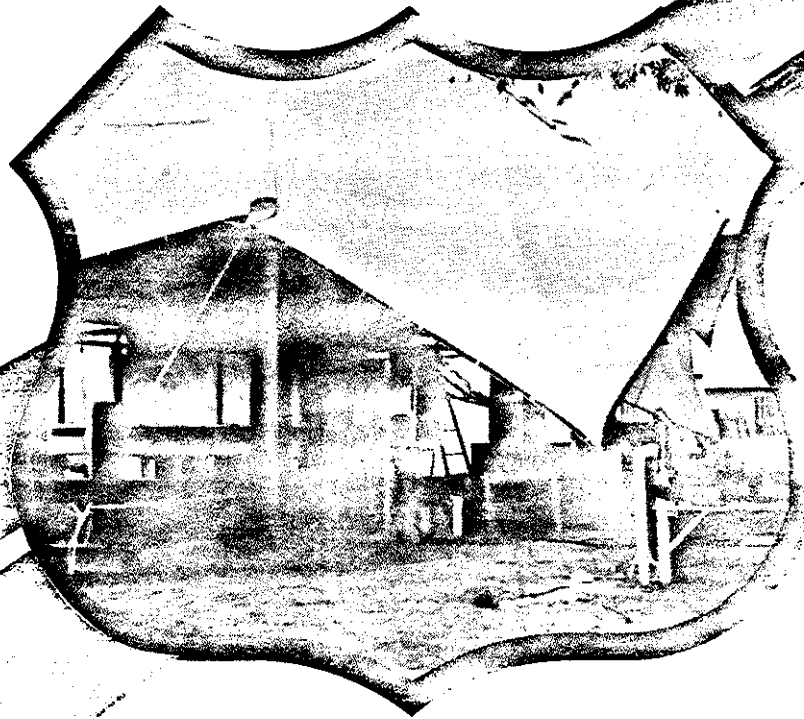


Report NO. FHWA/RD-81/005

FIELD STUDY OF PILE GROUP ACTION

Appendix C

March 1981
Final Report



Document is available to the public through
the National Technical Information Service,
Springfield, Virginia 22161



Prepared for
FEDERAL HIGHWAY ADMINISTRATION
Offices of Research & Development
Materials Division
Washington, D.C. 20590

1. Report No. FHWA/RD-81/005		2. Government Accession No.		3. Recipient's Catalog No.	
4. Title and Subtitle FIELD STUDY OF PILE GROUP ACTION (Appendix C)				5. Report Date October 1980	
				6. Performing Organization Code	
7. Author(s) L. J. Mahar and M. W. O'Neill				8. Performing Organization Report No.	
9. Performing Organization Name and Address RAYMOND INTERNATIONAL BUILDERS, INC. 2801 SOUTH POST OAK RD HOUSTON, TEXAS 77027				10. Work Unit No. (TRAIS) FCP 34H2-032	
				11. Contract or Grant No. DOT-FH-11-9526	
12. Sponsoring Agency Name and Address OFFICES OF RESEARCH AND DEVELOPMENT FEDERAL HIGHWAY ADMINISTRATION U.S. DEPARTMENT OF TRANSPORTATION WASHINGTON, D.C. 20590				13. Type of Report and Period Covered Final Report	
				14. Sponsoring Agency Code M/0685	
15. Supplementary Notes FHWA Contract Manager: Mr. Carl Ealy (HRS-21) Principal Investigator: Dr. Michael W. O'Neill, University of Houston Project Manager: Mr. Richard A. Hawkins, Raymond Technical Facilities, Inc.					
16. Abstract This report is the final report for a study involving the static vertical load testing of a full scale, instrumented pile group. The test group consisted of nine pipe piles instrumented for settlement, load transfer, pore pressures, total pressures and inclination. Two similarly instrumented reference (control) piles were also installed. Two smaller subgroups within the main group were also tested, and uplift tests were conducted on several of the individual piles. The soils at the test site consisted of clays that were overconsolidated by desiccation. It was determined that the efficiency of the main group and of the subgroups was essentially unity. Settlement ratios in the working load range were found to vary from about 1.2 to about 1.7, depending on the number of piles that were loaded. Failure was observed to be by plunging of the individual piles. Unit side load transfer varied essentially linearly with depth. Some dependence of load transfer patterns on residual stresses that remained after driving the piles was observed. The measured behavior of the group and subgroups was modeled by the "hybrid" algorithm, by means of Program PILGP1, which was developed for this study and documented in Appendices A and B. Good agreement between computed and measured results were achieved when the unit load transfer curves from the reference piles were used and when the soil modulus of deformation was appropriately adjusted to account for pile reinforcement of the soil and the presence of very small strains in the mass of soil around the group.					
17. Key Words Piles, Clay soils, Pile groups, computer model, pile driving			18. Distribution Statement No restrictions. This document is available to the public through the National Technical Information Service, Springfield, Virginia 22161		
19. Security Classif. (of this report) Unclassified		20. Security Classif. (of this page) Unclassified		21. No. of Pages 222	22. Price

NOTICE

This document is disseminated under the sponsorship of the Department of Transportation in the interest of information exchange. The United States Government assumes no liability for its contents or use thereof.

The contents of this report reflect the views of the author, who is responsible for the facts and the accuracy of data presented herein. The contents do not necessarily reflect the official view of the Department of Transportation. This report does not constitute a standard, specification, or regulation.

The United States Government does not endorse products or manufacturers. Trade or manufacturers' names appear herein only because they are considered essential to the object of this document.

Preface

This is the second and final report for a project entitled "Field Study of Pile Group Action." The Interim Report, dated March, 1979, precedes this report. The Interim Report describes several mathematical models for pile groups, presents an analysis of a proposed field experiment using one of the models, and describes details of instrumentation and procedures for that experiment. This report describes the results of the field experiment, which involved the load testing to failure of an instrumented, full-scale 9-pile group and two control (reference) piles at several times after installation. Two tests were also performed on subgroups of piles within the main 9-pile group, and uplift tests of several individual piles were also conducted.

This report is divided into a main text and six appendices, labeled A-F. The main text summarizes the prominent results of the study. Appendix A is a user's guide for Program PILGP1, a mathematical pile group model; Appendix B contains documentation for PILGP1; Appendix C contains detailed geotechnical data for the test site; Appendix D contains selected load-settlement, load distribution and load transfer plots; Appendix E is an evaluation of instrument performance; and Appendix F contains graphs and tables that support the main text that were not considered essential to the integrity of the main text. Appendices A-F are bound separately from the main body of the text and from each other.

The project was sponsored by the Offices of Research and Development, Federal Highway Administration, U.S. Department of Transportation. Raymond International Builders, Inc., was the prime research contractor. The University of Houston Central Campus (UHCC) was a subcontractor responsible for mathematical modeling, pile instrumentation, electronic data acquisition, analysis of results, and report preparation. Fugro Gulf, Inc., was a subcontractor responsible for the geotechnical study and for the ground instrumentation systems.

CONVERSION FACTORS, U. S. CUSTOMARY TO METRIC (SI)
UNITS OF MEASUREMENT

U. S. customary units of measurement used in this report can be converted to metric (SI) units as follows:

Multiply	By	To Obtain
Angstroms	0.0000001 (10^{-7})	millimetres
inches	2.54	centimetres
feet	0.3048	metres
miles (U. S. statute)	1.609344	kilometres
square inches	0.00064516	square metres
square feet	0.09290304	square metres
cubic feet	0.02831685	cubic metres
cubic yards	0.7645549	cubic metres
grams	0.001	kilograms
pounds (mass)	0.4535924	kilograms
tons (2000 pounds)	907.1847	kilograms
pounds (mass) per cubic foot	16.01846	kilograms per cubic metre
pounds (mass) per cubic yard	0.59327631	kilograms per cubic metre
pounds (force)	4.448222	newtons
pounds (force) per square inch	6894.757	pascals
pounds (force) per square foot	4.882428	kilograms per square metre
miles per hour	1.609344	kilometres per hour
degrees (angle)	0.01745329	radians
Fahrenheit degrees	5/9	Celsius degrees or Kelvins*

* To obtain Celsius (C) temperature readings from Fahrenheit (F) readings, use the following formula: $C = (5/9)(F - 32)$. To obtain Kelvin (K) readings, use: $K = (5/9)(F - 32) + 273.15$.

C O N T E N T S

	<u>Page</u>
INTRODUCTION	
General.	C1
Scope of Work Summary.	C2
Objectives	C4
INVESTIGATIVE PROCEDURES.	C7
Field Investigation	
General.	C7
Drilling and Sampling.	C7
Static Cone Penetrometer Soundings	C8
Pressuremeter Tests.	C9
Standard Penetration Test.	C10
Cross-Hole Seismic Wave Velocity Test.	C10
Laboratory Testing	
General.	C12
Classification and Index Property Tests.	C13
Strength Tests	C13
K _o Triaxial Tests.	C16
Remolded and Residual Strength Tests	C17
Consolidation Tests.	C18
REGIONAL GEOLOGY AND GENERAL SUBSURFACE SOIL CONDITIONS	
Regional Geology	C19
Local Subsurface Conditions.	C21
DISCUSSION OF FIELD AND LABORATORY TEST RESULTS	
General	C25
Soil Classification and Index Properties	C25
In situ Properties	C27
Undrained Shear Strength Profiles.	C29
Effective and Total Stress Parameters.	C31
Coefficient of Lateral Earth Pressure, K _o	C33
Consolidation Characteristics.	C35
Dynamic Properties	C36
Stress-Strain Properties	C37
Residual and Remolded Strength	C38
REFERENCES	
ILLUSTRATIONS AND TABLES	
ADDENDUM A: Field Logs and In Situ Test Data	
ADDENDUM B: Laboratory Test Curves	

INTRODUCTION

General

This appendix describes the detailed geotechnical site investigation and presents results of the Laboratory Testing Program conducted at the site of the full-scale pile group load test. The objective of the program was to define the general sub-surface soil conditions and soil engineering properties at the site to provide a basis for correlations to pile group and single pile behavior. The site is located on the campus of the University of Houston, Houston, Texas (see Figure C1). The project was sponsored by the Department of Transportation of the FHWA under contract with Raymond International Builders. Fugro Gulf, Inc., the University of Houston and Raymond Technical Facilities jointly conducted the program.

The investigative procedures used for the site investigation and laboratory testing program are described along with a discussion of the respective results. In addition, general background information such as regional geologic history and a general description of the investigation area is given. The scope of the investigation includes drilling and sampling, standard penetration tests, cone penetrometer soundings, cross-hole seismic velocity test and self-boring pressuremeter tests. Some discussion of the in situ field tests are presented to provide the reader an understanding of the applicability of the test results. The results of this investigation are included herein.

Scope of Work

The scope of work associated with the detailed site investigation and laboratory testing program included the following:

A. Undisturbed Drilling and Sampling in three boreholes;

1. Two boreholes drilled to a depth of 60 feet; one borehole to a depth of 120 feet.
2. Sampling continuously from grade to 50 feet, 5 foot intervals from 50 feet to 60 feet, and 10 foot intervals from 60 feet to 120 feet.
3. Field strength tests including pocket penetrometer and torvane conducted on each sample.
4. Field classification was made on the basis of field strengths and visual identification.

B. In situ Field Tests

1. Cross-hole seismic wave velocity tests were conducted at 5 foot intervals to a depth of 60 feet.
2. Standard penetration tests were conducted at 5 foot intervals to a depth of 60 feet.
3. Three static cone penetrometer test soundings were conducted to a depth of approximately 60 feet prior to the load test. Five additional tests were conducted upon completion of the load testing program.

4. Self-boring pressuremeter tests were conducted at approximately 10 foot intervals in two boreholes to a depth of 60 feet.

C. Laboratory Tests

1. Classification tests included gradation, Atterberg limits, specific gravities, water contents and unit weights.
2. Undrained shear strength tests included torvane, pocket penetrometer, unconfined compression, UU and \overline{CIU} triaxial compression tests.
3. K_0 triaxial tests.
4. Consolidation tests on horizontally and vertically trimmed specimens.
5. Remolded consolidated undrained triaxial compression tests.
6. Residual consolidated-drained direct shear tests.

Objectives

The principal objectives of the investigation and this presentation are summarized as follows:

1. To determine the general sub-surface conditions at the site of the group pile load test.
2. To determine in situ engineering properties of the soils along the length of the piles and beneath the pile tips.

3. To determine, in the laboratory, the physical engineering characteristics of the soils that may influence the behavior of the pile group acting under axial compression and tensile loading.
4. To provide a basis for determining design parameters needed to predict the performance of single piles and pile groups by available analytical procedures.
5. To provide preliminary information for the design of pile and ground instrumentation and for identification of the best penetration depth for the test piles and for the design of the load reaction system.

This investigation also provides a data base for correlation of various laboratory and in situ test data and pile design parameters such as soil-pile adhesion, load transfer characteristics and ultimate lateral and axial bearing factors to single and group pile behavior. Such correlations are presented within the main body of the report.

INVESTIGATIVE PROCEDURES

Laboratory testing techniques and in situ field tests were used to determine properties of the sub-surface soils at the test site. All field activities were conducted within 15 feet of the pile group with no borings or field tests being performed within the pile group itself to avoid site disturbance. The maximum depth of the investigation was 120 feet.

Field Investigation

General - The field investigation consisted of drilling and sampling, standard penetration, static cone penetrometer, pressuremeter and cross-hole seismic wave velocity tests. In addition, a groundwater observation well was placed to a depth of approximately 20 feet.

Standard penetration tests were conducted concurrently with the cross-hole test which served as the energy source while borings CB1 and CB3 were cased and served as receiver holes. The locations of all borings and field tests along with the general layout of the test pile group are shown on Figure C2.

Drilling and Sampling - Three boreholes were drilled to depths of 60, and 120 feet, respectively, below the existing grade using conventional wash boring procedures and a truck mounted Failing 750 drilling rig.

Undisturbed samples were taken by hydraulically pushing a 3-inch diameter thin walled Shelby sampler tube into the bottom of the borehole. In each boring, samples were taken continuously to a depth of 50 feet, at 5 foot intervals from 50 to 60 feet, in the deep boring, at 10 foot

intervals to the final penetration depth at 120 feet. In boring CB2, a split spoon sampler, driven with a standard penetration hammer, was used below 60 feet because soil stiffness exceeded the hydraulic push capability of the drill rig. Blow counts for these samples were recorded on field logs.

After retrieval of each sample, the soil in the end of the sample tube was visually classified and recorded on a field boring log along with soil strength values from the pocket penetrometer and torvane tests. A portion of each sample was then removed from the sample tube and placed in moisture tight jars. The remaining soil was left in the shelby tubes, sealed with wax and transported to the laboratory. The field logs are given in Addendum A.

Static Cone Penetrometer Soundings - Static cone penetrometer test soundings were conducted at the test site to provide an in situ measure of soil strength and consistency with depth and to provide information pertaining to the soil stratigraphy and site uniformity. Three soundings were performed and represent the initial in situ soil conditions in terms of cone resistance and sleeve friction at the test site. An additional five soundings were conducted at the completion of the load test program at locations in and around the pile group as shown on Figure C2.

The cone penetrometer soundings were accomplished using a truck-mounted electronic cone penetrometer system. Each sounding was conducted by positioning the twenty ton truck over the desired location and hydraulically pushing the electronic cone penetrometer through the soil at a constant rate of 2 cm/sec. Penetration was momentarily interrupted each three feet to add the next section of sounding rod.

The Fugro type electronic cone shown on Figure C3 measures both cone tip resistance (q_c) and friction sleeve resistance (f_s) electronically. The cone tip has a cross-sectional area of 10 square centimeters (1.54 square inches) and an apex angle of 60 degrees. The friction sleeve is located directly above the cone tip and has a total surface area of 150 square centimeters (23.3 square inches). Data from the cone tip and friction sleeve are recorded simultaneously on a two channel strip chart recorder calibrated to plot penetration depth, in feet, versus cone tip and friction sleeve resistance in tons per square foot. The CPT sounding records for the eight tests are presented in Addendum A.

Pressuremeter Tests - A self boring type pressuremeter, developed through research efforts at the University of Texas at Austin, was used to obtain in situ estimates of cohesive shear strengths, stress-strain behavior and estimates of in situ lateral earth pressures. The pressuremeter tests were conducted by drilling a starter hole with conventional wash boring techniques to 3 to 5 feet above each depth of interest. The pressuremeter was then attached to the drill string, inserted into the borehole and seated at the bottom. The drill string was then rotated, which causes the pressuremeter unit to advance slowly by cutting and washing away soil. A thin-wall cutting shoe is located at the end of the unit as shown in Figure C4. When the center of the pressure membrane reached the desired depth, a waiting period of approximately 30 minutes was allowed. Pressure increments of 2 psi were then applied until a circumferential strain of approximately 3 percent was reached. The increments were then increased to 5 psi for the remainder of the test. Expansion curves for each test conducted are included in Addendum A.

Eleven pressuremeter tests were performed at the test site in two boreholes to a maximum depth of 62 feet at approximately 10 foot intervals at each location (locations are shown on Figure C2). Due to difficulties encountered in the insertion of the probe into the very stiff soil at PM1, three of the tests were not successful and data from only eight are presented in this report.

Standard Penetration Test - A standard penetration test boring was drilled in accordance with ASTM standard D1586 to a depth of 60 feet below existing grade at location SPT1.

A standard 2-inch OD split spoon sampler was driven with a 140 pound hammer, dropped 30 inches by using two wraps of the hoisting rope on the "cat head", and released by throwing slack into the line and allowing the hammer to free fall. Blow count values were obtained on 5 foot intervals and recorded on a field log. Additional tests at 2.5 foot intervals were taken between 35 and 45 feet below grade to better define the soils where the pile tips were to be located.

Cross Hole Seismic Wave Velocity Tests - In situ measurements of shear and compression wave velocities were made by a cross-hole method similar to that described by Stokoe and Woods (C16) to determine dynamic values of shear and compression moduli.

The cross-hole method consisted of measuring the time for a mechanically produced body wave to travel from a source placed at the depth of interest to each of one or more receivers placed at the same depth at a known distance from the source. Both shear wave and compression wave travel times were determined from the response records

from the velocity transducers located at each receiver. Two three dimensional velocity transducers (geophones) were placed at each test depth by wedging them into cased boreholes spaced at 10 and 20 feet from the source in a linear array. The general test set up is shown on Figure C5.

The cross-hole tests were accomplished concurrently with the standard penetration tests such that after the SPT blow count value was determined at each test interval, the embedded split spoon was used as the energy source by striking the top of the drill string with a hammer connected electronically to the oscilloscope trigger. Boreholes CB1 and CB3 were used for receiver holes. Each hole was cased with 3-inch ID PVC pipe and grouted in place, as shown on Figure C5, several days prior to cross-hole testing. The response of the receivers to the passing body waves was recorded by a two channel storage oscilloscope which started recording at the instant the drill string was hit. A polaroid photograph was made of the response signal displayed on the scope from which compression and shear wave velocities were determined. Measurements were made at 5-foot intervals to a depth of 60 feet below the existing grade. Representative examples of the cross-hole response records are included in Addendum A.

LABORATORY TESTING

General - The laboratory testing program was developed to identify the general physical characteristics of each soil stratum which might influence the performance of the test pile group. Based on preliminary soil profiles obtained from the drilling and sampling program, a detailed laboratory testing program was selected as shown on Figure C6. From the preliminary profile five main soil strata were identified; two of which

(Strata III and IV) were considered as having the greatest potential influence on pile behavior.

The laboratory testing program consisted of five categories of tests as follows:

1. Classification and Index property tests,
2. Strength tests,
3. K_0 triaxial consolidation tests,
4. Remolded and Residual strength tests, and
5. One-dimensional Consolidation tests.

The tests were assigned in a manner that would allow delineation of specific soil properties in each stratum. Each category of tests is described in greater detail in the following sections.

Classification and Index Property Tests - Tests were conducted on soil from each sample interval to aid in the classification of the soil in each stratum and to determine its index properties. Soils were classified according to the unified soil classification system (ASTM SPEC. D2487). The following tests were included:

1. Natural water content,
2. Unit dry weight,
3. Specific gravity,
4. Gradation, and
5. Atterberg limits.

Water content and unit weight determinations were made in conjunction with each shear strength and consolidation test.

Specific gravity determinations were made at a minimum of one per each stratum for use in calculation of void ratio and degree of saturation. Soil gradation tests including sieve analysis, hydrometer tests and determinations of percent of fines (passing number 200 sieve) were conducted to classify the very silty soils in stratum V and to determine the variation of sand content with depth in the sandy clay of strata II and IV. Plastic and liquid limit tests (Atterberg limits) were conducted on soil from each sample interval for use in determining the plasticity and liquidity indices. The total number of these tests along with the other classification tests are given in Table C1.

Strength Tests - Since it may be desirable, in practice, to correlate general load-transfer characteristics to shear strength profiles obtained from routine laboratory strength tests, several types of undrained shear strength tests were conducted. In addition, a series of tests was conducted to determine normalized parameters as well as total and effective strength parameters to provide data necessary for a variety of ultimate pile capacity and load-settlement analytical procedures. The strength testing program included the following tests:

1. Pocket penetrometer and torvane,
2. Unconfined compression,
3. Unconsolidated-undrained triaxial compression,
4. Multi-specimen consolidated-undrained triaxial compression with pore pressure measurements, and
5. Consolidated-undrained triaxial compression rebounded to a specified over-consolidation ratio with pore pressure measurements.

The total numbers of each test conducted are given in Table C1 and the laboratory data for each test have been transmitted to the FHWA under separate cover.

Pocket penetrometer and torvane tests were conducted in the field at the time of sampling and in the laboratory in conjunction with each of the compressive strength tests. A factor of one-third to correlate penetrometer readings to undrained shear strength is commonly used in Texas for the type of soils encountered at the site and was therefore used in this program.

Unconfined compression tests were conducted on specimens from alternate sample intervals to a depth of 44 feet. The tests were run according to ASTM Standard D2166 (C3) on specimens trimmed to approximately 3-inches by 6-inches.

Unconsolidated-undrained (UU) triaxial compression tests were also conducted on specimens from alternate sample intervals. Confining pressures were selected approximately equal to the estimated effective vertical stress at the sample depth and, at selected depths, additional tests were conducted using higher confining pressures to determine any effect that confining pressure may have on the UU strengths. ASTM specification D2850 test procedures were used for these tests.

Multi-specimen, consolidated-undrained triaxial compression tests with pore pressure measurements (\overline{CIU} test) were conducted at five depth intervals to determine the effective and total strength parameters and to obtain the laboratory stress-strain characteristics of the soils. At each test interval, a series of three specimens, measuring 3-inches by

6-inches, were prepared for CIU tests. The three specimens were consolidated at pressures approximately equal to 1.25, 1.5 and 2 times the estimated effective overburden pressure for development of the effective and total stress failure envelopes. At the end of the consolidation phase, each sample was back-pressure-saturated at pressures sufficiently high to obtain a pore pressure coefficient, B, greater than 0.95. The sample was then sheared in compression at strain rates recommended by Bishop and Henkel (C6), based upon the measured consolidation rates. Each test was run to approximately 20 percent strain.

Normalized Shear Strength Tests - Consolidated undrained triaxial tests were conducted at four depths in which, during the consolidation phase, the specimens were consolidated isotropically at a pressure greater than approximately twice its maximum past pressure (p_o') and rebounded at a known over-consolidation ratio. At each of these depths (see Figure C2), a series of three tests was carried out using OCR values of approximately 2, 5 and 10. The normalized shear strength for each OCR value was then calculated by dividing the measured undrained shear strength with the consolidation pressure used (S_u/σ_{vc}').

Ladd and Foott (C7) have demonstrated that some clays exhibit a normalized behavior where, when tested as described above, the ratio, S_u/σ_{vc}' , remains constant for a given over-consolidation ratio, independent of the magnitude of the maximum consolidation pressure used. It is also presumed that the ratio of Young's modulus to vertical consolidation pressure, E/σ_{vc}' , remains constant. To demonstrate this for Beaumont clays, the maximum consolidation pressure used at the 20-22

foot depth interval was 67 percent higher (250 psi versus 150 psi) than that used at the 18-20 foot interval. The samples at both depth were then rebounded at known OCR values and the normalized strengths (S_u / σ_{vc}') compared. Stress-strain curves for these tests are presented in Addendum B and are denoted "NSP" triaxial compression tests.

K_0 Triaxial Consolidation Tests - To estimate the in situ coefficient of lateral earth pressure at rest in the laboratory for comparison to those determined from pressuremeter tests and to determine the stress history of the soil, a series of K_0 triaxial consolidation tests were conducted. The tests were carried out at four depths, as indicated on Figure C2, using a conventional triaxial cell and a procedure similar to that described by Bishop and Henkel (C6) and Abdelhamid and Krizek (C1).

In this procedure, the measurement of K_0 is made by imposing values of σ_1 and σ_3 in the triaxial cell such that no lateral deformation in the sample occurs during consolidation at these pressures. The ratio, σ_3 / σ_1 , which produces this condition is considered equal to K_0 for the imposed stress conditions. For overconsolidated clays, the K_0 value generally decreases as consolidation pressures increase until a normally consolidated condition is reached (i.e. when σ_1 becomes equal to the preconsolidation pressure). As consolidation pressures increase past this point, the value of K_0 remains constant. During the tests, several stages of increasing consolidation pressures were used and a curve of K_0 versus effective vertical consolidation pressure (σ_{vc}') was developed. From this relationship, the value of K_0 at the estimated in situ effective vertical overburden pressure was determined. It is also possible to estimate the maximum preconsolidation pressure and, thus, the overconsolidation ratio, as the point at which K_0 becomes constant.

Remolded and Residual Strength Tests - Remolded and residual strength tests were conducted in order to investigate the possibility that load transfer characteristics may be a clear function of the remolded or residual strength and thus provide a simple and rational means of predicting load transfer in over-consolidated clays.

Remolded consolidated-undrained triaxial compression tests with pore pressure measurements (\overline{CIU}_r) were conducted at four depth intervals. Two depth intervals were selected from each of strata III and IV for testing. At each depth, a series of three tests were run at consolidation pressures equal to approximately 1.25, 1.5 and 2 times the estimated effective overburden pressure. At two other test depths, the soil was consolidated under anisotropic conditions using a K value equal to the in situ K_0 as determined from the K_0 consolidation and pressuremeter tests and then sheared in compression while measuring the pore pressures. From these tests, the total and effective remolded strength envelopes were determined. Stress-strain curves, Mohr's diagrams and p' versus a curves are presented in Addendum B.

A residual strength envelope was determined from consolidated-undrained direct shear tests conducted on samples taken from two depth intervals. At each depth, three tests were conducted at consolidation pressures of approximately 1.25, 1.5 and 2.0 times the estimated effective overburden pressure. After consolidating, the sample was sheared within the direct shear apparatus in a consolidated-undrained conditions to create a pre-failed surface. The sample was then allowed to reconsolidate and the sample was again sheared but at a strain rate sufficiently slow to provide a drained condition (approximately 3 days to failure).

Consolidation Tests - One-dimensional consolidation tests were conducted on samples taken from five depth intervals. Using the ASTM standard D2435 procedure, each sample was consolidated in stages until virgin compression was observed and then rebounded to a pressure of 1/2 ton per square foot. The sample was then reloaded to a maximum vertical pressure of about 28 tsf and rebounded one more time at the completion of the test.

At four depth intervals, an additional consolidation test was conducted on horizontally trimmed samples to determine the lateral stress history. From this, an inferred value of K_0 can be calculated from the ratio of the maximum preconsolidation pressure from horizontally oriented samples to that of the vertically oriented samples. These tests were conducted in the same manner as the vertically oriented samples. Consolidation curves are presented in Addendum B.

REGIONAL GEOLOGY AND LOCAL SUBSURFACE CONDITIONS

Regional Geology

The test site is located on the Texas Gulf coastal plain. The soils outcropping along a band extending inland approximately 70 to 100 miles from the Gulf of Mexico are of the Quaternary system. The earlier Quaternary deposits, the Pleistocene series, are composed of several formations. It is the two most recent formations, the Beaumont and the Montgomery, that are of interest in this study. The Beaumont formation, the more recent of the two, is composed mainly of stiff over-consolidated clay and it is exposed along most of the Texas Gulf coast to a distance of approximately 40 to 50 miles inland (see Figure C7). Although the maximum thickness of this formation is believed to be about 700 feet (Sellards, Adkins, and Plummer, C13), the Beaumont Formation tapers out northwest of downtown Houston where the older, underlying Montgomery Formation outcrops.

The Beaumont Clay was deposited during the recession of the ice sheet in the Wisconsin Ice Age, approximately 75,000 to 100,000 years ago (Bernard, LeBlanc, and Major, C5). Beaumont sediments were deposited primarily in distributaries of rivers (deltas) and in shallow lagoons. It is presumed that the depositional environment resembled the Mississippi delta region of the present. The soil in the Houston area is non-marine, and appears to have been deposited by distributaries of the Brazos River, which took a more northerly course at the time of deposition than it does today (Van Siclen, C17).

The formation is somewhat heterogeneous, with inclusions of sand and silt being quite prevalent, as would be expected from the alluvial process of deposition. The clay portion typically presents a red or tan

and gray mottled appearance. The mineralogical composition of the red, tan, and gray portions appears to be about the same (O'Neill, C11).

The following account of the formation's structure and stress history was presented by Al-Layla in (C2):

The Beaumont clay was deposited on broad flat plains during periods of overflow. During dry seasons the clay shrunk and a network of cracks were opened. As repeated flooding continued, new material was deposited in these cracks and on top of the previous layer. Alternating periods of deposition and no-deposition coupled with drying continued for a considerable time span. The repeated wetting and drying produced joint systems in the clay which are now visible. Different colors found on joint surfaces are either due to varied materials deposited on them, or to the fact that these joints served as planes which allowed water seepage. Seeping water may have produced chemical reactions which changed the color along the joints. Between joints, clay blocks contain randomly oriented fissures formed similarly when the clay was subjected to repeated cycles of wetting and drying. Variations in clay mineral types probably caused differential swelling and contraction and, these differential movements were accompanied by internal strains, large enough to cause structural damage and produce tension fissures.

The Beaumont clay was over-consolidated by desiccation as a result of exposures to weathering during the late Wisconsin glacial stage when the sea level was more than 400 feet lower than at present. When the clay was exposed to air at the surface, water began to move from the interior soil mass, by a capillary process toward the surface where it evaporated. This process reduced the water content and created a capillary pressure or tension in the pore water of the soil whose magnitude increased with decreasing soil moisture content; however, the total normal stress remained practically unchanged. Since the total stress is equal to the sum of the pore pressure and effective stress, decreasing the pore pressure causes equivalent increases of the effective stress. This increased effective stress acts all around the soil and causes it to consolidate, not by increasing the total pressure with additional overburden or surcharge weights, but by increasing the negative pore pressure. Also, since more swelling under those circumstances was possible in the vertical than in the horizontal direction, the Beaumont clay can be considered an anisotropic material.

The Beaumont formation appears to extend from the surface to a depth of 26 feet at the test site. The change in formations is evidenced by an abrupt change in several of the soil properties, most notably a rise in the percentage of sand size particles which is typical of the older formations underlying the Beaumont.

Local Subsurface Conditions

A generalized soil profile developed from the boring and cone penetration test results is presented on Figure C8. As shown, the site subsurface soils within the upper 60 feet consist of five main strata as follows:

<u>Stratum</u>	<u>Depth, Ft.</u>		<u>Soil Description</u>
	<u>From</u>	<u>To</u>	
I	0	8	Stiff to Hard Gray and Tan Clay
II	8	12	Stiff to Very Stiff Gray and Tan Sandy Clay with Calcareous Nodules
III	12	26	Very Stiff to Hard Red and Light Gray Clay, Slickensided
IV	26	46	Stiff to Hard Light Gray and Tan Sandy Clay
V	46	60	Red and Light Gray Silt, Interbedded with Clay and Sand Layers

Subsurface conditions were relatively uniform across the test site, as revealed by the soil test borings and cone penetrometer soundings (Figure C9). The surface stratum (Stratum I) generally has fine organic material and some small roots to a depth of 3 to 6 feet. Calcareous and ferrous nodules were found dispersed within this stratum generally below a depth of 4 feet. The average natural moisture content in these upper

clays was approximately 20 percent. Atterberg limits tests indicate that this stratum is moderately to highly plastic with liquid limits in the range of 34 to 56 and plasticity indices increase with depth from 20 to 44 percent. Dry unit weight ranged from about 105 to 108 pcf. The results of the various field and laboratory strength tests indicate average cohesion values of between 0.8 and 1.4 tons per square foot (tsf). Static cone penetrometer resistances (q_c) ranged from 10 to 25 tsf resulting in average undrained shear strength between 1.1 and 2.0 tsf. Standard Penetration resistances (N-values) were recorded at between 5 and 10 blows per foot.

Stratum II consists of a four foot layer where the percentage of sand (and calcareous nodules) increases to about 37 percent. Moisture content in this stratum was measured between 20 and 25 percent while the Liquid Limit and Plasticity Index reduce to about 35 and 21 percent, respectively. Along with calcareous nodules, some sand pockets are encountered within this stratum. Field and Laboratory strength tests indicate an average cohesion value of about 0.9 tsf while the CPT undrained shear strength increased markedly to an average maximum value of about 5 tsf at 12 feet.

Underlying this sandy clay stratum is a 14 foot thick stratum of slickensided clay containing occasional calcareous nodules (Stratum III). This highly plastic stratum has an average liquid limit of 66 and average plasticity indices between 40 and 55 percent. Natural moisture contents ranged from 23 to 33 percent, and dry unit weights were measured at 93 to 100 pcf. Strength tests indicate that this over-consolidated stratum (by desiccation) has an average laboratory undrained cohesion value on the order of 1.3 tsf. The average computed undrained shear strength from the

CPT was fairly uniform at approximately 2.5 tsf. N-values ranged between 12 and 19 blows per foot. Based on consolidation tests and experience the overconsolidation ratios (OCR) was estimated between 8 and 15.

Below a depth of 26 feet, almost all of the soil parameters exhibit a rather abrupt change. It is generally believed that, at this depth, a change in geologic formations is encountered. The upper three strata are believed to be of the Beaumont formation while the underlying strata are believed to be in the Montgomery formation. Stratum IV generally has natural moisture contents and liquid limits below 20 and 30 percent, respectively, and plasticity indices between 15 and 20 percent. The percent of sand size particles rises from about 20 to about 40 percent while dry unit weights were generally between 110 and 120 pcf. Cohesion values dropped to around 0.5 tsf near the top of the stratum but generally rise to between 1 and 2 tsf between 30 and 40 feet. Many sand pockets and seams and calcareous nodules were encountered. This stratum appears less homogeneous than Stratum III, as demonstrated by the CPT point resistance logs. N-Values recorded within this stratum ranged between 7 and 35 blows per foot.

Underlying this sandy clay stratum is a 12 foot thick stratum consisting primarily of silt. This stratum is interbedded with clay and sand seams and layers and the interbedded nature is clearly visible in CPT point resistance logs. The CPT soundings indicate that the silt is relatively dense.

Although one soil test boring penetrated deeper than stratum V, the details of soils encountered deeper than 60 feet below existing grade are not presented here. See the boring logs in Addendum A for further details.

A stabilized groundwater level of approximately 7 feet below existing grade was recorded in the observation well at the time of the field work (February, 1979). February is generally considered the middle of the rainy season for the upper Texas Gulf coast and, therefore, this groundwater level is probably higher than the groundwater during the dry season.

DISCUSSION OF FIELD AND LABORATORY TEST RESULTS

General

A general discussion is presented here of the results of the Field and Laboratory Testing Program. Data are presented as measured in the field or lab and reduced to commonly used geotechnical engineering properties and parameters. In addition, a discussion of the general form of the data and suggested explanations for anomalous or erroneous information is presented to aid in interpretation of the data. A more detailed, and in some instances revised, interpretation of these data with respect to the pile load test results is presented in the main body of the report.

Soil Classification And Index Properties

As previously discussed, the soil profile in the upper 60 feet can be divided into five general strata (see Figure C8) based on visual descriptions as well as the results of Atterberg limits, unit weight and water content determinations. These test results are given on the boring logs presented in Addendum B and on Figures C10 through C17. The soil in each of these strata were classified according to the unified classification system as shown on Figure C8. Plasticity soil classification charts for strata I through IV are given in Figures C10, C11 and C12.

Strata II and IV are described as a light gray and tan sandy clay with calcareous nodules. The variation of sand content with depth in these layers is considered important to the assessment of their engineering properties and to load transfer characteristics. Based upon the grain size distribution of these soils, the average sand content in stratum II is approximately 37 percent while the sand content in Stratum IV generally increases with depth and nearly becomes a clayey sand at

approximatley 42 feet as seen on Figure C13. This high sand content at about 42 feet shows up as a spike on the CPT point resistance plots on Figure C8 and on the cone sounding records in Addendum A. Complete gradation curves for samples at selected depths in strata II, IV and V are also included in Addendum A.

The unit weights and water contents were determined in conjunction with each strength and consolidation test. As can be seen from Figure C14, the data plots with little scatter, and strata breaks in the profile can be easily seen. The increased amount of scatter shown in the data below 46 feet is due to the presence of clay and sand layers and seams within a stratum of predominately silt. This interbedding can be seen more clearly from the cone sounding records shown on Figure C8.

The void ratio, e , and plasticity index, PI, variations with depth (Figures C15 and C16) demonstrate similar characteristics. The relatively low values of void ratio measured are somewhat typical of Beaumont clay and the very low values of e and PI found below about 26 feet are believed to be due to the presence of sand and silt sized particles within the clay. Numerical values obtained from the Atterberg limit tests along with results of tests to determine percent passing the number 200 sieve and specific gravity are summarized on Table C2.

The liquidity index was determined using average values of natural water content and plasticity index from Figures C14 and C16. As seen from Figure C17, the liquidity index is generally less than 0.30 at depths less than about 40 feet, indicating natural water contents at or near the plastic limit. This corresponds to a sensitivity of less than about 1.5 according to the relationship of liquidity index versus sensitivity presented by Skempton and Northey (C14).

In situ Properties

The results of the in situ field tests including the cone penetrometer, pressuremeter, cross-hole seismic and standard penetration tests are presented in Addendum A. Some interpretation of these data are offered within this report in the form of profiles developed from available correlations to certain common geotechnical engineering properties such as undrained shear strength and elastic constants to correlate with the load-transfer characteristics. However, it is anticipated that direct correlation between in situ data and load-transfer characteristics may be possible.

The cone penetrometer sounding records in Addendum A represent a continuous account of the penetration resistance in tons per square foot acting on a cone tip, q_c , and on a friction sleeve, f_s . It has been shown that, in most soils, an identification of material type can be made by determining the friction ratio, FR (f_s/q_c). It was found, however, that the published correlation between material type and friction ratio (Schmertmann, C12) did not apply to the soils encountered at this site due to the high degree of over-consolidation and the presence of slickensided surfaces which resulted in lower friction ratios. Friction ratio values are plotted along with the q_c and f_s profiles in Addendum A.

As can be seen on the CPT records, the soil in strata I and III can be characterized as having fairly uniform values of q_c of approximately 20 and 28 tons per square foot, respectively. The friction sleeve resistance values are approximately 0.5 and 0.7 tons per square foot, respectively, for these strata. The friction ratio in these layers is generally greater than 2 percent, which is common for clay soils.

Also note that the q_c and f_s records within stratum III are comparatively smooth, indicative of the absence of large numbers of calcareous nodules, sand and silt pockets or lenses and other anomolous conditions.

At the top of stratum IV, the average value of cone resistance remained approximately the same as that of stratum III, however, it can be seen, particularly on sounding D-2, that upon entering the sandy clay of stratum IV, the q_c record clearly becomes non-uniform with the average q_c value increasing with depth to a maximum average value of about 35 tsf at 46 feet. The non-uniform q_c profile in this statum, which is characteristic of a soil containing sand is supported by the decrease in the average friction ratio to about 1.8 percent, also indicating sandy material. The spike in the q_c record at about 41 feet was caused by the very high sand content (see Figure C14) at that depth.

Below 46 feet, the cone records can be characterized as very non-uniform with many high spikes reaching q_c values of 275 tsf and f_s values of 4 tsf or more and thin layers of lower q_c and f_s values averaging about 50 and 1.0 tsf respectively. This is the result of the cone penetrating the interbedded silt and clay with sand pockets and lenses in the stratum. These records were used in deciding to place the test pile tips at a depth which avoids the interbedded soil in stratum IV.

In comparing the CPT records from soundings conducted prior to test pile installation to those conducted after completion of the load testing, very little change in q_c and f_s values were noted. Figure C9 shows a comparison of soundings D1, D2 and D3. As can be seen, there was close agreement between soundings, which indicates lateral uniformity of soil conditions at the test site.

In relating this type of in situ data to the behavior of piles, Nottingham and Schmertmann (C10), have presented a method of predicting pile capacity directly from cone penetration test records. Schmertmann (C12) has also presented methods for using CPT data for many other engineering applications including load-settlement characteristics of driven piles. However, the method presented is based upon correlations with the Menard pressuremeter and is considered very conservative. Therefore, it seems reasonable to use CPT data in direct correlation to the load-transfer characteristics of driven piles.

Undrained Shear Strength Profiles

In order to correlate pile load-transfer characteristics with routinely obtained soil strength data, an undrained shear strength profile was obtained from the following laboratory and in situ field tests:

1. Pocket penetrometer
2. Torvane
3. Unconfined compression
4. Unconsolidated-undrained triaxial compression
5. Self boring pressuremeter
6. Static cone penetration

Pocket penetrometer and torvane values were obtained in the field and on each triaxial or consolidation test specimen. The values of each of these tests are plotted with respect to depth on Figures C18 and C19. Data from the tests conducted in the field are recorded on the boring logs in Addendum A. Unconfined compression and unconsolidated undrained triaxial compression test results are plotted together on Figure C20 and given in tabular form on Table C3.

From the pressuremeter test results, the undrained shear strength was determined using the method suggested by Wroth and Hughes (C18) in which a stress-strain curve is constructed from the pressuremeter expansion curve. The undrained shear strength is then taken as the peak of the stress-strain curve. Values of the undrained shear strength are plotted with respect to depth on Figure C21 and given on Table C6. The stress-strain and pressuremeter expansion curves used in this determination are included in Addendum A.

It is also possible to obtain values of undrained shear strength from the static cone penetrometer test as recommended by Nottingham and Schmertmann (C10) and Schmertmann (C12) using the equation:

$$S_u = \frac{q_c - \gamma_z}{N_c}$$

Where: S_u = undrained shear strength

q_c = cone tip resistance

γ_z = total overburden pressure at depths of q_c

N_c = dimensionless cone tip bearing factor

The value of N_c has been found to vary depending on many factors including type of cone, penetration rate and soil type. For the Fugro type electronic cone penetrometer, an N_c value in the range of 10 to 15 is recommended (Schmertmann, C12). The undrained shear strength profile using the above equation and N_c values of both 10 and 15 is shown on Figure C22 along with values from the pressuremeter and the UU triaxial tests for comparison. The cone penetrometer sounding records from which this undrained shear strength profile was determined is included in Addendum B.

A composite profile showing the results of all the conventional laboratory undrained shear strength tests is shown on Figure C24. The large variation of data shown in the profile is typical and has been shown in other laboratory investigations in Beaumont clay (Al-Layla, C2). In stratum III, this can be partially attributed to the presence of prefailed surfaces of various orientations found in most of the specimens. In stratum IV, however, it appears that the data scatter in the composite shear strength profile is more likely the result of the variation of sand content and the presence of sand pockets within the stratum (Figure C13). At depths of 40 to 43 feet (Stratum IV), the undrained shear strength decreased considerably due to this very high sand content.

In addition, at depths from about 26 feet to 30 feet in the composite profile (Figure C23), the data appear to be more consistent with a lesser degree of scatter. However, these data indicate a fairly significant decrease in shear strength which is inconsistent with the fact that both water content and void ratio decrease sharply below 26 feet and that sand content is relatively low at those depths (less than 20%). A possible explanation is that the strata break at 26 feet defines the lower boundary of the Beaumont formation and the top of the Montgomery foundation. The top of the Montgomery formation has likely been exposed to a high degree of weathering resulting in higher percentage of silt size particles and lower undrained shear strengths. The lower void ratio and water content in this zone can also be explained by presence of this silt and sand sized particles in the soil.

Effective And Total Stress Parameters

The effective and total stress strength parameters (ϕ' , c' , ϕ and

c), were determined from consolidated-undrained triaxial compression tests with pore pressure measurements ($\overline{\text{CIU}}$ Test). The results from these tests are summarized in Table C5.

The friction angle and intercept cohesion, c , for effective stress reported in the table were determined from a set of three Mohr's diagrams drawn from the results of the $\overline{\text{CIU}}$ tests conducted at each assigned test interval. Difficulty was experienced while attempting to draw a straight line through the three Mohr's circles due to scatter in the data and, in order to improve the determination of ϕ and c , the stress-strain-pore pressure data were plotted in terms of p' and q where:

$$p' = \frac{1}{2} (\sigma'_1 + \sigma'_3) \text{ and}$$

$$q = \frac{1}{2} (\sigma_1 - \sigma_3)$$

The locus of points defined by p' and q for a particular test is termed the stress path (Lambe and Whitman, C8). A failure envelope can then be determined to represent the three ($\overline{\text{CIU}}$) tests conducted at various consolidation pressures by drawing a line which best approximates a tangent to the three stress path curves. The angle of inclination, α and intercept, a , of this failure envelope is related to the Mohr Coulomb failure envelope as follows:

$$\tan \alpha = \sin \phi'$$

$$a = c' \frac{\tan \alpha}{\tan \phi'}$$

For the sandy clay of strata II and IV, it was found from these plots that the stress conditions reached the failure envelope at strains much lower than indicated from the stress-strain curves, where the maximum deviator stress had not yet occurred within 20 percent strain and the samples experienced a considerable amount of "bulge" type deformation.

For these tests, failure was assumed, for the purpose of plotting the Mohr's diagrams, to occur at the point where the stress path on the p' - q plot became parallel or intersected the interpreted failure envelope. With failure defined in this manner, the scatter in the Mohr-Coulomb presentation improved considerably. Both representations of the \overline{CIU} test data (Mohr-Coulomb and p' versus q curves) are presented in Addendum B along with the respective stress-strain and pore pressure strain curves.

Stress-History - The stress history of the soil at the project site was estimated using the results of both one-dimensional and K_o triaxial consolidation tests.

For the one-dimensional consolidation tests, the preconsolidation pressure was determined using the Casagrande construction procedure. The over-consolidation ratio was then determined using the estimated in situ overburden pressure shown on Figure C24 and plotted versus depth on Figure C25. Due to high nonlinearity of the e - $\log p$ curves and resulting difficulty in identifying the preconsolidation pressure scatter, in the calculated values of OCR was experienced and less weight was given to these value in determining the average OCR profile shown.

For the K_o triaxial consolidation tests, the preconsolidation pressures were determined as the point on the K_o versus σ_{vc} curve (see Figures C26 thru C29) where K_o becomes constant. The over-consolidation ratios calculated using these values of preconsolidation pressure are also plotted versus depth on Figure C25.

An average OCR profile was then developed based on these results and is indicated on Figure C25 as a solid line. The dashed lines and shaded region present the range of values calculated. The OCR values determined from one-dimensional consolidation at depths of 9 and 33 feet

seemed inconsistent and were not considered in the development of this average curve.

Normalized Strength Profile - An undrained shear strength profile was developed based on the results of the normalized shear strength tests described earlier. This was done by plotting the normalized shear strength, S_u / σ_{vc}' , against the overconsolidation ratio for each depth interval (Figures C30 thru C33). Using this relationship and an estimated OCR value from Figure C25, a value of S_u / σ_{vc}' was determined. This value was then multiplied by the estimated in situ overburden pressure from Figure C24 to arrive at an undrained shear strength value.

In order for this concept to be valid, Ladd and Foott (C7) recommend verifying that the soil of interest behaves in a normalized manner by conducting the normalized strength tests on specimens from the same soil type using different maximum consolidation pressures and re-bounding at known OCR values. The concept is then valid if the normalized shear strength remains constant in each case for given OCR value. This is demonstrated by comparing the OCR versus S_u / σ_{vc}' curves from 19 and 21 feet where close agreement can be found (see Figures C30 and C31).

The values of undrained shear strength calculated from this method are plotted versus depth along with UU strength values on Figure C34. A summary of results of the Normalized Strength Parameter triaxial tests is given on Table 5. It was found that the undrained shear strengths derived from normalized strength parameters correlated well with the laboratory unconsolidated undrained shear strength values.

Coefficient of Lateral Earth Pressure, K_0

The coefficient of lateral earth pressure at rest, K_0 was evaluated using the self-boring pressuremeter and checked in the

laboratory with the K_o -consolidation triaxial tests as discussed earlier. In addition, an independent assessment was made from the results of one-dimensional consolidation tests on horizontally and vertically trimmed specimen.

To determine values of K_o from pressuremeter test results, the following must be known: the location of the water table, the variation of soil unit weight with depth, and most critically, the initial horizontal total stress in the soil, P_o , for each test. A three step iterative procedure, suggested by Marsland and Randolph (C9) was used to estimate P_o . First, a value of P_o is assumed; next, this value is used to find a value of undrained shear strength, S_u , by the graphical procedure proposed by Wroth and Hughes (C18), and finally, the value ($P_o + S_u$) is checked on the expansion curve for proximity to the region at which the curve becomes non-linear. The process is repeated with new values of P_o until the third step yields a satisfactory result. It is suggested by Marsland and Randolph that the pressure ($P_o + S_u$) corresponds to that point where the soil adjacent to the pressuremeter membrane begins to fail in shear. After P_o is found, the value of K_o is calculated using the expression:

$$K_o = \frac{p_o - u}{\sigma'_v}$$

where: u = hydro static pore water pressure

σ'_v = effective overburden pressure

Values of K_o derived from this procedure are given in Table C6 and plotted versus depth in Figure C35. The expansion curves from which these values were derived with values of P_o indicated are included in Addendum A.

It was also possible to estimate the lateral earth pressure coefficient using the results of the consolidation tests on horizontal and vertically trimmed samples. Although it was not possible to accurately determine the preconsolidation pressure from the e -log p curves (Addendum B) due to the highly non-linear characteristics of the curves, K_o values were estimated by the following procedure (refer to Figure C36):

1. The e -log p curve for the test on the horizontally trimmed sample was superimposed on the curve from the vertically trimmed sample such that the void ratios at the initial stage of loading for each curve coincided.
2. Horizontal lines were drawn through both curves at several points corresponding to pressures higher than the estimated preconsolidation pressure.
3. The average ratio of pressures corresponding to the points of intersection of the horizontal lines with the two curves, as indicated on Figure C26, was determined.

It was assumed that the ratio defined above was a good approximation of the ratio of horizontal to vertical preconsolidation pressures, as illustrated on Figure C36, and is an estimate of K_o . It was found, by using the above procedure, that the ratio remained relatively constant along the curves and the values of K_o calculated agreed well with those determined from the pressuremeter.

Determination of K_o from this procedure was carried out at five depth intervals. In each case, the e-log p curve for the horizontally trimmed sample plotted to the right of the curve for the vertically trimmed samples which resulted in values of K_o greater than one. The K_o values determined from one-dimensional consolidation tests are shown on Figure C25.

A third determination of the coefficient of lateral earth pressure at rest was made from the K_o triaxial consolidation tests. This was done by reading the K_o value directly from the K_o versus σ_{vc} relationships presented on Figures C26 thru C29 taking the estimated effective overburden pressure from Figure 6 equal to σ_{vc} for each depth. Values of K_o determined from this procedure were then plotted versus depth on Figure C35 along with those values from one-dimensional consolidation and in situ pressuremeter tests. An average line was drawn through the points, indicated by the solid line. The dashed lines and shaded region represent the range of values calculated.

A K_o profile can also be developed from the average oveconsolidation ratio profile and plasticity information by utilizing the relationship between K_o , plasticity index, and OCR proposed by Brooker and Ireland (C19) shown on Figure 37. Values of K_o determined from this relationship are also plotted versus depth on Figure 38 along with the curve determined from the field and laboratory tests. Very close agreement is demonstrated here.

Consolidation Characteristics

The results of the one dimensional consolidation tests are presented in Addendum B in the form of e-log p curves plotted along with the

coefficient of consolidation, c_v . The square root of time method was used to determine the void ratio from the sample height at the end of primary consolidation (D_{100}) at each load stage.

The general shape of the e -log p curves for both the red and light gray slickensided clays of stratum III and the light gray and tan sandy clays of strata II and IV can be described as very non-linear. The virgin compression portion of the curves is typically parabolic in shape and concave downward. Since the initial recompression portion of the curve is also non-linear, it became very difficult to identify a point of greatest curvature and thus, the determination of the preconsolidation pressure from these curves was difficult.

Other published work on Beaumont and other desiccated clays have described similar difficulty in determining stress history from one dimensional consolidation tests (Al-Layla, C2). However, in general, the soil at the test site can be described as over-consolidated by desiccation with an estimated over-consolidation ratio ranging from approximately 8 to 15 near the surface and decreasing to about 2 to 4 at 46 feet.

Dynamic Properties

Dynamic soil properties were determined from the results of the cross-hole seismic wave velocity tests and are presented on Table C7. Values of dynamic shear and compression modulus and poissons ratio were developed from the shear and compression wave velocity profiles shown on Figure C39.

Using theory of elasticity and wave propagation, the values of shear (G) and compression (E) modulus given in the table were determined

from the shear wave velocity measurements follows:

$$G = \frac{\gamma}{g} v_s^2$$
$$E = 2G (1 + \nu)$$

where: γ = unit weight

g = acceleration of gravity

ν = Poisson's ratio

V_s = shear wave velocity

Elastic constants are dependent upon the level of strain such that, as the strain level decreases, the value of G and E increases to some maximum value at very low strain. The values determined from the above equation, therefore, can be considered as upper bound values since the strain level in a cross-hole seismic test, using a mechanical source, is generally less than 10^{-3} percent.

Stress-Strain Properties

The stress-strain relationship for each laboratory strength test was plotted and presented in Addendum B from which the laboratory values of the elastic constants can be determined. It is believed, however, that the stress-strain characteristics of the soil encountered at this site are sensitive to sample disturbance caused by stress relief, and therefore, more emphasis is placed here on the determination of the elastic modulus from in situ test results.

The self-boring pressuremeter provides an ideal tool for establishing the in situ stress-strain relationship. The modulus of elasticity, E , was determined from the pressuremeter test by finding the initial slope, $\Delta p / \Delta \epsilon$, of the expansion curve in the range between the

horizontal earth pressure, P_p , and the point on the expansion curve, $(P_o + s_u)$, where plastic behavior begins. Assuming a value of Poisson's ratio of 0.5 for a saturated clay, the value of E was calculated from the following equation (Baguelin et al, C4):

$$E = 2 (1 + \nu) [0.5 (\Delta p / \Delta \epsilon)]$$

where: $\Delta \epsilon$ = change in radial strain over
the given pressure range

p = change in pressure

ν = Poisson's ratio

The values of E determined from the pressuremeter are given on Table C6 and plotted versus depth on Figure C28.

On Figure C29, the elastic moduli determined from the cross-hole seismic test are plotted on the same graph with pressuremeter values for comparison. From this figure it can be seen that the value of E from in situ seismic tests is about four times the value from the pressuremeter.

Residual And Remolded Strength

The effective stress strength parameters were determined for remolded specimens from strata III and IV by a consolidated undrained triaxial compression test as outlined earlier. The p' - q curves and total and effective stress Mohr's diagrams for these tests are included in Addendum B along with the respective stress-strain curves. The parameters determined from these curves are given on Table C5.

The results of the anisotropically consolidated undrained triaxial tests on remolded specimens is summarized in Table 2. At the 16 to 18 foot depth interval a K_o stress condition of 1.0 was imposed on the test

specimen. Since this is an isotropic condition no significant difference was noticed in the results from the other remolded tests in the red clay. At the 34 to 36 foot depth, the samples were consolidated with a σ_3/σ_1 ratio of 0.8. A noticeable increase in the friction angle was noticed when comparing to similar material at the 30 to 32 foot depth interval tested under isotropic conditions. However, part of this increase may have been due to a higher sand content at the 34 to 36 foot depth intervals. Stress-strain curves at Mohr's diagrams for these remolded tests are given in Addendum B. The results of two of the remolded tests seemed unreasonable (shown as dashed line) and were not considered in drawing strength envelopes.

The residual effective strength envelope was also determined from multi-specimen, consolidated-drained direct shear tests on soils in strata III and IV. It is important to note that the failure envelope from these tests (given in Addendum B) represents the peak effective shear stress along a pre-failed surface which had been permitted to reconsolidate. Actual residual strengths associated with repeated failure resulting in a minimum residual strength would be expected to yield a lower value than reported here. The effective strength parameters determined from these tests are given on Table C5.

REFERENCES

- C1 Abdelhamid, M. S., and Krizek, R. J., July 1976, "At-Rest Lateral Earth Pressure of a Consolidating Clay", Journal of the Geotechnical Engineering Division, ASCE, VOL.102, No. GT7, pp. 721-739.
- C2 Al-Layla, M. T., 1970, "Study of Certain Geotechnical Properties of Beaumont Clay", Ph. D. Thesis, Texas A & M University.
- C3 American Society for Testing and Materials, 1979 Annual Book of ASTM Standards.
- C4 Baguelin, F., Jezequel, J. F., and Shields, D. H., 1978, The Pressuremeter and Foundation Engineering, Trans Tech Publications, Clausthal, Germany.
- C5 Bernard, H. A., LeBlanc, R. J., and Major, C. F., 1962 "Recent and Pleistocene Geology of Southeast Texas" Geology of the Gulf Coast and Central Texas and Guide Book of Excursions, Houston Geologic Society pp. 175-224.
- C6 Bishop, A. W., and Henkel, D. J., 1957, The Measurement of Soil Properties in the Triaxial Test, Edward Arnold (Publishers) Ltd., London.
- C7 Ladd, C. C., and Foott, R., July, 1974 "New Design Procedure for Stability of Soft Clays" Journal of the Geotechnical Engineering Division, ASCE, Vol. 100, No. GT7, pp. 763-787.
- C8 Lambe, W. T., and Whitman, R. V., 1969, Soil Mechanics, John Wiley and Sons, Inc., New York.
- C9 Marsland A., and Randolph, M. F., 1978, "Comparisons of the Results from Pressuremeter Tests and Large In Situ Plate Tests in London Clay", Geotechnique, Vol. 27, No. 2, pp. 217-243.
- C10 Nottingham, L. C., and Schmertmann, J. H., Sept. 1975, "An Investigation of Pile Capacity Design Procedures", Final Report, D629 to Florida Dept. of Transportation from Dept. of Civil Engineering, University of Florida.
- C11 O'Neill, M. W., December, 1970, "Behavior of Axially Loaded Drilled Shafts in Beaumont Clay" Ph. D. Thesis, The University of Texas at Austin.
- C12 Schmertmann, J. H. February, 1978, "Guidelines for Cone Penetration Test, Performance and Design" Report FHWA-TS-78-209 Federal Highway Administration.
- C13 Sellards, E. H., Adkins, W. S. and Plummer, R. B., 1954, "The Geology of Texas" The University of Texas Bulletin No. 3232, Austin.

- C14 Skempton, A. W., and Northey, R. P., March, 1952, "The Sensitivity of Clays", Geotechnique No. 1 pp. 30-53.
- C15 Steussy, D. K. and Reese, L. C., May, 1979, "Interim Report on Use of the Self-Boring Pressuremeter" A report to Fugro, Inc. by The University of Texas.
- C16 Stokoe, K. H. II and Woods, R. P., May, 1972, "In Situ Shear Wave Velocity by Cross-Hole Method" Journal of the Soil Mechanics and Foundations Division, ASCE, Vol. 98, No. SMS, pp. 443-460.
- C17 Van Siclen, D. C., 1961, "Surface Geology in and Near Houston", Geology of Houston and Vicinity, Texas, Houston Geological Society, Houston, Texas.
- C18 Wroth, C.P. and Hughes, J.M., August, 1974, "Development of a Special Instrument for the In Situ Measurement of the Strength and Stiffness of Soils", Proceedings of the Conference on Subsurface Exploration for Underground Excavation and Heavy Construction, New Hampshire.
- C19 Brooker, E.W., and Ireland, H.O., February 1965, "Earth Pressures at Rest Related to Stress History", Canadian Geotechnical Journal, Vol. II, page 1-15.

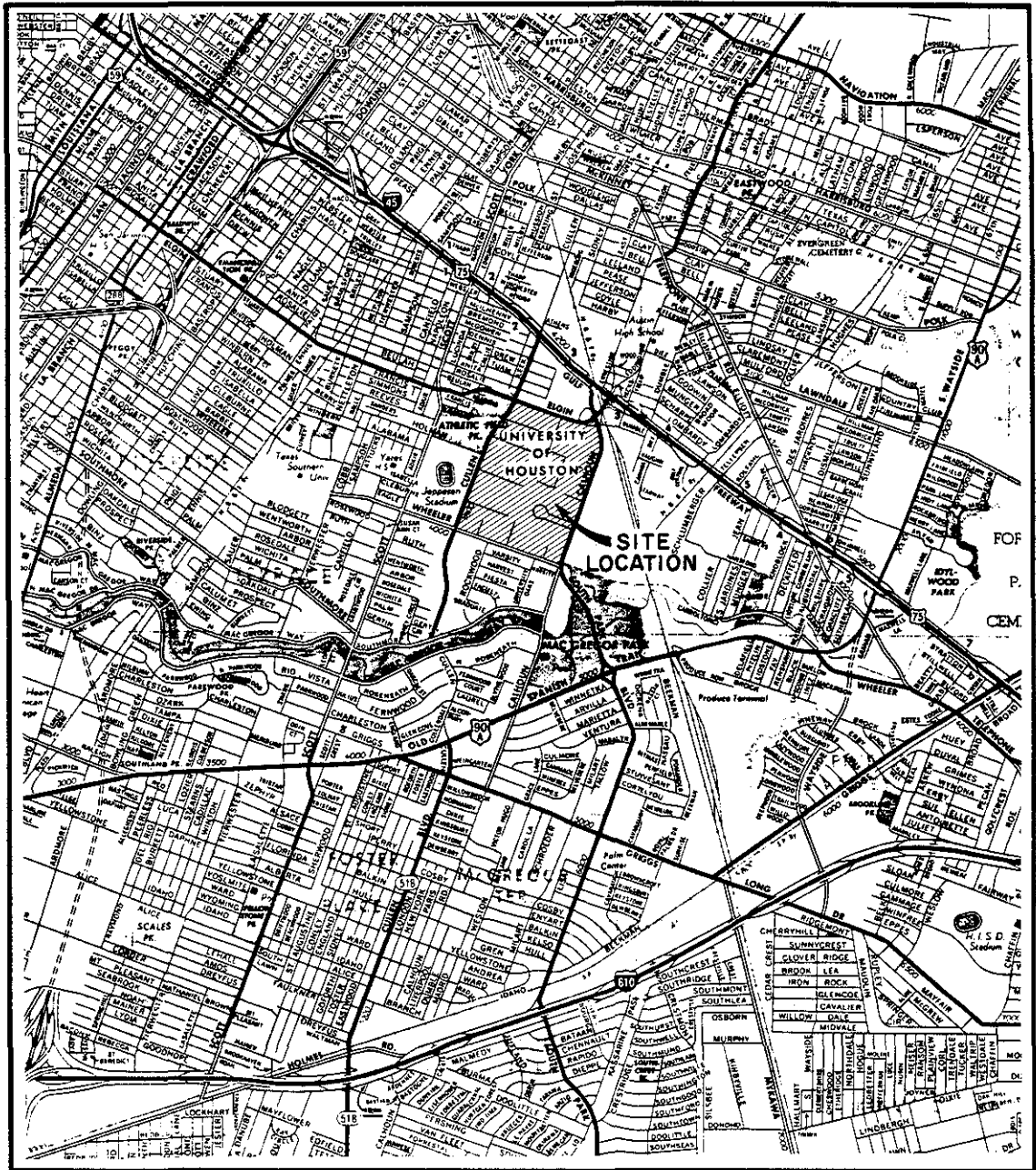


FIGURE C1. SITE LOCATION MAP

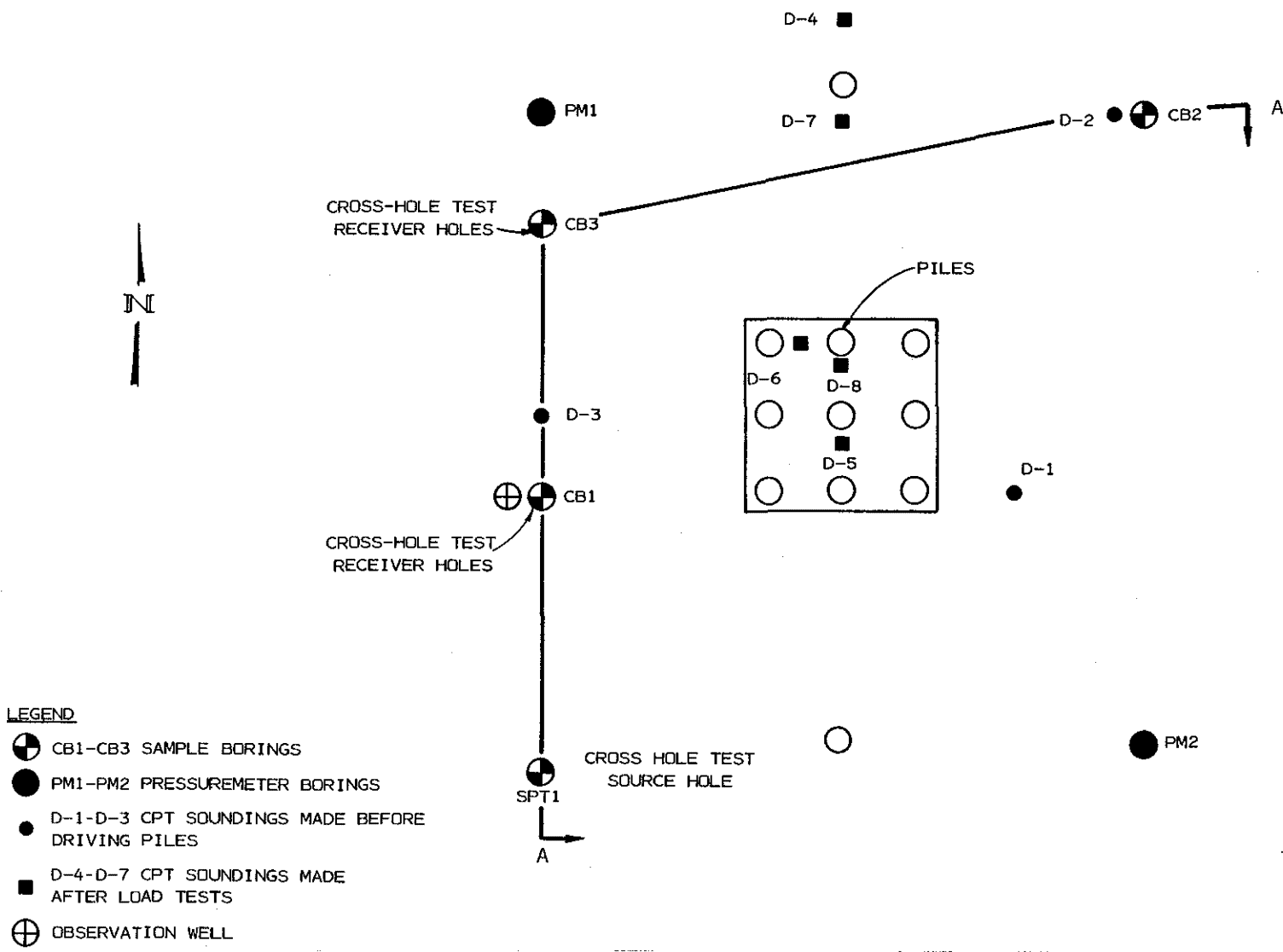
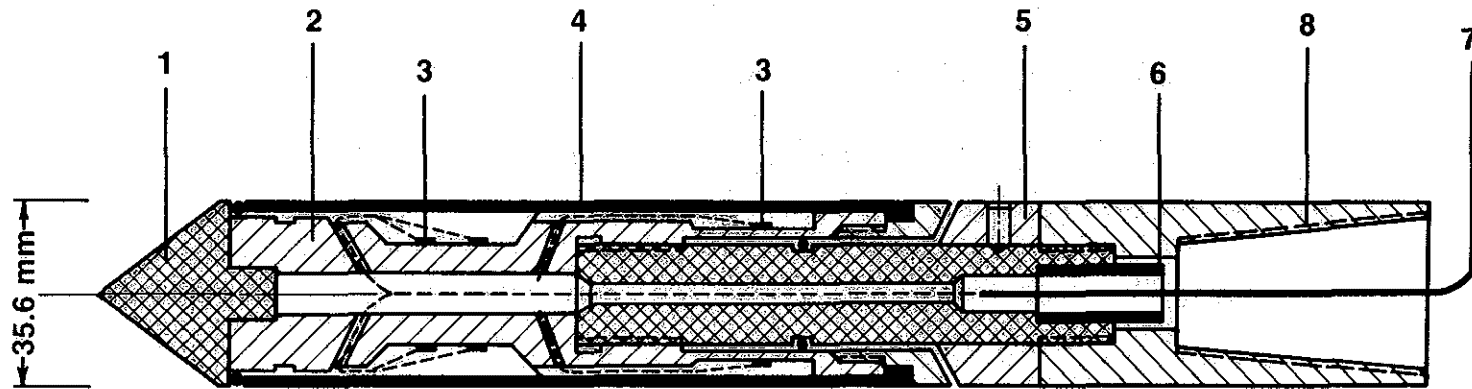


FIGURE C2. SITE INVESTIGATION GENERAL LOCATION PLAN



- | | |
|---------------------------------------|-------------------------|
| 1. Conical Point (10cm ²) | 5. Adjustment Ring |
| 2. Load Cell | 6. Waterproof Bushings |
| 3. Strain Gauges | 7. Cable |
| 4. Friction Sleeve | 8. Connection with Rods |

FIGURE C3. CROSS-SECTION OF FRICTION CONE PENETROMETER

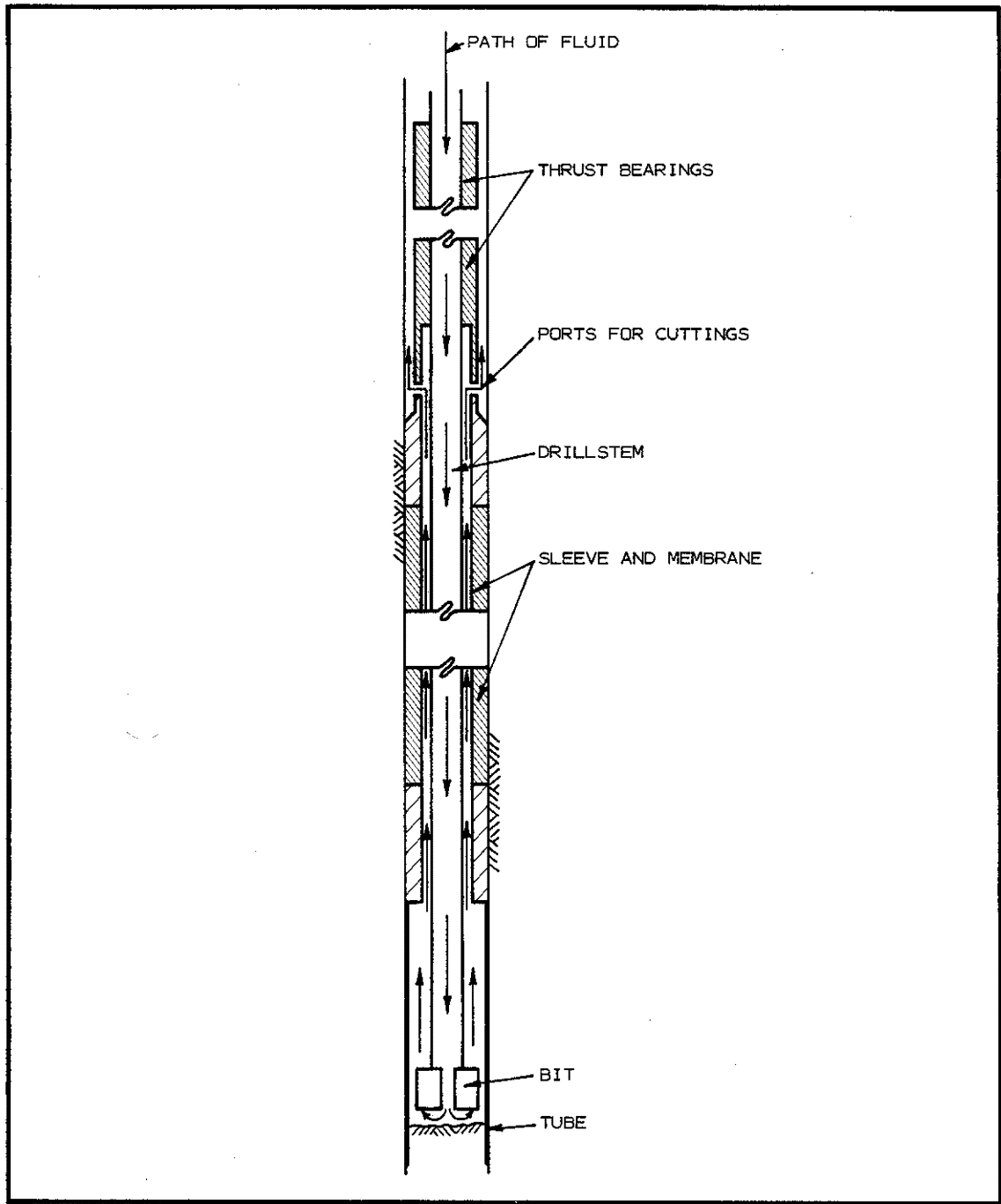


FIGURE C4. THE SELF-BORING PRESSUREMETER

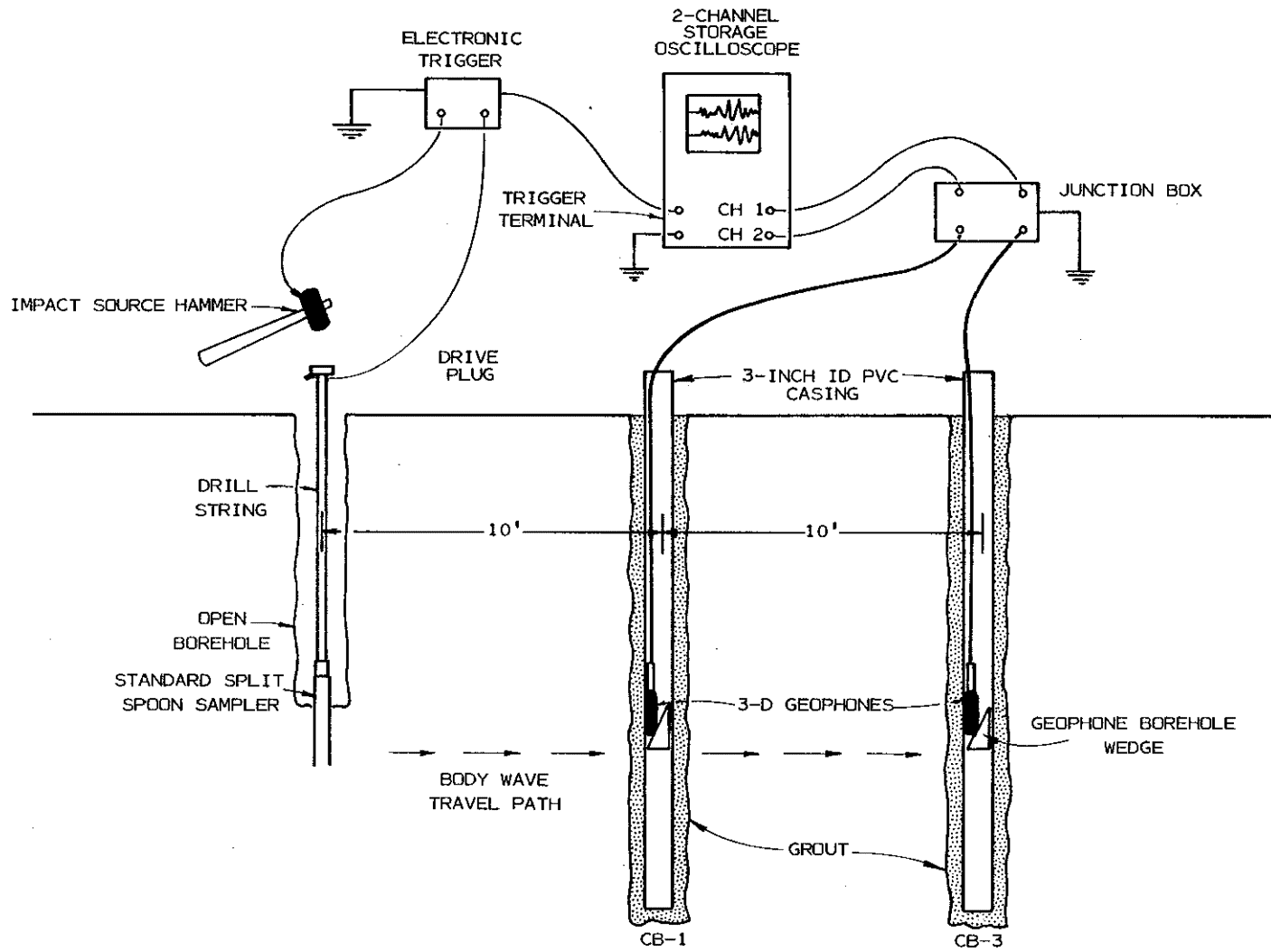


FIGURE C5. CROSS-HOLE SEISMIC WAVE VELOCITY TEST SET-UP

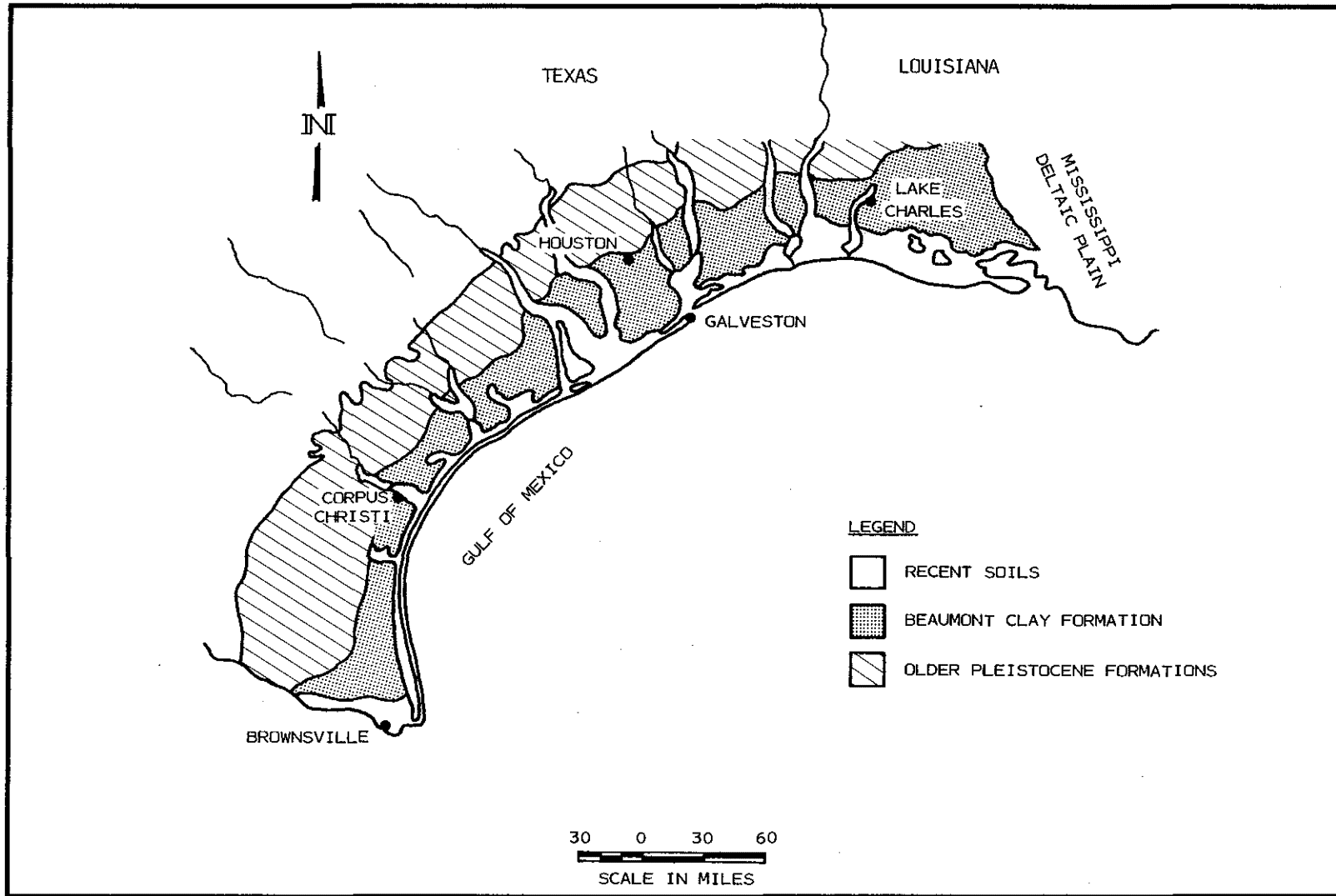


FIGURE C7. GEOGRAPHIC DISTRIBUTION OF BEAUMONT CLAY

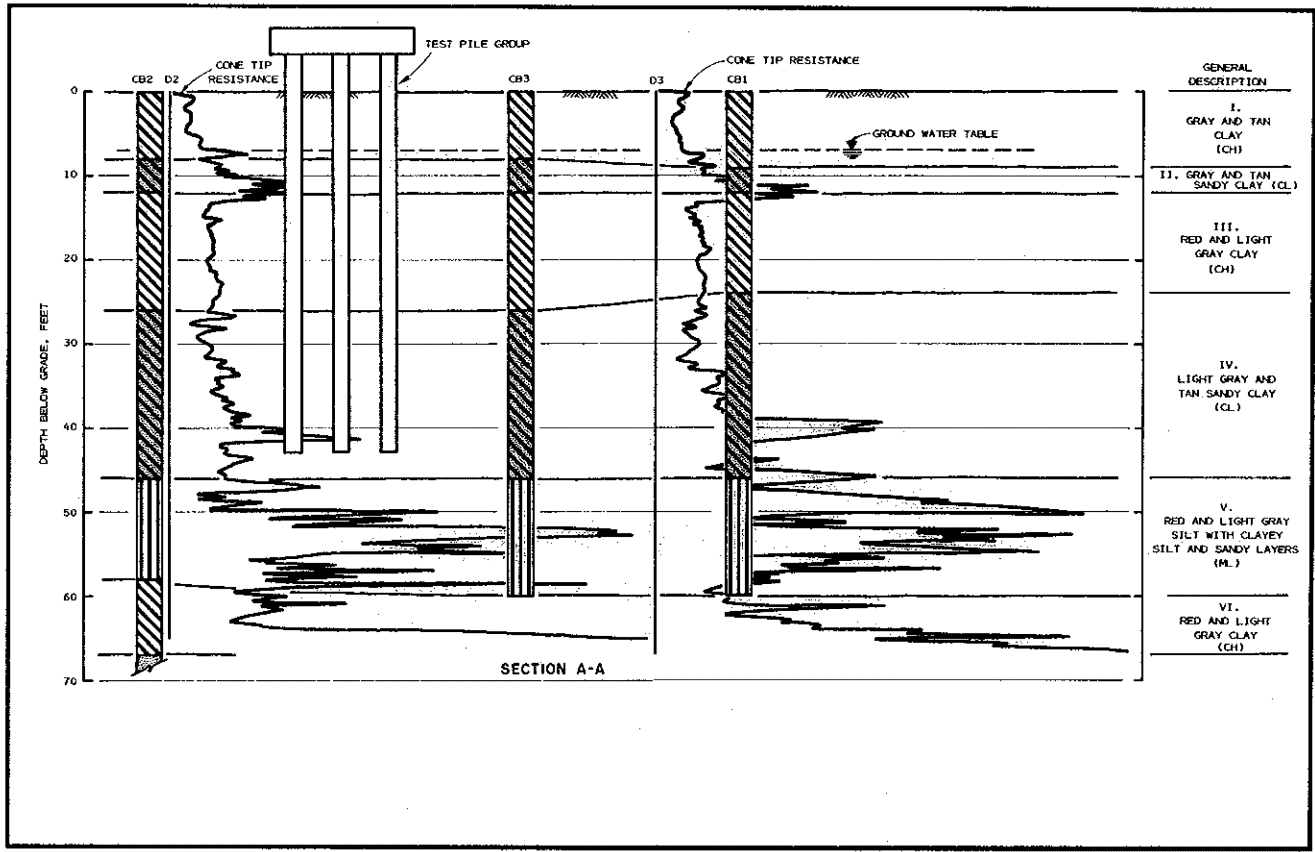


FIGURE C8. GENERALIZED SOIL PROFILE

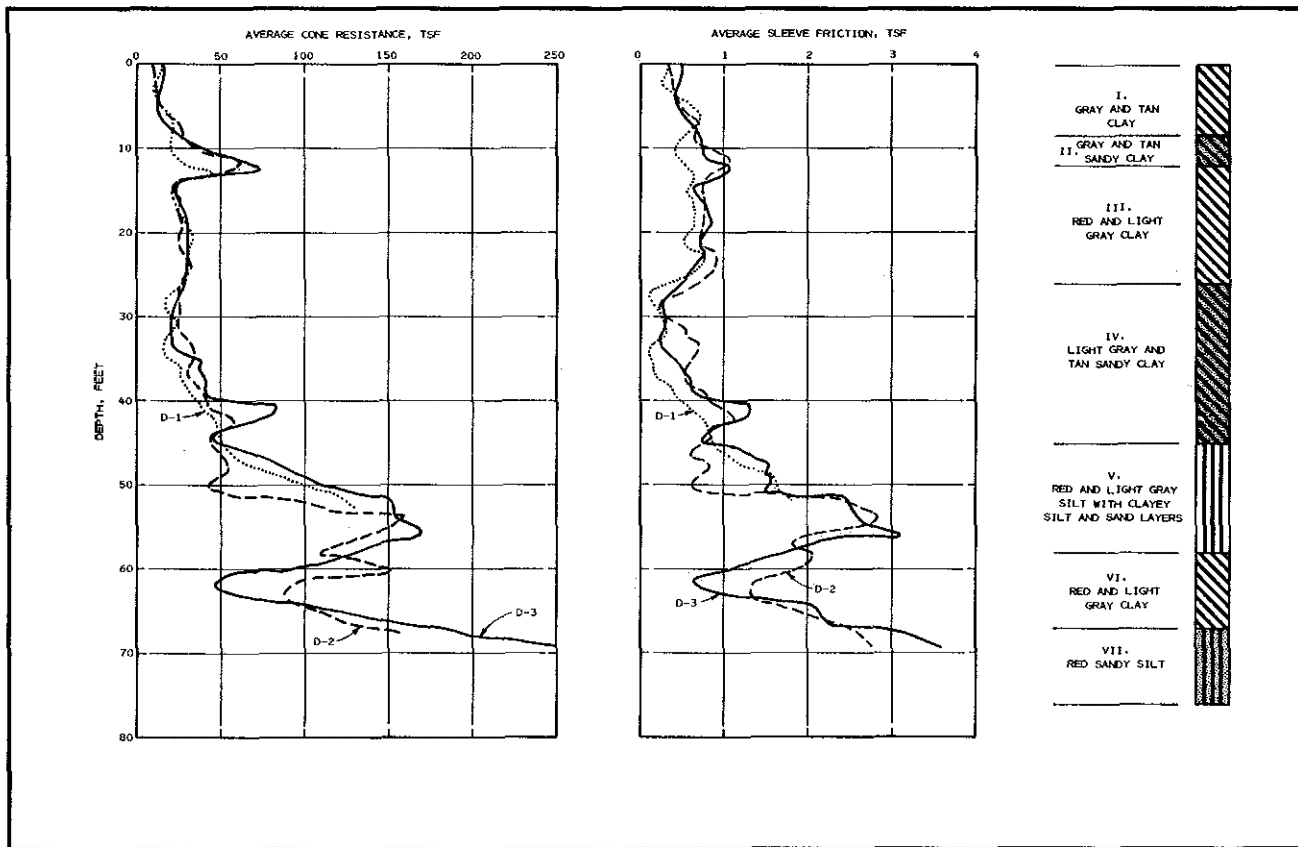


FIGURE C9. CORRELATION BETWEEN CONE SOUNDINGS AND BORING LOGS

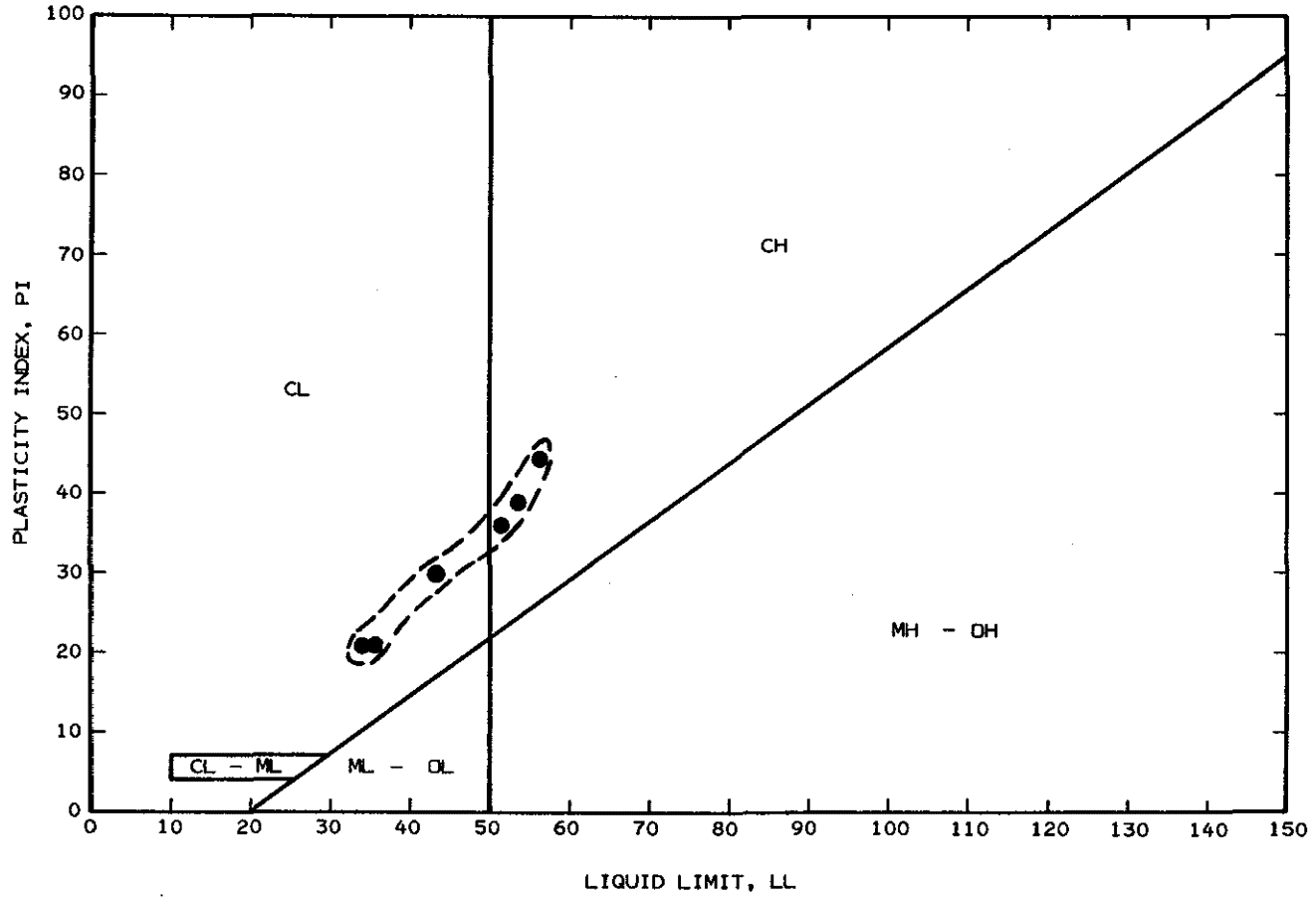


FIGURE C10. PLASTICITY CHART FOR STRATA I AND II

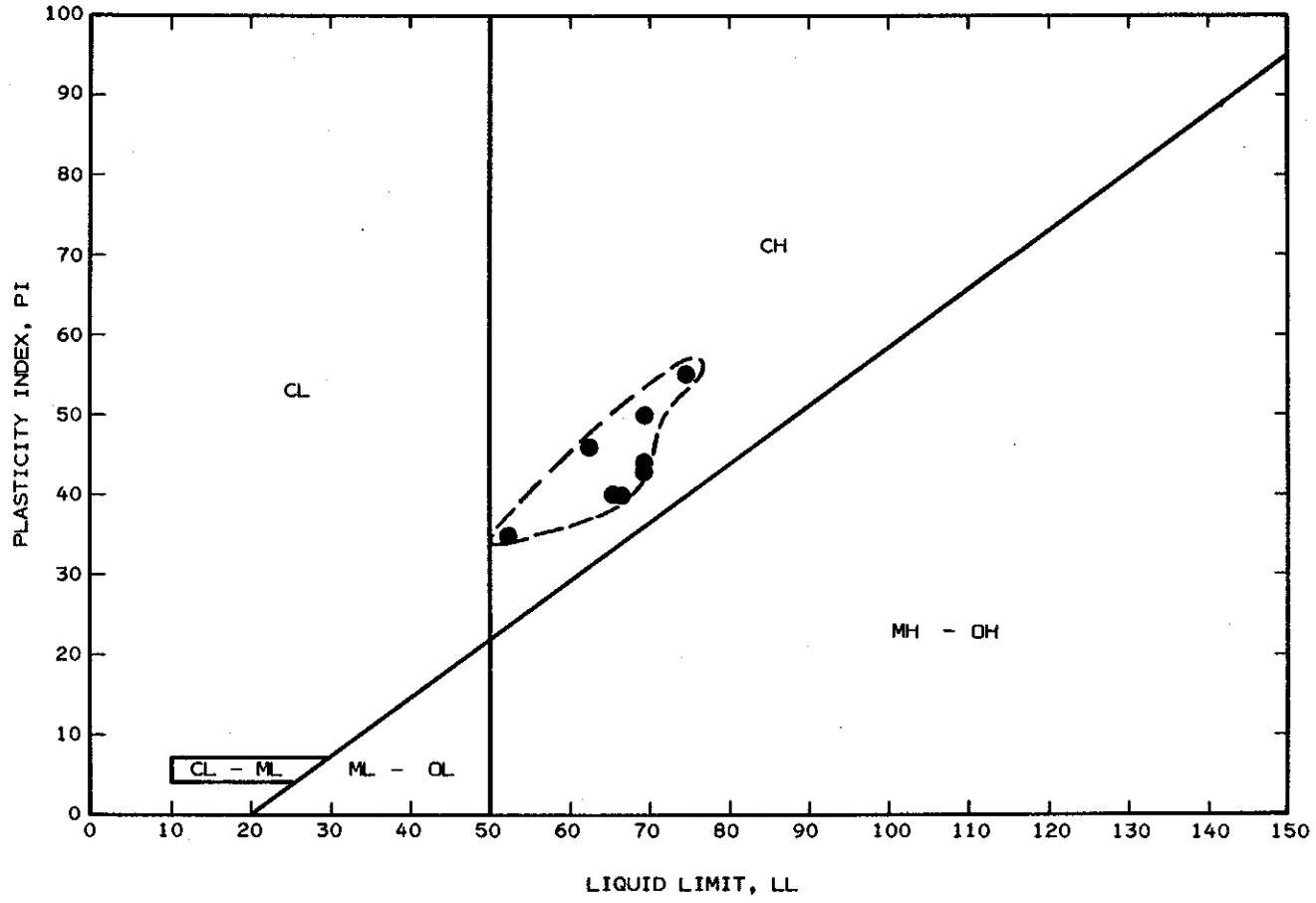


FIGURE C11. PLASTICITY CHART FOR STRATUM III

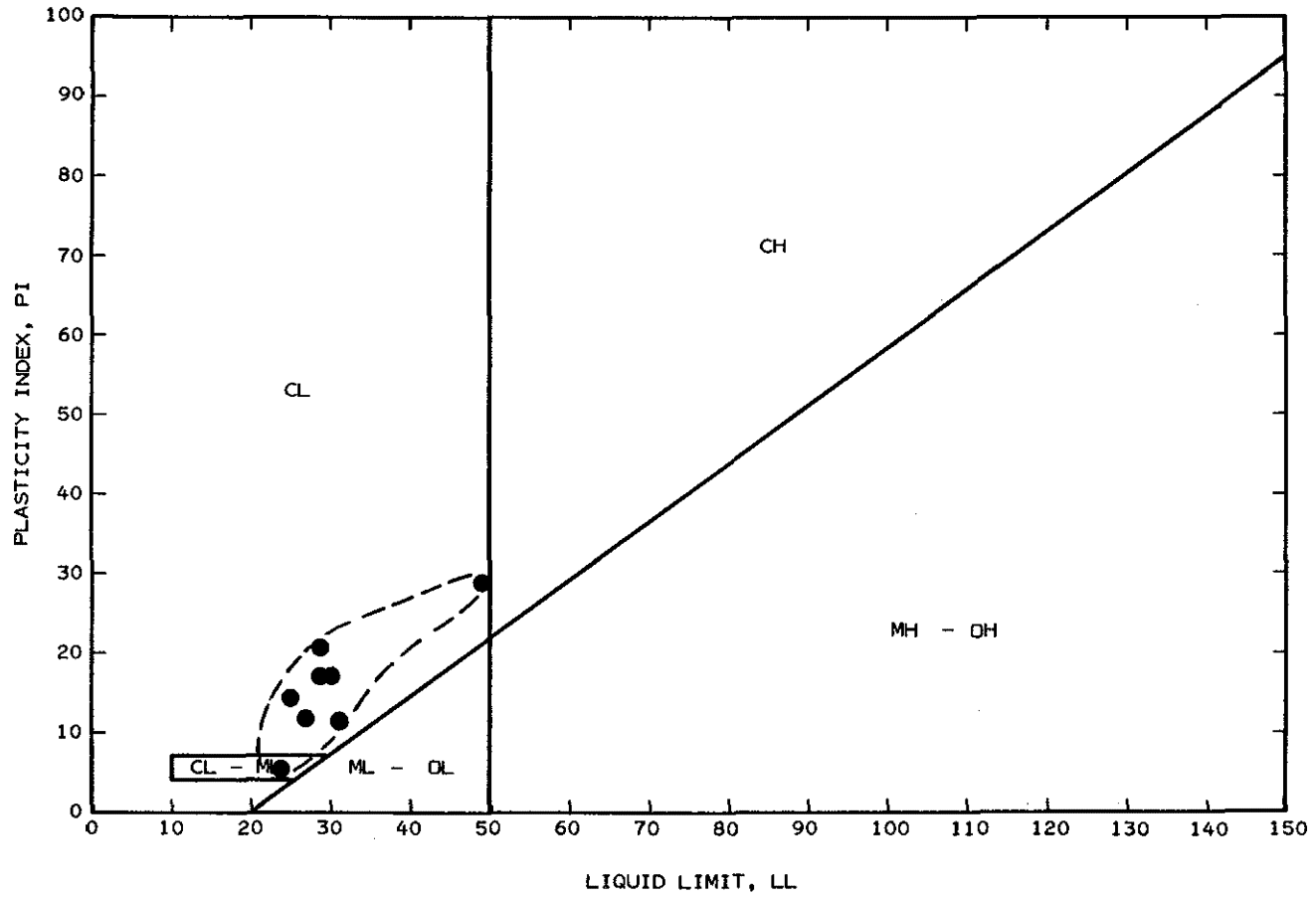


FIGURE C12. PLASTICITY CHART FOR STRATUM IV

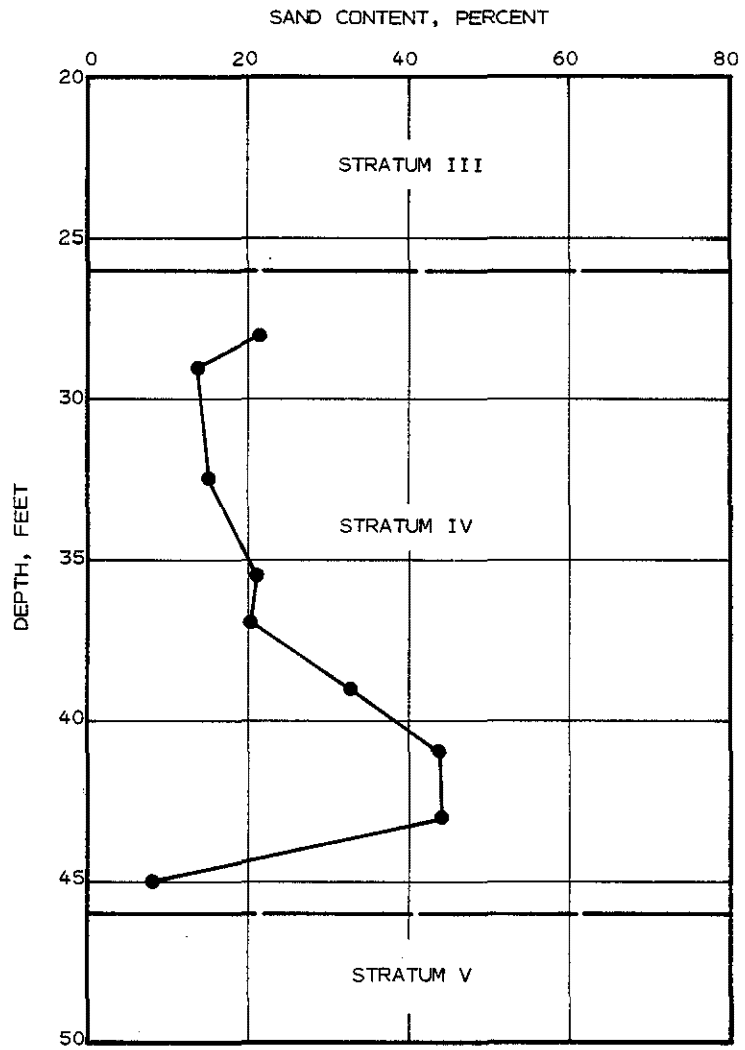


FIGURE C13. VARIATION OF SAND CONTENT IN STRATUM IV

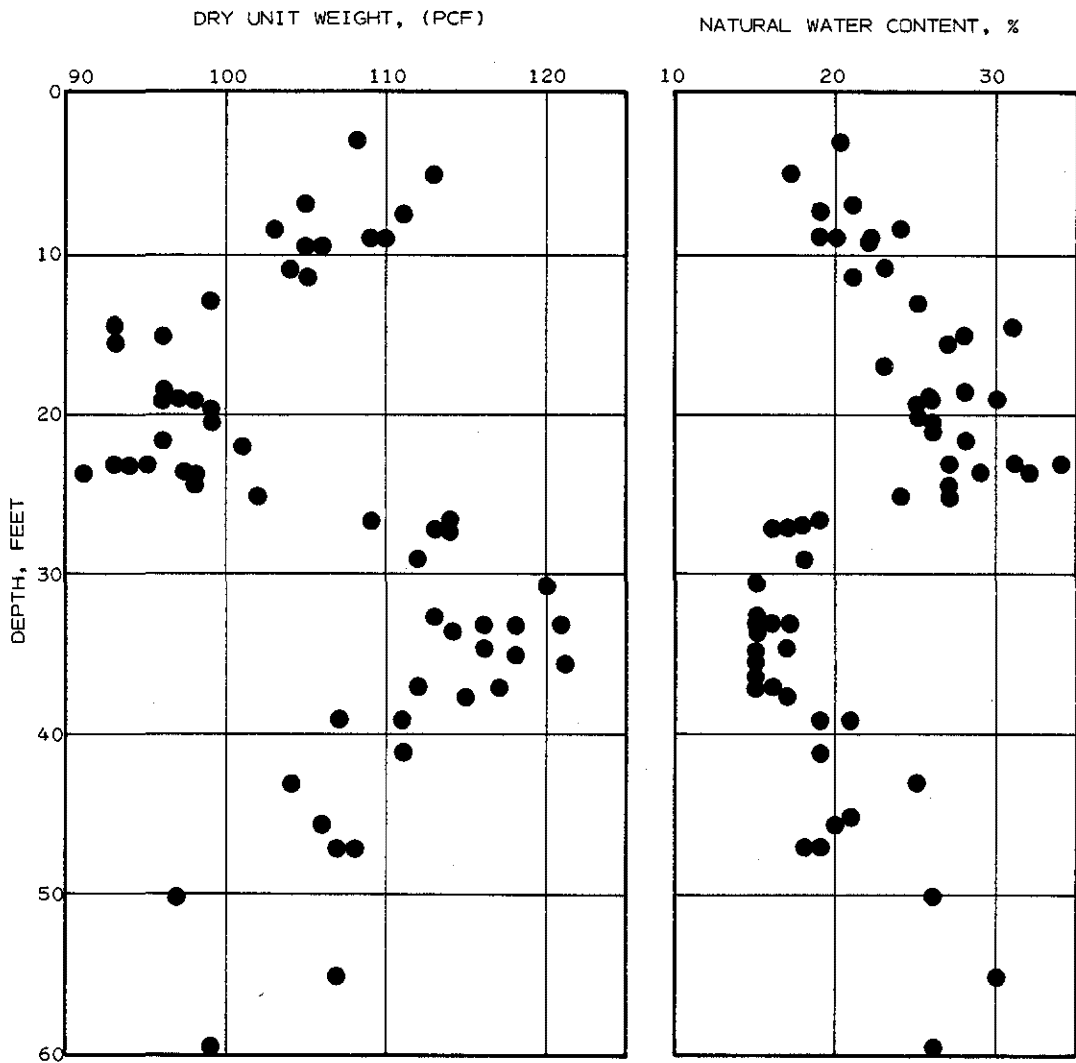


FIGURE C14. DRY UNIT WEIGHT AND NATURAL WATER CONTENT VARIATION WITH DEPTH

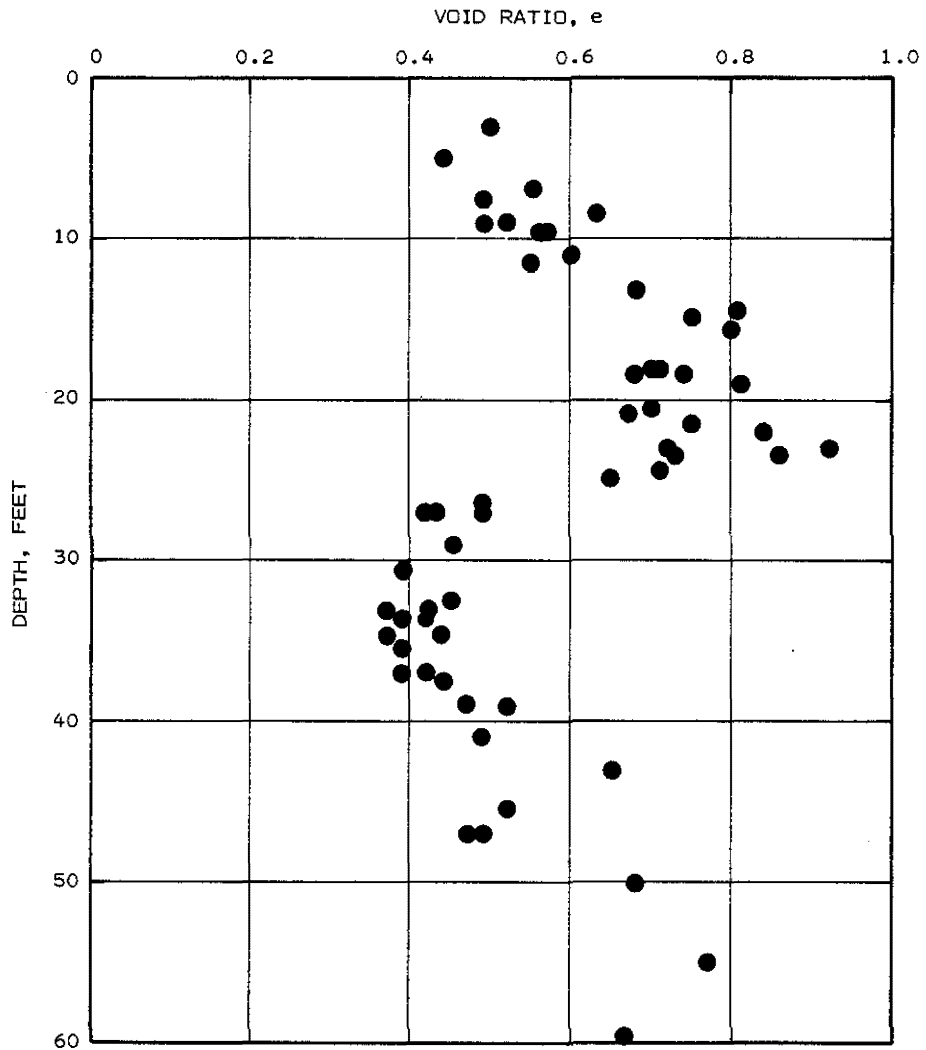


FIGURE C15. VOID RATIO VARIATION WITH DEPTH

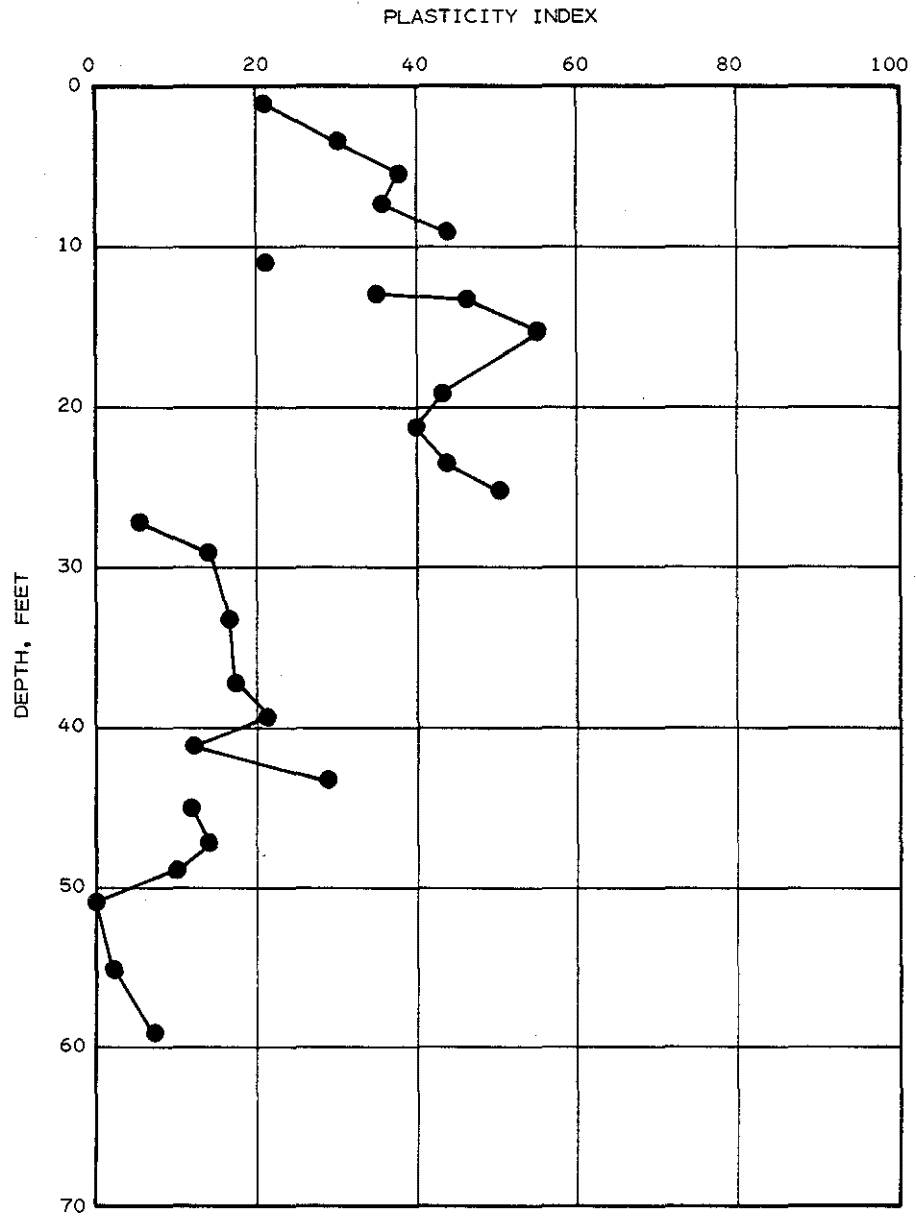


FIGURE C16. PLASTICITY INDEX VARIATION WITH DEPTH

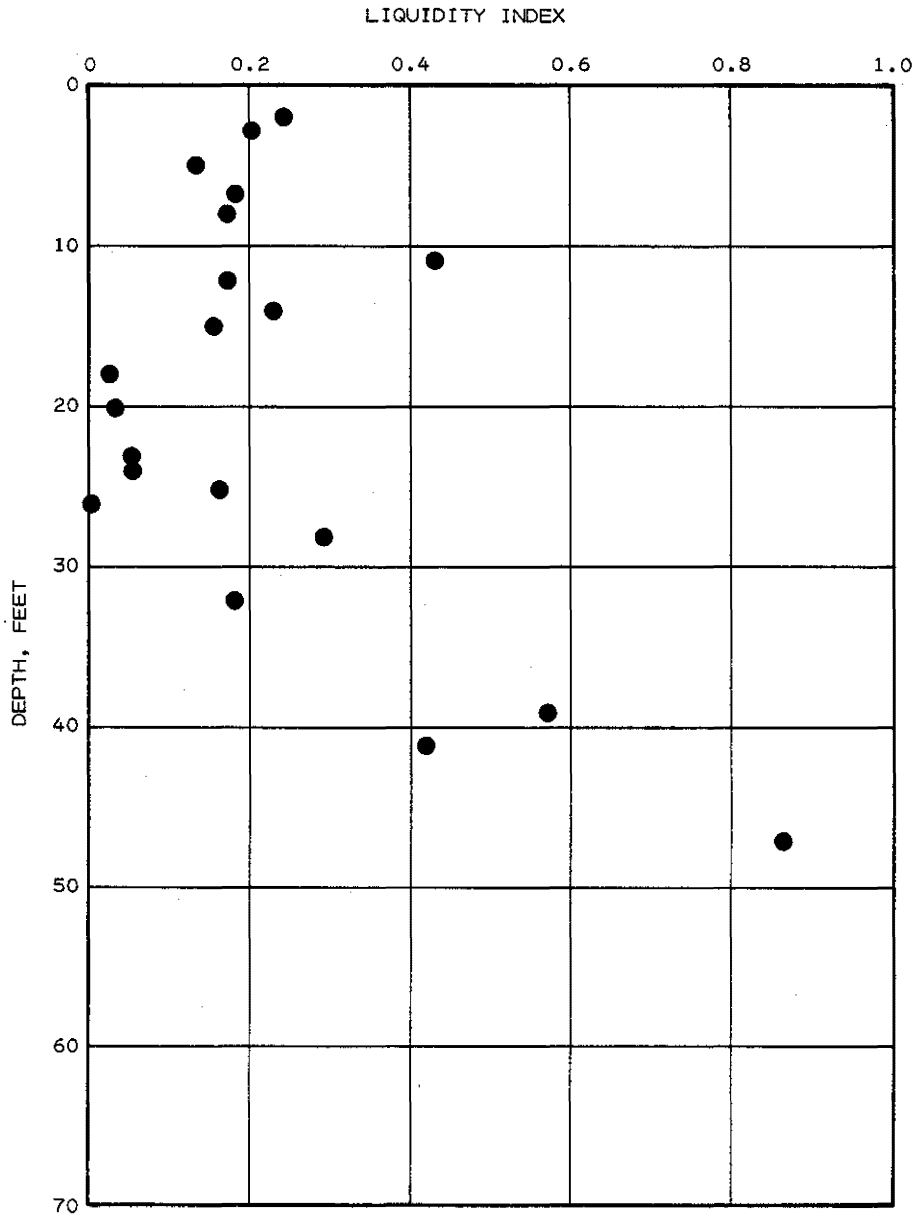


FIGURE C17. LIQUIDITY INDEX VARIATION WITH DEPTH

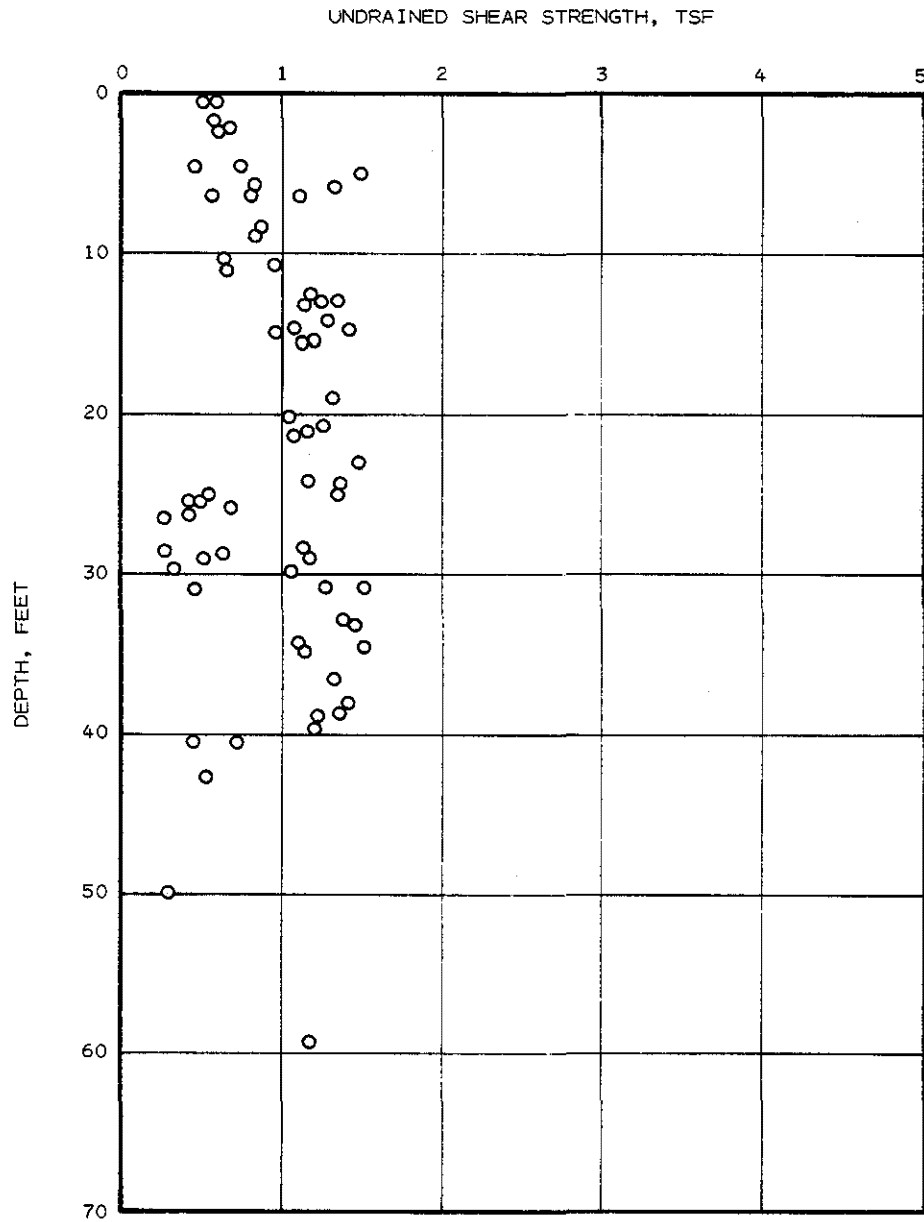


FIGURE C18. UNDRAINED SHEAR STRENGTH FROM TORVANE VALUES

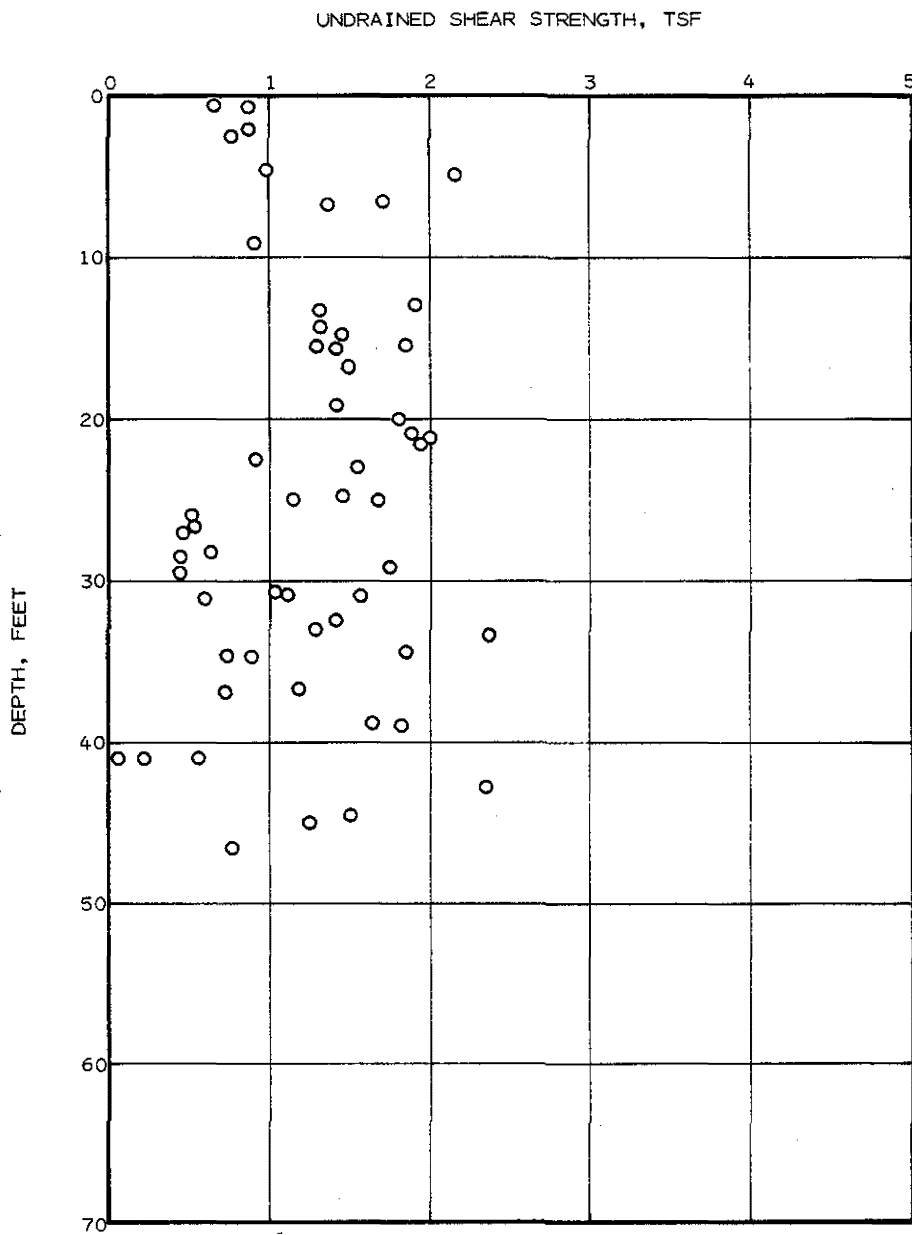


FIGURE C19. UNDRAINED SHEAR STRENGTH TORVANE VALUES

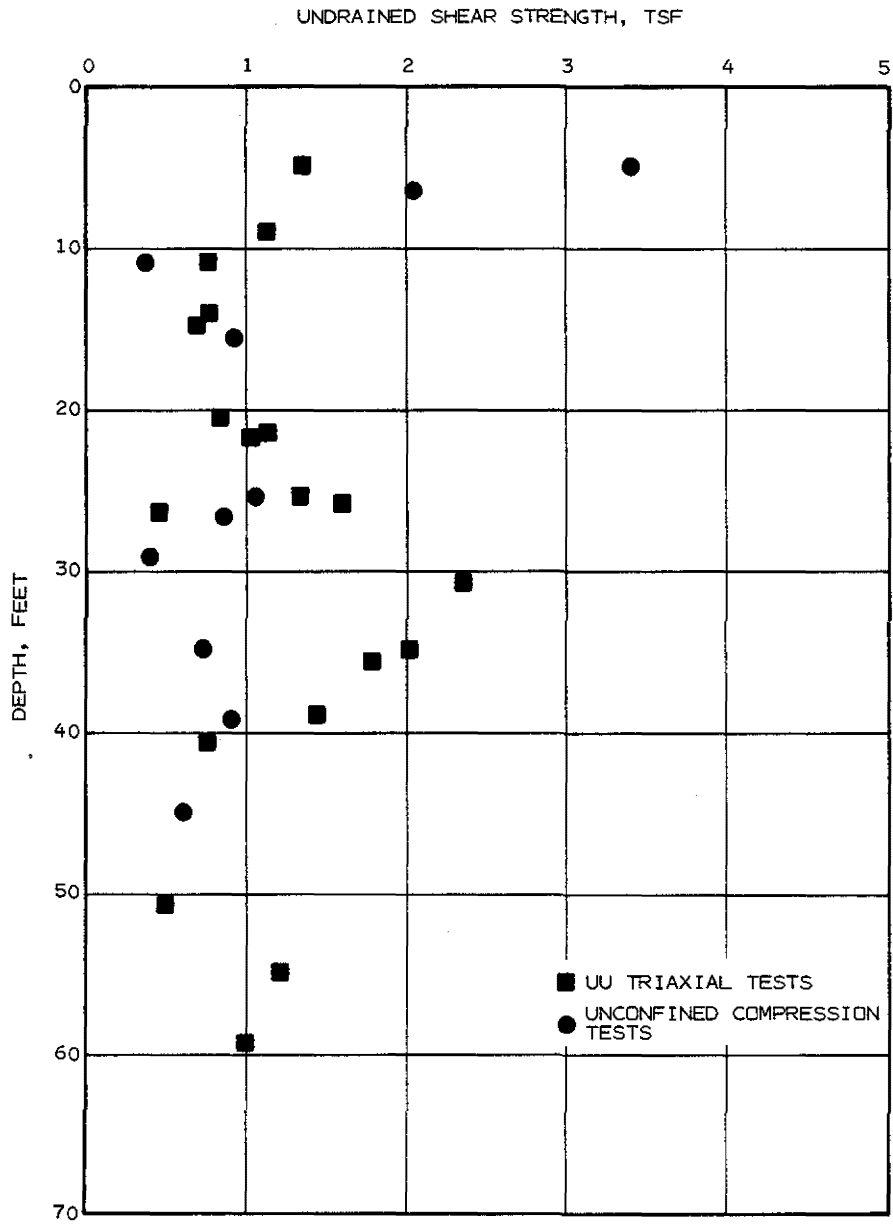


FIGURE C20. LABORATORY UNDRAINED SHEAR STRENGTH RESULTS

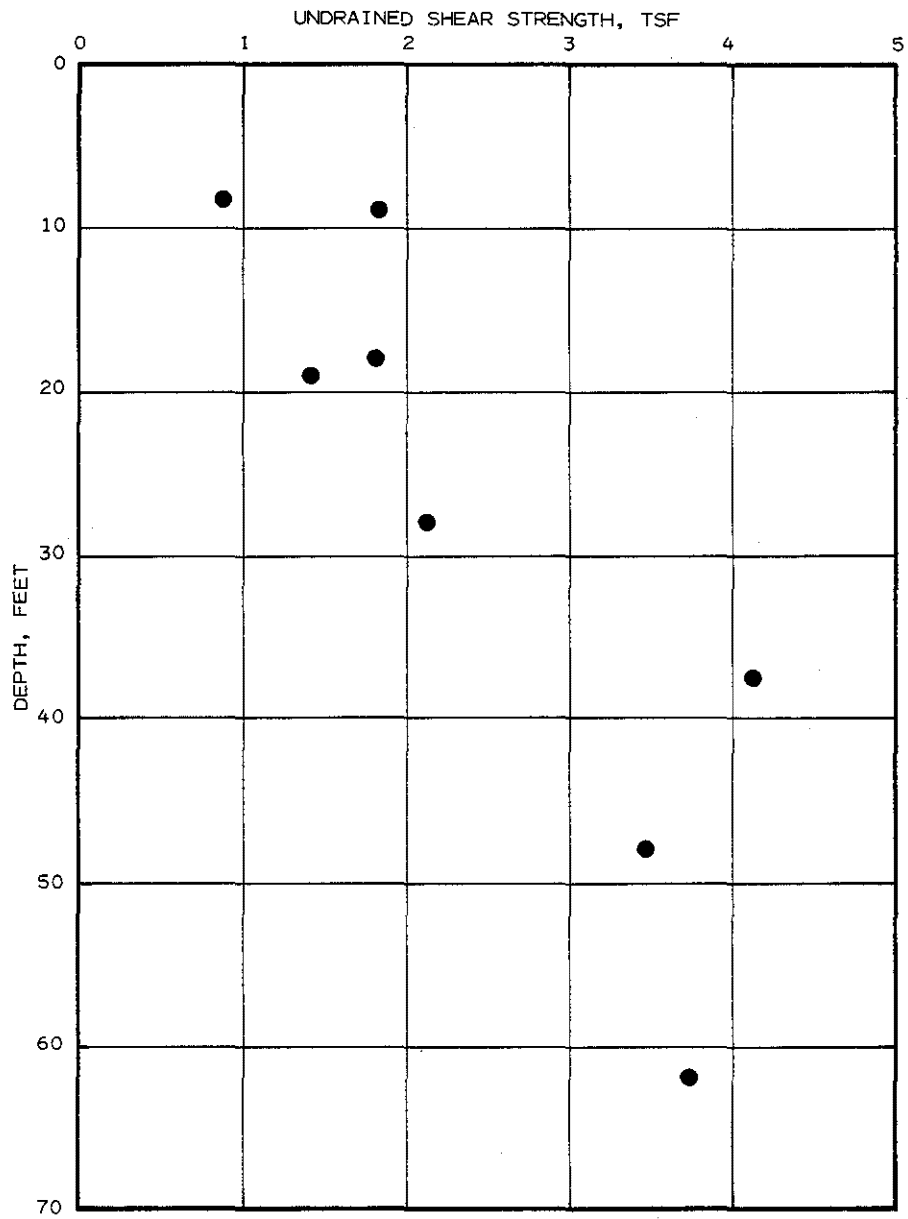


FIGURE C21. UNDRAINED SHEAR STRENGTH PROFILE FROM SELF-BORING PRESSUREMETER TEST

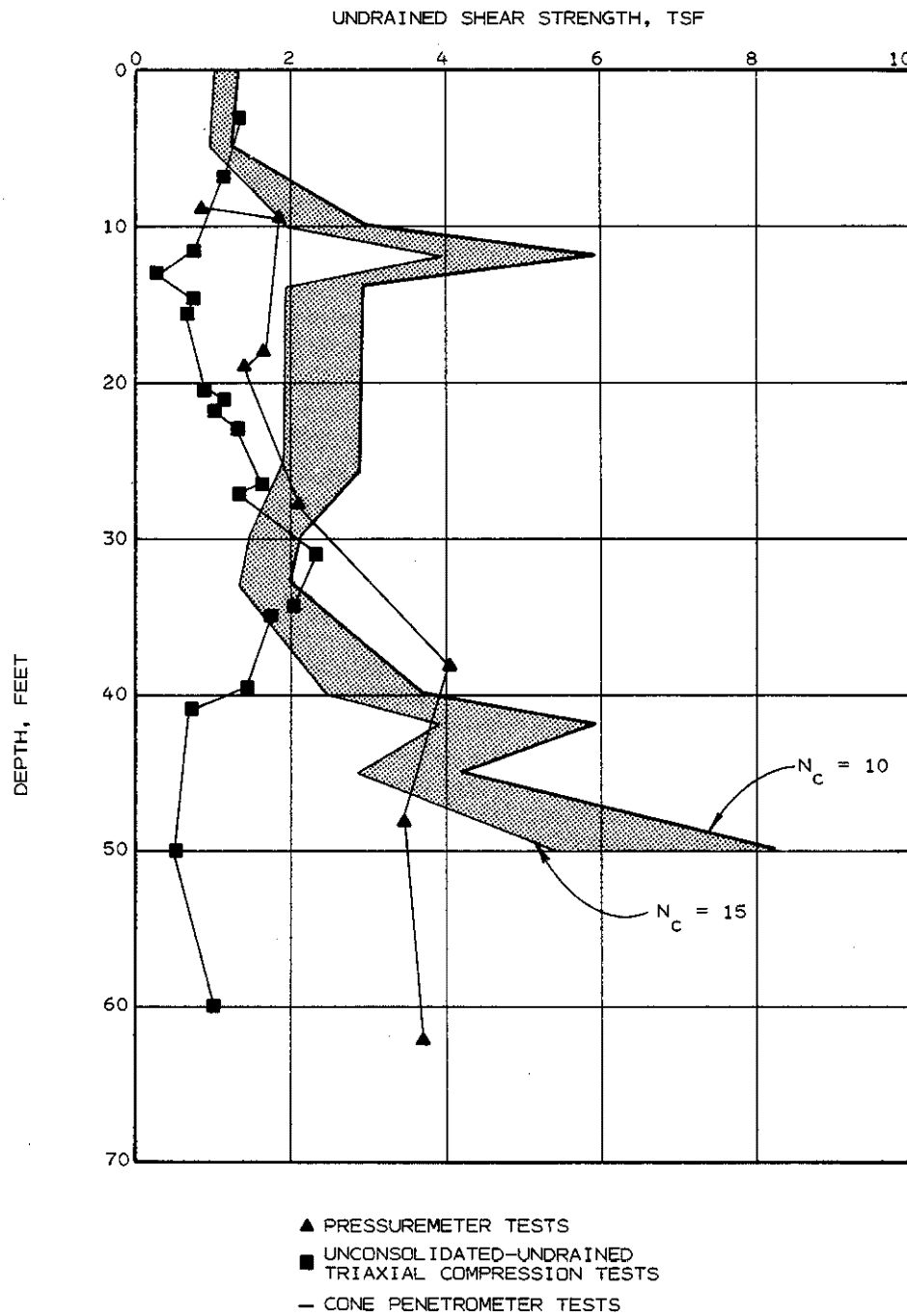


FIGURE C22. UNDRAINED SHEAR STRENGTH FROM IN SITU AND
UU TRIAXIAL TESTS

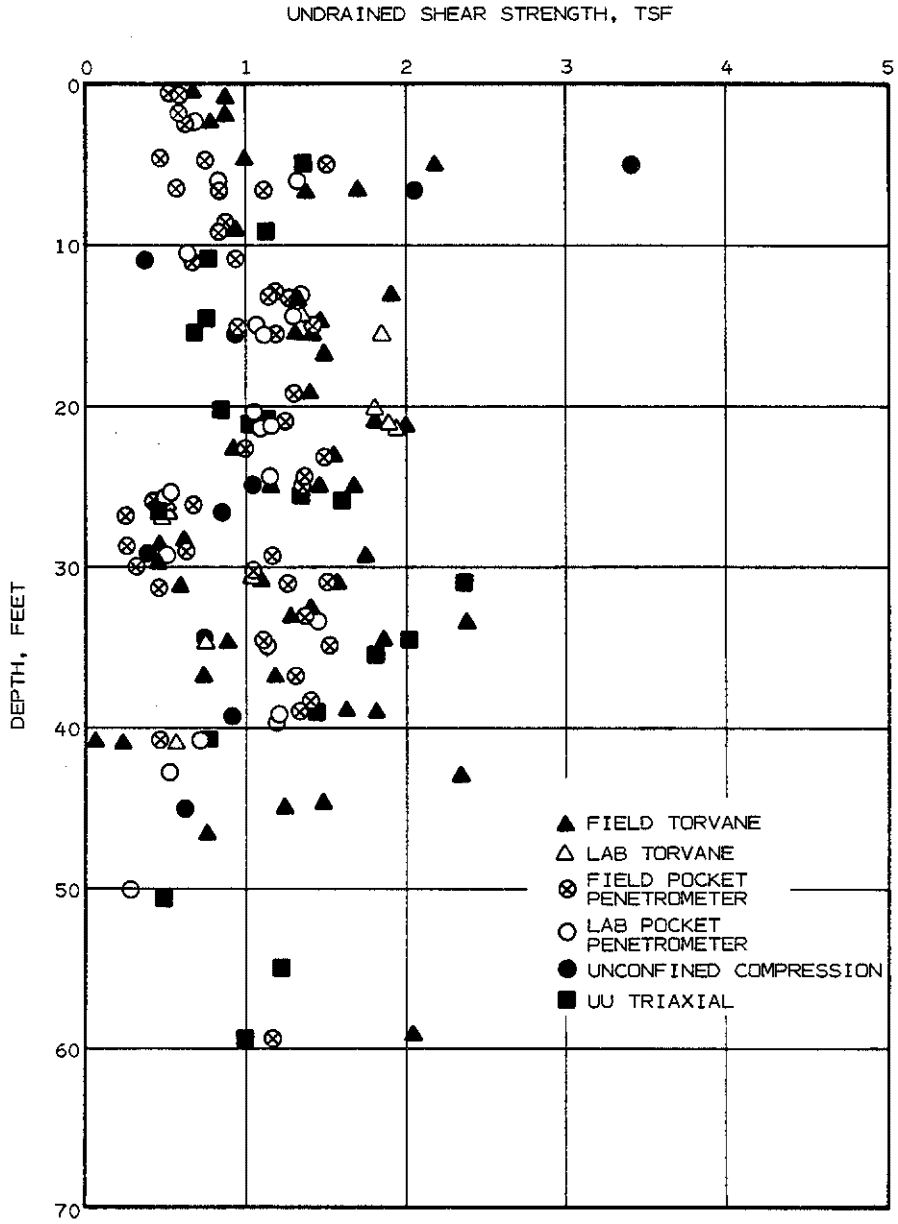


FIGURE C23. COMPOSITE UNDRAINED SHEAR STRENGTH TEST RESULTS

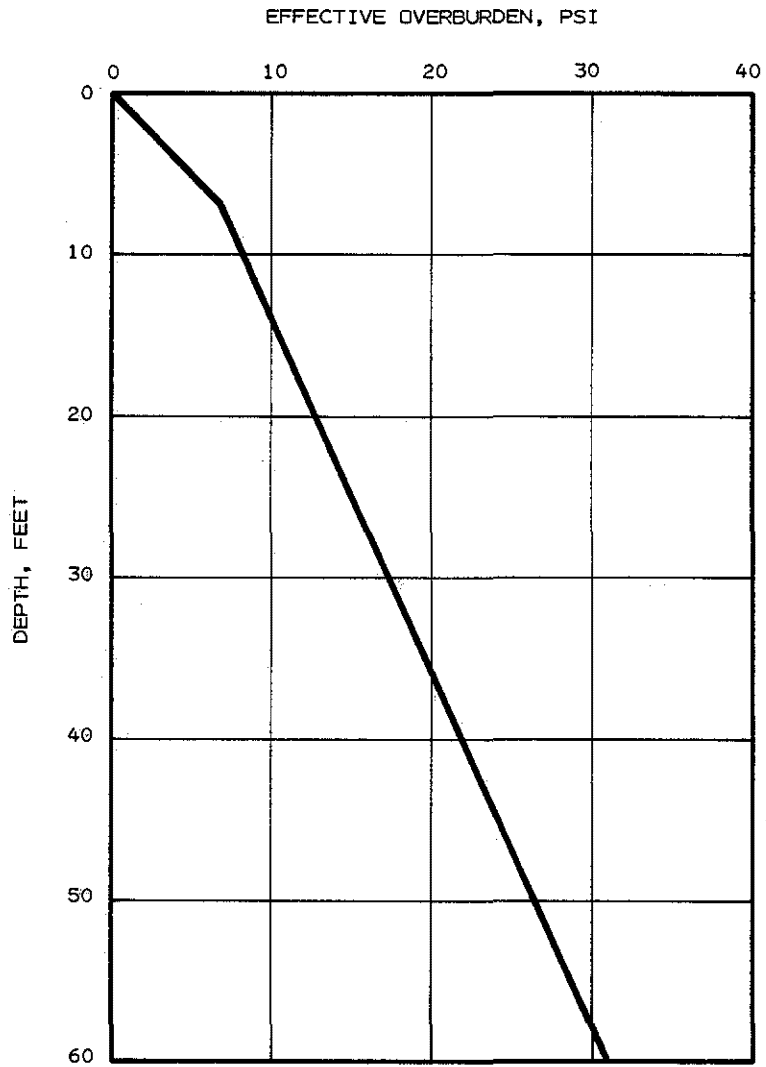


FIGURE C24. VERTICAL EFFECTIVE OVERBURDEN PRESSURE PROFILE

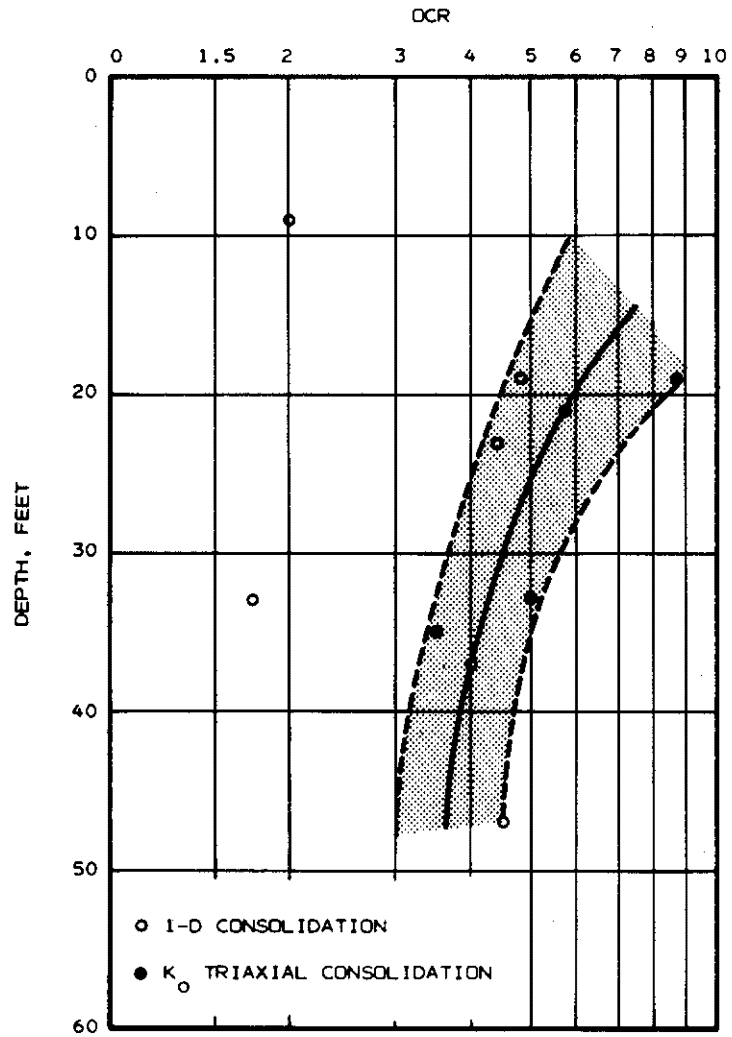


FIGURE C25. OVERCONSOLIDATION RATIO VERSUS DEPTH

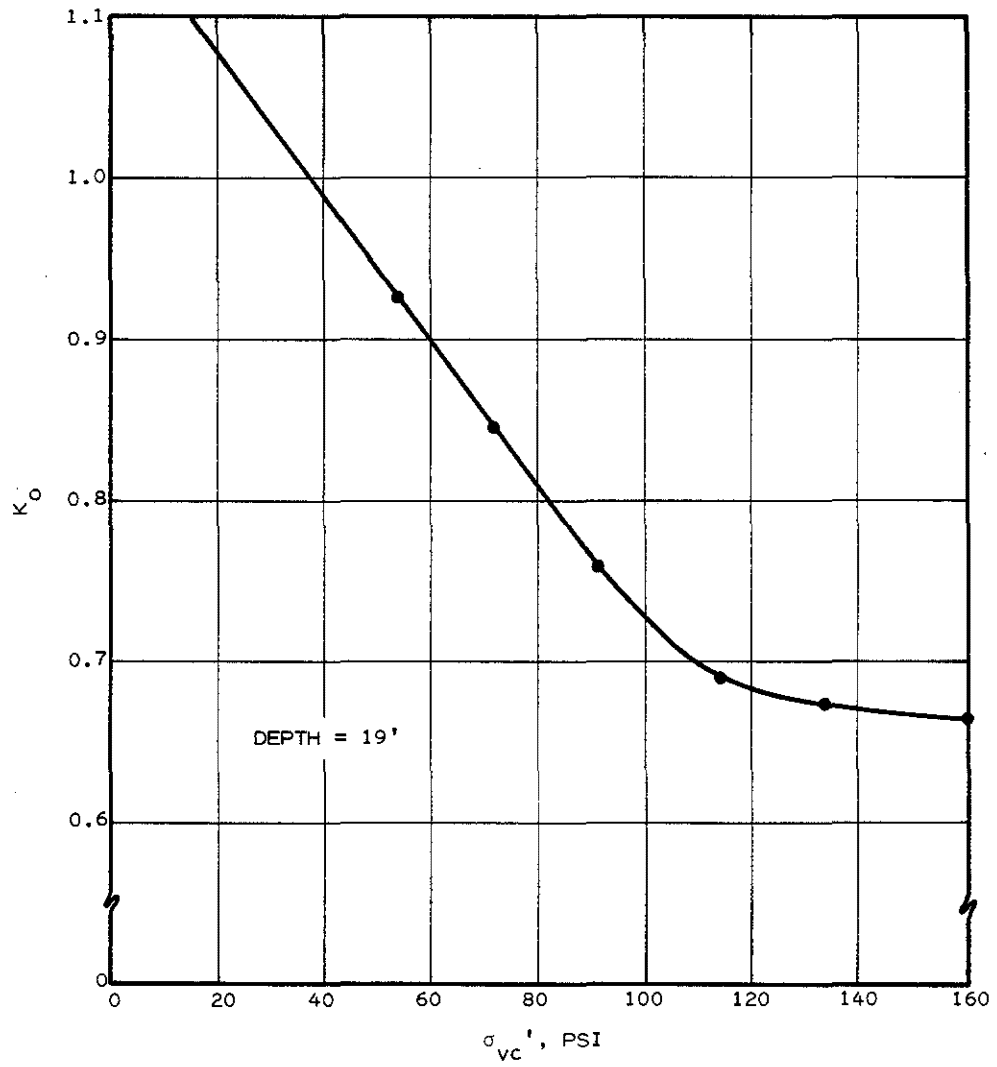


FIGURE C26. VERTICAL EFFECTIVE CONSOLIDATION PRESSURE (σ'_{vc}) VERSUS K_0

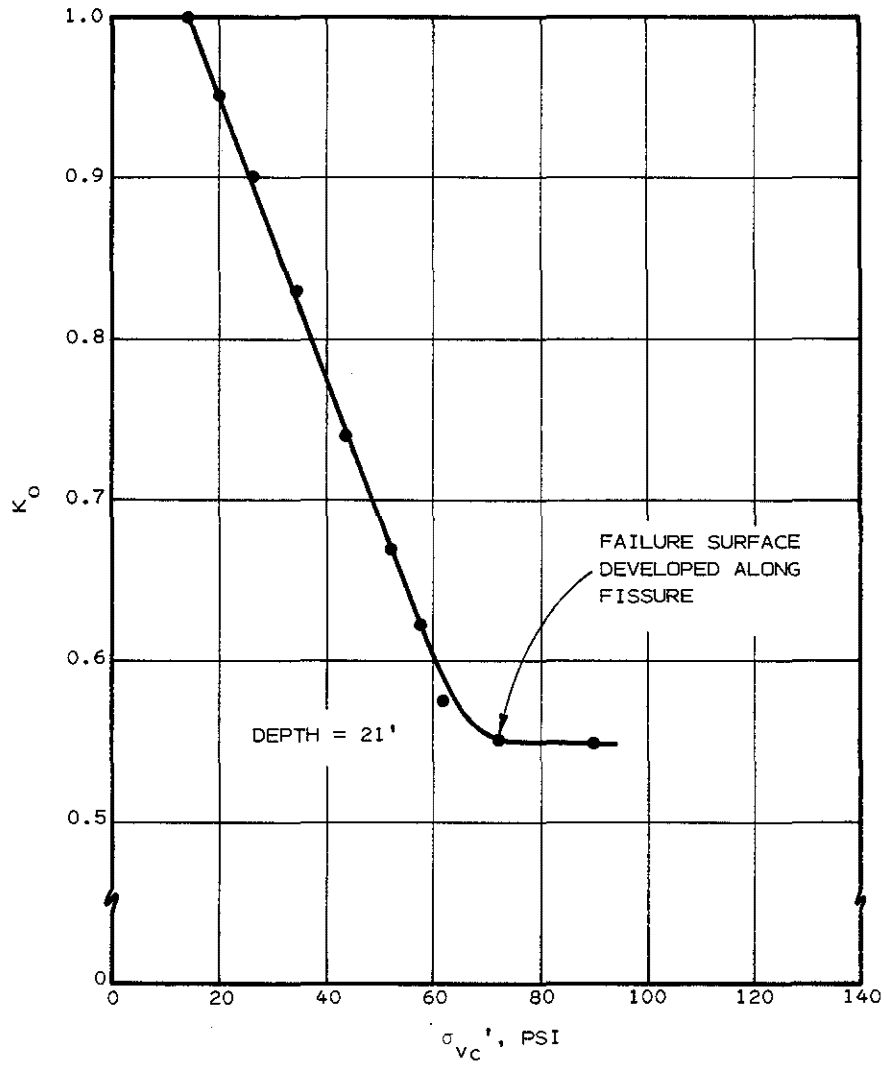


FIGURE C27. VERTICAL EFFECTIVE CONSOLIDATION PRESSURE (σ'_{VC}) VERSUS K_0

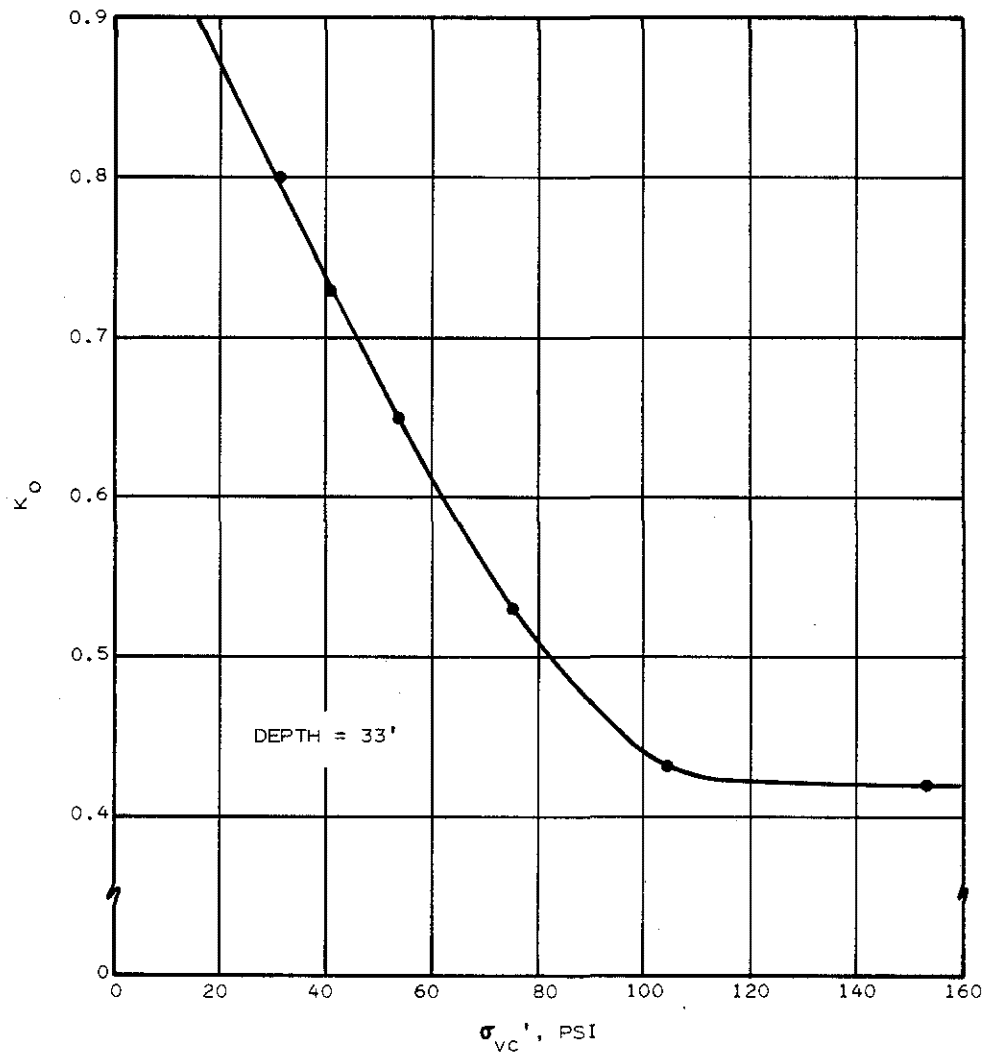


FIGURE C28. VERTICAL EFFECTIVE CONSOLIDATION PRESSURE (σ_{VC}') VERSUS K_0

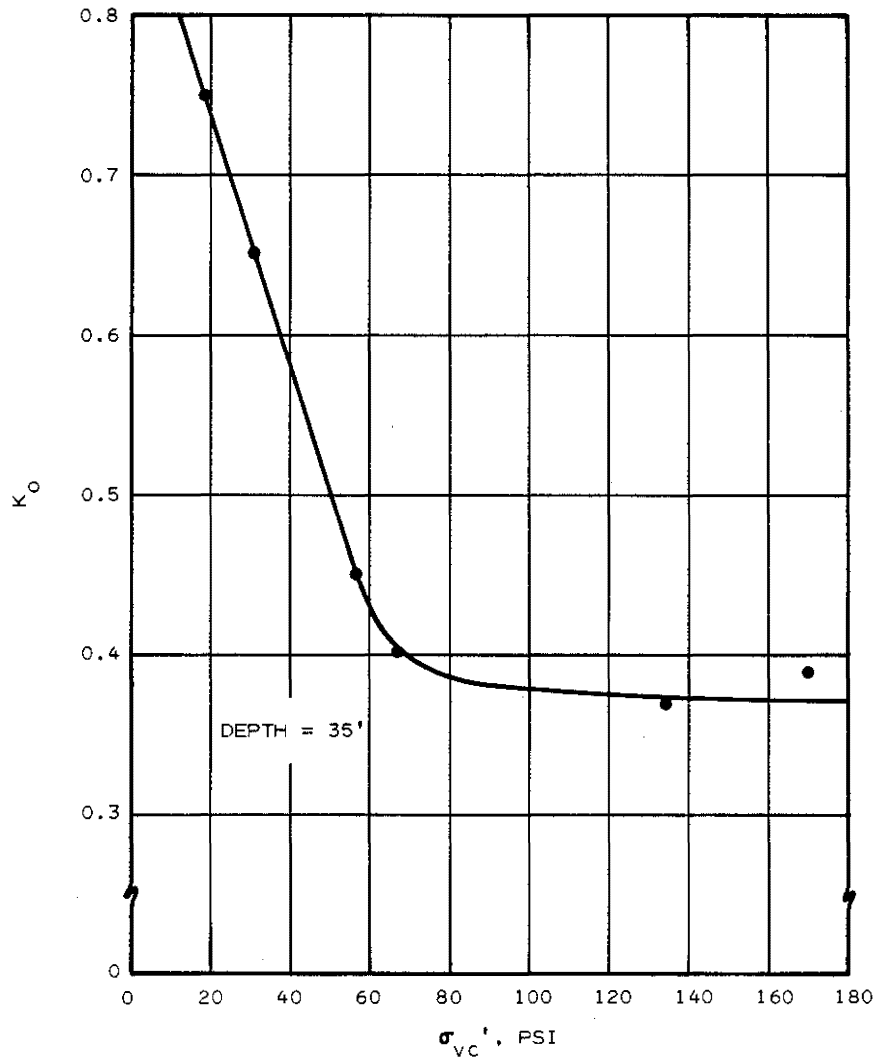


FIGURE C29. VERTICAL EFFECTIVE CONSOLIDATION PRESSURE (σ'_{vc}) VERSUS K_0

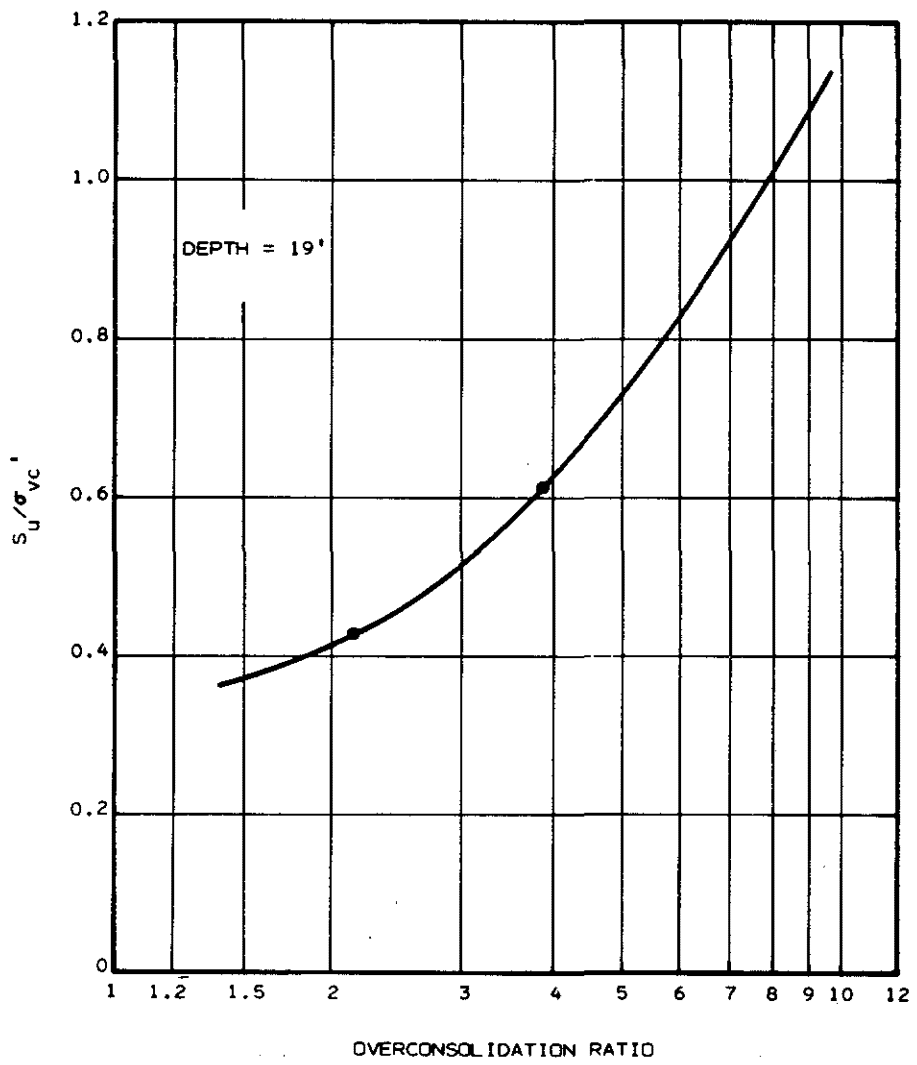


FIGURE C30. NORMALIZED SHEAR STRENGTH VERSUS OCR

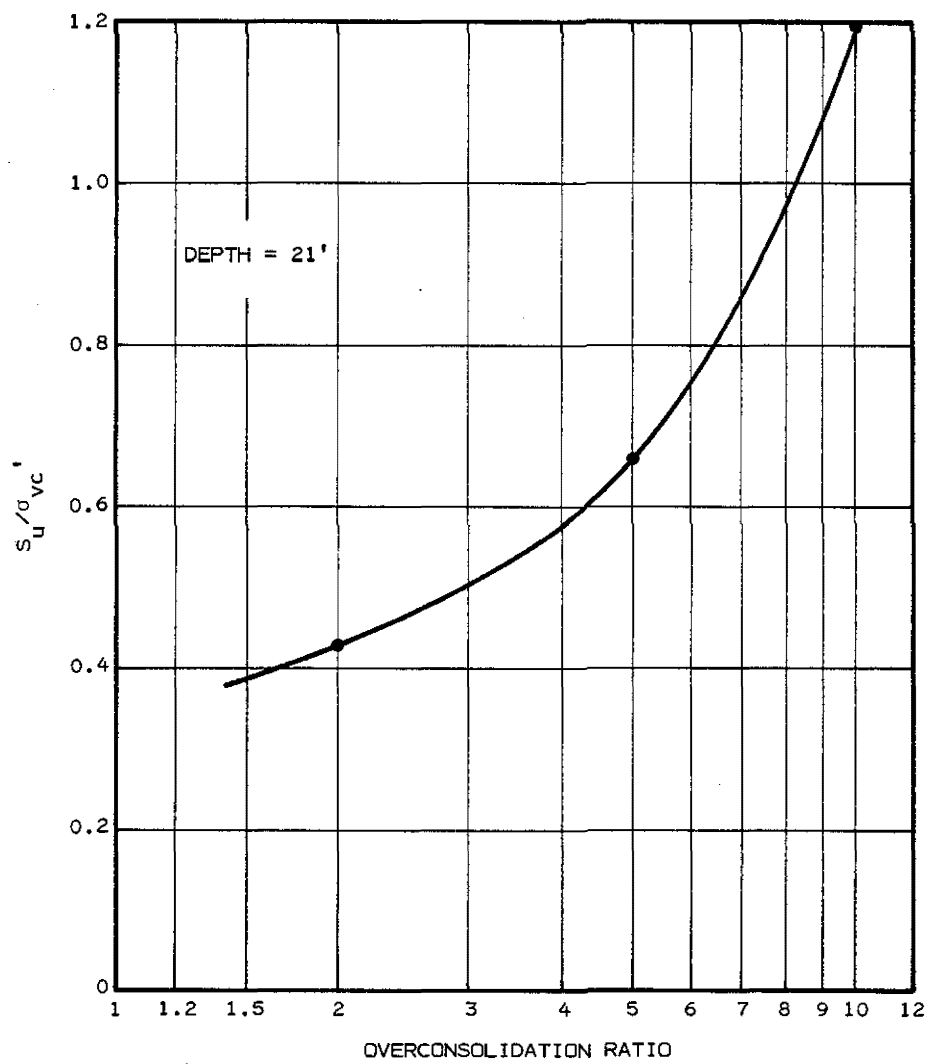


FIGURE C31. NORMALIZED SHEAR STRENGTH VERSUS OCR

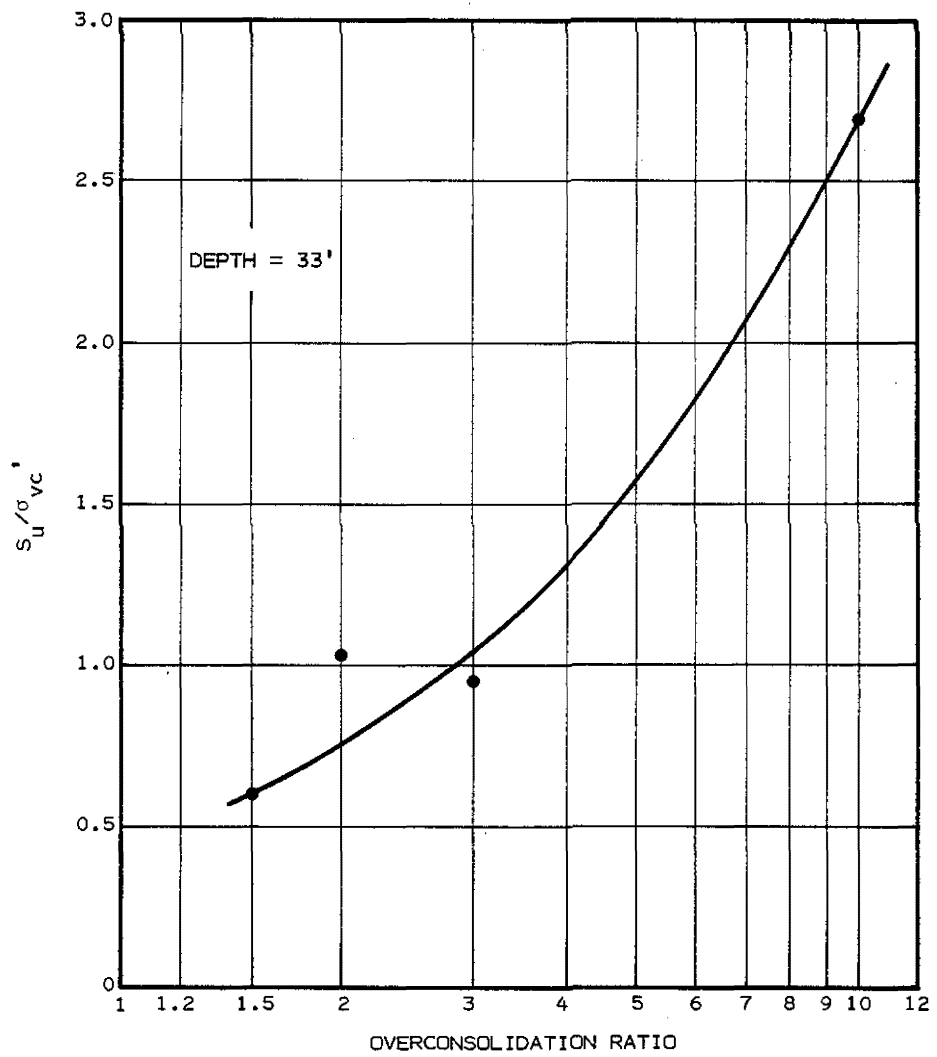


FIGURE C32. NORMALIZED SHEAR STRENGTH VERSUS OCR

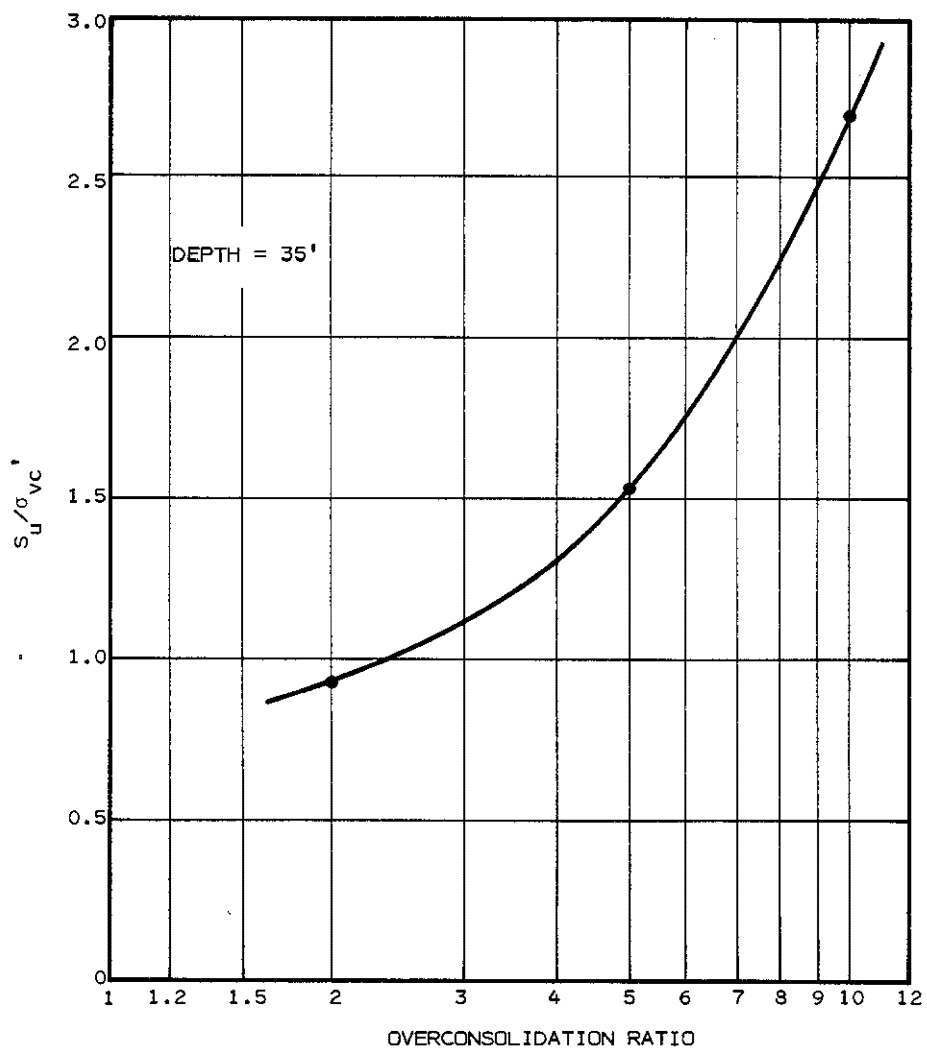


FIGURE C33. NORMALIZED SHEAR STRENGTH VERSUS OCR

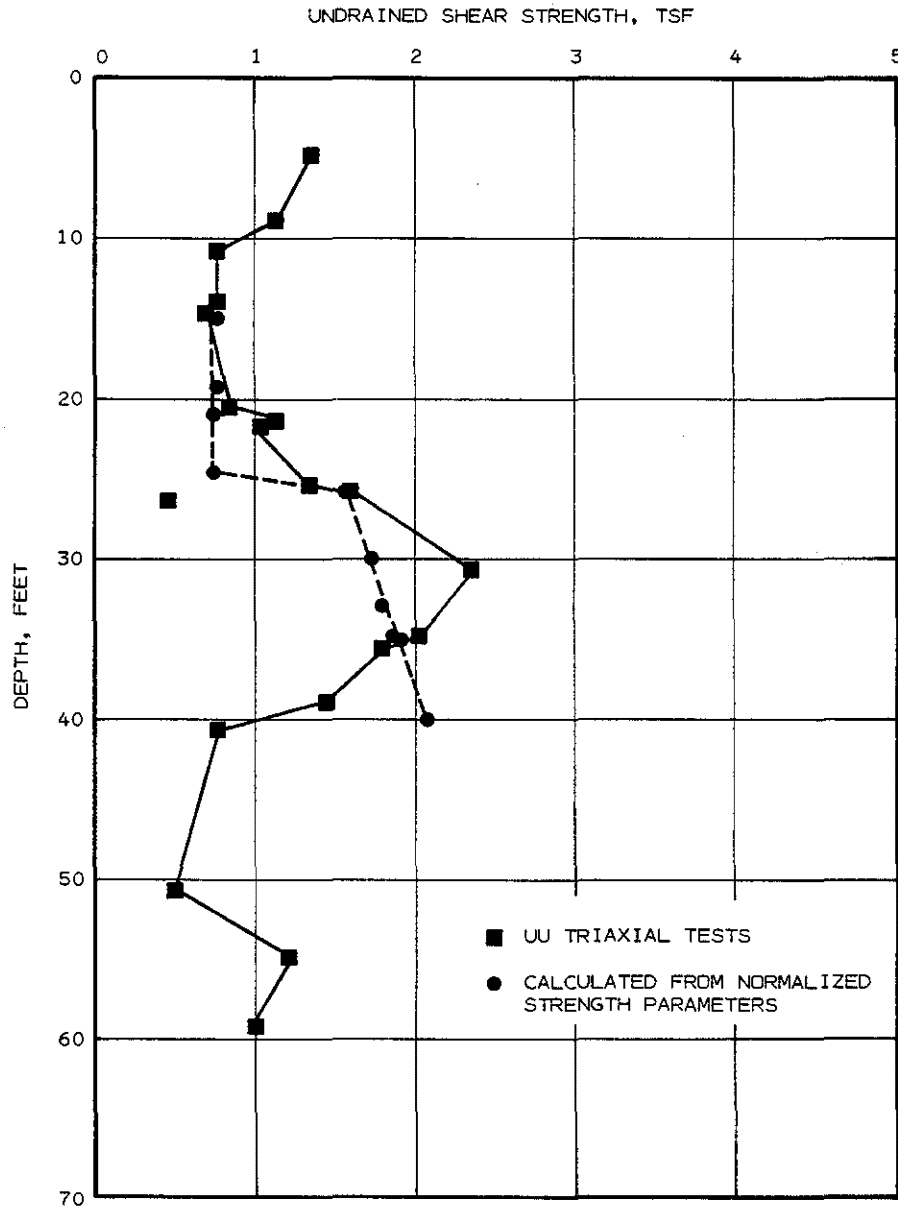


FIGURE C34. COMPARISON OF NORMALIZED SHEAR STRENGTH TO UNCONSOLIDATED-UNDRAINED TRIAXIAL STRENGTH

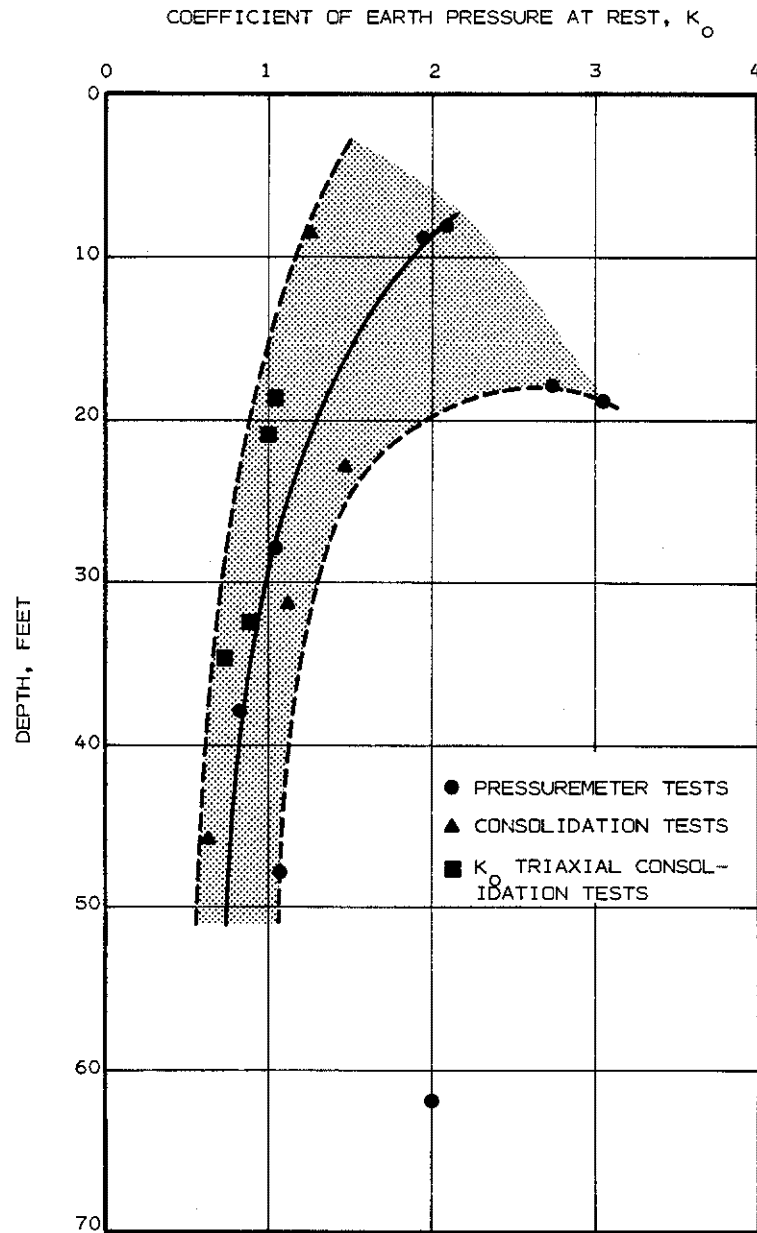


FIGURE C35. K_0 PROFILE FROM SELF BORING PRESSUREMETER AND CONSOLIDATION TESTS

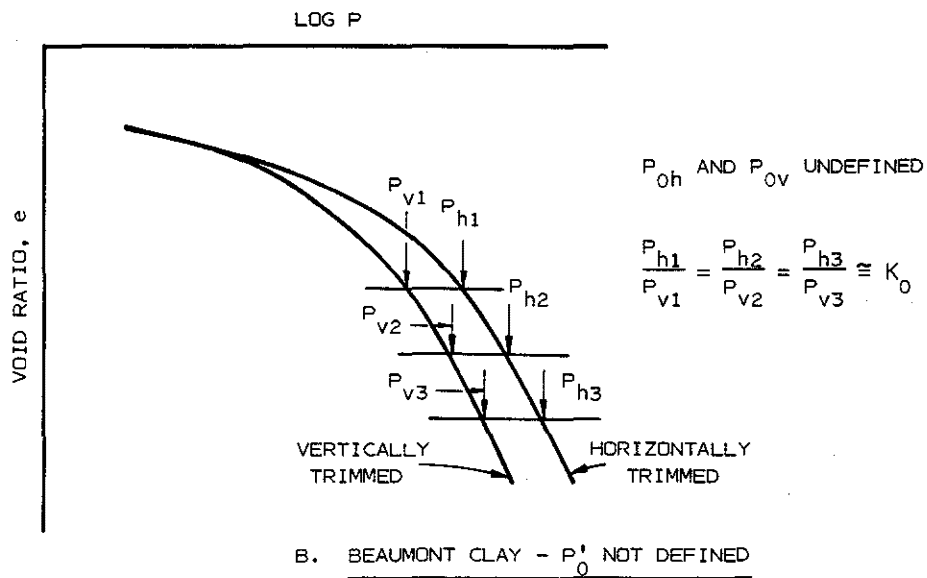
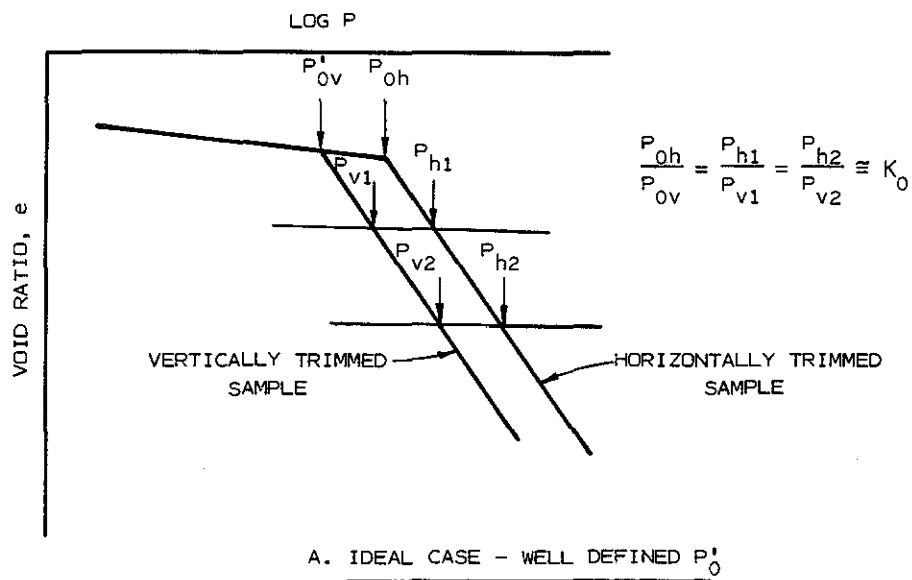


FIGURE C36. PROCEDURE FOR DETERMINING K_0 FROM CONSOLIDATION TESTS

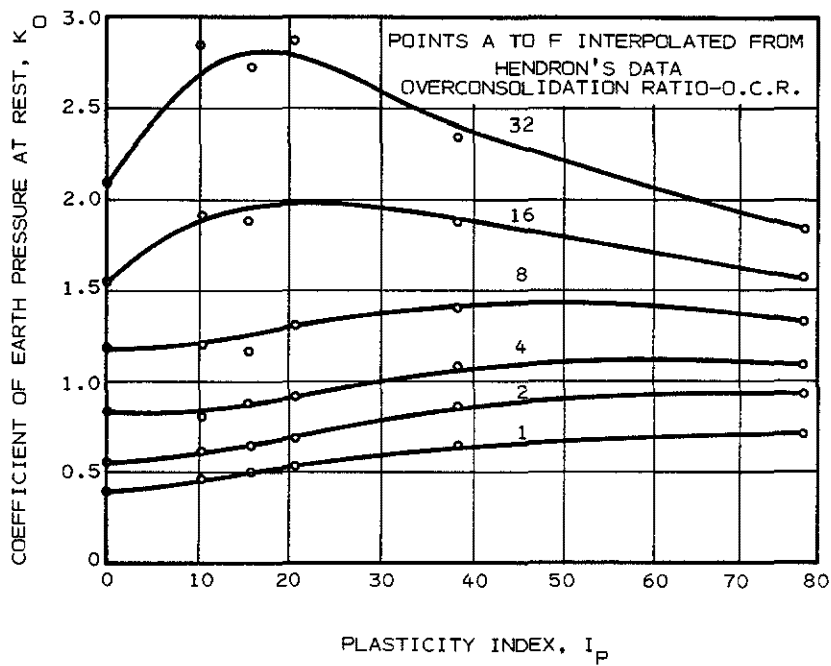


FIGURE C37. RELATIONSHIP BETWEEN K_0 , I_p , AND OCR

COEFFICIENT OF EARTH PRESSURE AT REST, K_0

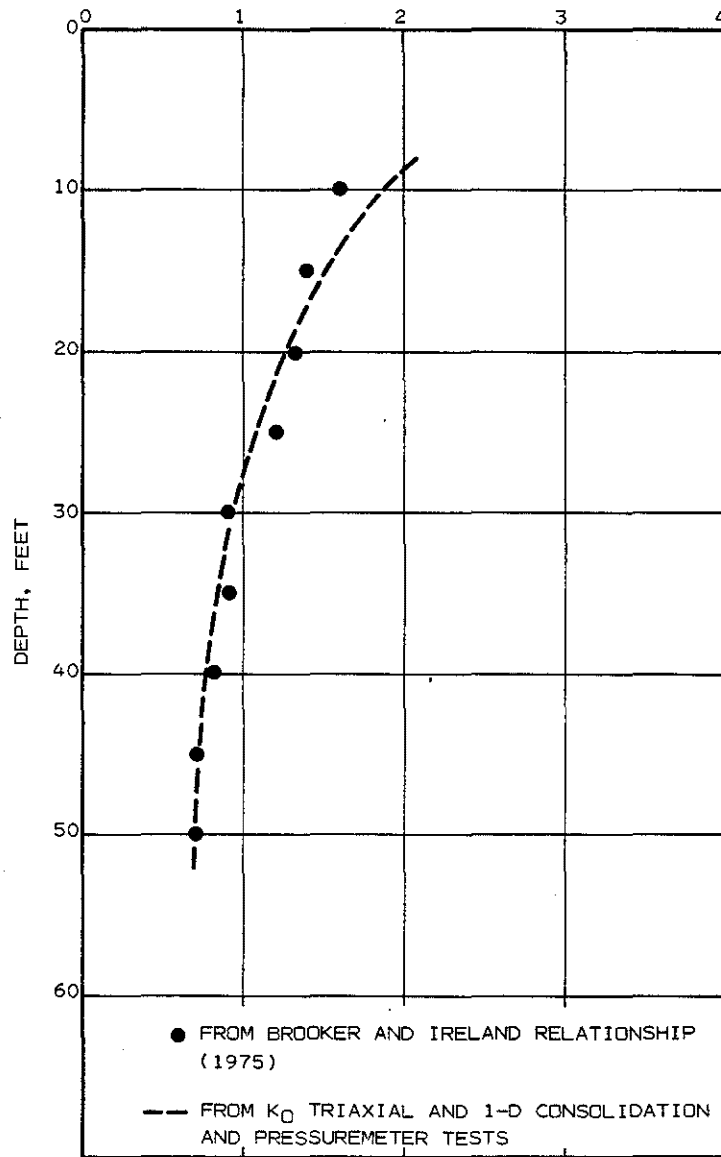


FIGURE C38. COMPARISON OF MEASURED K_0 VALUES TO CALCULATED VALUES FROM BROOKER AND IRELAND'S RELATIONSHIP

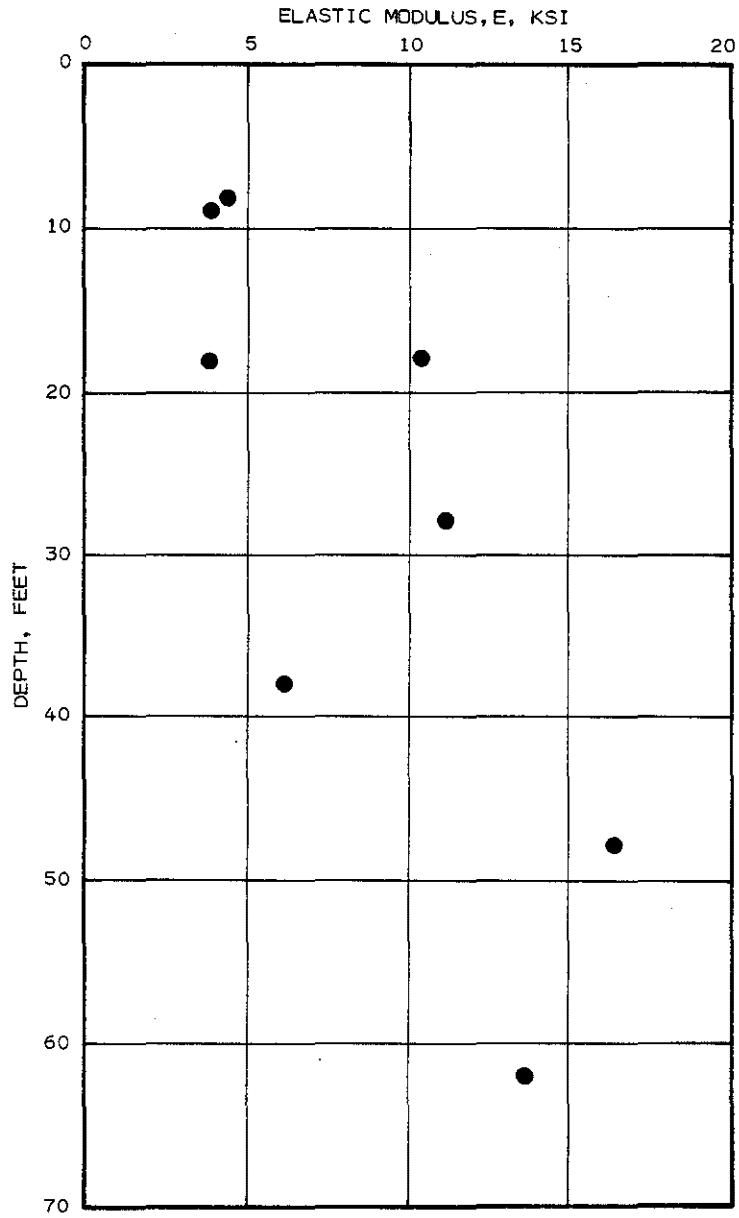


FIGURE C40. ELASTIC MODULUS PROFILE FROM SELF BORING PRESSUREMETER TESTS

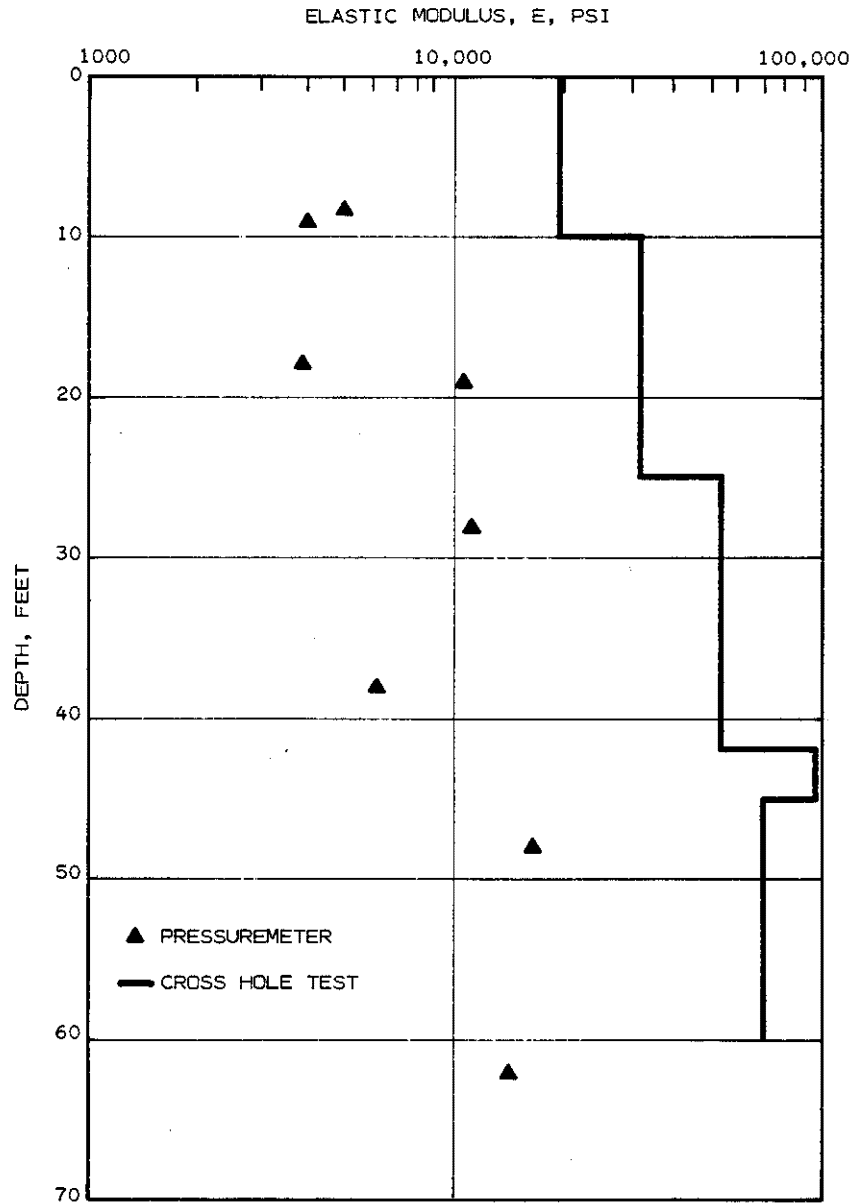


FIGURE C41. COMPARISON BETWEEN ELASTIC MODULUS DETERMINED FROM CROSS-HOLE SEISMIC TESTS AND SELF-BORING PRESSUREMETER TESTS

DESCRIPTION	NO. OF TESTS RUN
ATTERBERG LIMITS	31
SPECIFIC GRAVITY	10
SIEVE	5
PERCENT PASSING NO. 200 SIEVE	8
HYDROMETER	5
UNCONFINED COMPRESSION*	12
UNCONSOLIDATED-UNDRAINED TRIAXIAL*	21
CONSOLIDATED-UNDRAINED TRIAXIAL* WITH PORE PRESSURE MEASUREMENTS	15
REMOLEDDED CONSOLIDATED-UNDRAINED* TRIAXIAL WITH PORE PRESSURE MEASUREMENTS	12
RESIDUAL DIRECT SHEAR*	6
CONSOLIDATION*	10
CIU, CONSOLIDATED AT HIGH PRESSURE* AND REBOUNDED AT KNOWN OCR. (NSP TRIAXIAL)	12
K_o TRIAXIAL CONSOLIDATION TESTS*	4

*WATER CONTENTS AND UNIT WEIGHTS ARE RUN WITH EACH OF THESE TESTS.

TABLE C1. NUMBER OF LABORATORY TESTS CONDUCTED

SAMPLE INTERVAL, FEET	%PASSING #200 SIEVE	SPECIFIC GRAVITY	LIQUID LIMIT	PLASTIC LIMIT	PLASTICITY INDEX PI
0 - 2			34	13	21
2 - 4			43	13	30
4 - 6			53	15	38
6 - 8			51	15	36
			56	12	44
8 - 10		2.70			
		2.63			
		2.58			
10 - 12	63.0		35	14	21
12 - 14			52	17	35
			62	16	46
14 - 16			74	19	55
16 - 18	99.0				
18 - 20		2.67	69	26	43
20 - 22			66	26	40
22 - 24		2.72	65	25	40
			69	25	44
24 - 26			69	19	50
26 - 28	78.1		24	19	5
28 - 30	86.0		25	11	14
32 - 34		2.62	29	12	17
		2.63			
36 - 38	80.0	2.59	31	19	12
38 - 40	67.3		28	7	21
40 - 42	56.0		27	15	12
42 - 44	61.0		49	20	29
44 - 46	92.0		31	19	12
46 - 48	88.0	2.62	29	15	14
		2.59			
48 - 50	87.0		23	23	0
			28	18	10
53 - 55			23	21	2
58 - 60			26	22	4
			27	20	7
68 - 70			79	21	58
78 - 80			71	21	50
88 - 90			51	14	37

TABLE C2. SUMMARY OF INDEX PROPERTY TESTS

SAMPLE INTERVAL	DEPTH, FT.	CONFINING PRESSURE, TSF	WATER CONTENT, %	DRY UNIT WT. PCF	MAXIMUM SHEAR STRESS	PERCENT STRAIN
2 - 4	3.0	0.72	20	108	1.33	16.7
6 - 8	7.0	0.72	21	105	1.12	20.0
10 - 12	11.5	0.72	21	105	0.76	20.0
12 - 14	13.0	0.72	25	99	0.27	2.8
14 - 16	15.5	0.86	27	93	0.67	2.4
	14.5	1.73	31	93	0.77	3.5
20 - 22	20.5	1.08	26	99	0.83	5.7
	21.0	1.66	26	101	1.13	7.4
	21.5	2.20	28	96	1.01	2.2
22 - 24	24.5	1.01	27	98	1.32	10.0
26 - 28	26.5	1.10	19	109	1.64	6.9
	27.0	1.15	16	114	1.34	5.2
	27.0	1.15	18	113	0.45	14.9
30 - 32	30.5	1.51	15	120	2.35	20.0
34 - 36	35.5	1.69	15	121	1.79	14.1
	34.5	3.38	17	116	2.01	16.8
38 - 40	39.5	1.51	21	107	1.45	6.3
40 - 42	41.0	1.51	19	111	0.72	19.9
50 - 52	50.0	1.66	26	97	0.49	15.5
53 - 55	55.0	1.94	25	107	1.21	11.7
58 - 60	59.5	2.09	26	99	1.00	8.9

TABLE C3. SUMMARY OF UU TRIAXIAL TESTS

SAMPLE INTERVAL	DEPTH, FT.	DRY UNIT WT., PCF	WATER CONTENT, %	S _u (TSF)	% STRAIN AT FAILURE
4 - 6	5.0	113	17	3.41	9.5
6 - 8	7.5	111	19	2.06	14.3
10 - 12	11.0	104	23	0.38	5.8
14 - 16	15.0	96	28	0.96	2.8
24 - 26	25.0	102	24	1.04	1.7
26 - 28	27.0	114	17	0.89	6.4
28 - 30	29.0	112	18	0.40	5.3
34 - 36	35.0	118	15	0.72	3.4
38 - 40	39.0	111	19	0.96	2.4
42 - 44	43.0	104	25	1.57	6.3
46 - 48	45.5	106	20	0.61	3.6
46 - 48	47.0	103	23	0.30	4.3

TABLE C4. SUMMARY OF UNCONFINED COMPRESSION TEST RESULTS

DEPTH FT.	γ DRY PCF	WATER CONTENT %	EFFECTIVE STRESS		TOTAL STRESS	
			φ'	C', TSF	φ	C, TSF
CIU TESTS, UNDISTURBED SPECIMENS						
8 - 10	105	20	26	0.20	17	0.35
18 - 20	98	25	24	0	11	0.35
22 - 24	97	26	26	0	11	0.45
32 - 34	116	15	30	0.50	17	0.60
36 - 38	116	15	30	0.27	17	0.80
CIU TESTS, REMOLDED SPECIMENS						
20 - 22	100	27	17	0.36	13	0.60
30 - 32	119	14	25	0	18	0.55
*** RESIDUAL CD DIRECT SHEAR						
16 - 18	100	24	12	0.23	-	-
30 - 32	115	15	30	0	-	-
CAU TESTS, REMOLDED SPECIMENS						
* 16 - 18	101	24	16	0.60	20	0.40
** 34 - 36	117	16	33	0	22	0.70

* CONSOLIDATED AT $K_o = 1.0$ STRESS CONDITION

** CONSOLIDATED AT $K_o = 0.8$ STRESS CONDITION

*** VALUES FROM INTERM REPORT REVISED HERE

TABLE C5. SUMMARY OF NORMALIZED STRENGTH PARAMETER
TRIAxIAL TEST RESULTS

DEPTH, FT.	BORING	C_u , PSF	E, PSI	K_σ
8.3	PM-1	1730	4390	2.08
9.0	PM-2	3820	3980	1.95
18.0	PM-2	3210	3930	2.73
19.0	PM-1	2810	10,450	3.04
28.0	PM-1	4250	11,060	1.04
38.0	PM-1	8210	6100	0.82
48.0	PM-1	6910	16,360	1.06
62.0	PM-1	7490	13,680	2.00

TABLE C6. RESULTS OF SELF-BORING PRESSUREMETER TESTS

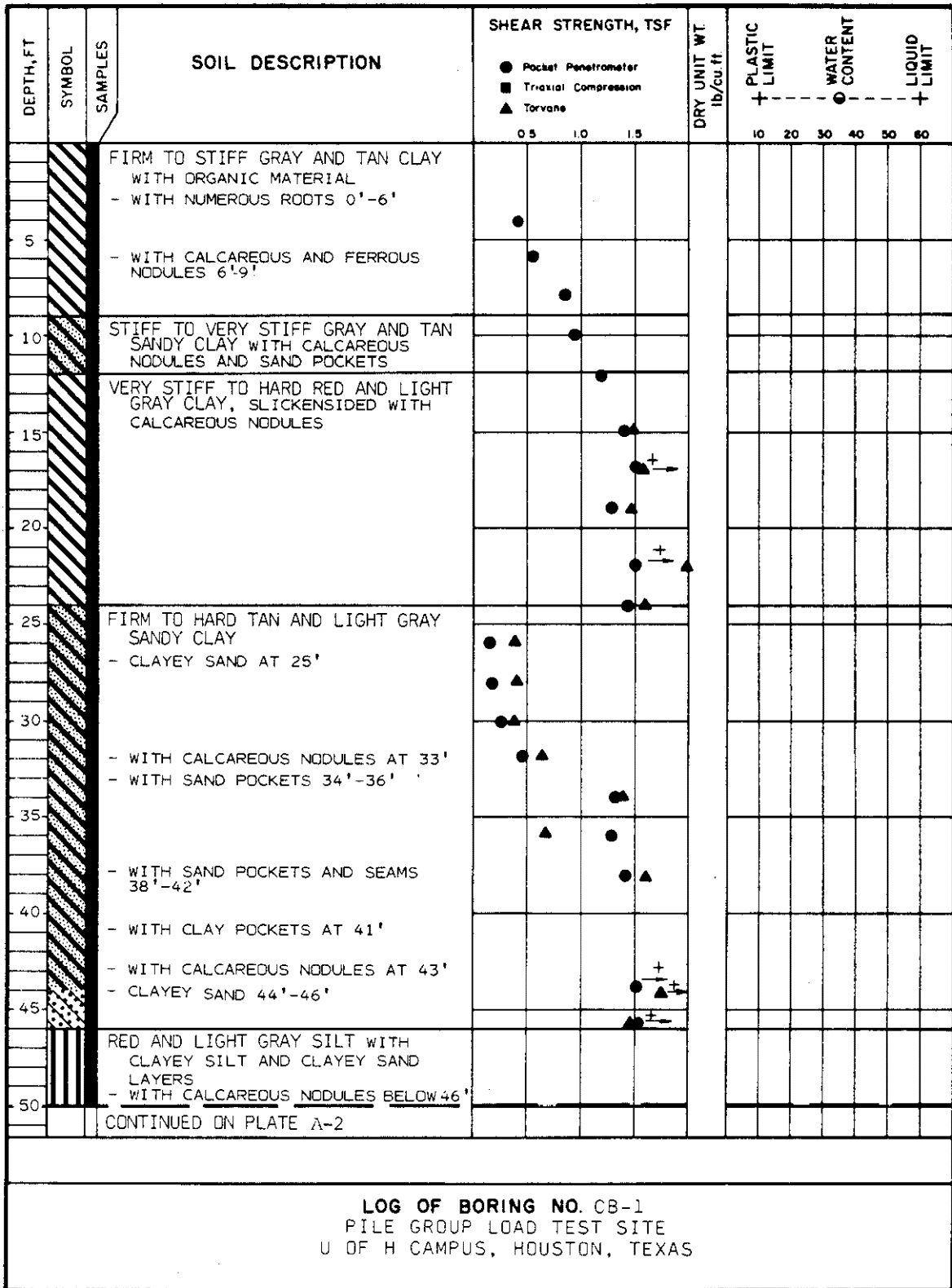
DEPTH, FEET	AVERAGE UNIT WT. LBS/FT ³	POISSON'S RATIO	SHEAR WAVE VELOCITY FT/SEC	COMPRESSION WAVE VELOCITY, FT/SEC	SHEAR MODULUS, G, PSI	YOUNG'S MODULUS, E, PSI
0 - 10	131	0.49	480	4000	6520	19,460
10 - 25	126	0.49	630	6100	10,800	32,290
25 - 42	132	0.49	800	4700	18,250	54,200
42 - 45	132	0.49	1070	6300	32,640	96,960
45 - 60	127	0.49	920	5800	23,220	69,056

TABLE C7. AVERAGE DYNAMIC PROPERTIES BASED ON
CROSS-HOLE SEISMIC TESTS

DEPTH FT.	MAXIMUM CONSOLIDATION PRESSURE PSI	FINAL CONSOLIDATION PRESSURE, σ_{VC} PSI	DCR	S_U PSI	S_U/σ_{VC}
18 - 20	150	72	2.10	30.1	0.43
18 - 20	150	38	3.95	23.3	0.61
20 - 22	250	25	10.0	30.0	1.20
20 - 22	250	50	5.0	33.1	0.66
20 - 22	250	125	2.0	53.3	0.43
32 - 34	150	15	10.0	40.3	2.69
32 - 34	150	50	3.0	47.4	0.95
32 - 34	150	75	2.0	77.0	1.03
32 - 34	250	167	1.5	100.0	0.60
34 - 36	150	15	10.0	42.2	2.68
34 - 36	150	50	5.0	45.8	1.53
34 - 36	150	75	2.0	69.9	0.93

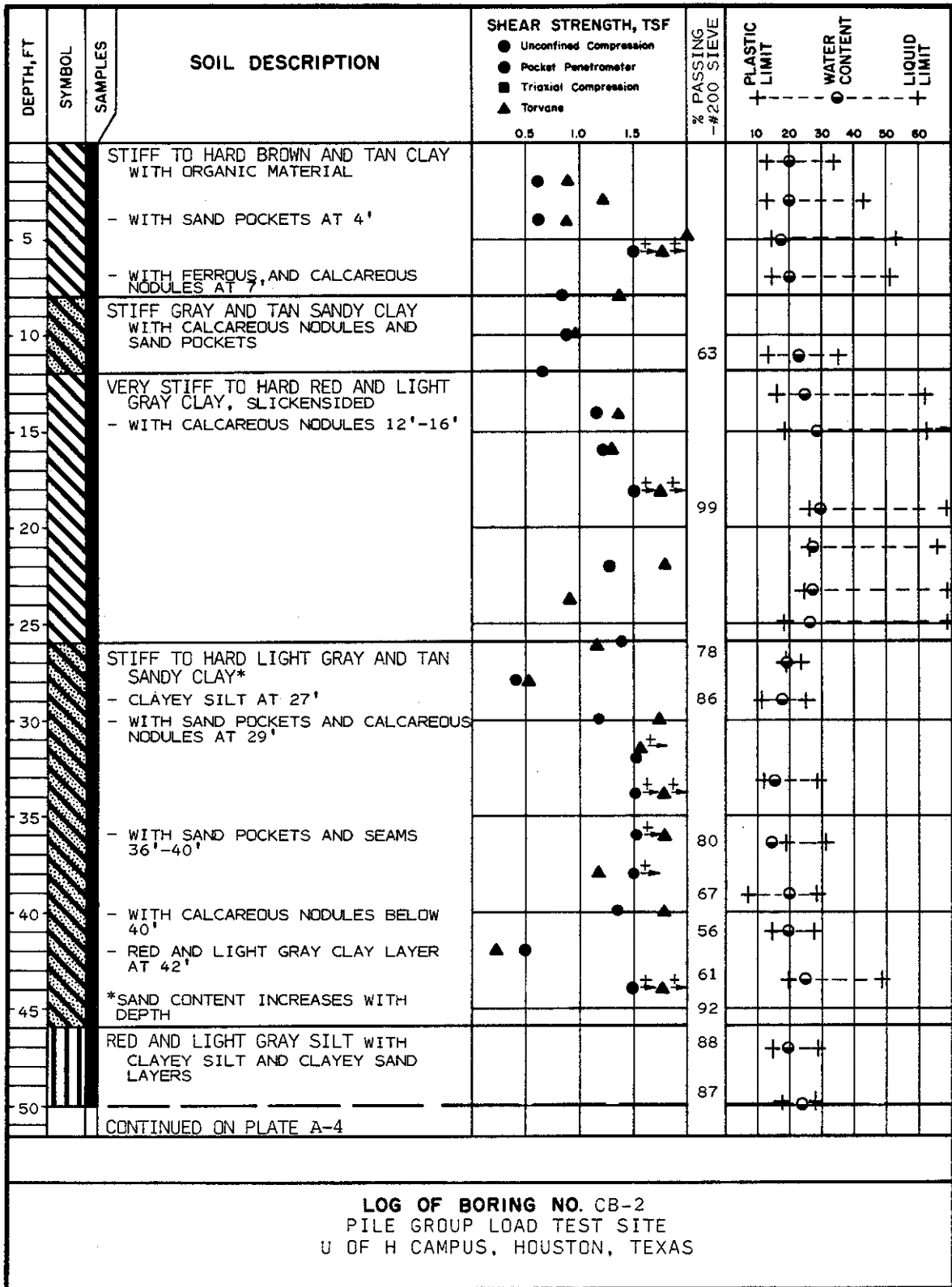
TABLE C8. RESULTS OF RESIDUAL DIRECT SHEAR AND CIU
TESTS ON UNDISTURBED AND REMOLDED SPECIMENS

ADDENDUM A

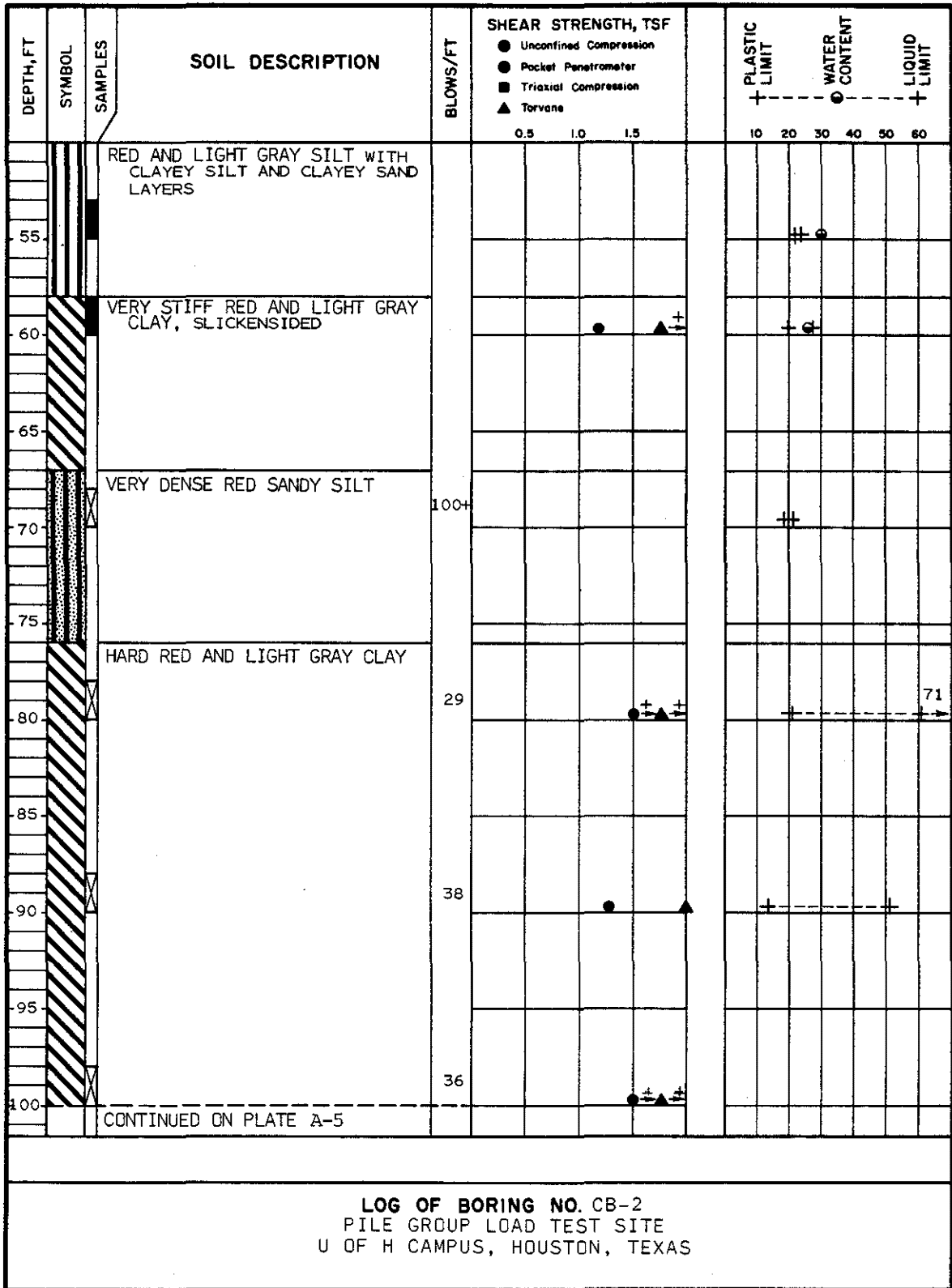


LOG OF BORING NO. CB-1
PILE GROUP LOAD TEST SITE
U OF H CAMPUS, HOUSTON, TEXAS





DEPTH, FT	SYMBOL	SAMPLES	SOIL DESCRIPTION	SHEAR STRENGTH, TSF			DRY UNIT WT. lb/cu. ft.	PLASTIC LIMIT	WATER CONTENT	LIQUID LIMIT
				0.5	1.0	1.5				
55			RED AND LIGHT GRAY SILT WITH CLAYEY SILT AND CLAYEY SAND LAYERS - WITH NUMEROUS SILTSTONES AND CLAY SEAMS 53'-55'							
60			- CLAYEY SAND 58'-60'							
65										
70										
75										
80										
85										
90										
95										
100										
COMPLETION DEPTH: 60'			LOCATION: SEE FIGURE 2			DEPTH TO WATER: 7.0'				
DATE: 2/8/79						DATE: 2/19/79				
LOG OF BORING NO. CB-1 PILE GROUP LOAD TEST SITE U OF H CAMPUS, HOUSTON, TEXAS										



LOG OF BORING NO. CB-2
 PILE GROUP LOAD TEST SITE
 U OF H CAMPUS, HOUSTON, TEXAS



LOG OF BORING NO. CB-2
 PILE GROUP LOAD TEST SITE
 U OF H CAMPUS, HOUSTON, TEXAS

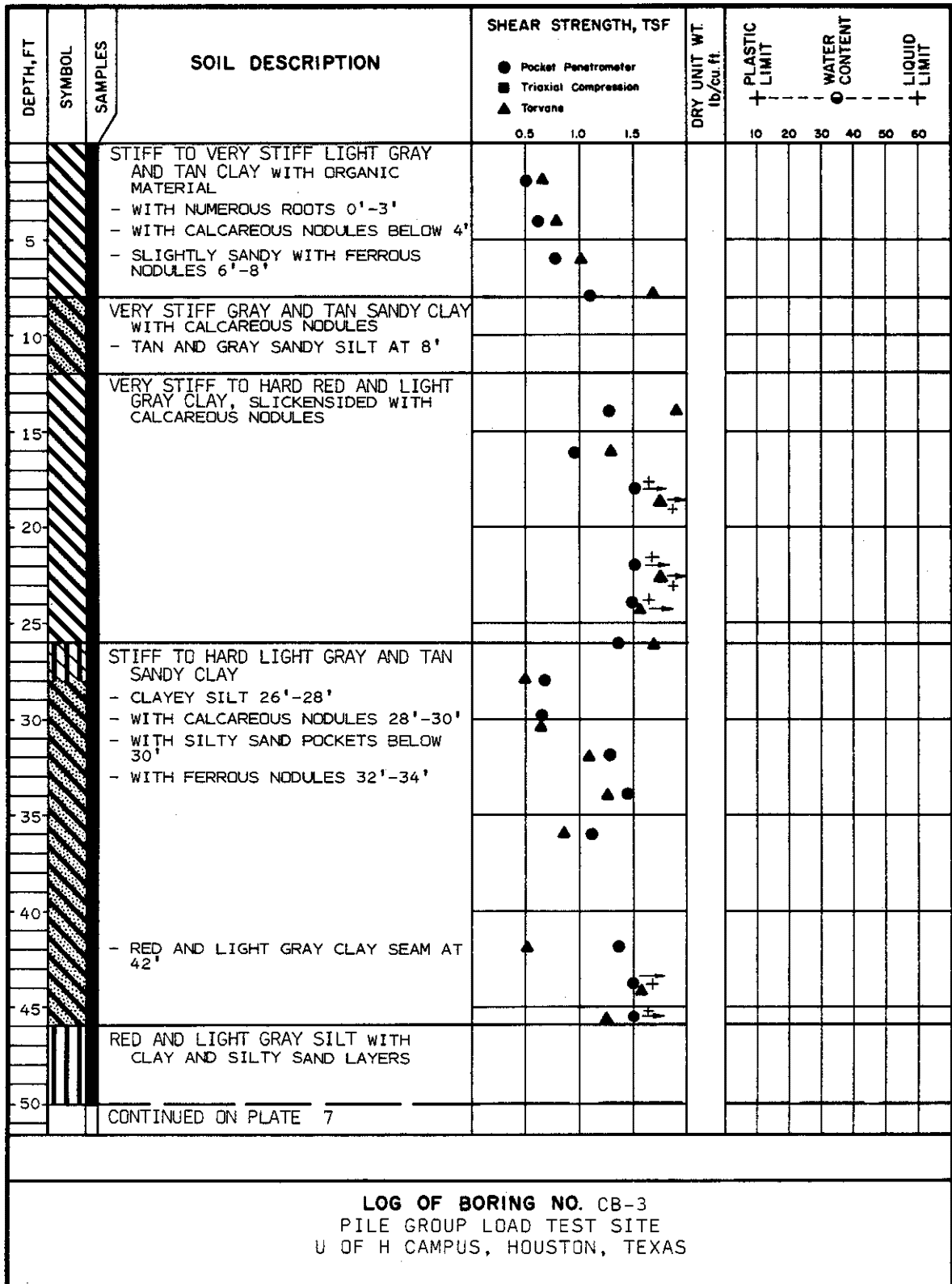
DEPTH, FT	SYMBOL	SAMPLES	SOIL DESCRIPTION	BLOWS/FT	SHEAR STRENGTH, TSF			PLASTIC LIMIT	WATER CONTENT	LIQUID LIMIT			
					● Unconfined Compression	○ Pocket Penetrometer	■ Triaxial Compression				▲ Torvane		
					0.5	1.0	1.5	10	20	30	40	50	60
105			HARD RED AND LIGHT GRAY CLAY										
110			VERY DENSE TAN FINE SAND	100+									
115													
120				100+									
125													
130													
135													
140													
145													
150													

COMPLETION DEPTH: 120'
DATE: 1/24/79

LOCATION: SEE FIGURE 2

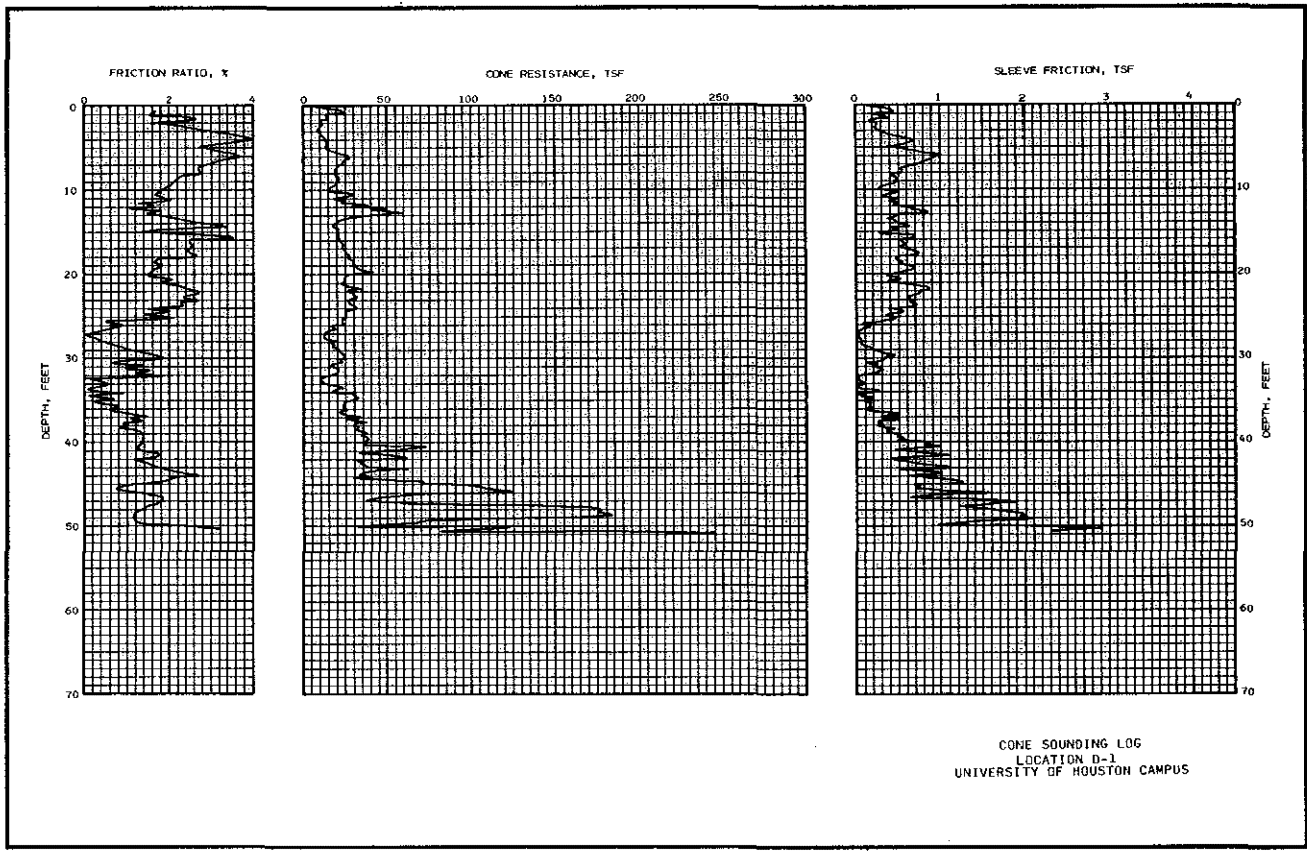
DEPTH TO WATER: 7.0'
DATE: 1/24/79

LOG OF BORING NO. CB-2
PILE GROUP LOAD TEST SITE
U OF H CAMPUS, HOUSTON, TEXAS

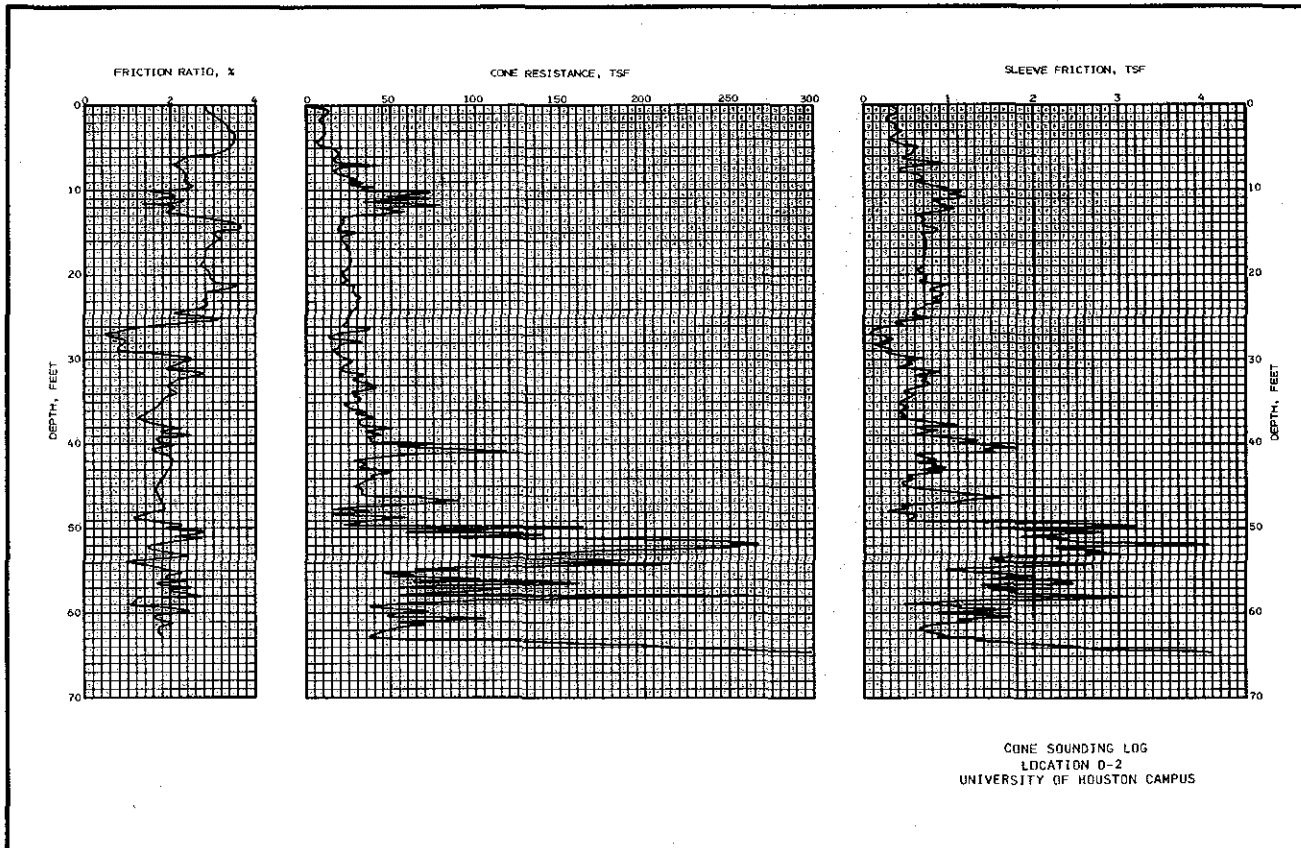


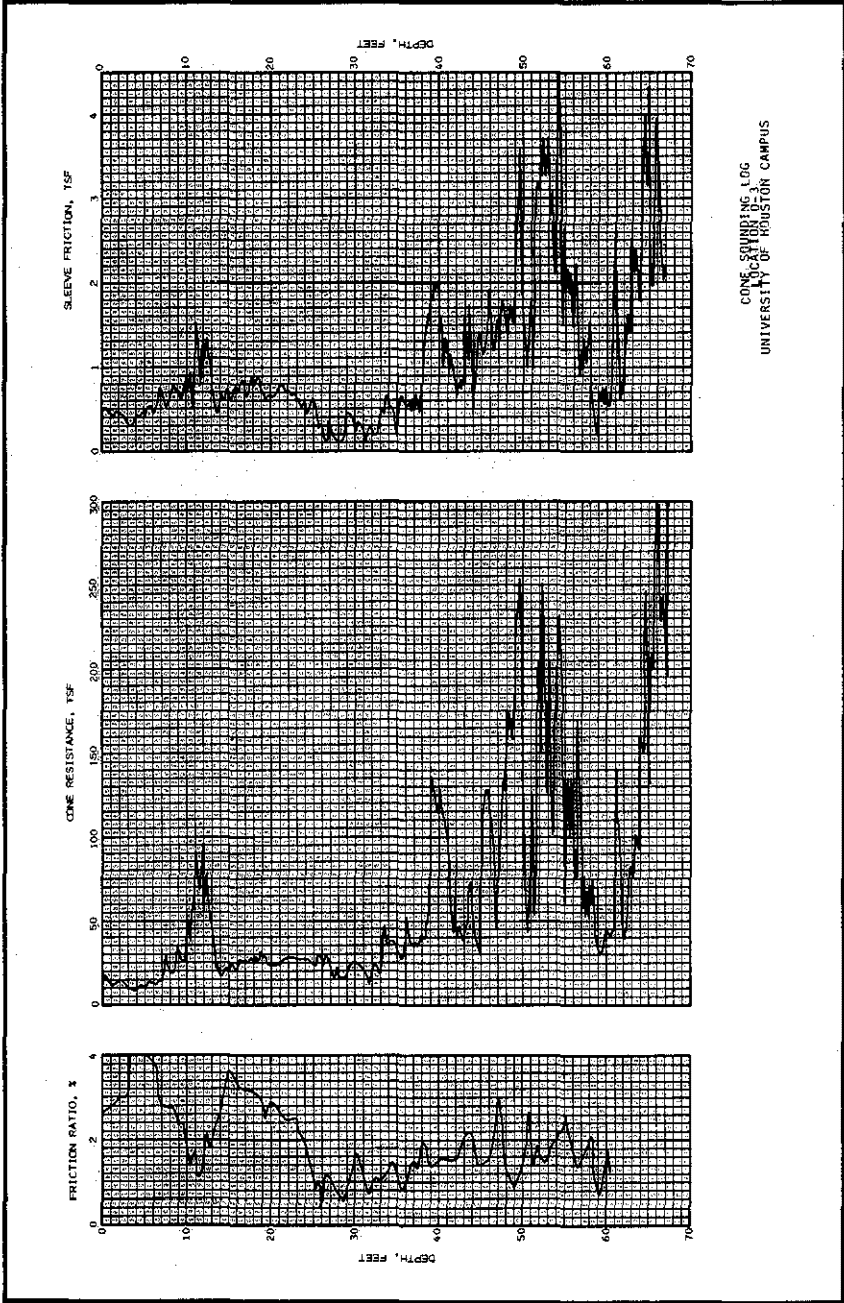
LOG OF BORING NO. CB-3
PILE GROUP LOAD TEST SITE
U OF H CAMPUS, HOUSTON, TEXAS

DEPTH, FT	SYMBOL	SAMPLES	SOIL DESCRIPTION	SHEAR STRENGTH, TSF			DRY UNIT WT lb/cu. ft.	PLASTIC LIMIT	WATER CONTENT	LIQUID LIMIT
				0.5	1.0	1.5				
55			RED AND LIGHT GRAY SILT WITH CLAY AND SILTY SAND LAYERS - SANDY SILT 53'-55'							
60			- CLAYEY AT 60'							
65										
70										
75										
80										
85										
90										
95										
100										
COMPLETION DEPTH: 60'			LOCATION: SEE FIGURE 2			DEPTH TO WATER: 7.0'				
DATE: 1/30/79						DATE: 2/19/79				
LOG OF BORING NO. CB-3 PILE GROUP LOAD TEST SITE U OF H CAMPUS, HOUSTON, TEXAS										

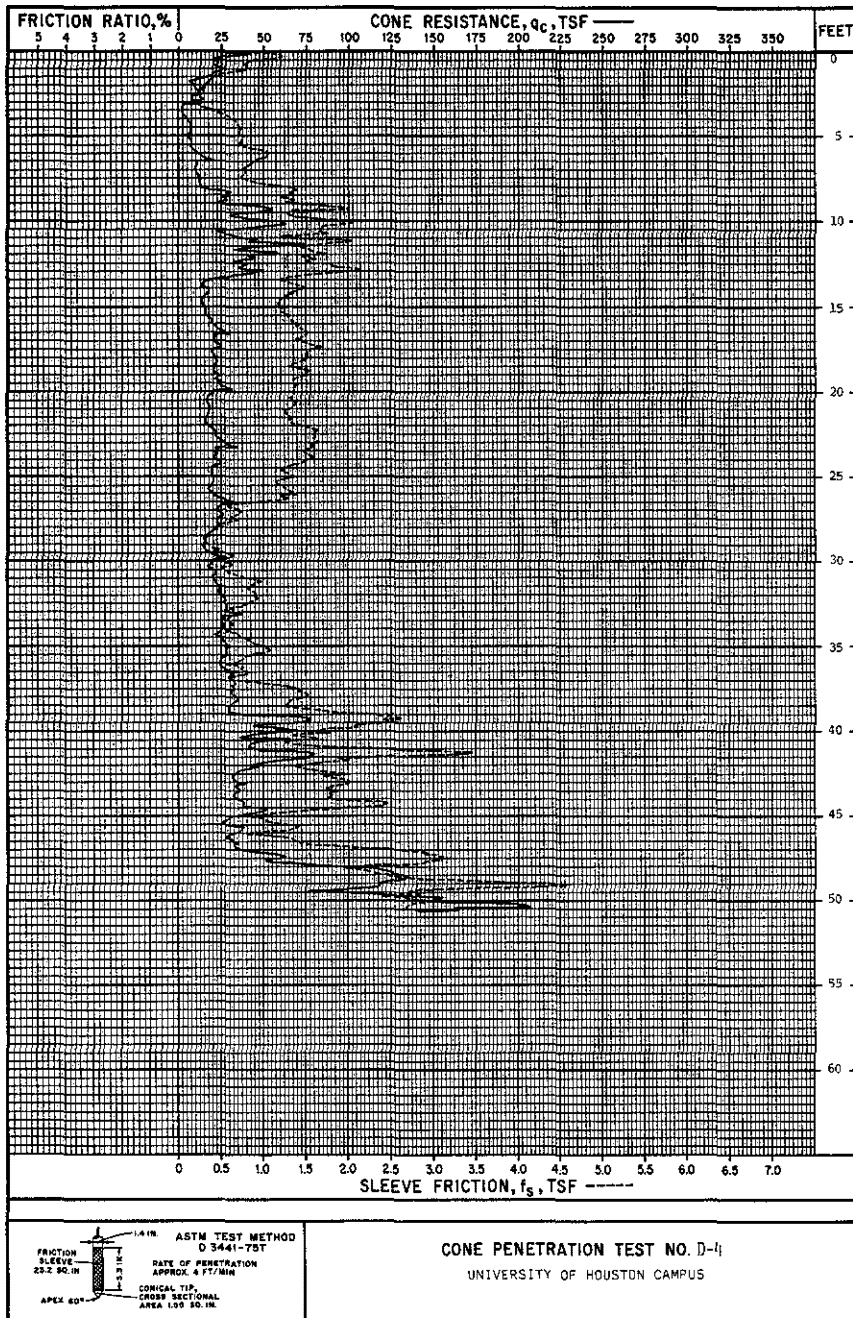


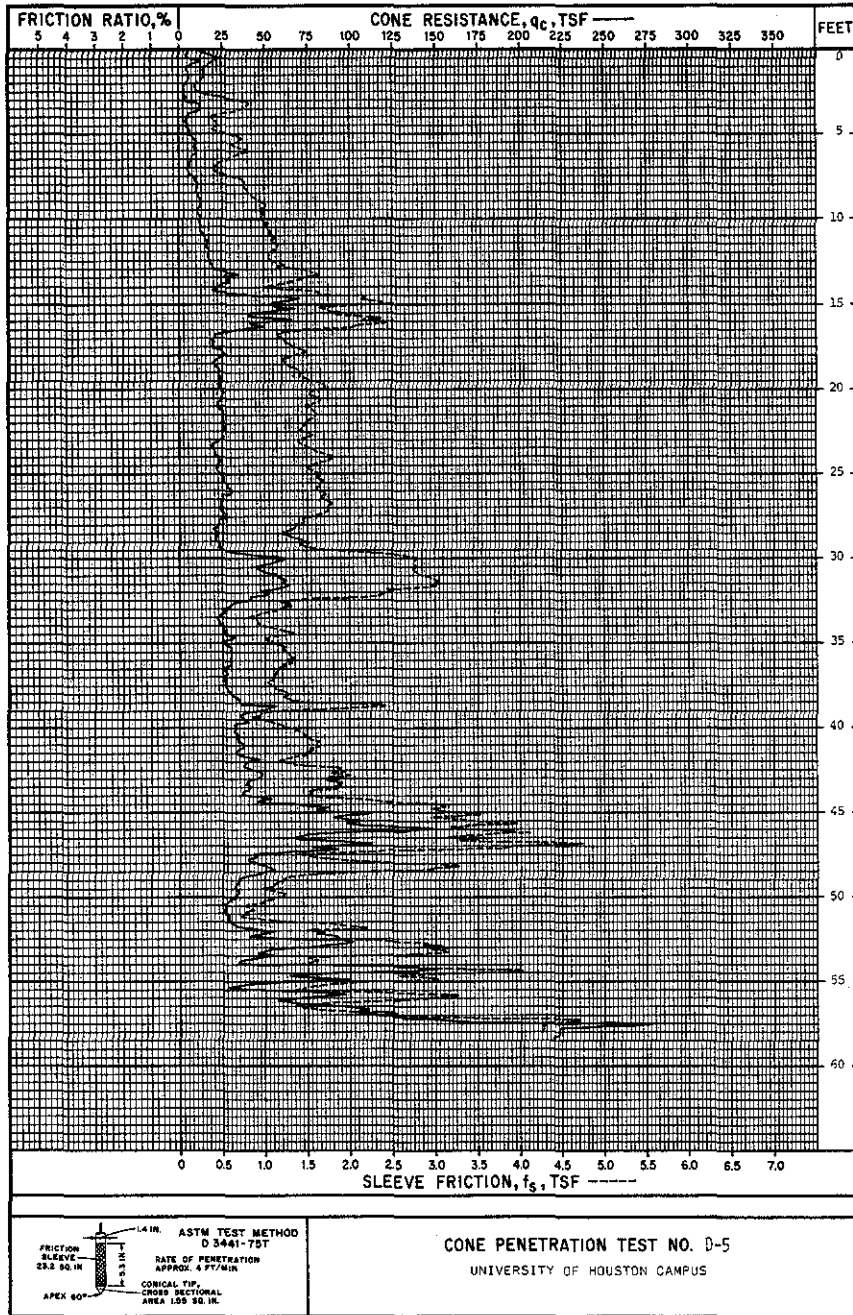
C100

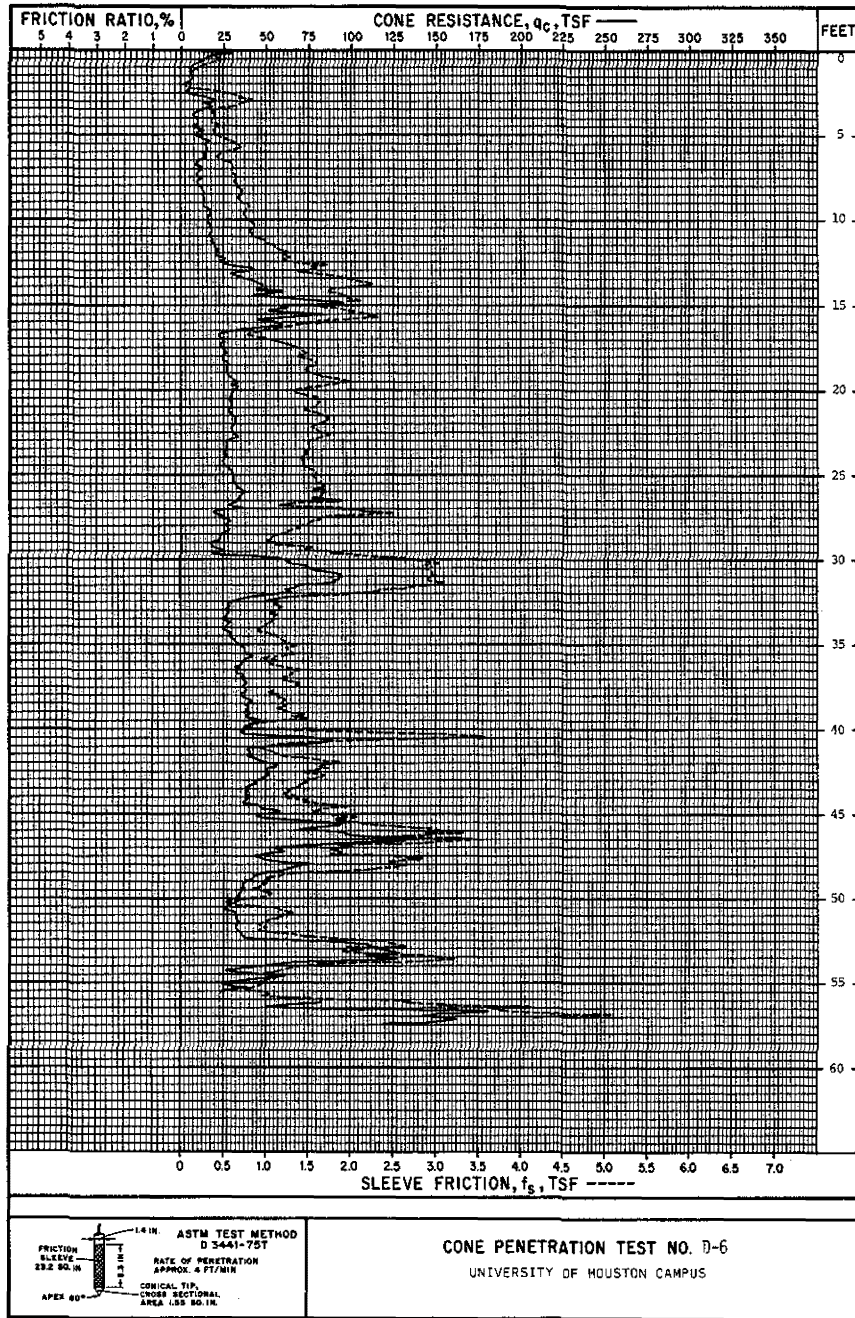


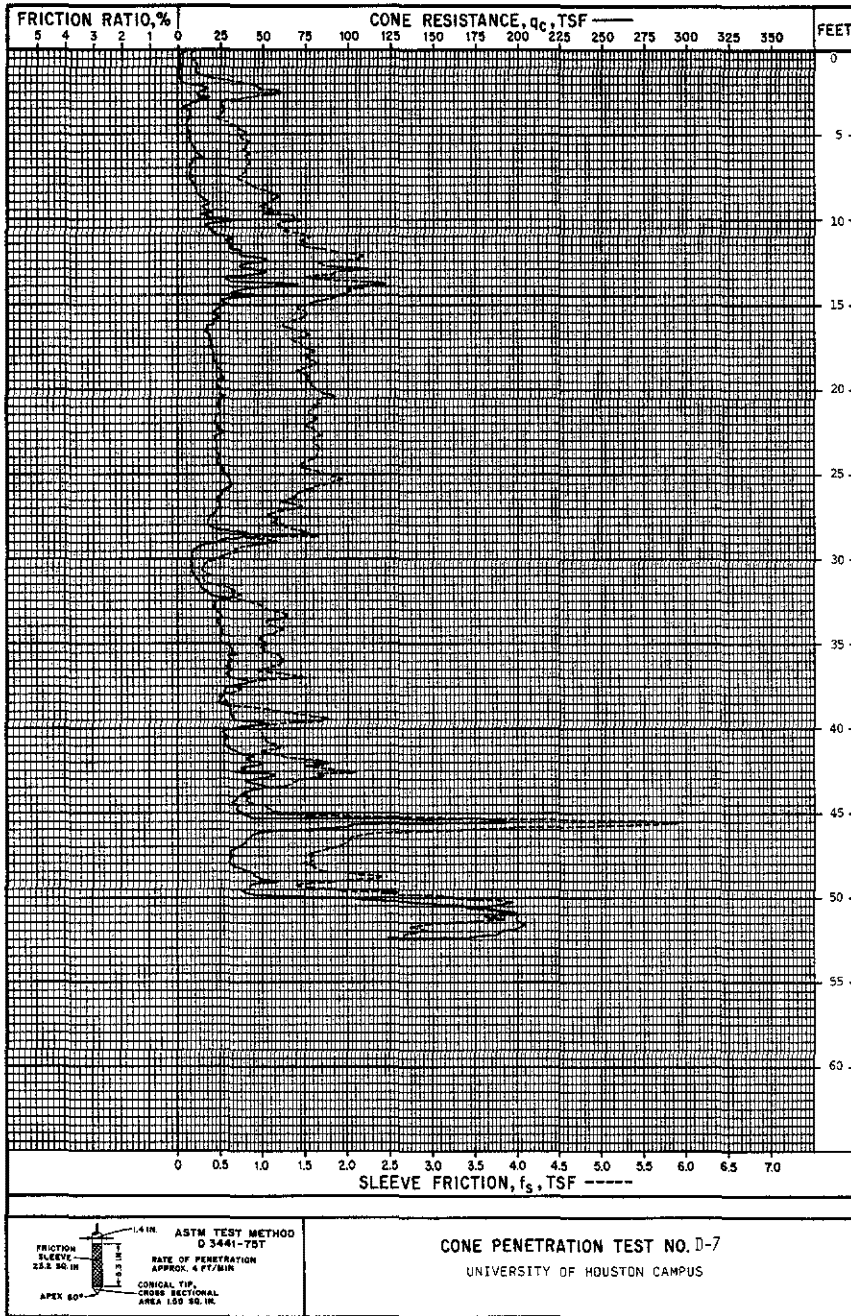


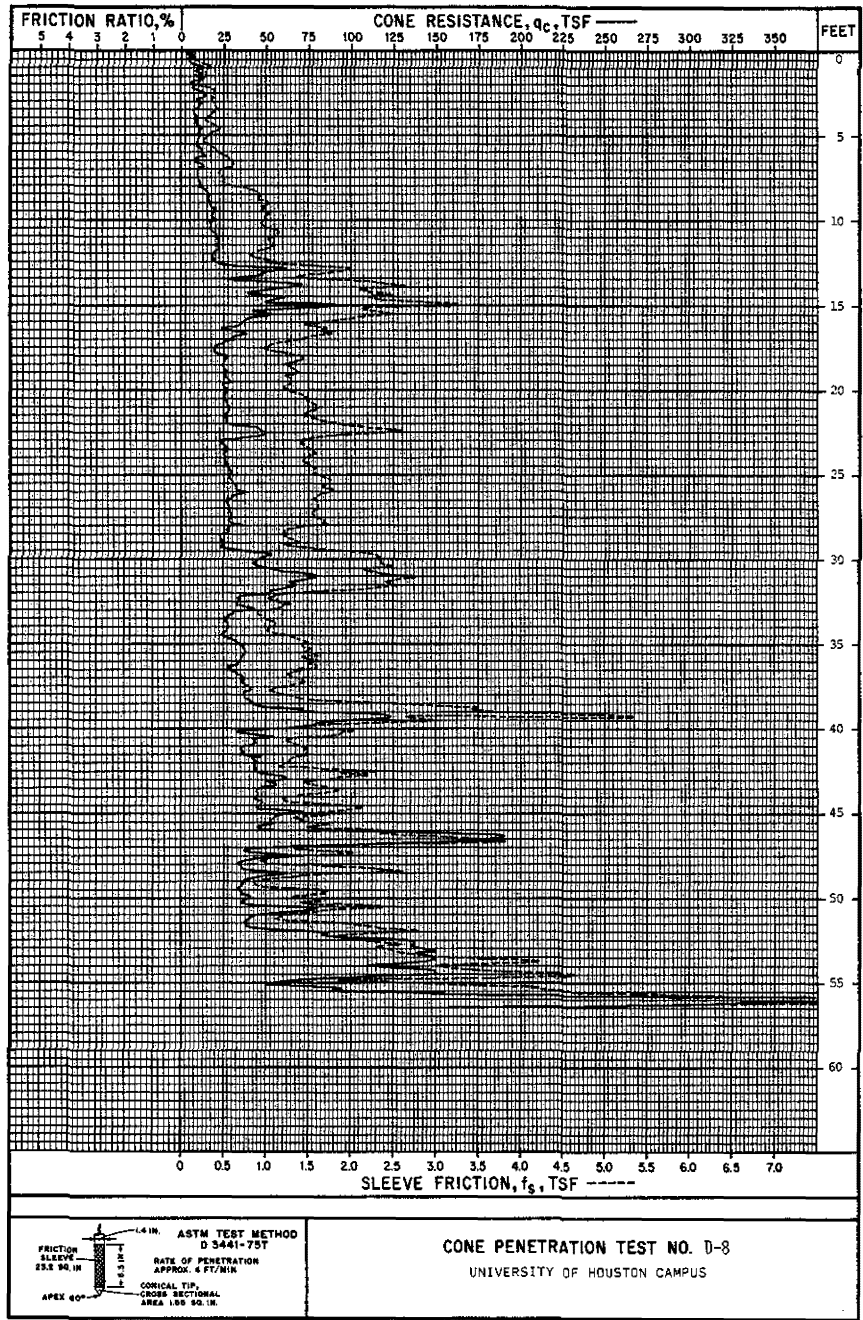
CONE SOUNDING LOG
 LOCATION OF
 UNIVERSITY OF HOUSTON CAMPUS

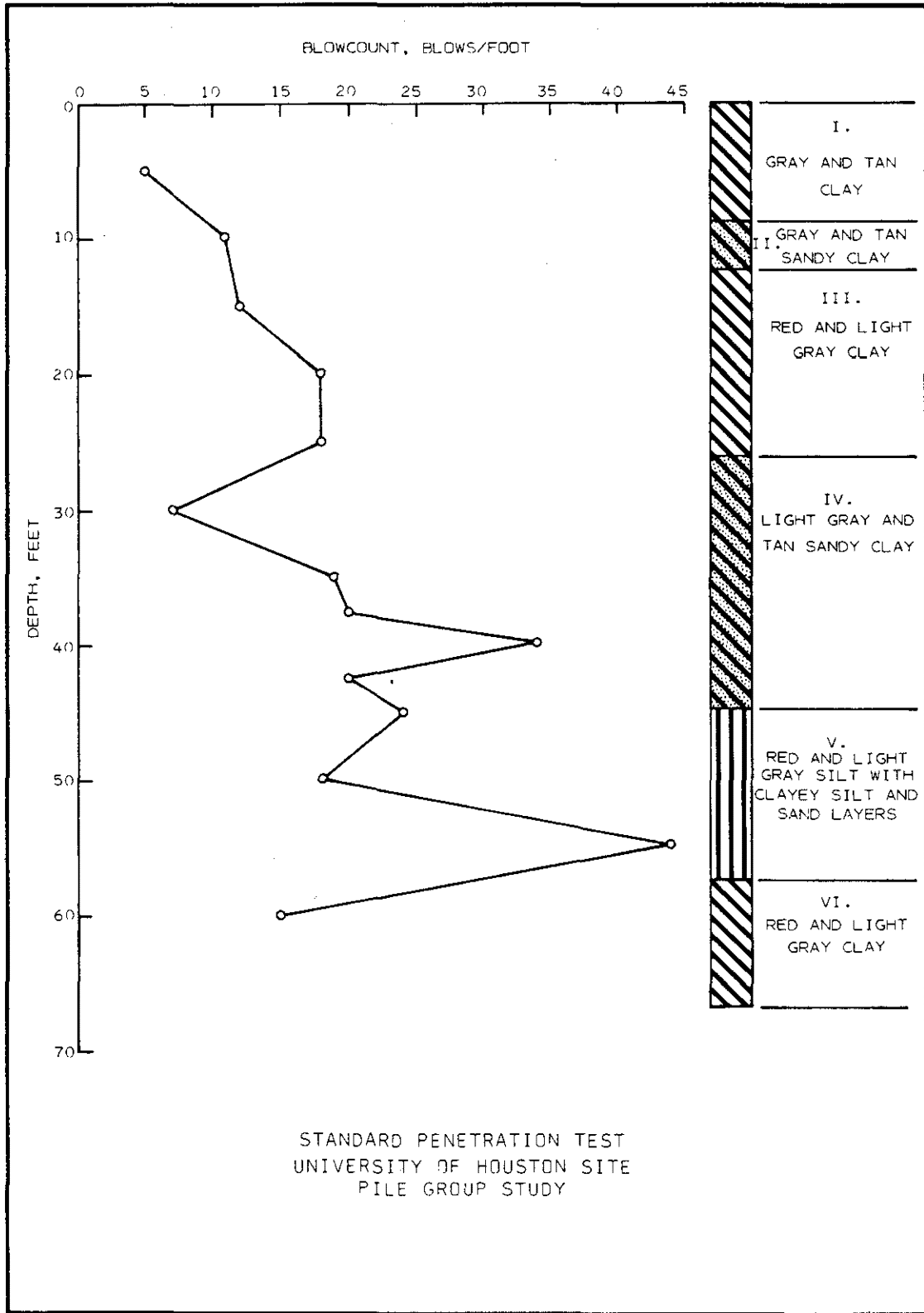


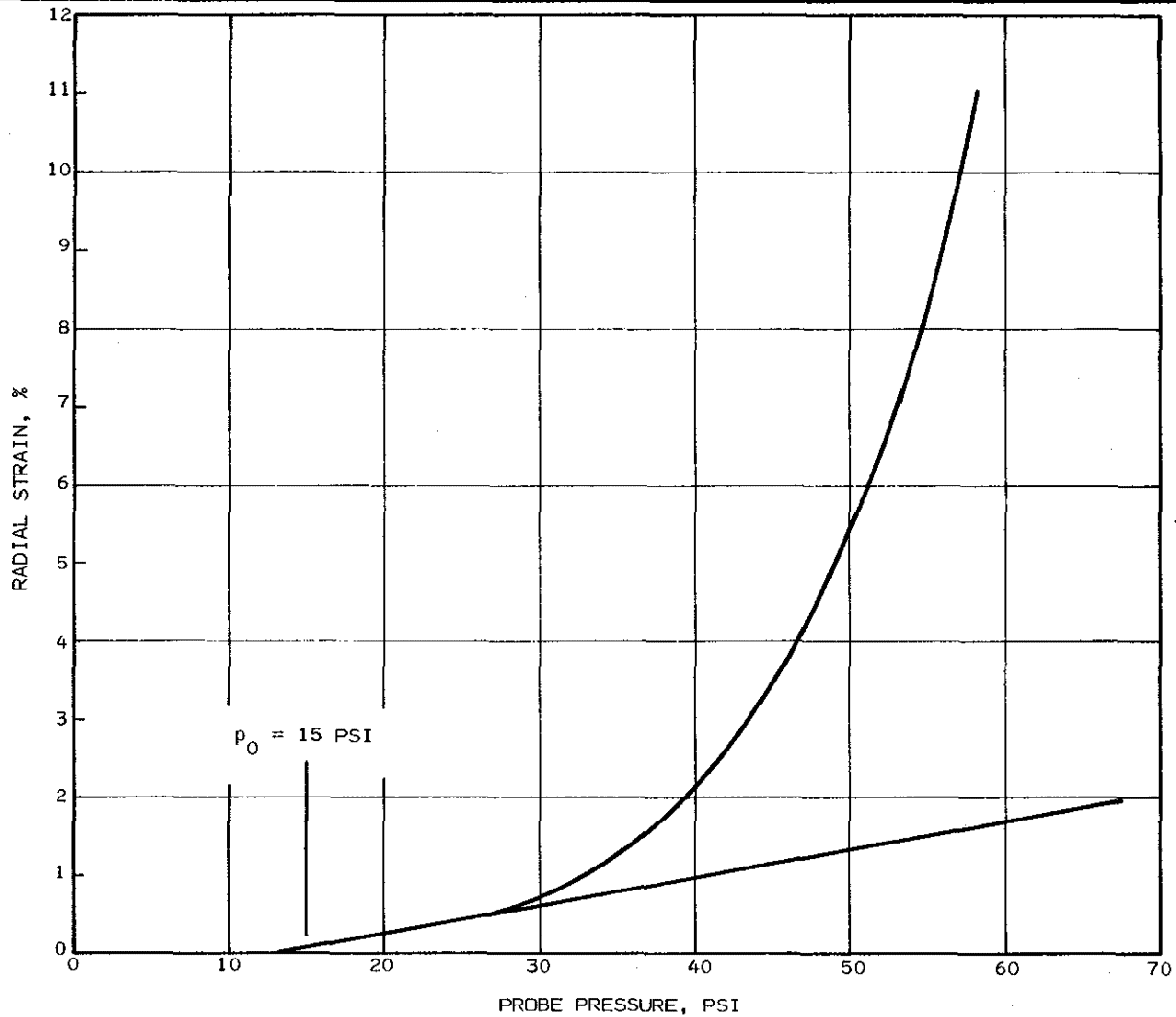






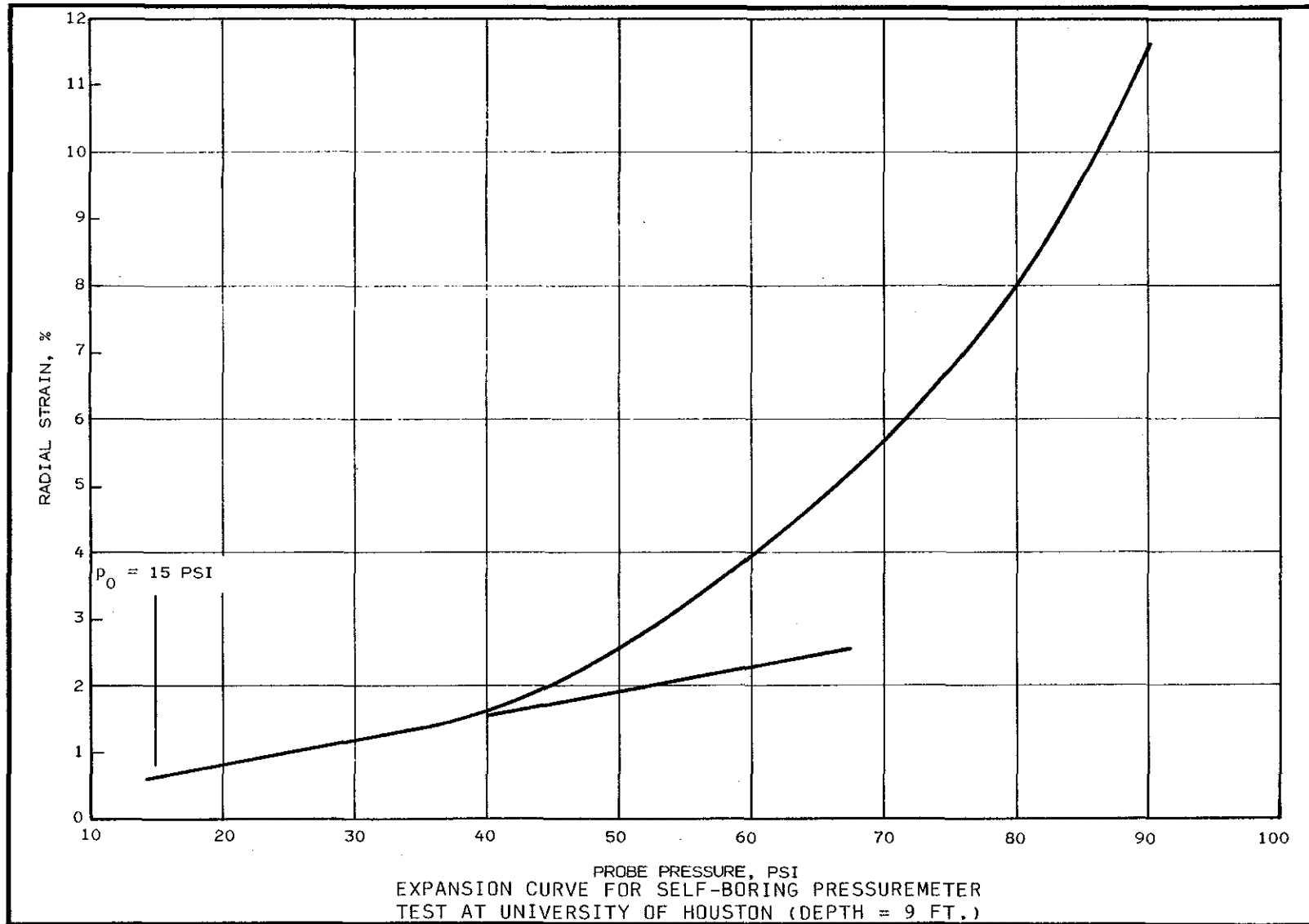


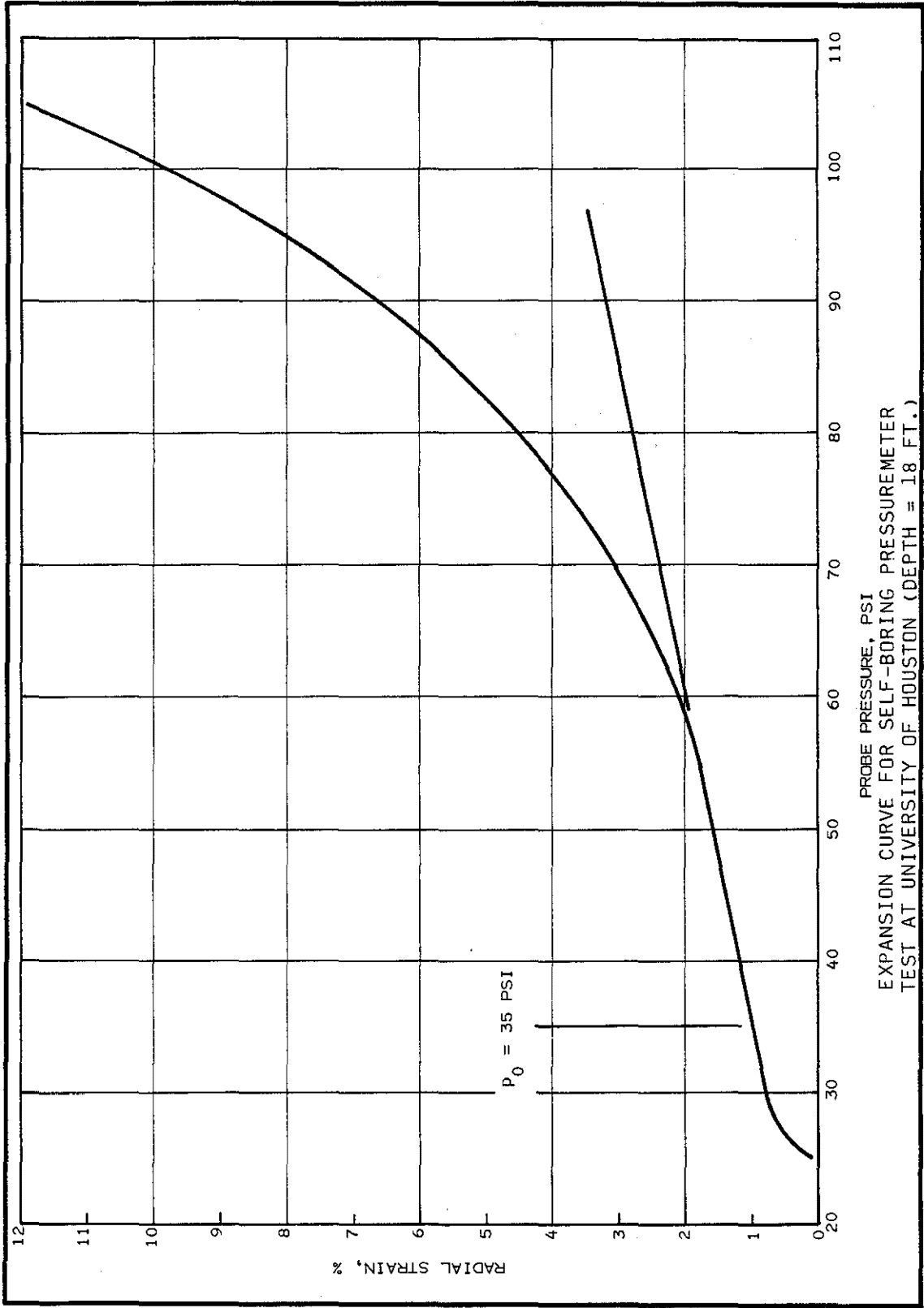




EXPANSION CURVE FOR SELF-BORING PRESSUREMETER
TEST AT UNIVERSITY OF HOUSTON (DEPTH = 8.3 FT.)

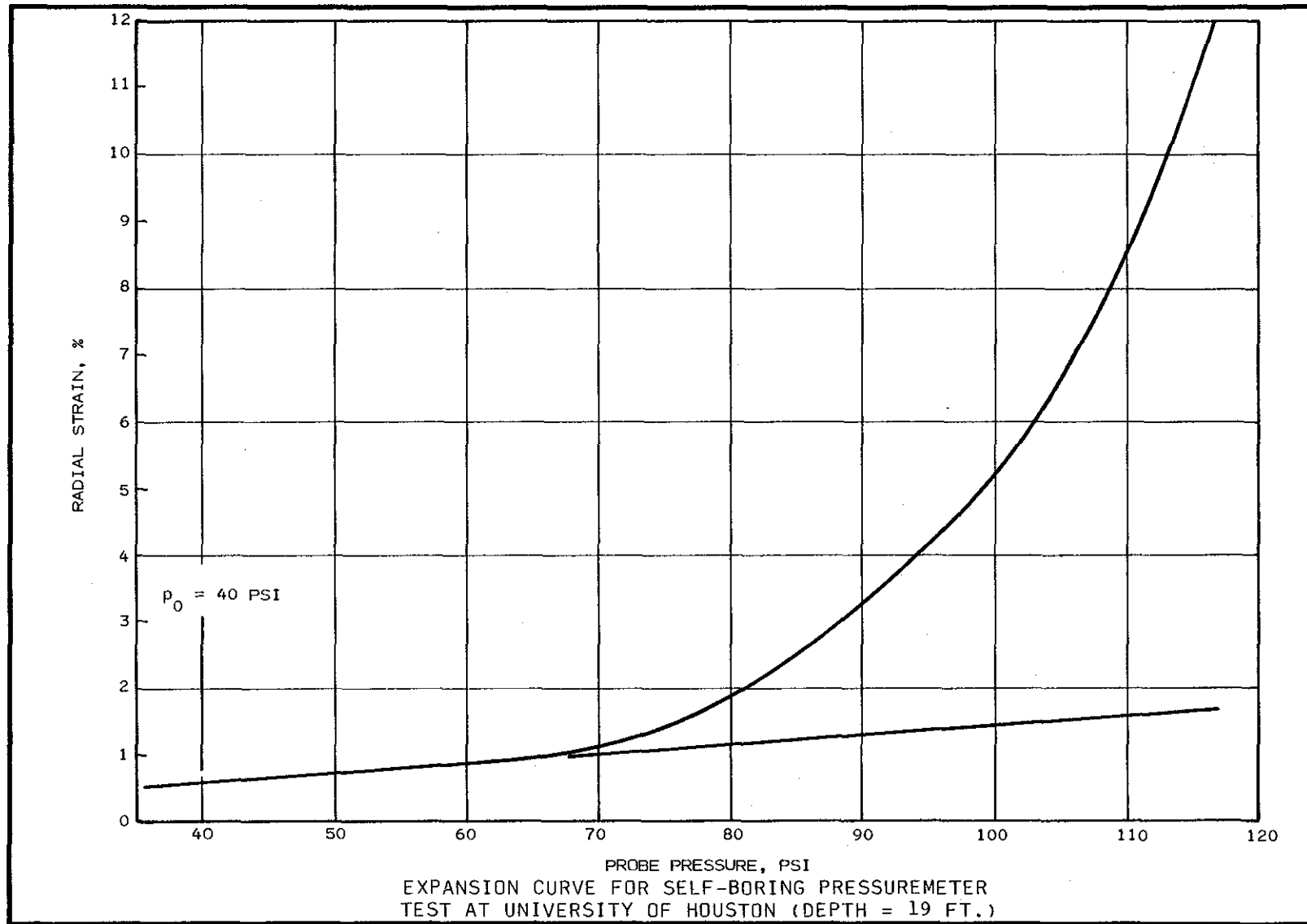
C109

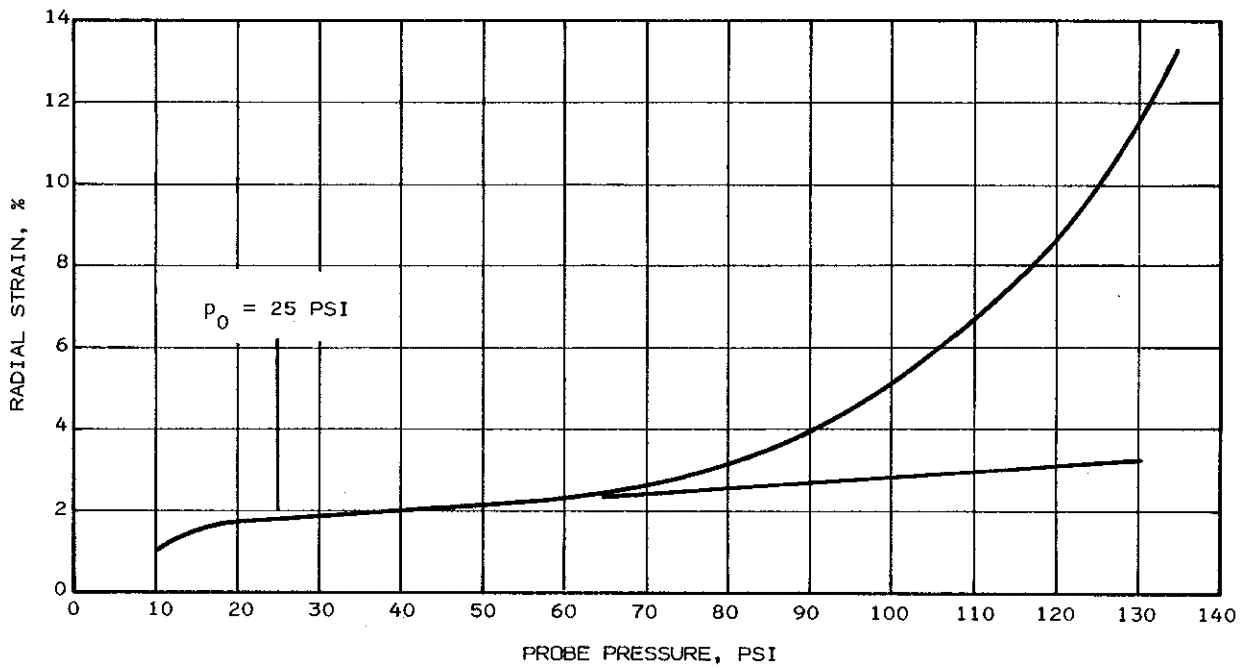




EXPANSION CURVE FOR SELF-BORING PRESSUREMETER
 TEST AT UNIVERSITY OF HOUSTON (DEPTH = 18 FT.)

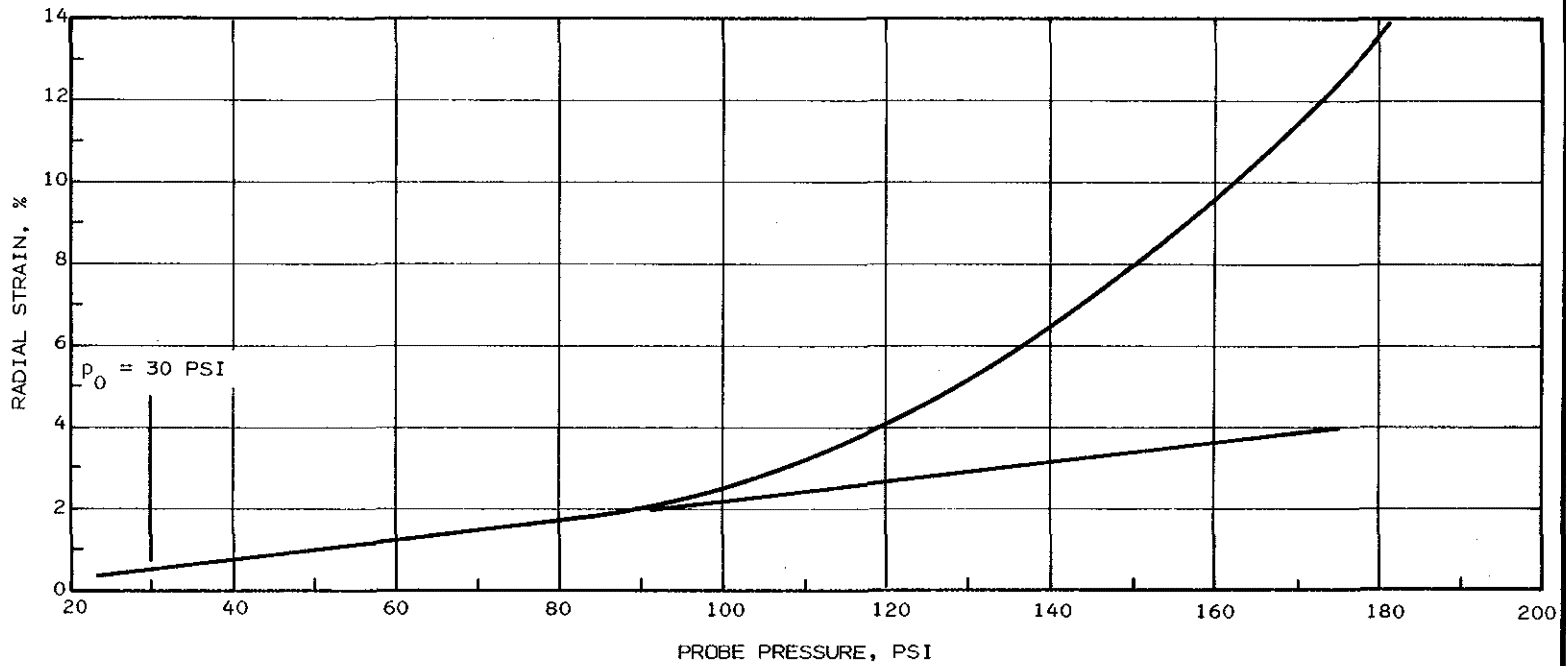
C117





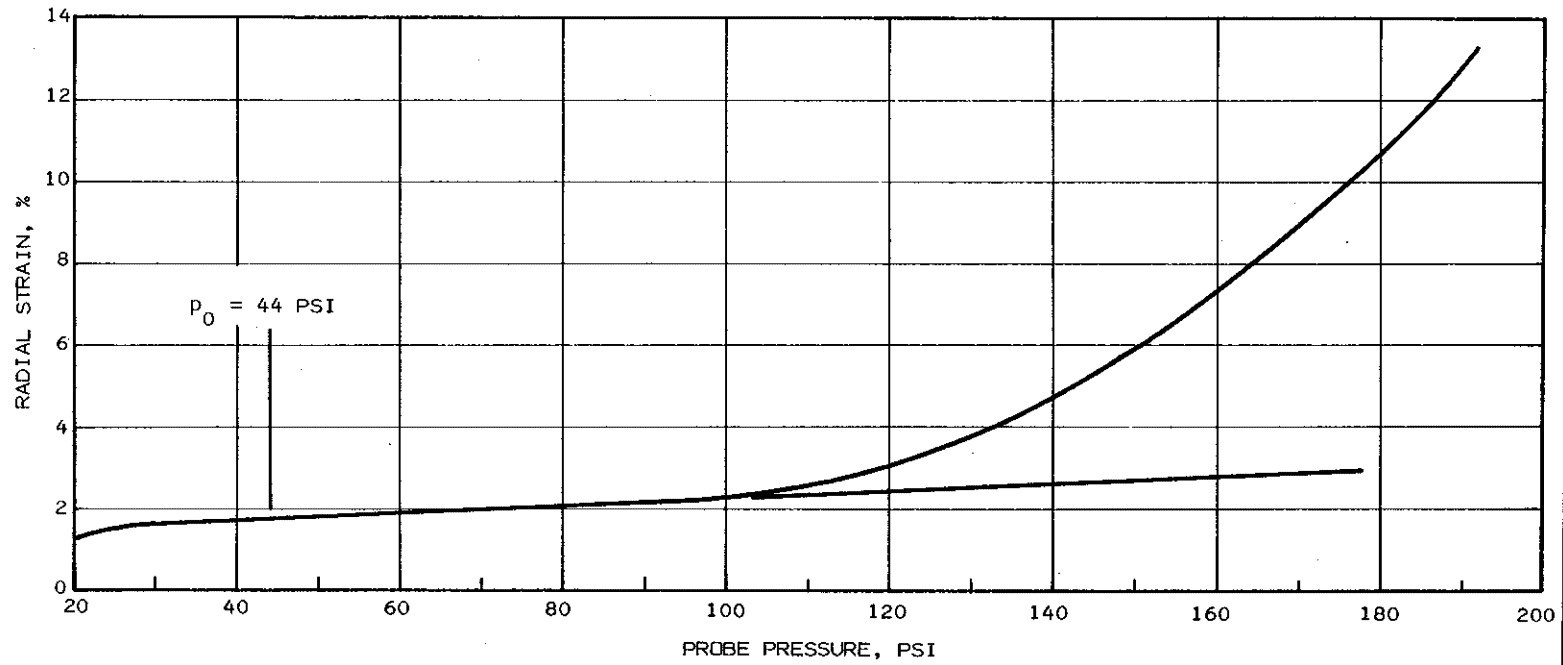
EXPANSION CURVE FOR SELF-BORING PRESSUREMETER
TEST AT UNIVERSITY OF HOUSTON (DEPTH = 28 FT.)

C112

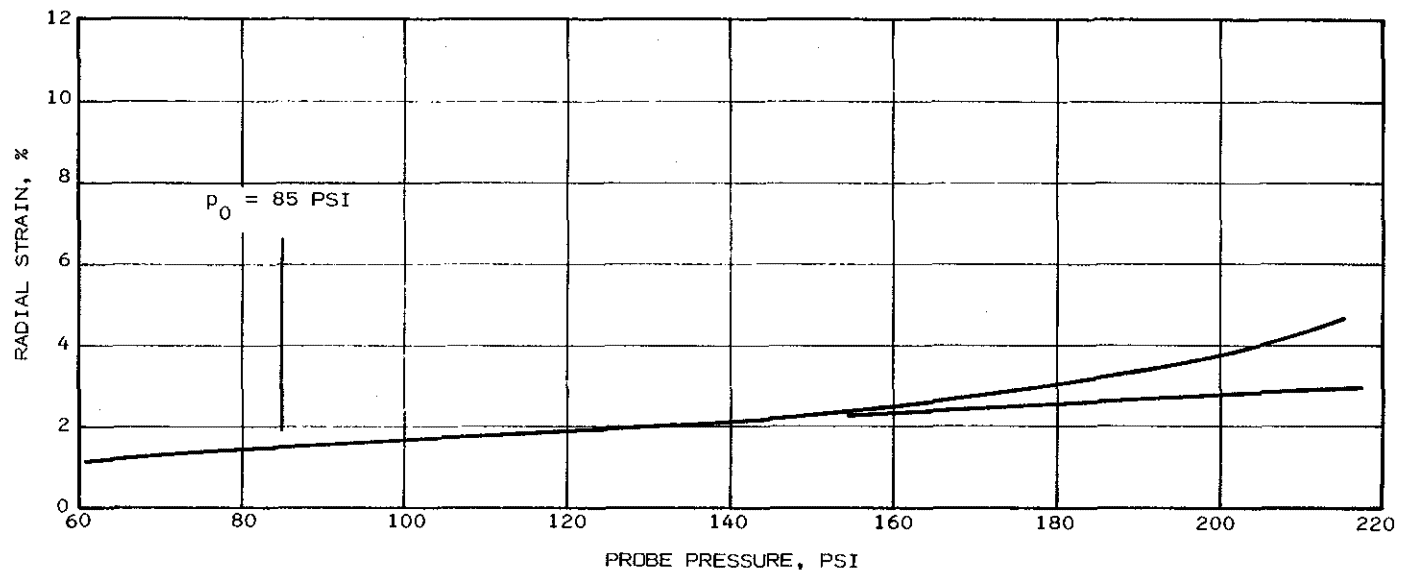


EXPANSION CURVE FOR SELF-BORING PRESSUREMETER
TEST AT UNIVERSITY OF HOUSTON (DEPTH = 38 FT.)

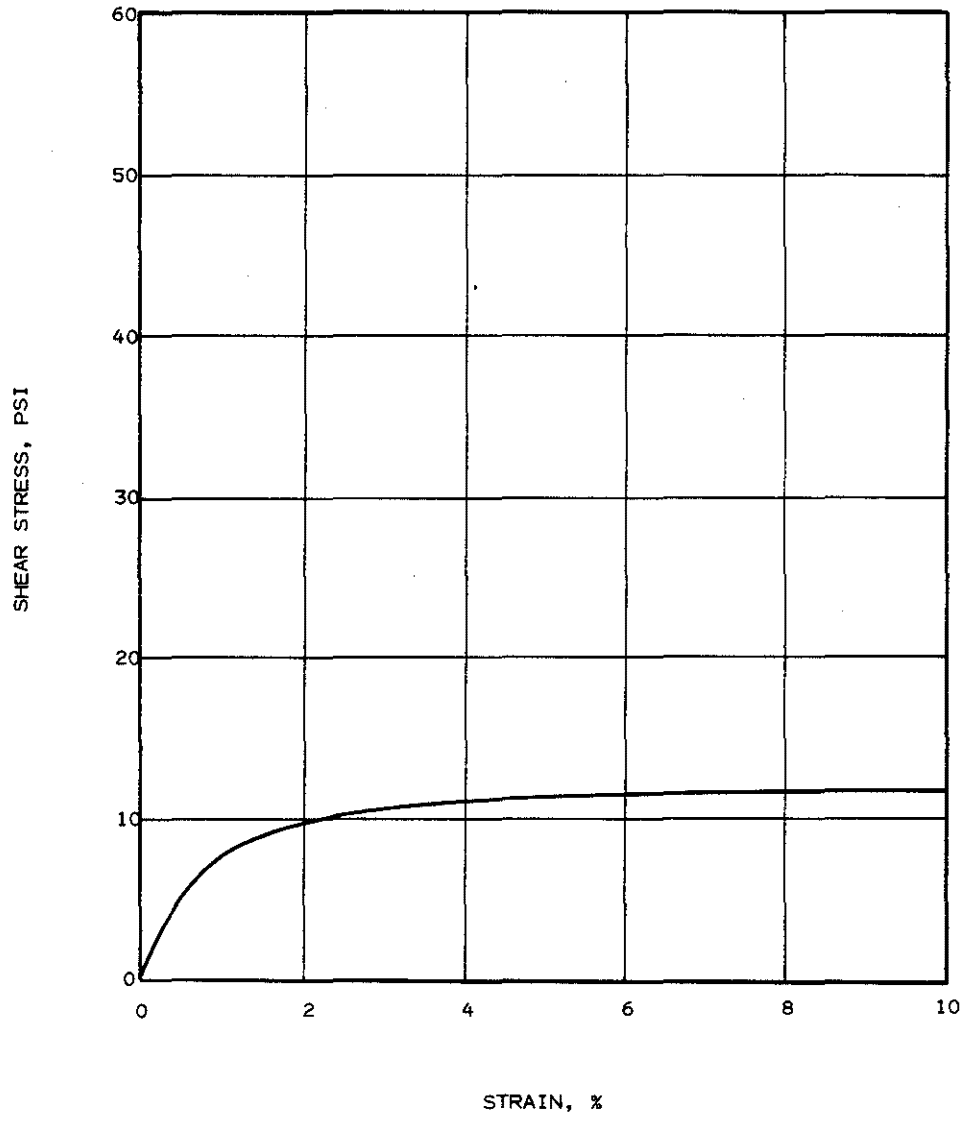
C114



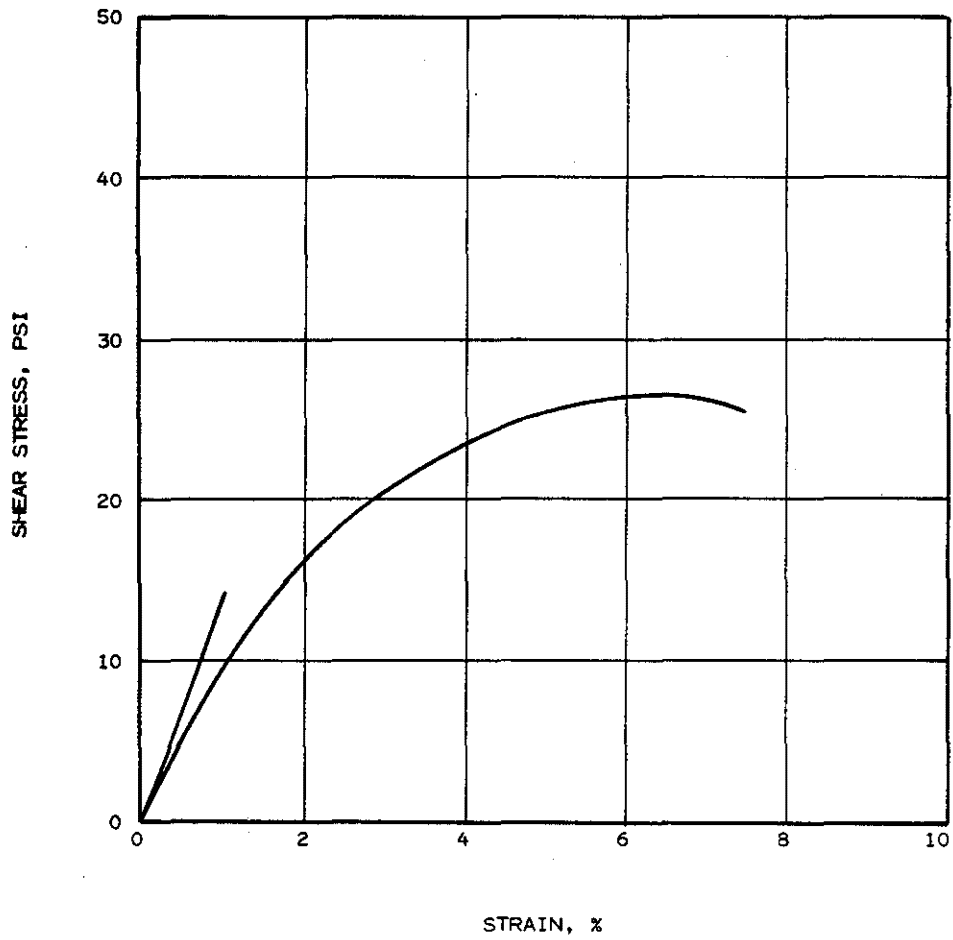
EXPANSION CURVE FOR SELF-BORING PRESSUREMETER
TEST AT UNIVERSITY OF HOUSTON (DEPTH = 48 FT.)



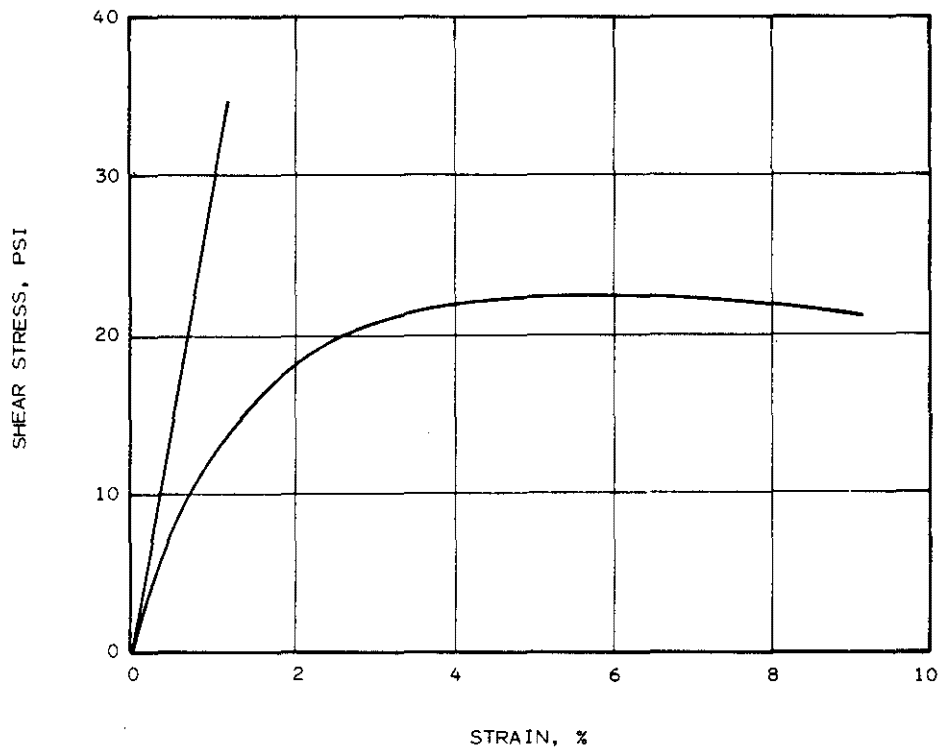
EXPANSION CURVE FOR SELF-BORING PRESSUREMETER
TEST AT UNIVERSITY OF HOUSTON (DEPTH = 62 FT.)



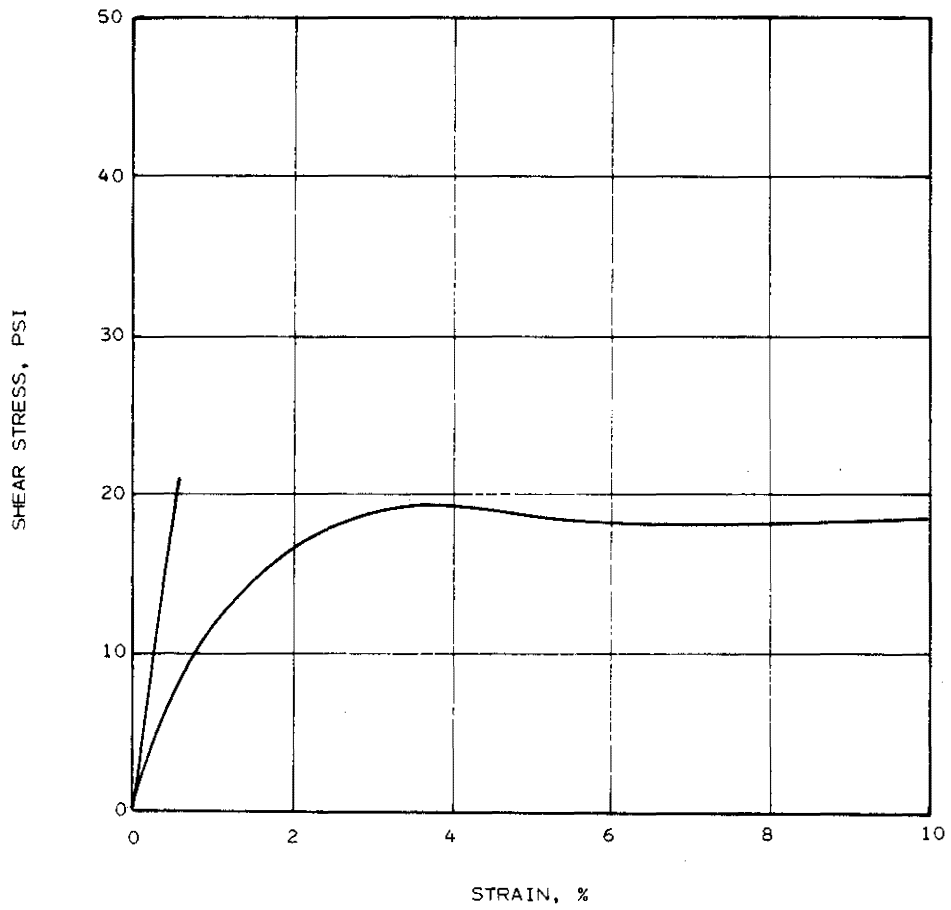
STRESS - STRAIN CURVE
FROM PRESSUREMETER TESTS
DEPTH = 8.3 FEET
AT PM1



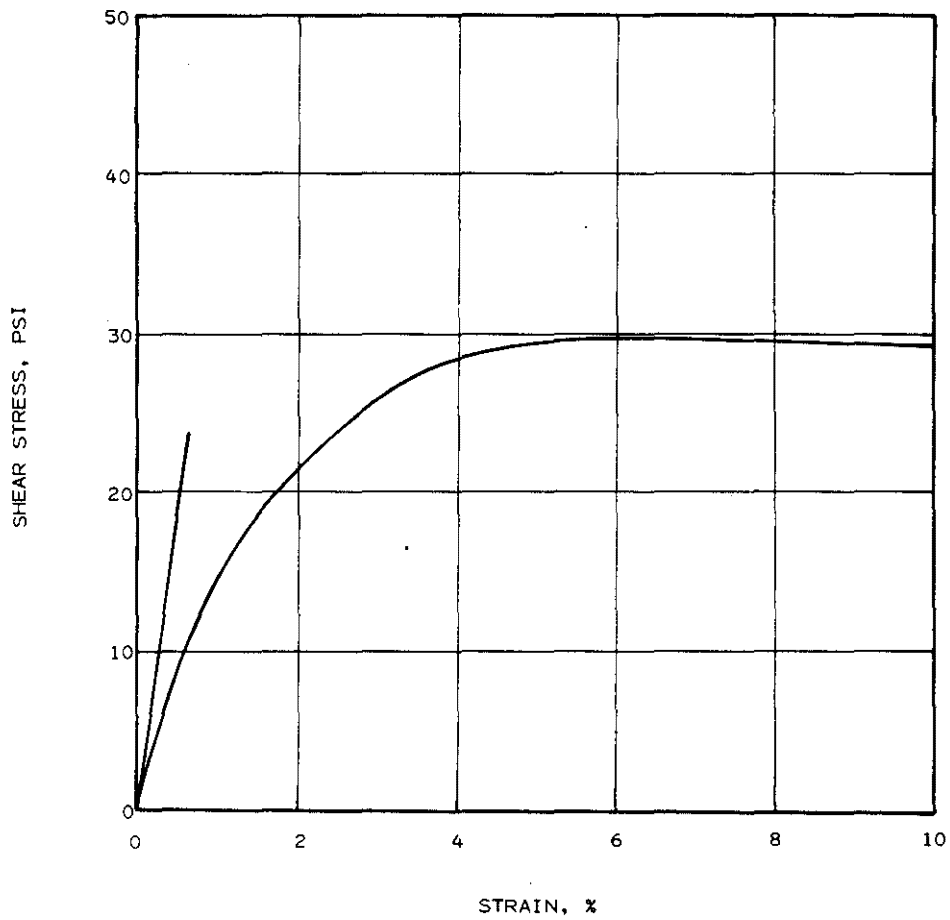
STRESS - STRAIN CURVE
FROM PRESSUREMETER TESTS
DEPTH = 9 FEET
AT PM2



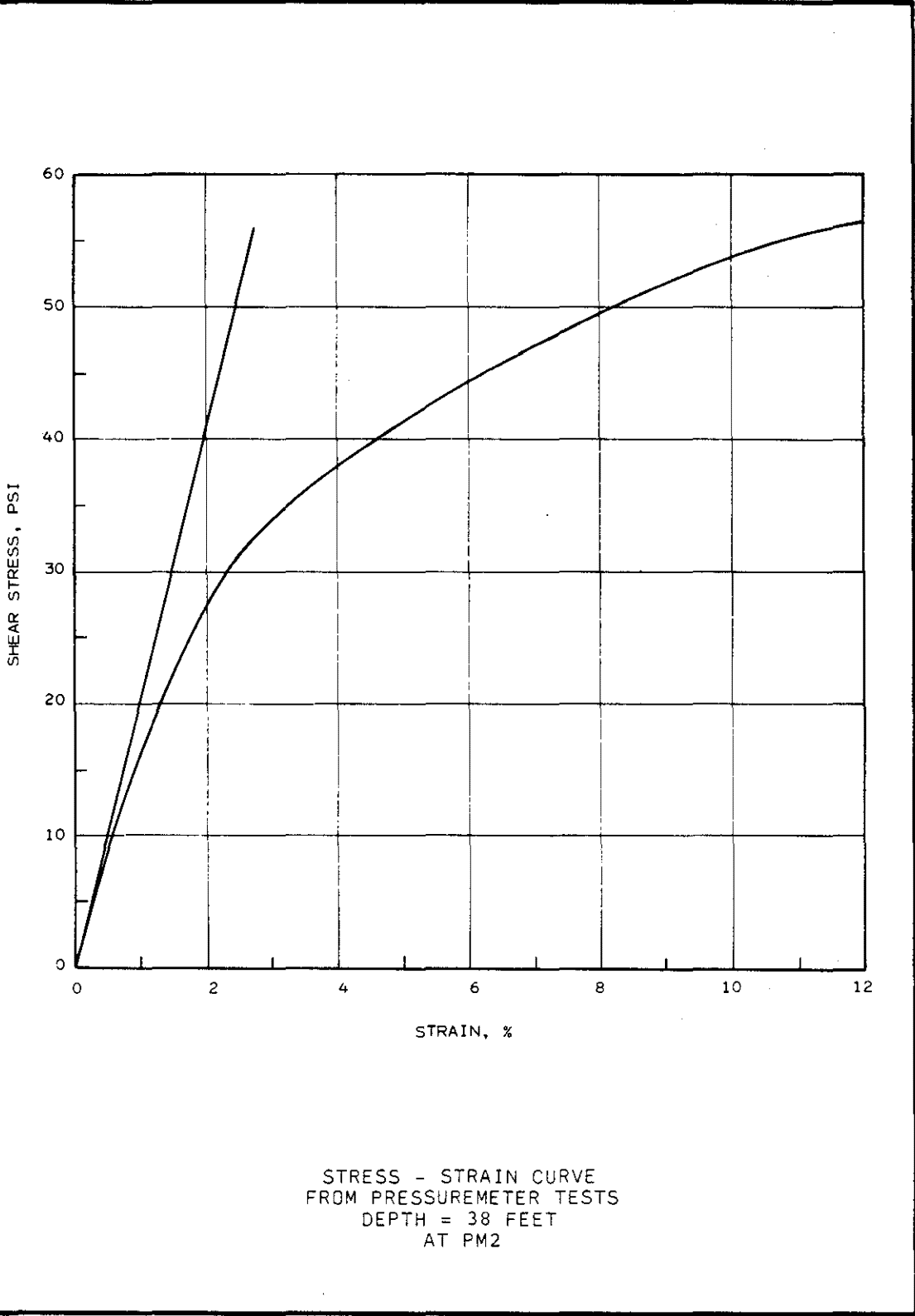
STRESS - STRAIN CURVE
FROM PRESSUREMETER TESTS
DEPTH = 18 FEET
AT PM2



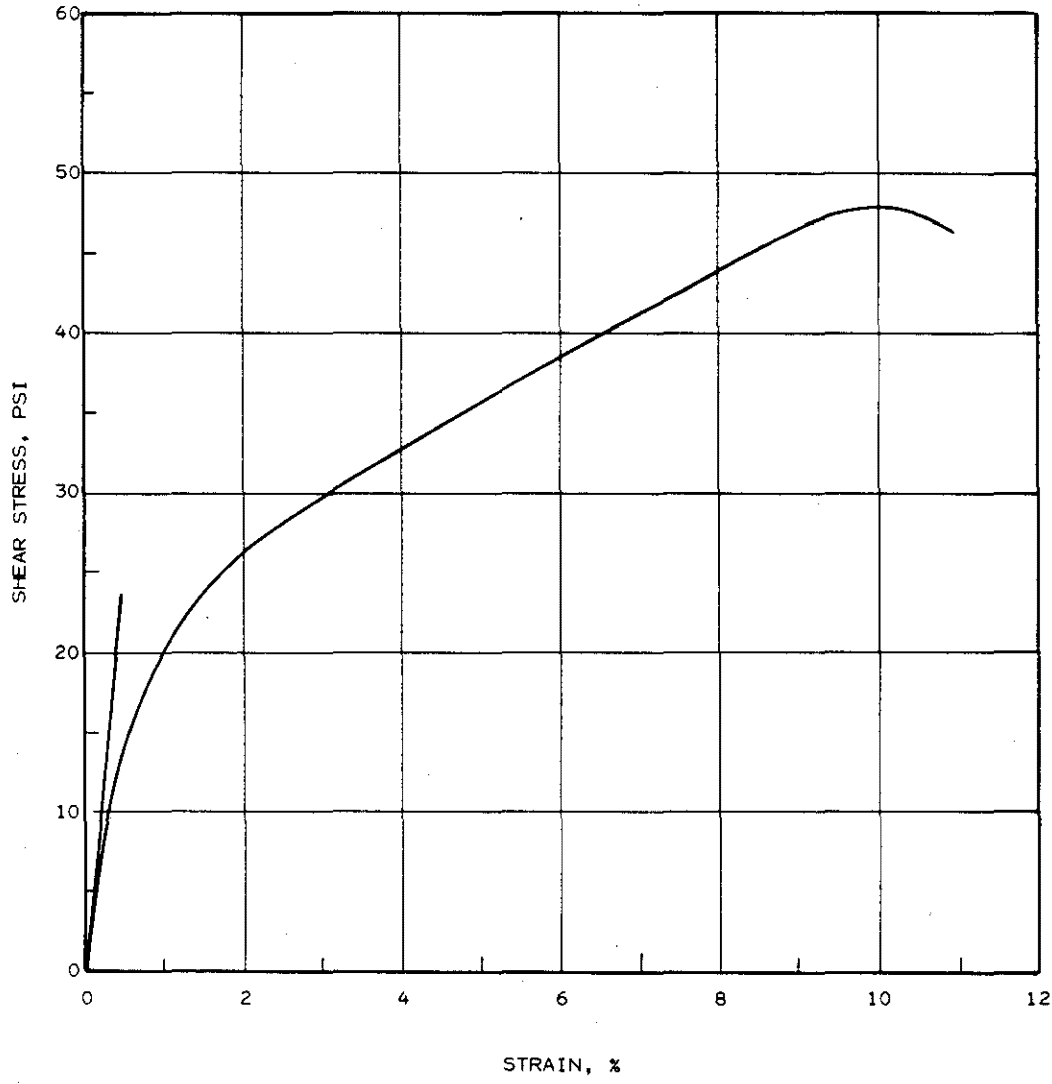
STRESS - STRAIN CURVE
FROM PRESSUREMETER TESTS
DEPTH = 19 FEET
AT PM1



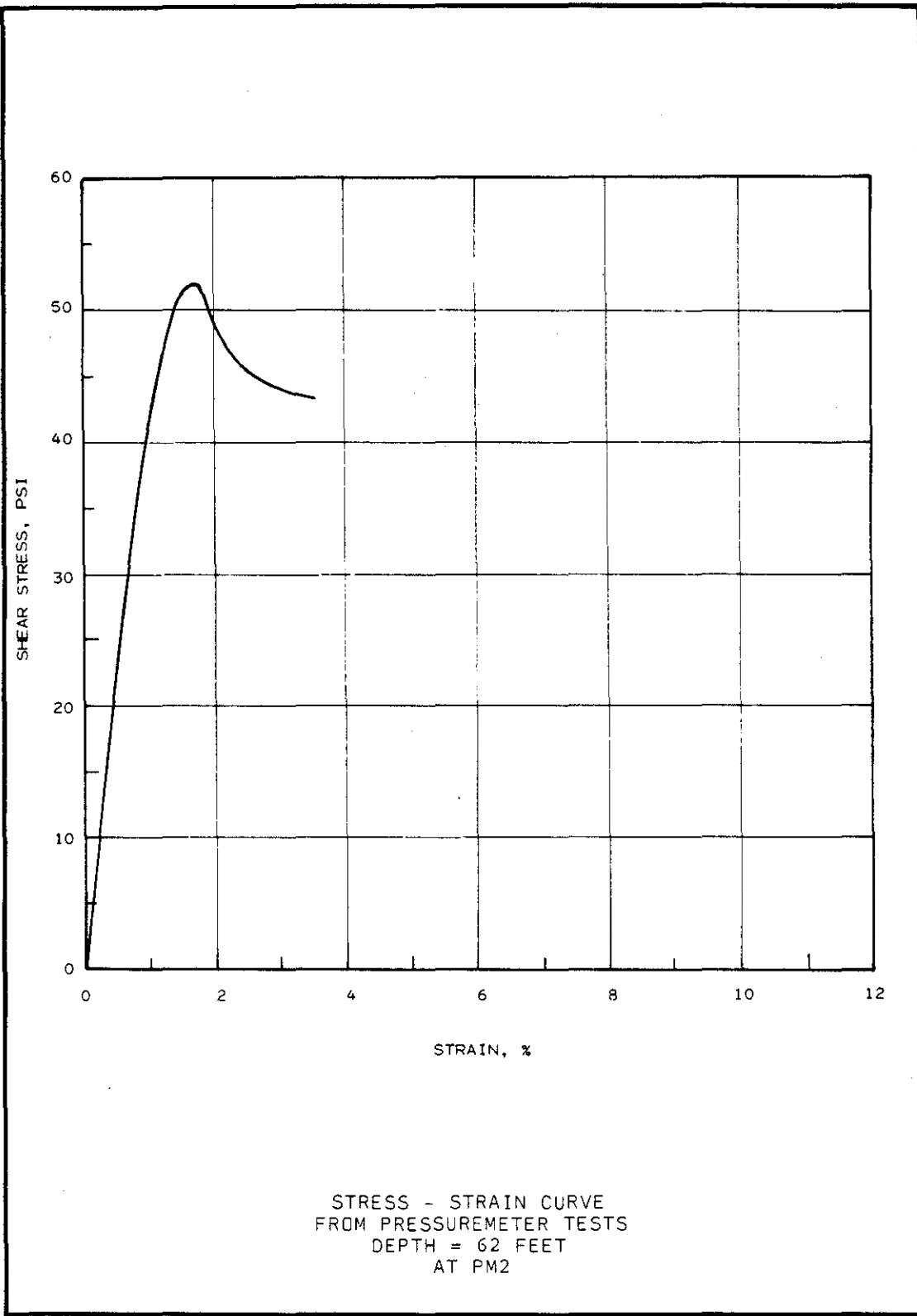
STRESS - STRAIN CURVE
FROM PRESSUREMETER TESTS
DEPTH = 28 FEET
AT PM2



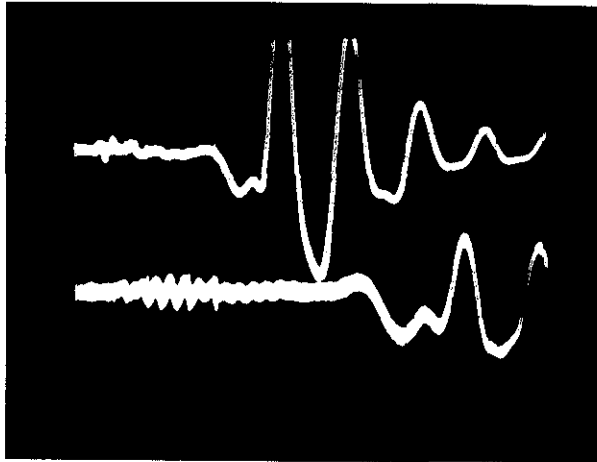
STRESS - STRAIN CURVE
FROM PRESSUREMETER TESTS
DEPTH = 38 FEET
AT PM2



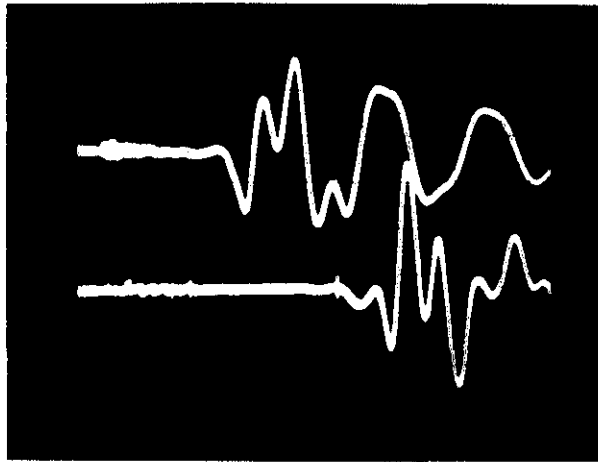
STRESS - STRAIN CURVE
FROM PRESSUREMETER TESTS
DEPTH = 48 FEET
AT PM2



STRESS - STRAIN CURVE
FROM PRESSUREMETER TESTS
DEPTH = 62 FEET
AT PM2

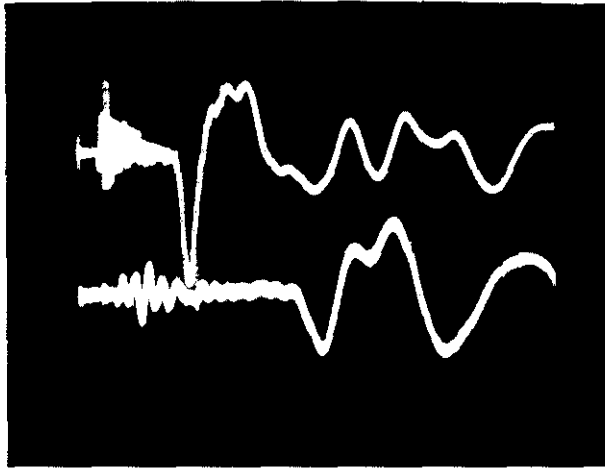


DEPTH = 15'
SWEEP RATE = 5MS/DIV.
SENSITIVITY:
CHANNEL 1 = 5MV./DIV.
CHANNEL 2 = 5MV./DIV.

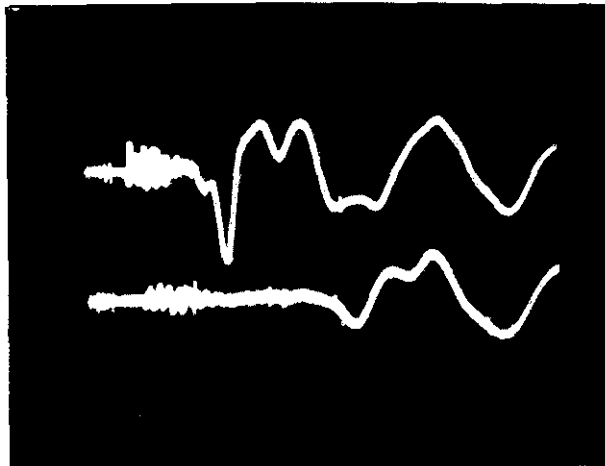


DEPTH = 25'
SWEEP RATE = 5MS/DIV.
SENSITIVITY:
CHANNEL 1 = 50 MV./DIV.
CHANNEL 2 = 20 MV./DIV.

EXAMPLE CROSS HOLE TEST RECORDS

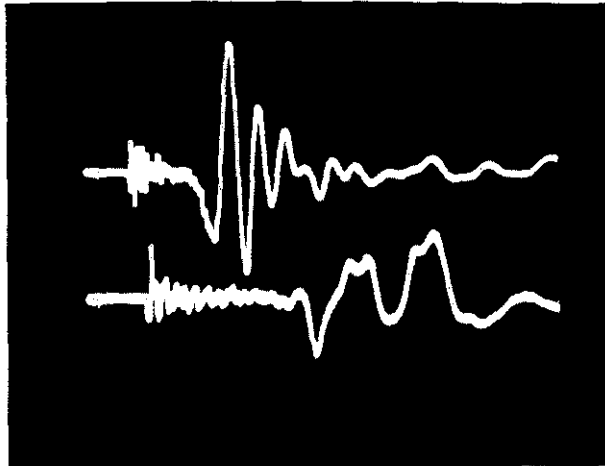


DEPTH = 37'
SWEEP RATE = 5MS/DIV.
SENSITIVITY:
CHANNEL 1 = 10MV./DIV.
CHANNEL 2 = 5MV./DIV.



DEPTH = 40'
SWEEP RATE = 5MS/DIV.
SENSITIVITY:
CHANNEL 1 = 10MV./DIV.
CHANNEL 2 = 5MV./DIV.

EXAMPLE CROSS HOLE TEST RECORDS



DEPTH = 50'
SWEEP RATE = 5MS/DIV.
SENSITIVITY:
CHANNEL 1 = 20MV./DIV.
CHANNEL 2 = 5MV./DIV.

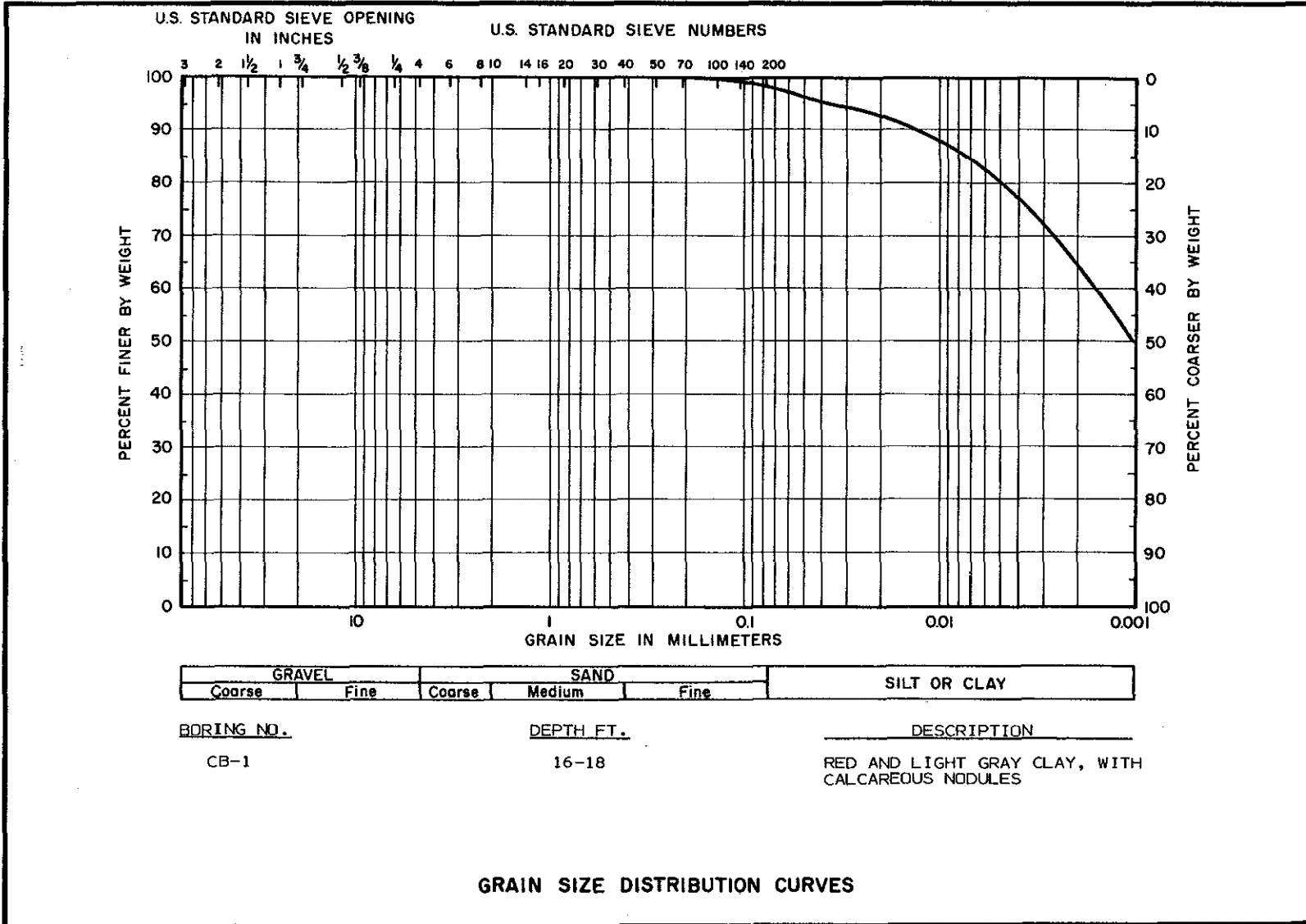


DEPTH = 59'
SWEEP RATE = 5MS/DIV.
SENSITIVITY:
CHANNEL 1 = 20MV./DIV.
CHANNEL 2 = 10MV./DIV.

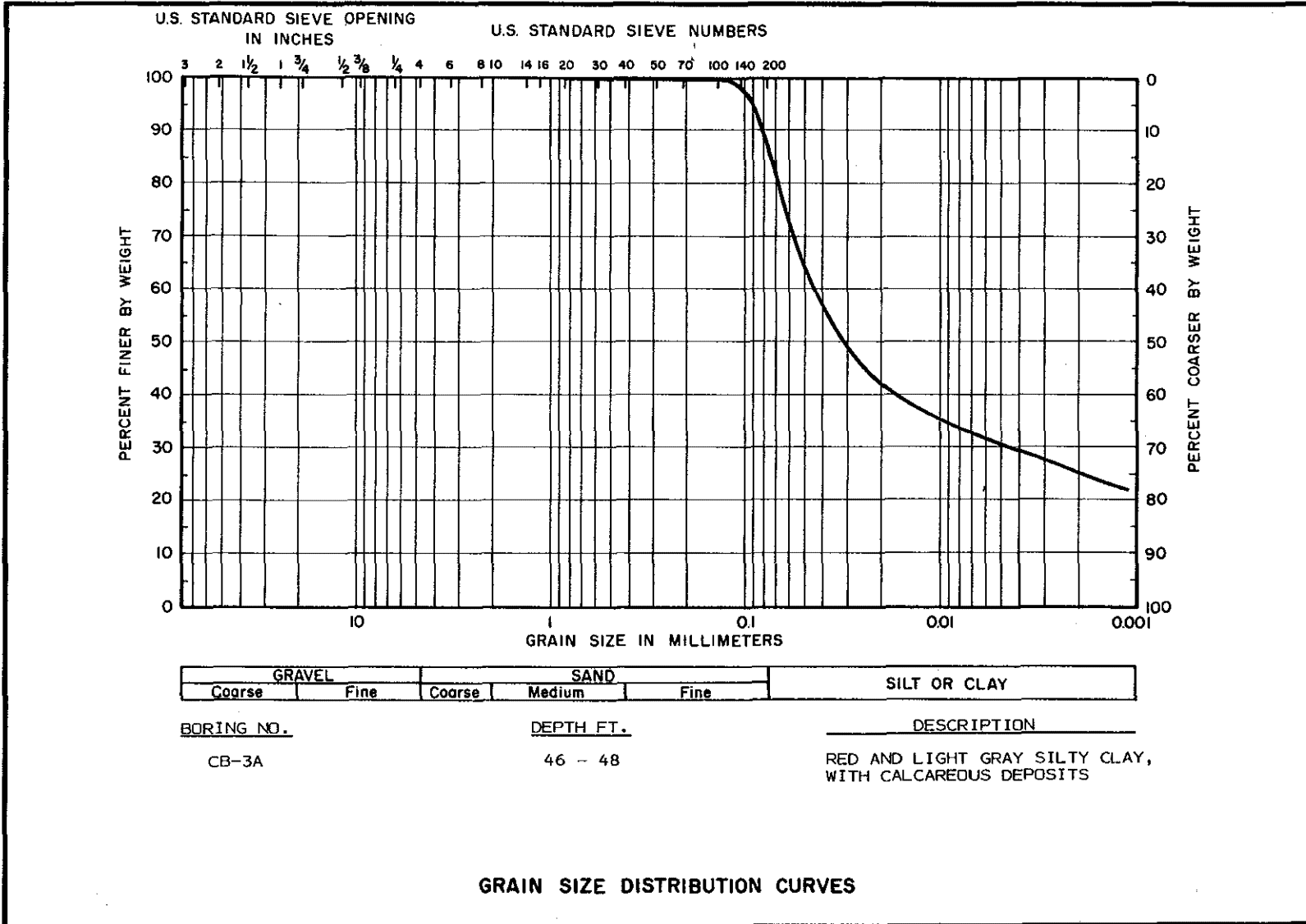
EXAMPLE CROSS HOLE TEST RECORDS

ADDENDUM B

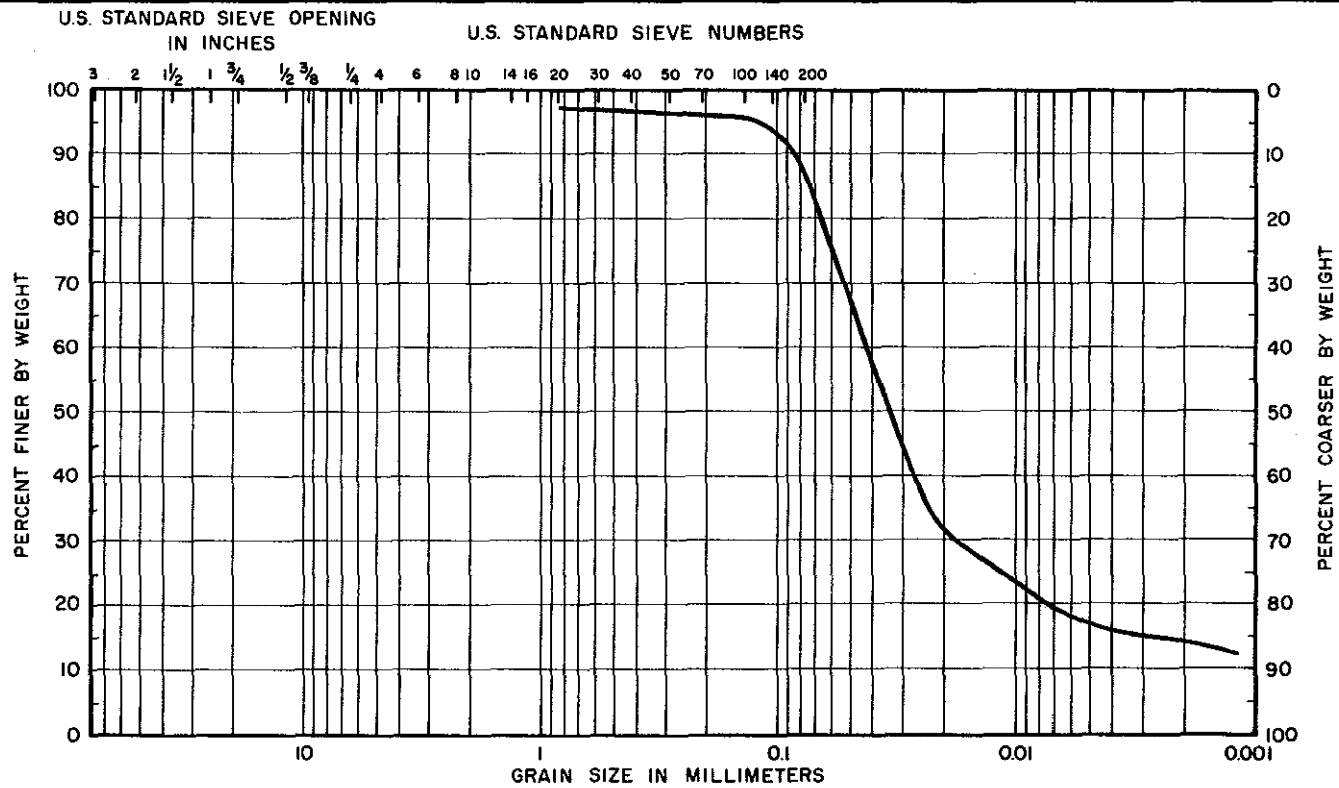
C128



C131



C132



GRAVEL		SAND			SILT OR CLAY
Coarse	Fine	Coarse	Medium	Fine	

BORING NO.

CB-3A

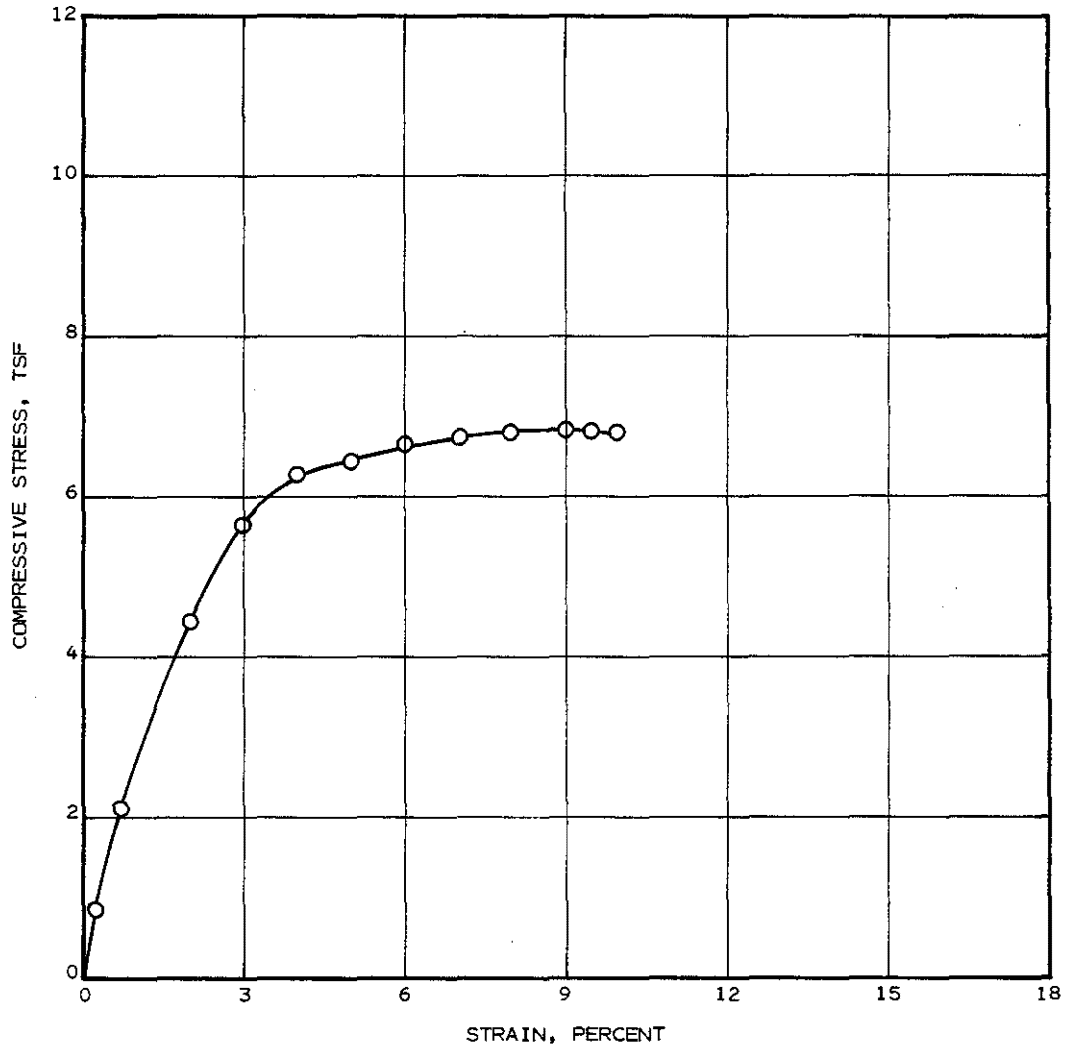
DEPTH FT.

48 - 50

DESCRIPTION

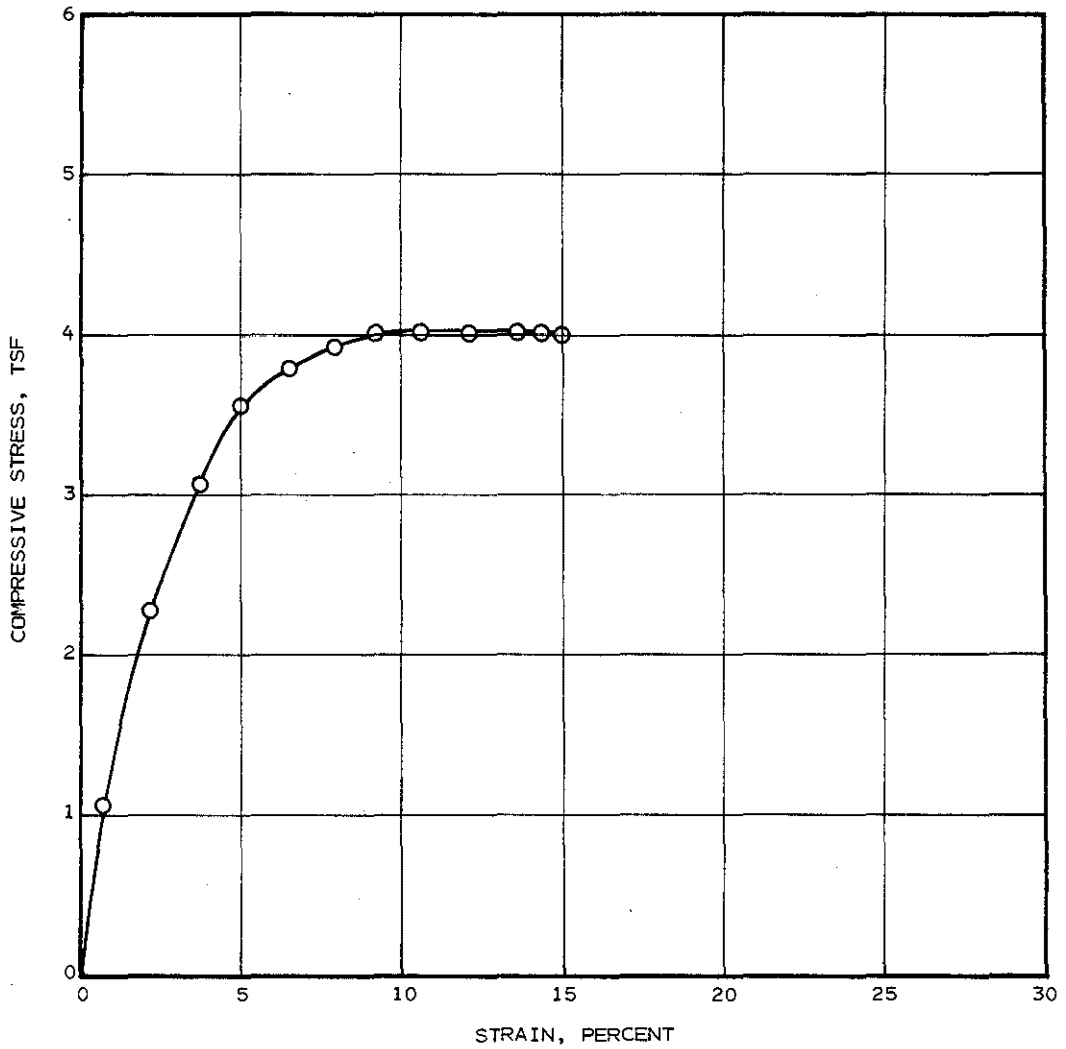
RED SILTY CLAY WITH CALCAREOUS NODULES

GRAIN SIZE DISTRIBUTION CURVES



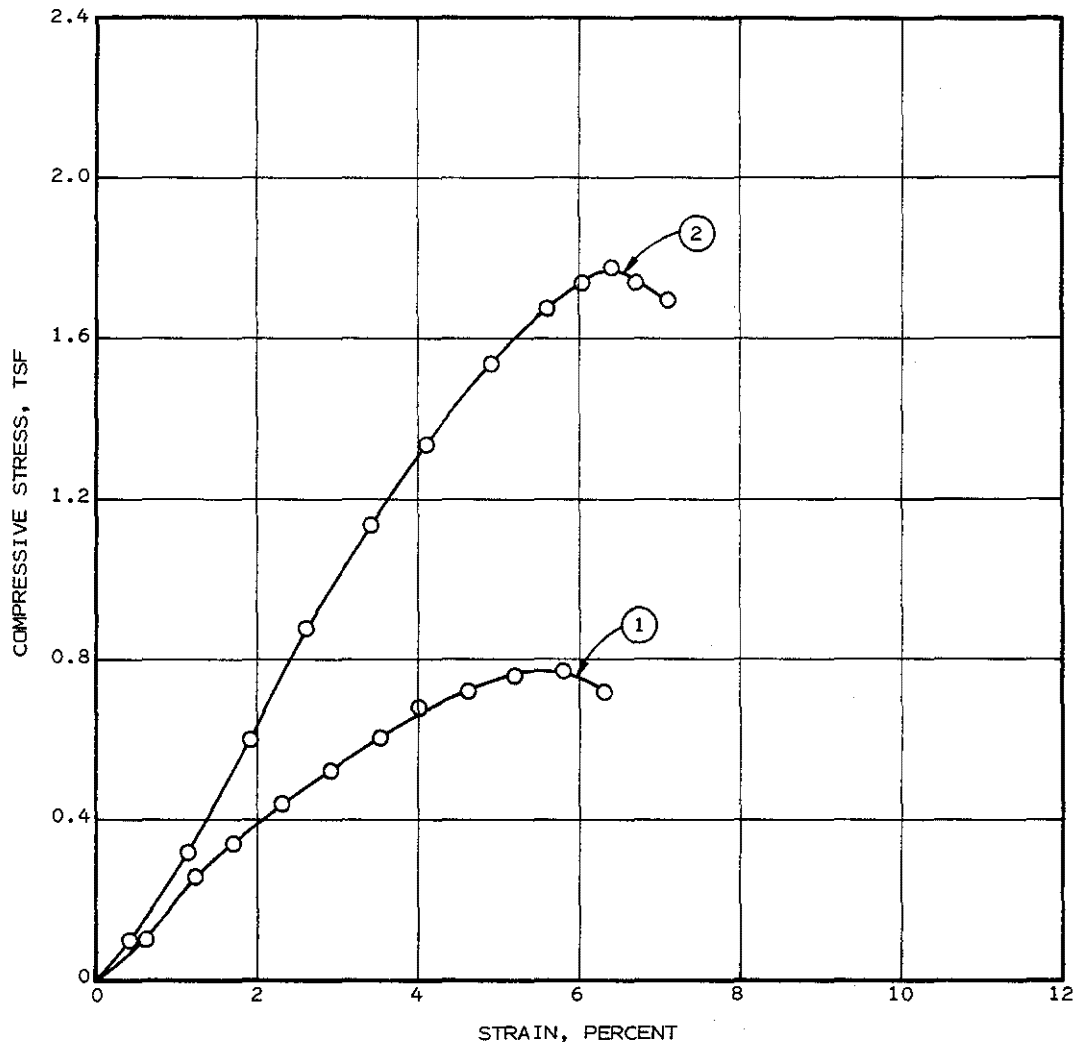
<u>BORING NO.</u>	<u>DEPTH, FT.</u>	<u>MATERIAL</u>
CB-2	5	HARD BROWN CLAY WITH ORGANIC MATERIAL

STRESS-STRAIN CURVES
UNCONFINED COMPRESSION TEST



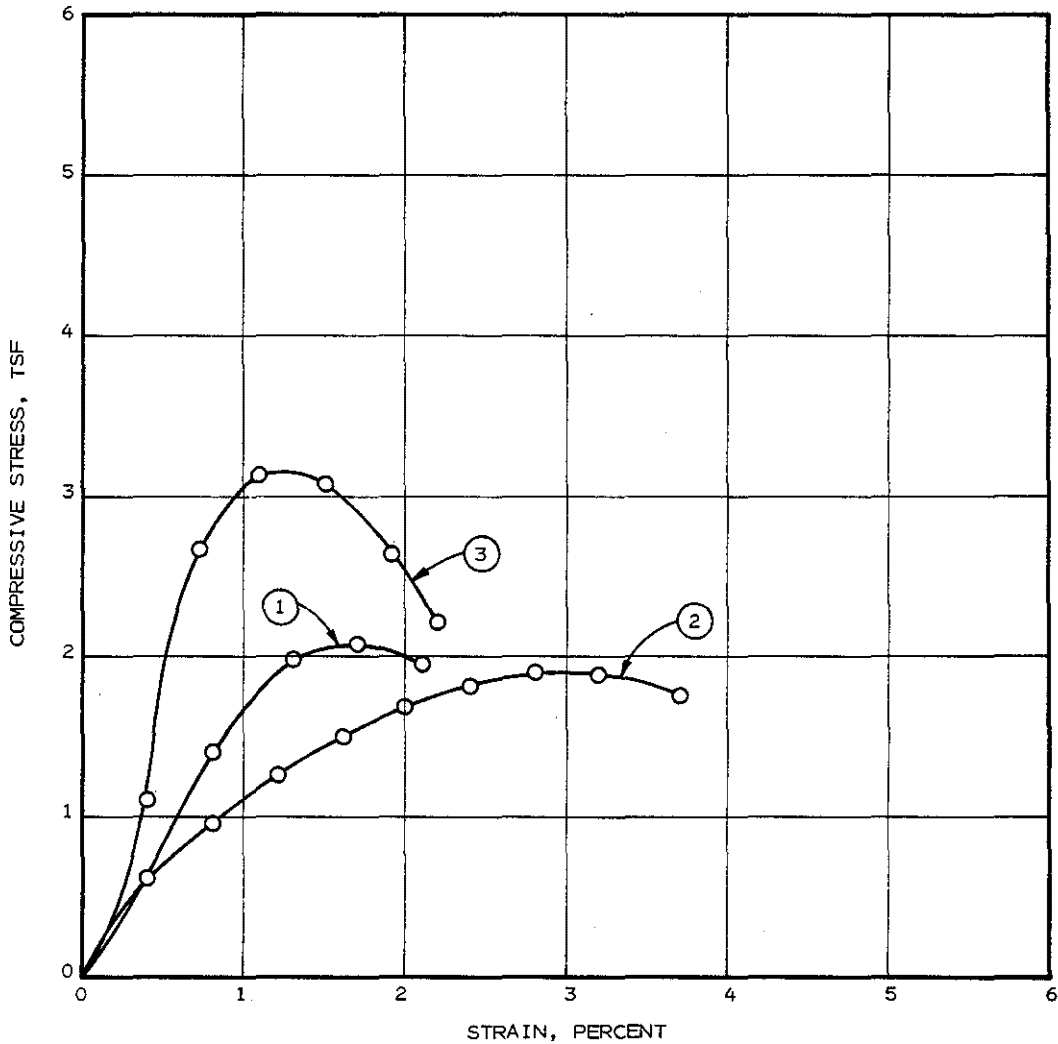
<u>BORING</u> NO.	<u>DEPTH,</u> FT.	<u>MATERIAL</u>
CB-2	7.5	HARD BROWN CLAY WITH ORGANIC MATERIAL AND FERROUS NODULES

STRESS-STRAIN CURVES
UNCONFINED COMPRESSION TEST



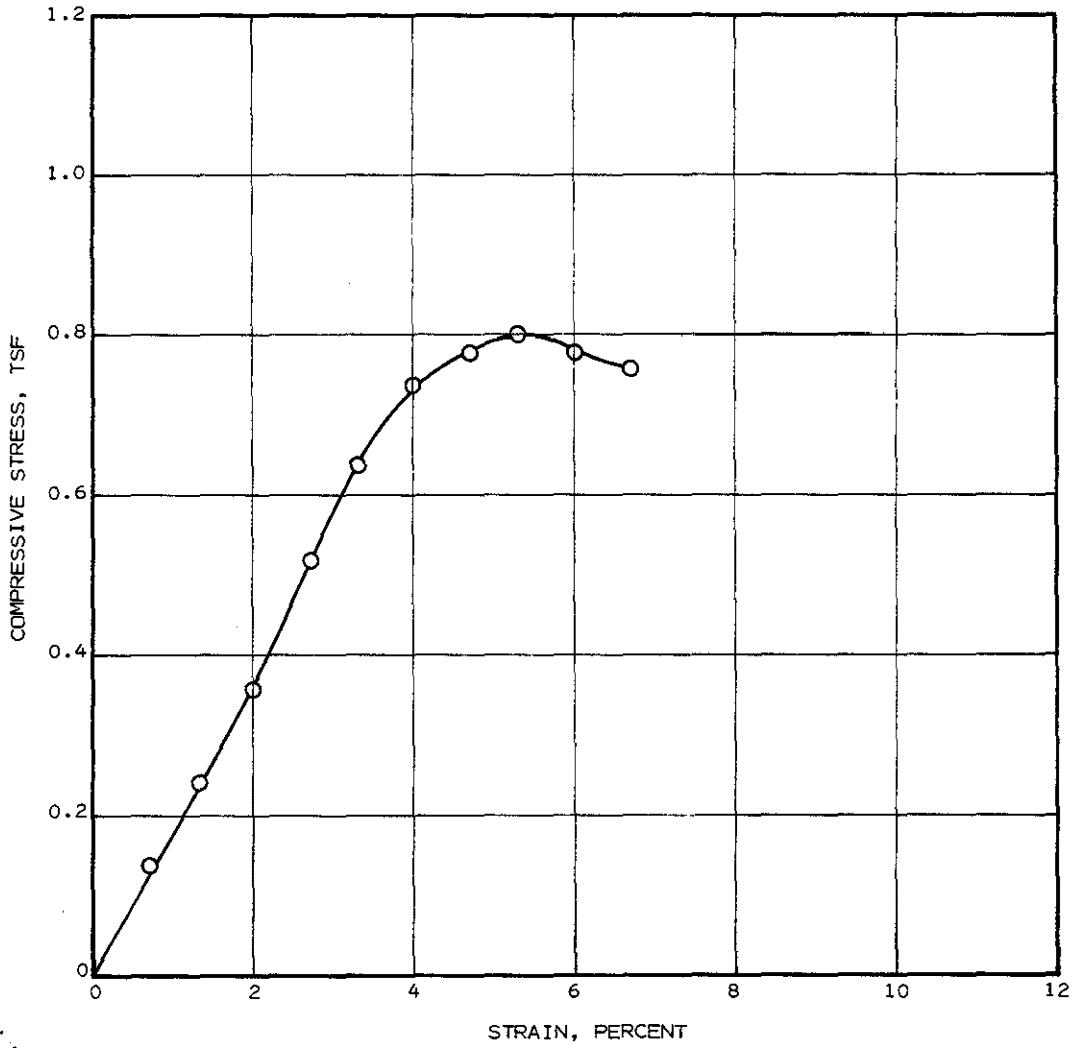
<u>CURVE NO.</u>	<u>BORING NO.</u>	<u>DEPTH, FT.</u>	<u>MATERIAL</u>
1	CB-2	11	STIFF TAN AND GRAY CLAYEY SAND TO SANDY CLAY WITH CALCAREOUS DEPOSITS
2	CB-3	27	VERY STIFF TAN SANDY CLAY

STRESS-STRAIN CURVES
UNCONFINED COMPRESSION TEST



CURVE NO.	BORING NO.	DEPTH, FT.	MATERIAL
1	CB-1	25	VERY STIFF RED AND LIGHT GRAY CLAY, SLICKENSIDED
2	CB-2	15	HARD RED AND LIGHT GRAY CLAY, SLICKENSIDED WITH CALCAREOUS NODULES
3	CB-3	43	VERY STIFF TO HARD RED AND GRAY SANDY CLAY WITH CLAY POCKETS

STRESS-STRAIN CURVES
UNCONFINED COMPRESSION TEST



BORING
NO.

CB-2

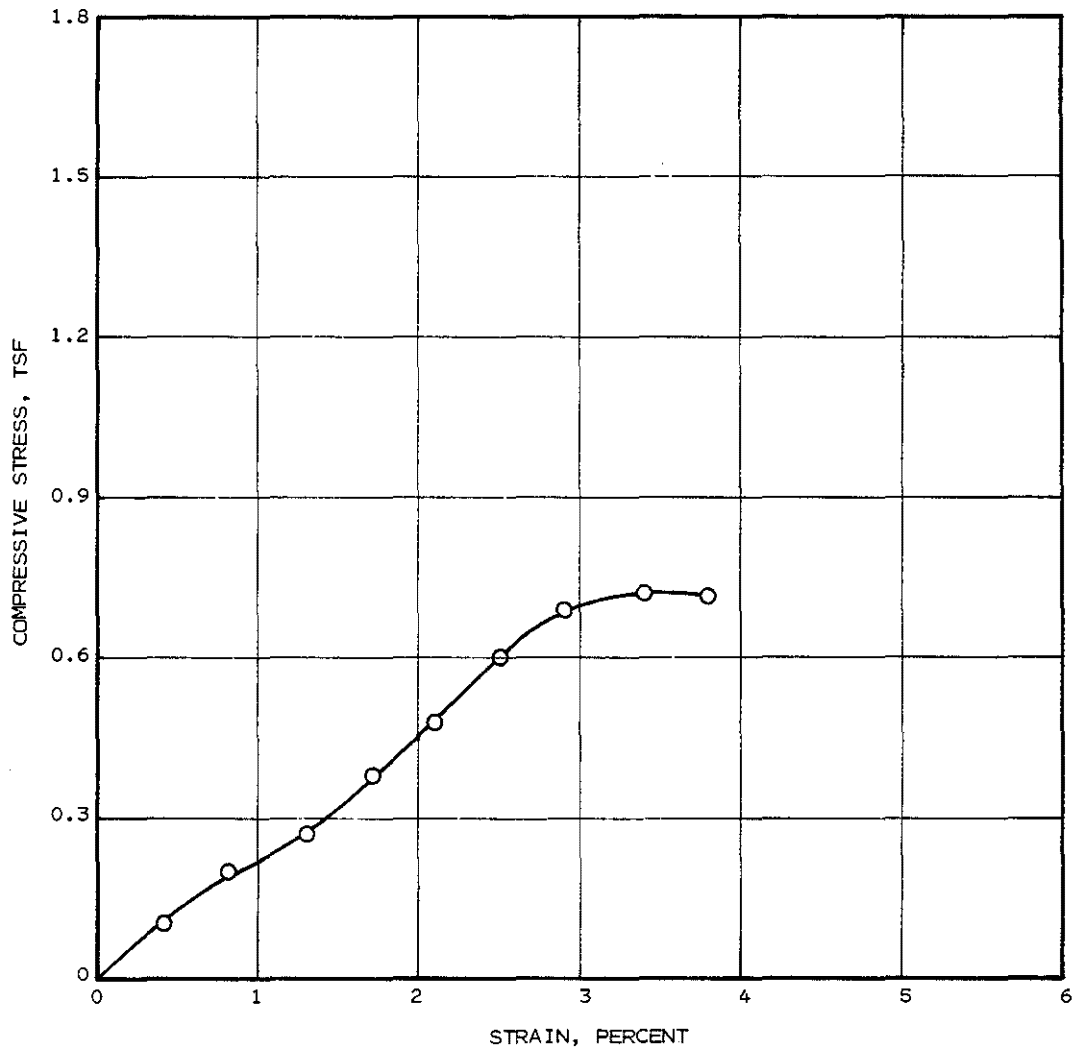
DEPTH,
FT.

29

MATERIAL

VERY STIFF LIGHT GRAY AND TAN VERY SILTY CLAY

STRESS-STRAIN CURVES
UNCONFINED COMPRESSION TEST

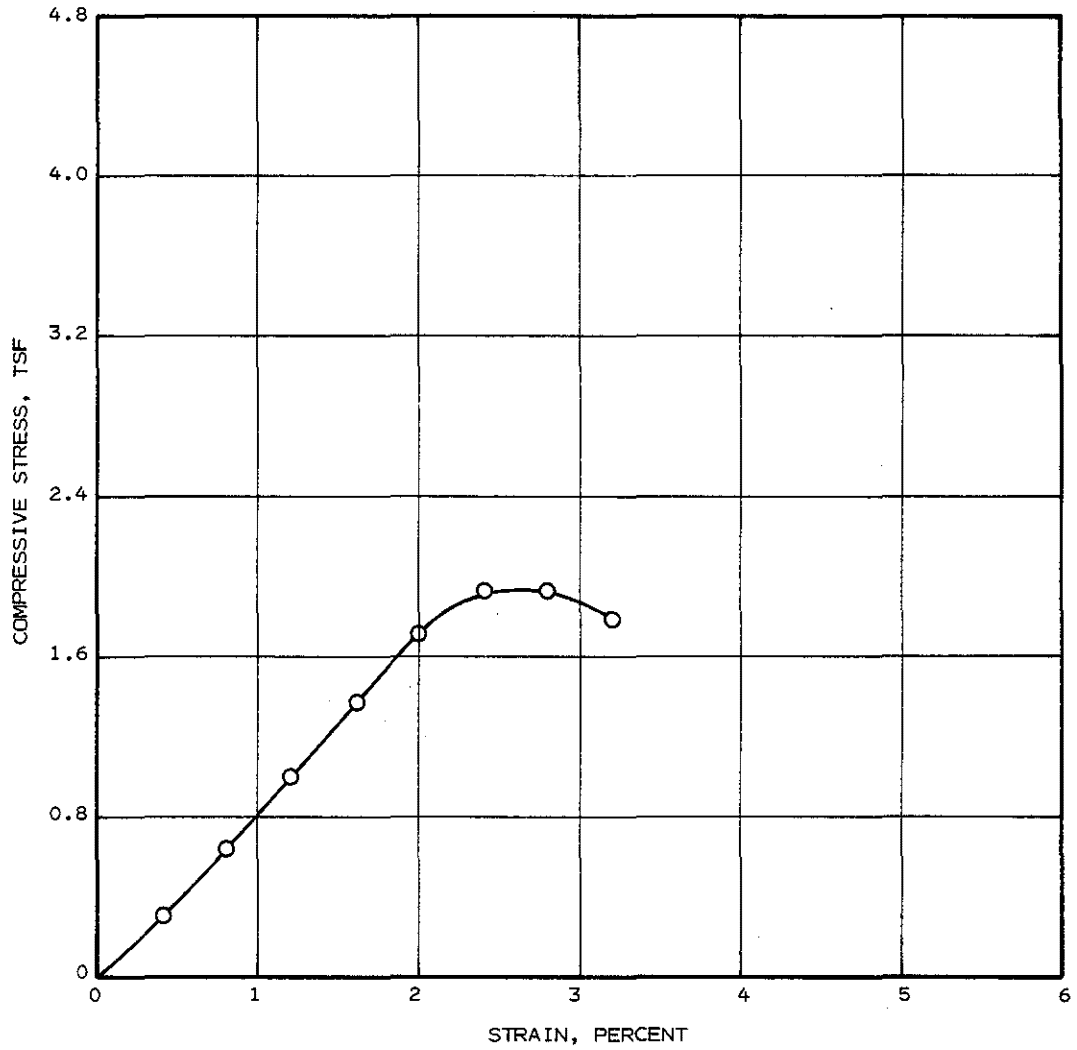


BORING
NO.
CB-3

DEPTH,
FT.
35

MATERIAL
TAN AND LIGHT GRAY SANDY CLAY

STRESS-STRAIN CURVES
UNCONFINED COMPRESSION TEST



BORING
NO.

CB-2

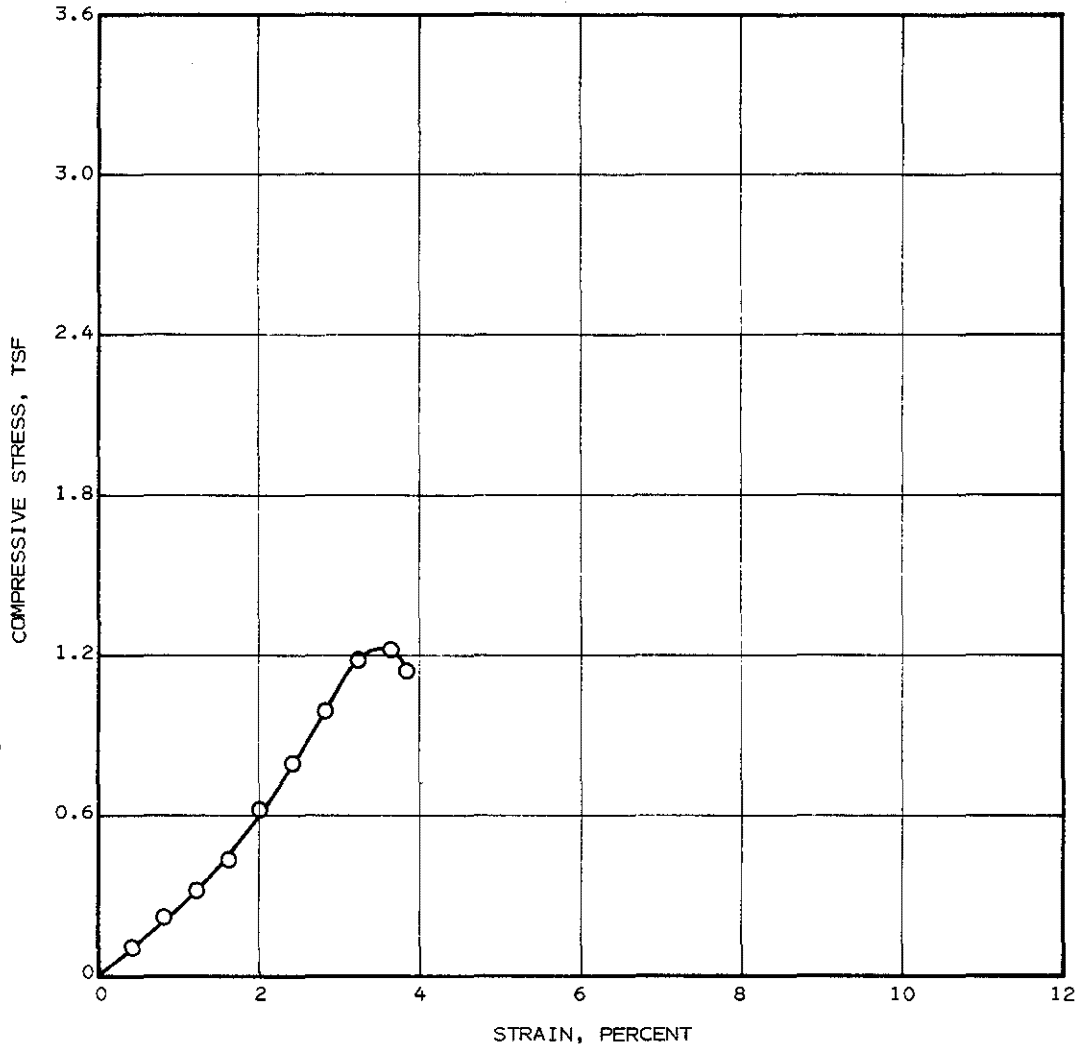
DEPTH,
FT.

39

MATERIAL

VERY STIFF TAN, GRAY AND LIGHT GRAY SANDY
CLAY WITH ORGANIC MATERIAL

STRESS-STRAIN CURVES
UNCONFINED COMPRESSION TEST



BORING
NO.

CB-1

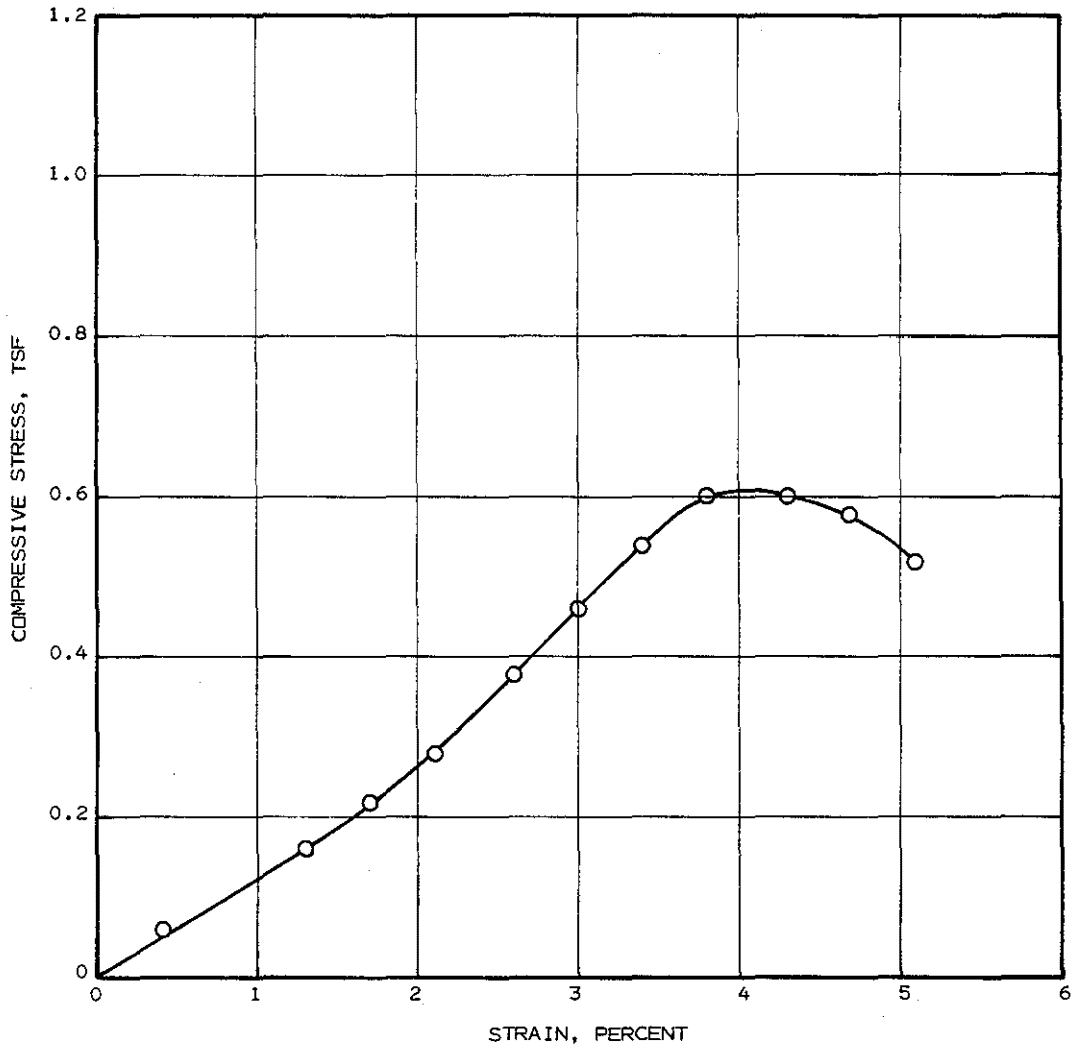
DEPTH,
FT.

45.5

MATERIAL

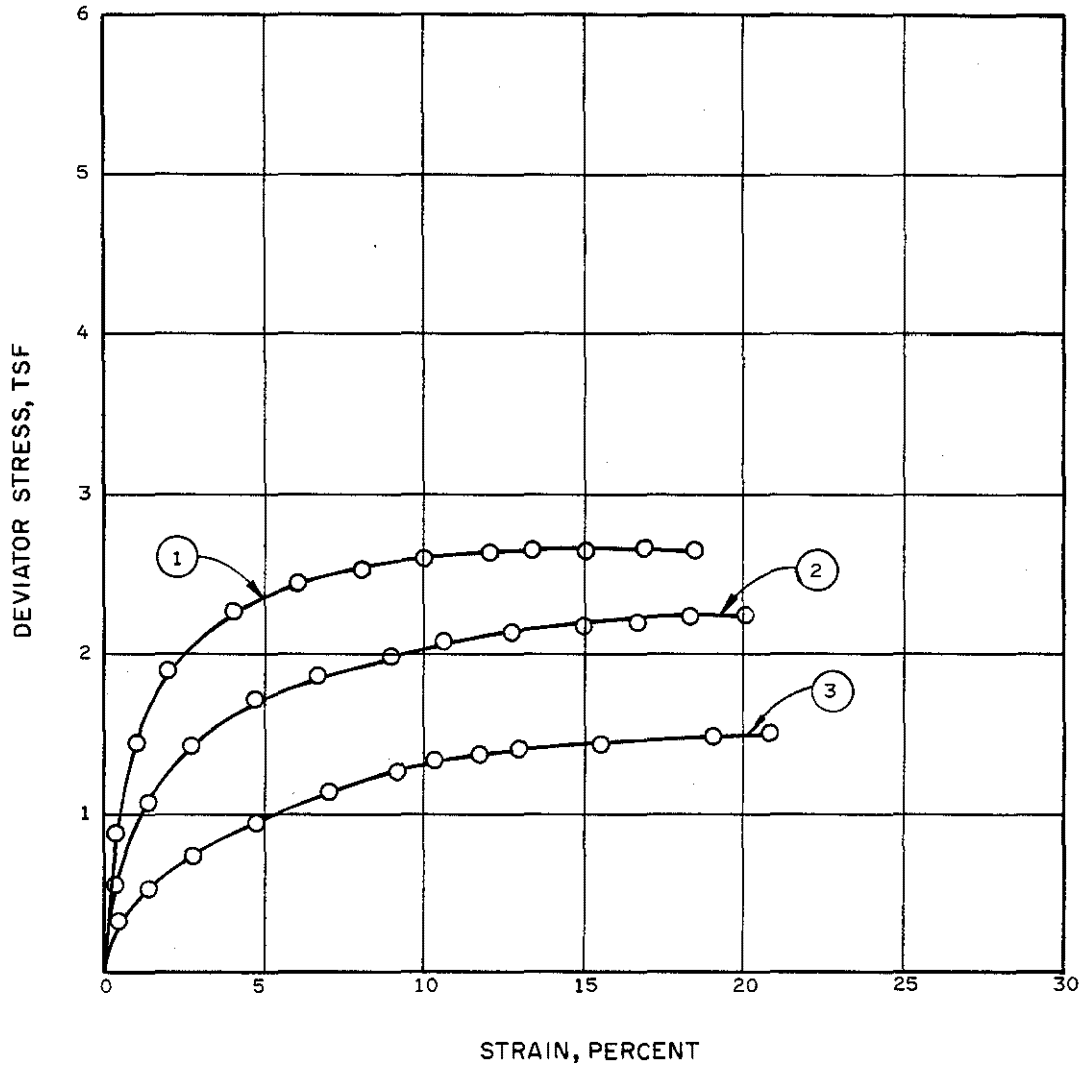
LIGHT GRAY AND TAN CLAYEY SAND WITH SAND
POCKETS

STRESS-STRAIN CURVES
UNCONFINED COMPRESSION TEST



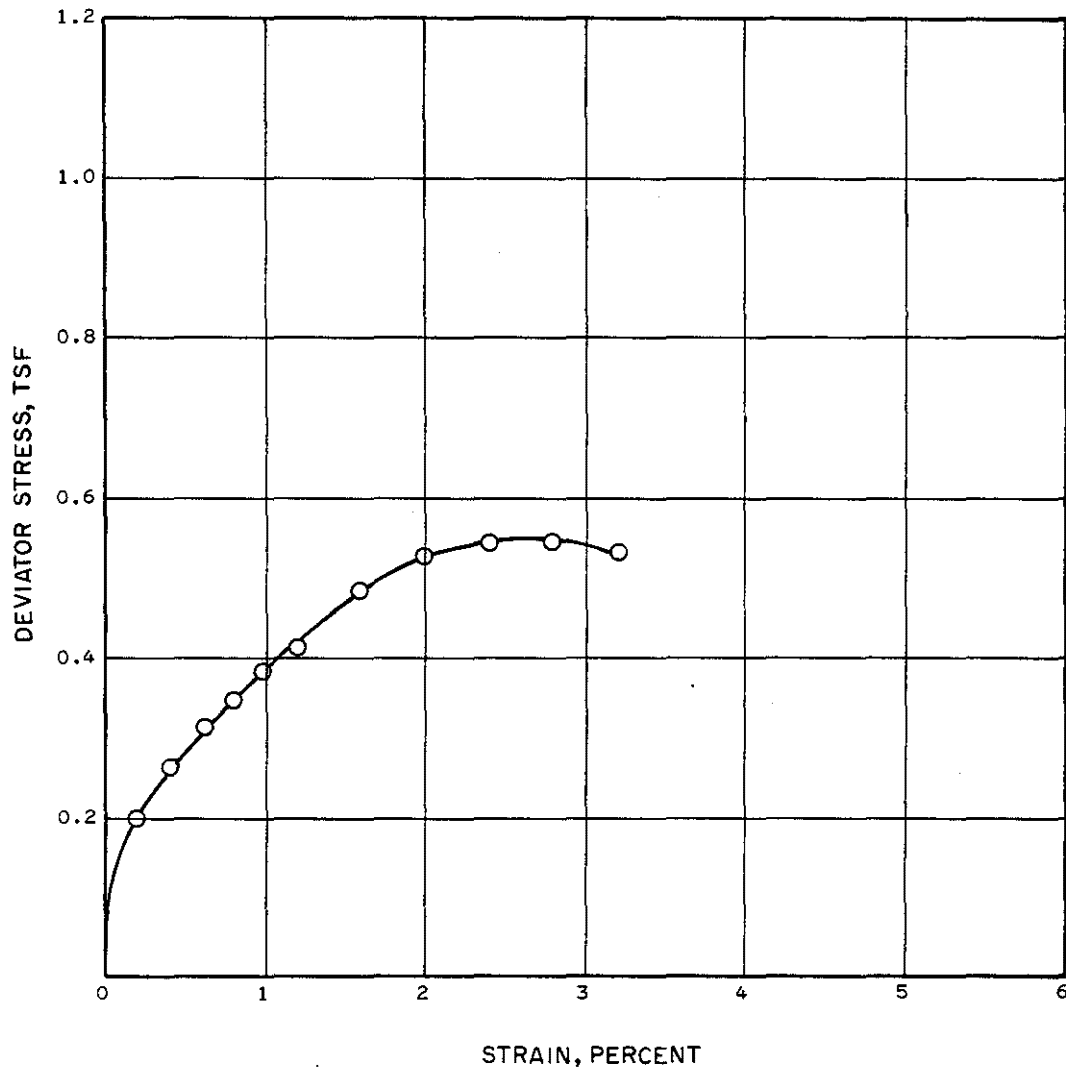
<u>BORING</u> NO.	<u>DEPTH,</u> FT.	<u>MATERIAL</u>
CB-2	47	FIRM REDDISH BROWN AND GRAY SANDY SILT WITH CLAY POCKETS

STRESS-STRAIN CURVES
UNCONFINED COMPRESSION TEST



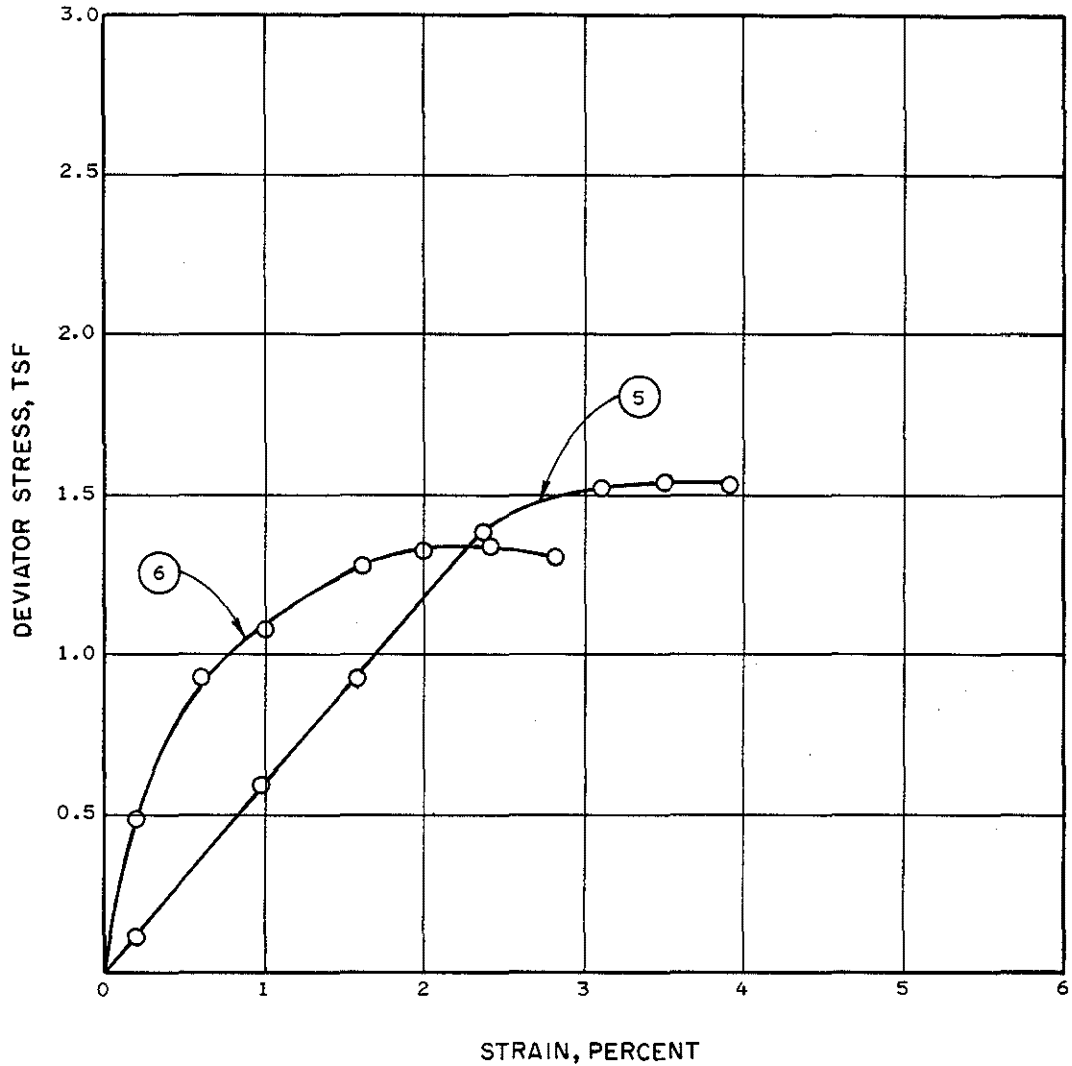
CURVE NO.	BORING NO.	DEPTH, FT.	CONFINING PRESSURE, TSF	MATERIAL
1	CB-2	3	0.72	VERY STIFF BROWN AND TAN CLAY WITH ROOTS, SAND POCKETS AND ORGANIC MATERIAL
2	CB-3	7	0.72	VERY STIFF BROWN AND TAN SLIGHTLY SANDY CLAY, WITH ORGANICS AND FERROUS NODULES, SLIGHTLY SLICK-ENSIDED
3	CB-2	11.5	0.72	STIFF TAN AND GRAY SANDY CLAY WITH SAND POCKETS, SLIGHTLY SLICKENSIDED

STRESS-STRAIN CURVES
TRIAxIAL COMPRESSION TEST
 UNCONSOLIDATED UNDRAINED



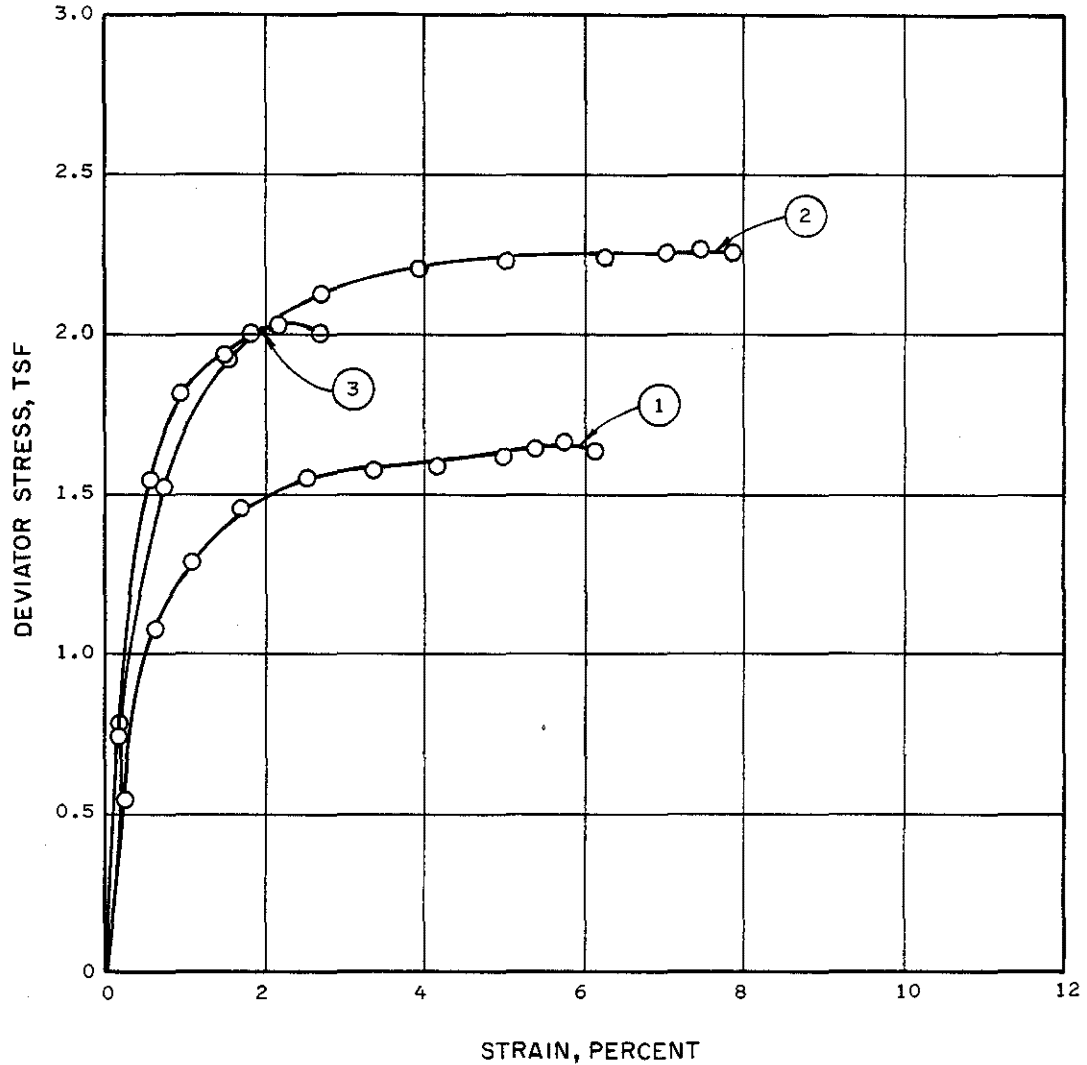
CURVE NO.	BORING NO.	DEPTH, FT.	CONFINING PRESSURE, TSF	MATERIAL
4	CB-3	13	0.72	HARD RED AND LIGHT GRAY CLAY, CALCAREOUS DEPOSITS

STRESS-STRAIN CURVES
TRIAXIAL COMPRESSION TEST
 UNCONSOLIDATED UNDRAINED



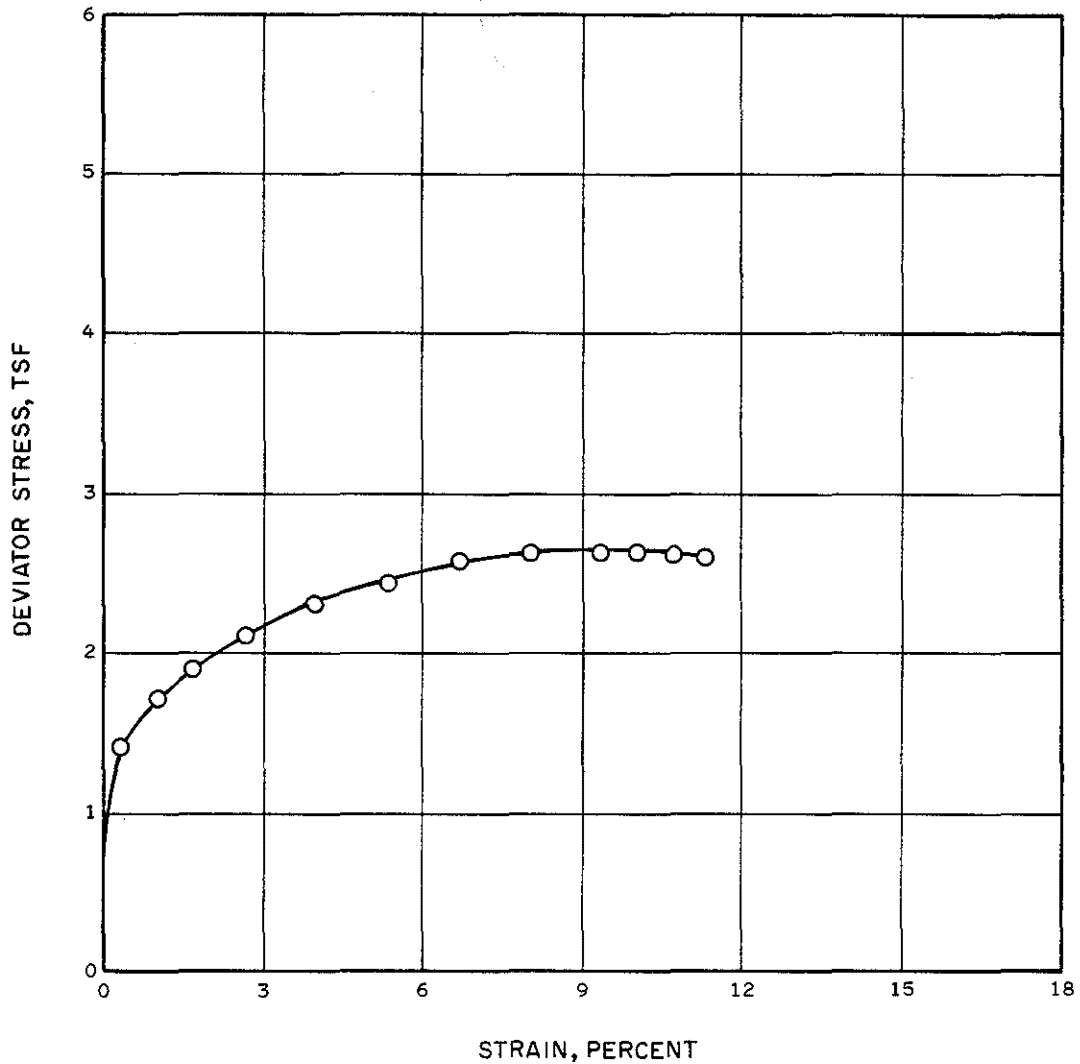
CURVE NO.	BORING NO.	DEPTH, FT.	CONFINING PRESSURE, TSF	MATERIAL
5	CB-1	14.5	1.73	VERY STIFF RED CLAY, SLICKENSIDED
6	CB-1	15.5	0.86	VERY STIFF RED CLAY, SLICKENSIDED

STRESS-STRAIN CURVES
TRIAxIAL COMPRESSION TEST
 UNCONSOLIDATED UNDRAINED



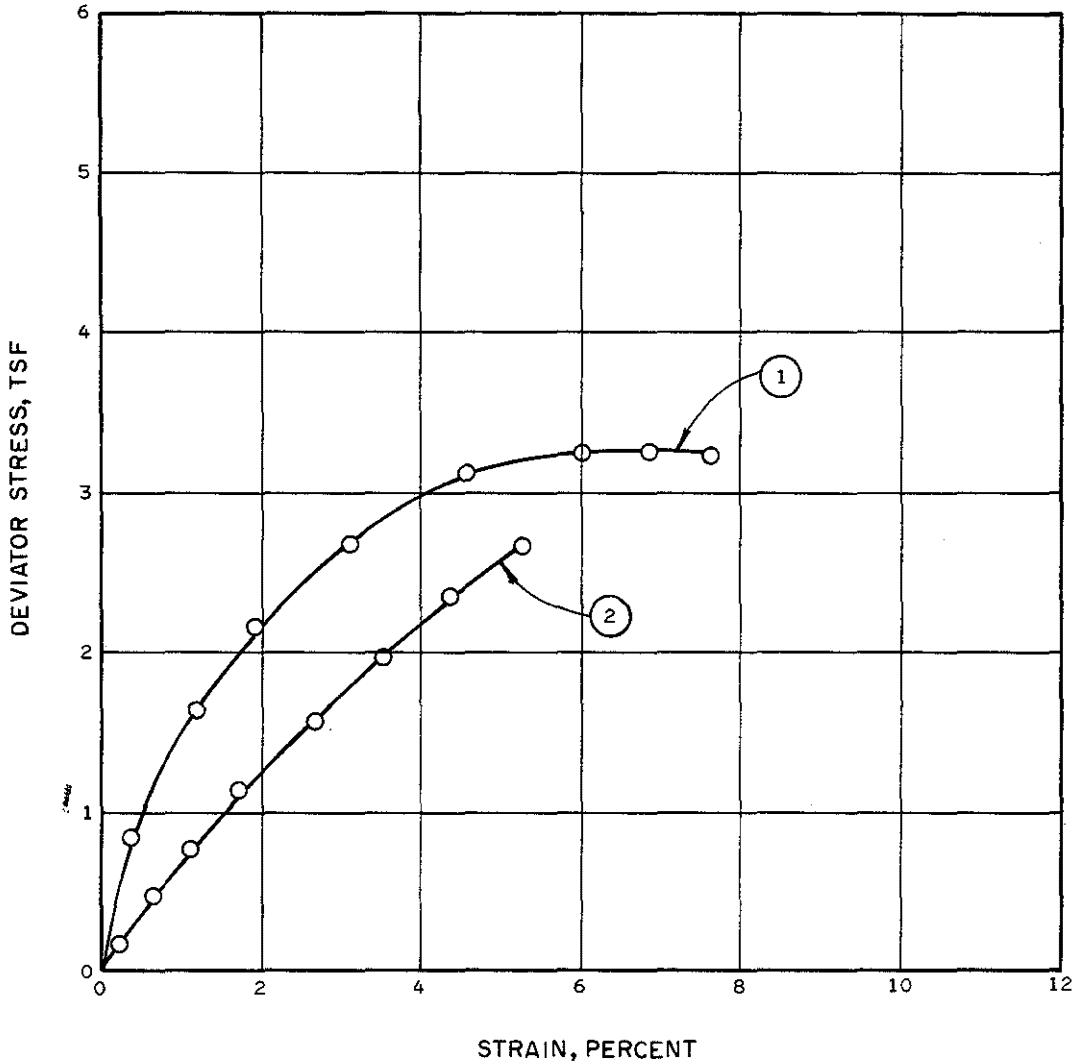
CURVE NO.	BORING NO.	DEPTH, FT.	CONFINING PRESSURE, TSF	MATERIAL
1	CB-3	20.5	1.08	VERY STIFF YELLOW, RED AND LIGHT GRAY CLAY, SLICKENSIDED
3	CB-3	21.5	2.20	VERY STIFF RED AND LIGHT GRAY CLAY, SLICKENSIDED
2	CB-3	21.0	1.66	VERY STIFF RED AND LIGHT GRAY CLAY, SLICKENSIDED

STRESS-STRAIN CURVES
TRIAxIAL COMPRESSION TEST
 UNCONSOLIDATED UNDRAINED



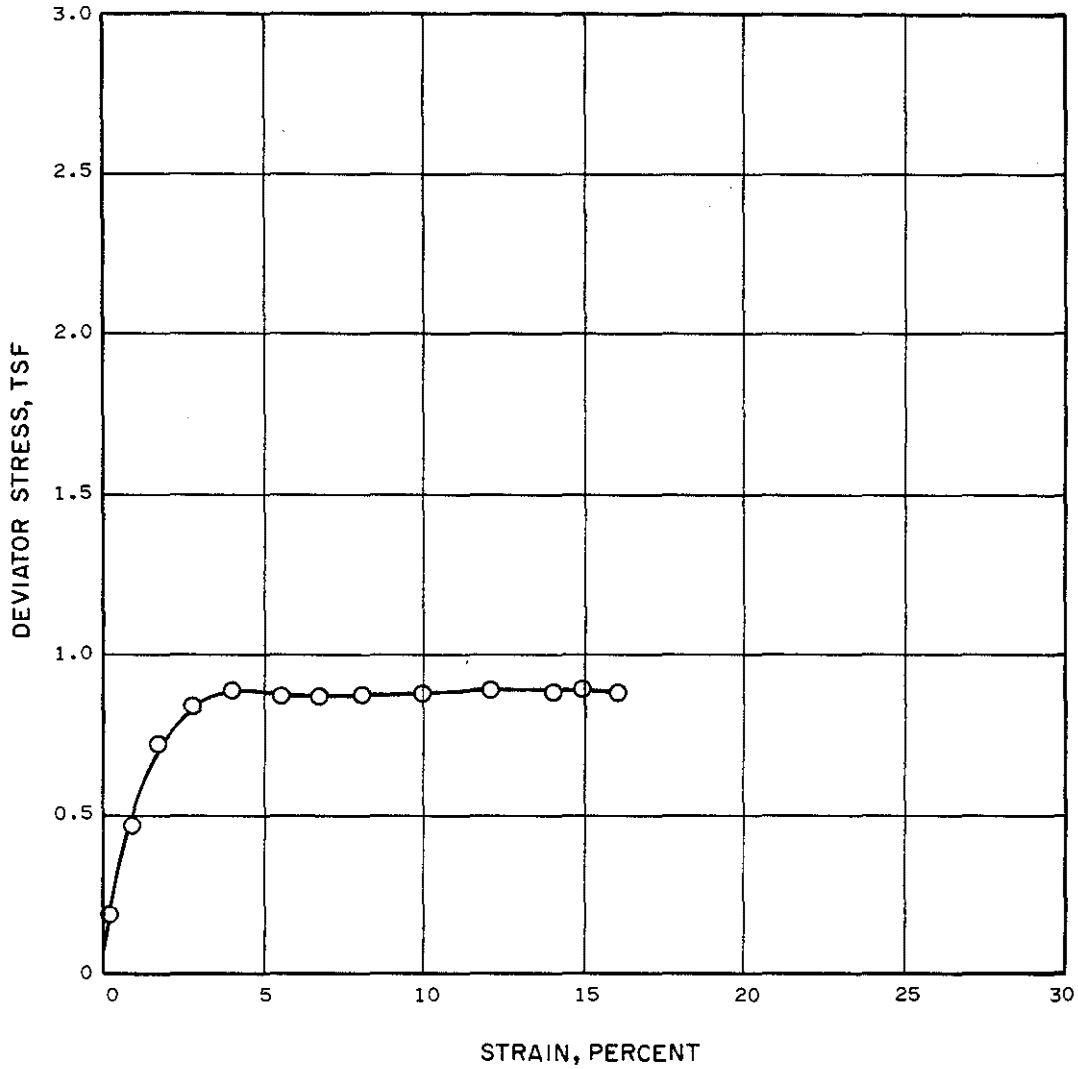
<u>BORING NO.</u>	<u>DEPTH, FT.</u>	<u>CONFINING PRESSURE, TSF</u>	<u>MATERIAL</u>
CB-2	24.5	1.01	VERY STIFF RED AND LIGHT GRAY CLAY, SLICKENSIDED

STRESS-STRAIN CURVES
TRIAxIAL COMPRESSION TEST
 UNCONSOLIDATED UNDRAINED



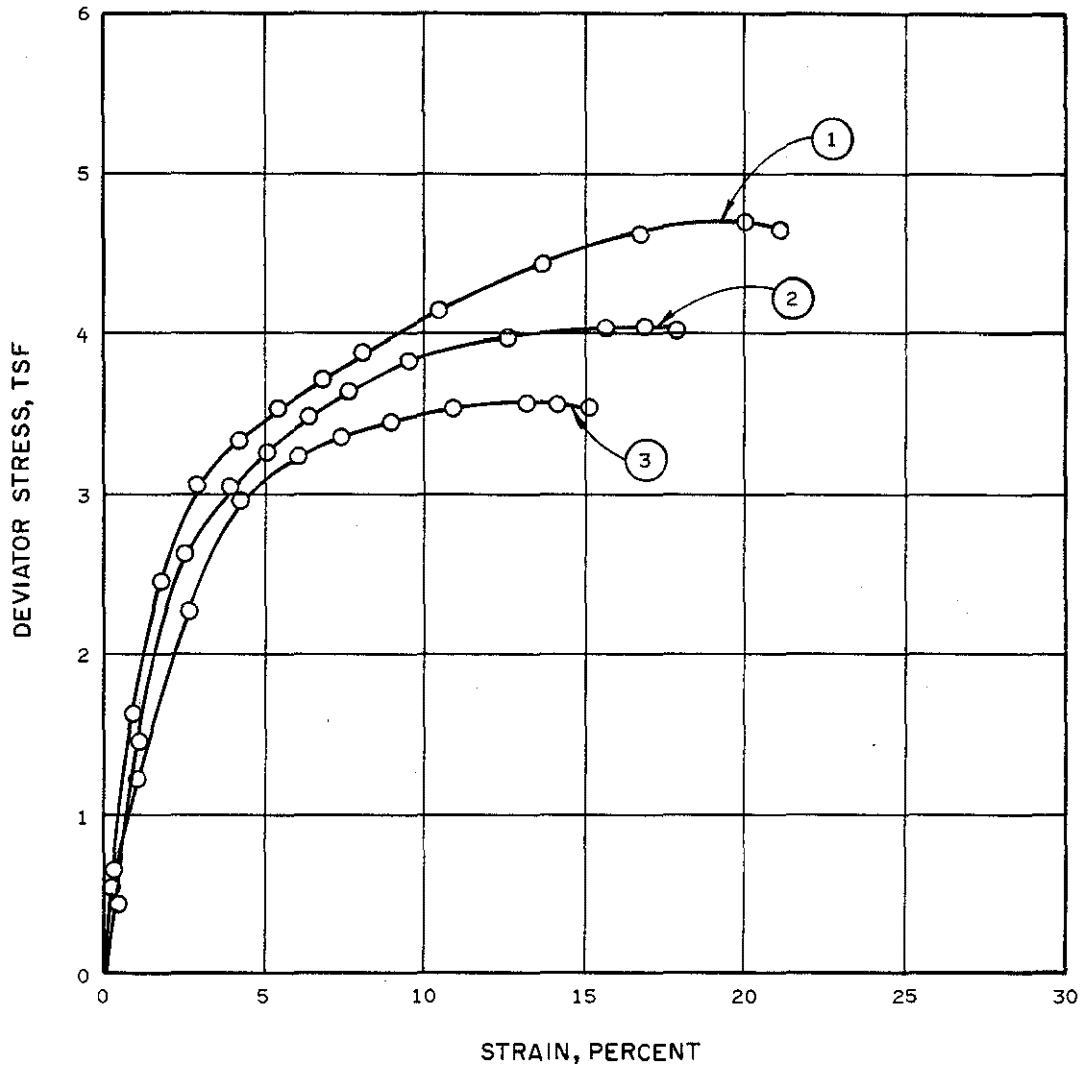
CURVE NO.	BORING NO.	DEPTH, FT.	CONFINING PRESSURE, TSF	MATERIAL
1	CB-3	26.5	1.08	STIFF BROWN, TAN AND GRAY CLAY, WITH SANDY CLAY SEAMS AND NUMEROUS CALCAREOUS NODULES
2	CB-3	27	1.15	STIFF TAN SLIGHTLY SANDY CLAYEY SILT

STRESS-STRAIN CURVES
TRIAXIAL COMPRESSION TEST
 UNCONSOLIDATED UNDRAINED



<u>BORING NO.</u>	<u>DEPTH, FT.</u>	<u>CONFINING PRESSURE, TSF</u>	<u>MATERIAL</u>
CB-2	27	1.15	TAN CLAYEY SLIGHTLY SANDY SILT

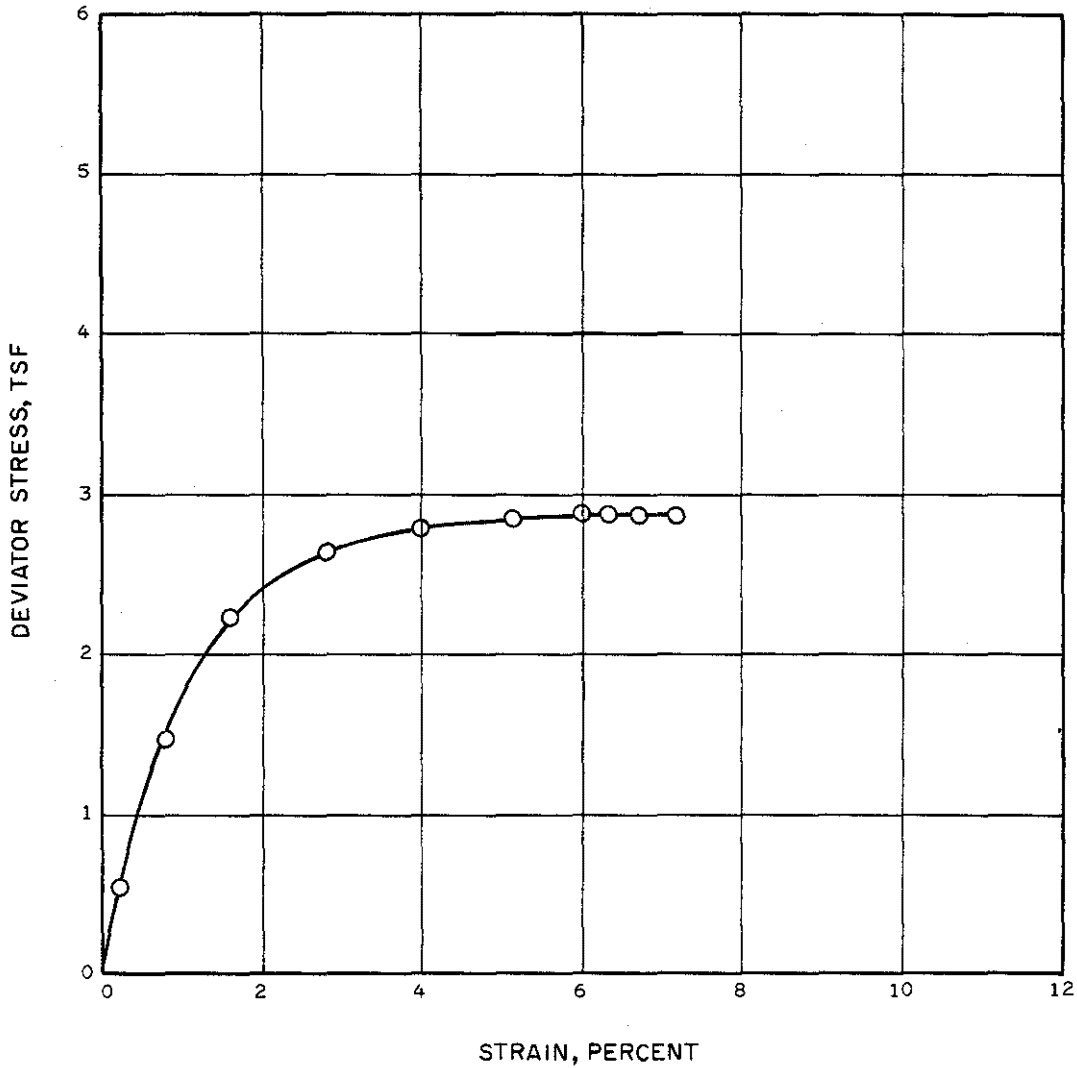
STRESS-STRAIN CURVES
 TRIAXIAL COMPRESSION TEST
 UNCONSOLIDATED UNDRAINED



CURVE NO.	BORING NO.	DEPTH, FT.	CONFINING PRESSURE, TSF	MATERIAL
1	CB-3	30.5	1.51	TAN AND LIGHT GRAY SANDY CLAY WITH CALCAREOUS DEPOSITS AND NODULES
2	CB-3	34.5	3.38	LIGHT GRAY AND TAN CLAYEY SAND
3	CB-3	35.5	1.69	VERY STIFF TAN AND LIGHT GRAY SANDY CLAY

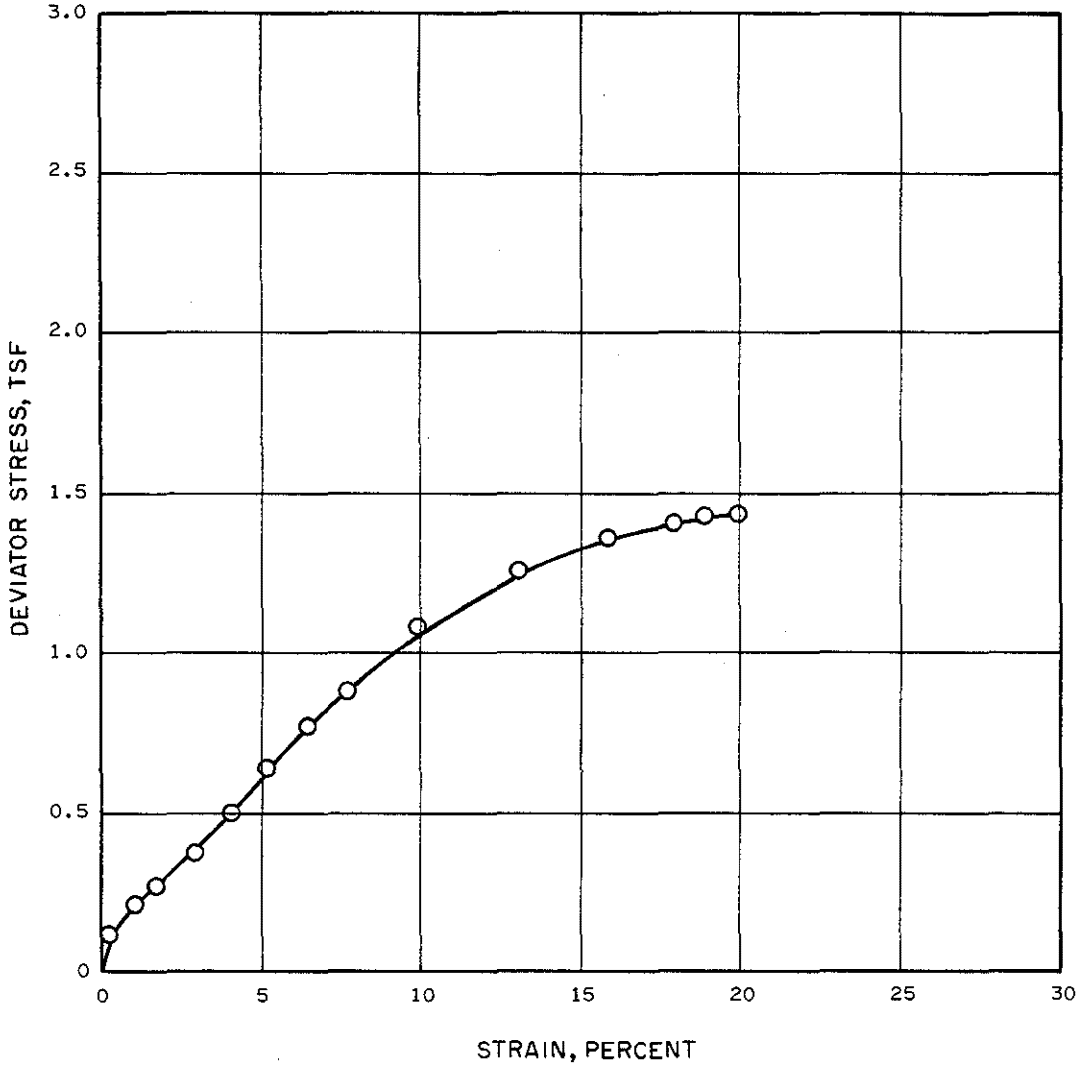
**STRESS-STRAIN CURVES
 TRIAXIAL COMPRESSION TEST**

UNCONSOLIDATED UNDRAINED



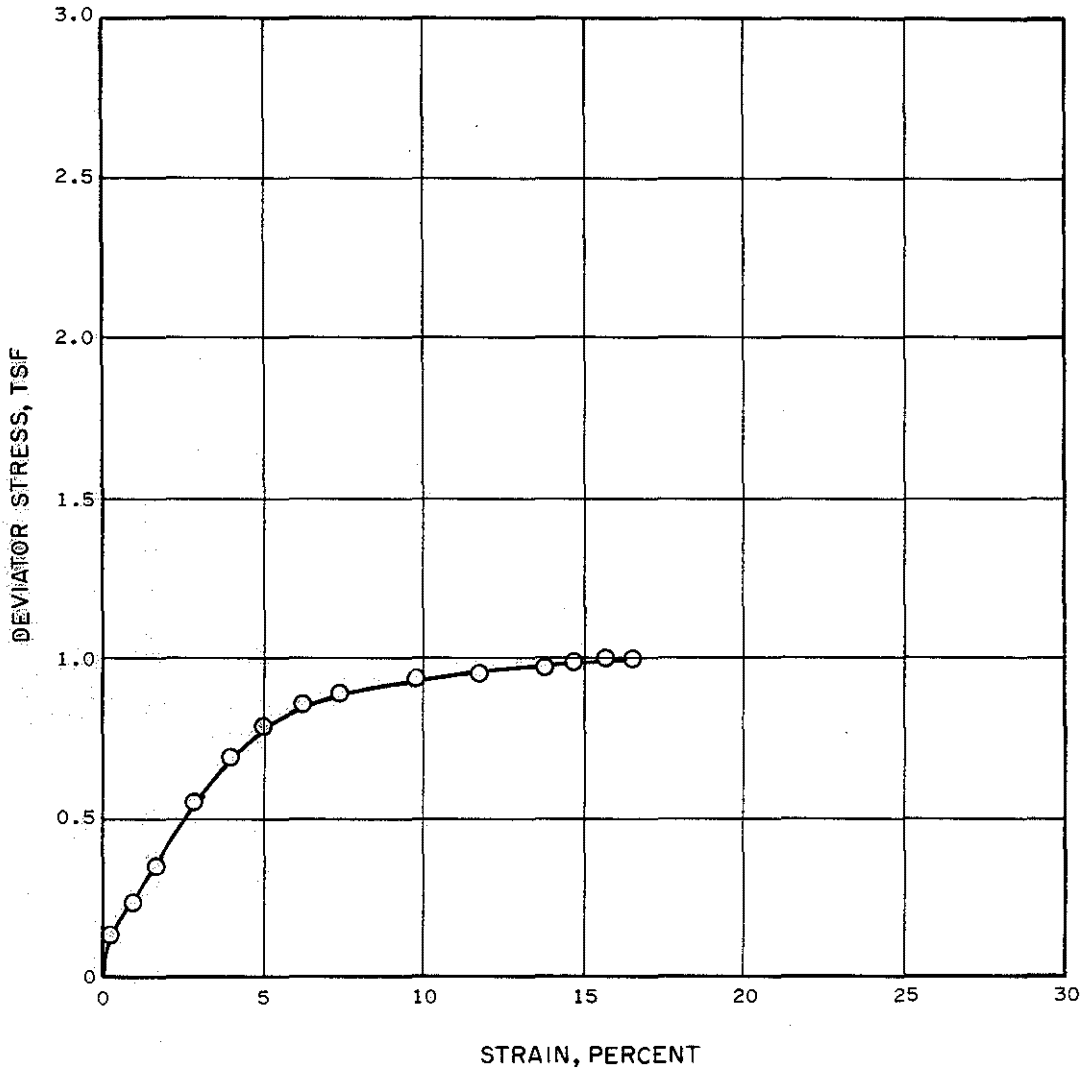
<u>BORING NO.</u>	<u>DEPTH, FT.</u>	<u>CONFINING PRESSURE, TSF</u>	<u>MATERIAL</u>
CB-2	39.5	1.51	VERY STIFF TAN, GRAY AND LIGHT SANDY CLAY, WITH ORGANICS

STRESS-STRAIN CURVES
 TRIAXIAL COMPRESSION TEST
 UNCONSOLIDATED UNDRAINED



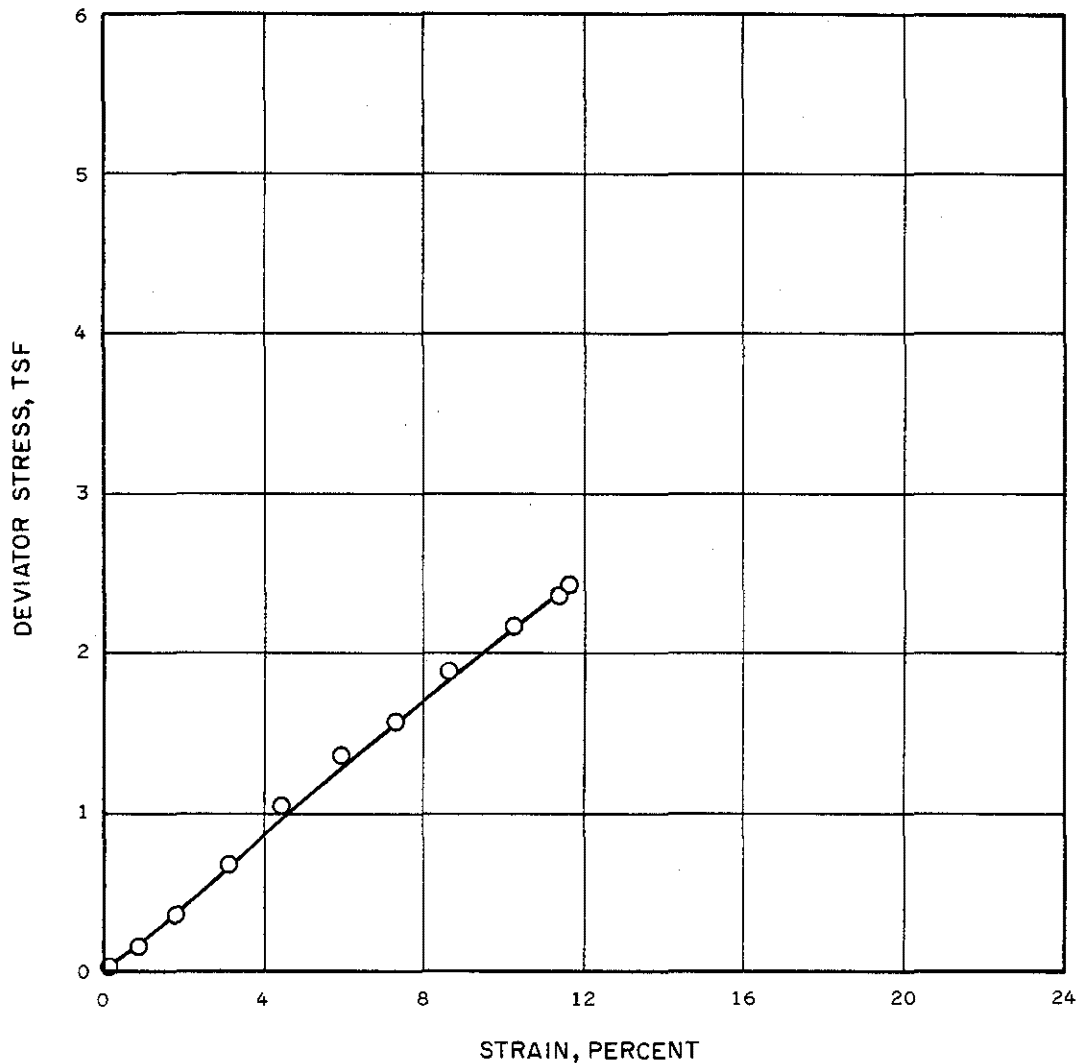
<u>BORING NO.</u>	<u>DEPTH, FT.</u>	<u>CONFINING PRESSURE, TSF</u>	<u>MATERIAL</u>
CB-2	41	1.51	FIRM TAN AND LIGHT GRAY SANDY CLAY, WITH ORGANICS AND CALCAREOUS NODULES

STRESS-STRAIN CURVES
TRIAXIAL COMPRESSION TEST
 UNCONSOLIDATED UNDRAINED



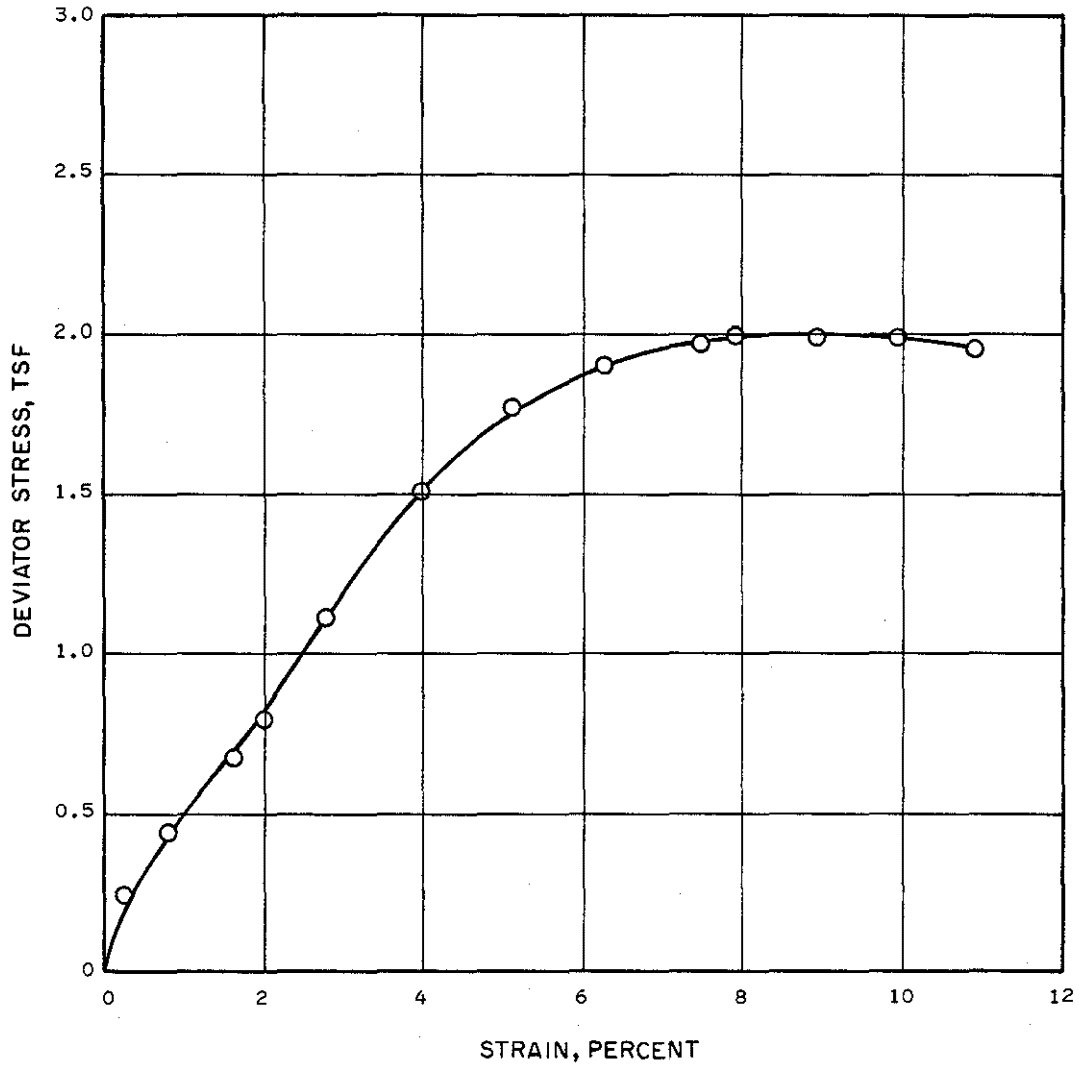
<u>BORING NO.</u>	<u>DEPTH, FT.</u>	<u>CONFINING PRESSURE, TSF</u>	<u>MATERIAL</u>
CB-2	50	1.66	FIRM RED, TAN AND LIGHT GRAY CLAYEY SILT WITH CALCAREOUS NODULES

STRESS-STRAIN CURVES
TRIAXIAL COMPRESSION TEST
 UNCONSOLIDATED UNDRAINED



<u>BORING NO.</u>	<u>DEPTH, FT.</u>	<u>CONFINING PRESSURE, TSF</u>	<u>MATERIAL</u>
CB-2	55	1.94	RED AND GRAY SILT

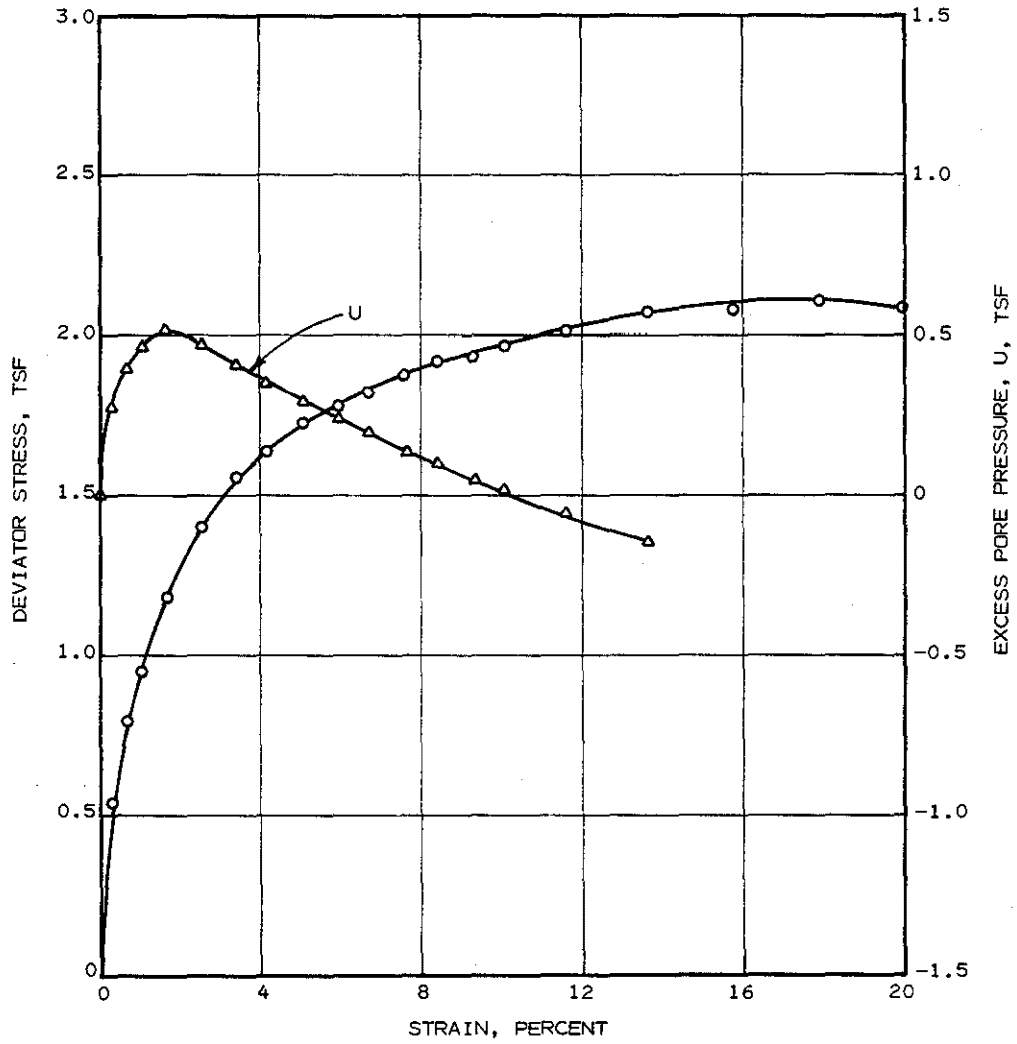
STRESS-STRAIN CURVES
TRIAxIAL COMPRESSION TEST
 UNCONSOLIDATED UNDRAINED



<u>BORING NO.</u>	<u>DEPTH, FT.</u>	<u>CONFINING PRESSURE, TSF</u>	<u>MATERIAL</u>
CB-2	59.5	2.09	STIFF RED AND GRAY CLAYEY SILT, WITH CALCAREOUS NODULES

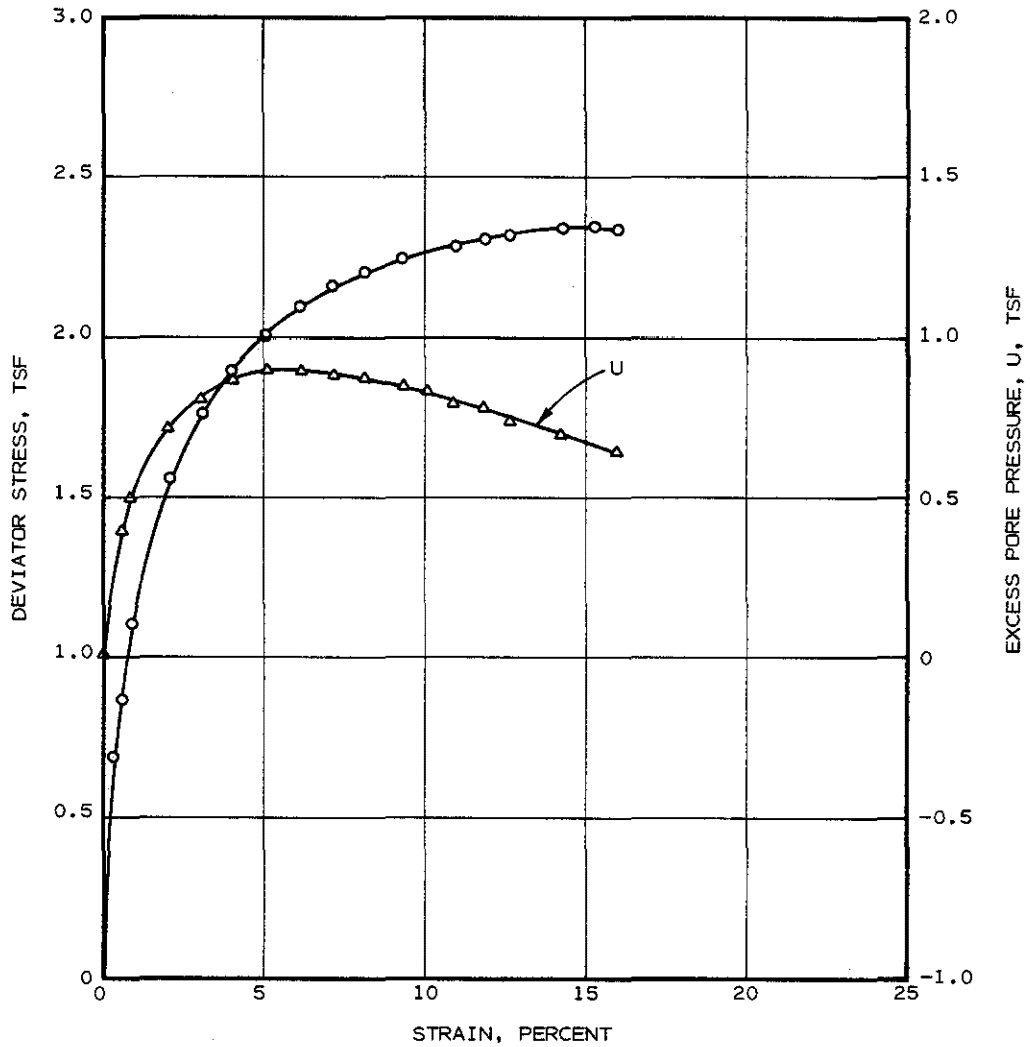
**STRESS-STRAIN CURVES
TRIAxIAL COMPRESSION TEST**

UNCONSOLIDATED UNDRAINED



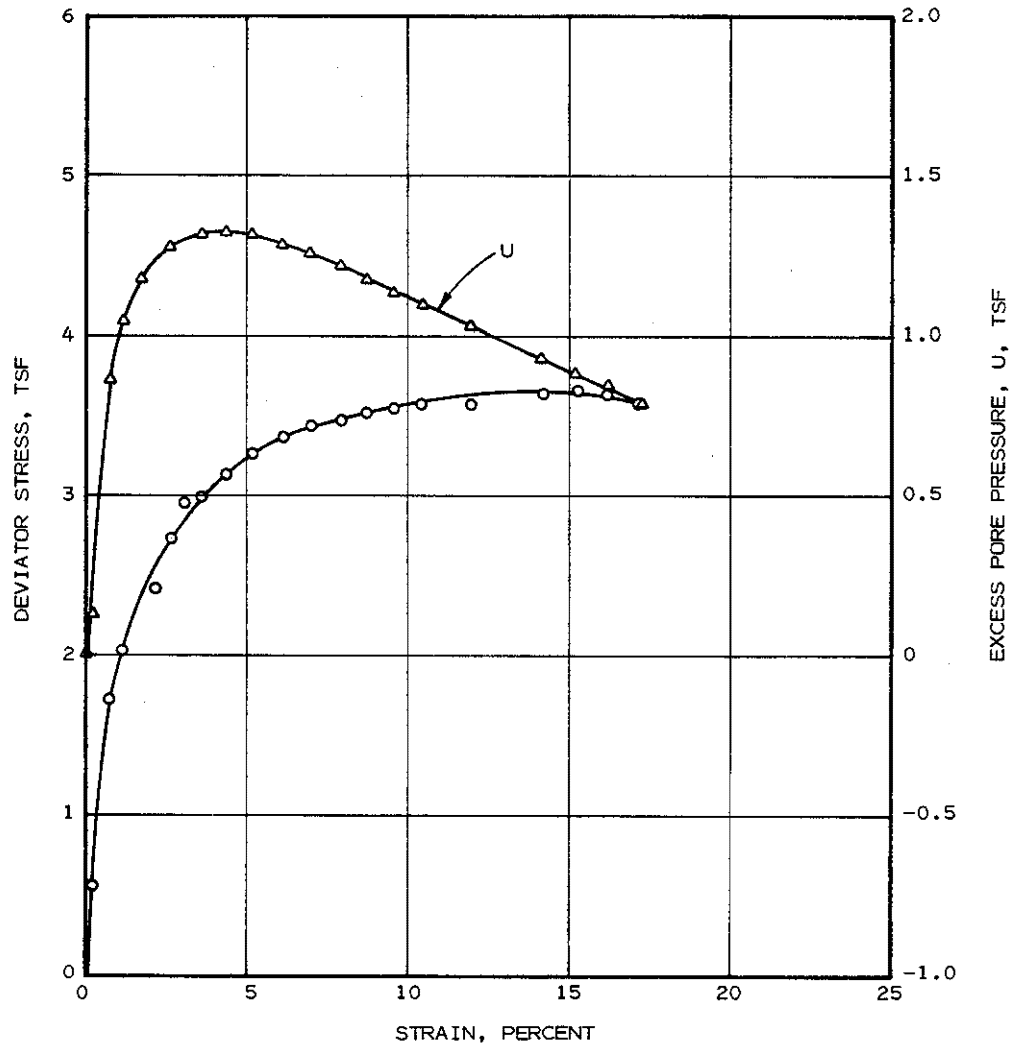
BORING NO.	DEPTH, FT.	CONFINING PRESSURE, TSF	MATERIAL
CB-1	8.5	0.72	VERY STIFF BROWN AND LIGHT GRAY CLAY

PORE PRESSURE-STRAIN AND
STRESS-STRAIN CURVES
TRIAXIAL COMPRESSION TEST
CONSOLIDATED UNDRAINED



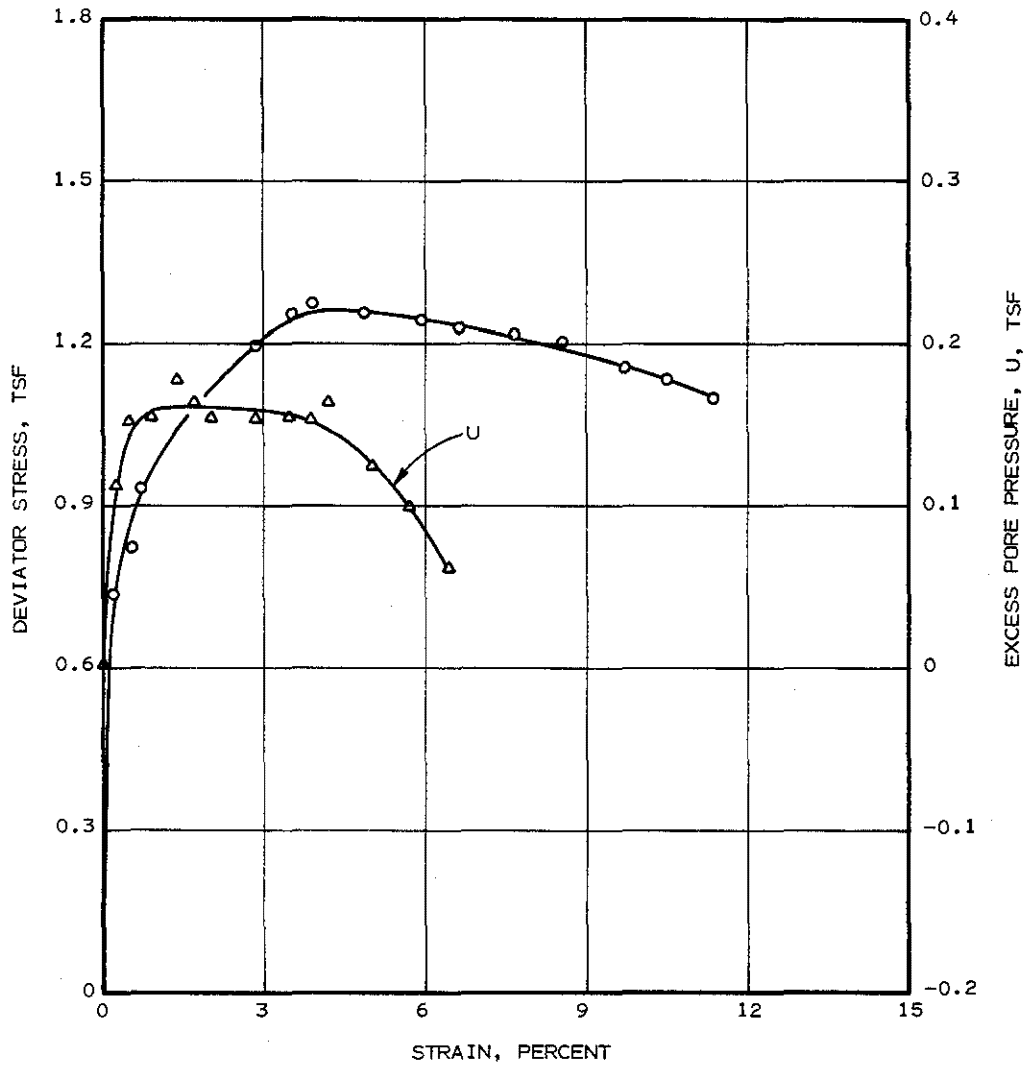
<u>BORING NO.</u>	<u>DEPTH, FT.</u>	<u>CONFINING PRESSURE, TSF</u>	<u>MATERIAL</u>
CB-3	9.5	2.30	VERY STIFF BROWN AND LIGHT GRAY CLAY

PORE PRESSURE-STRAIN AND
STRESS-STRAIN CURVES
TRIAxIAL COMPRESSION TEST
CONSOLIDATED UNDRAINED



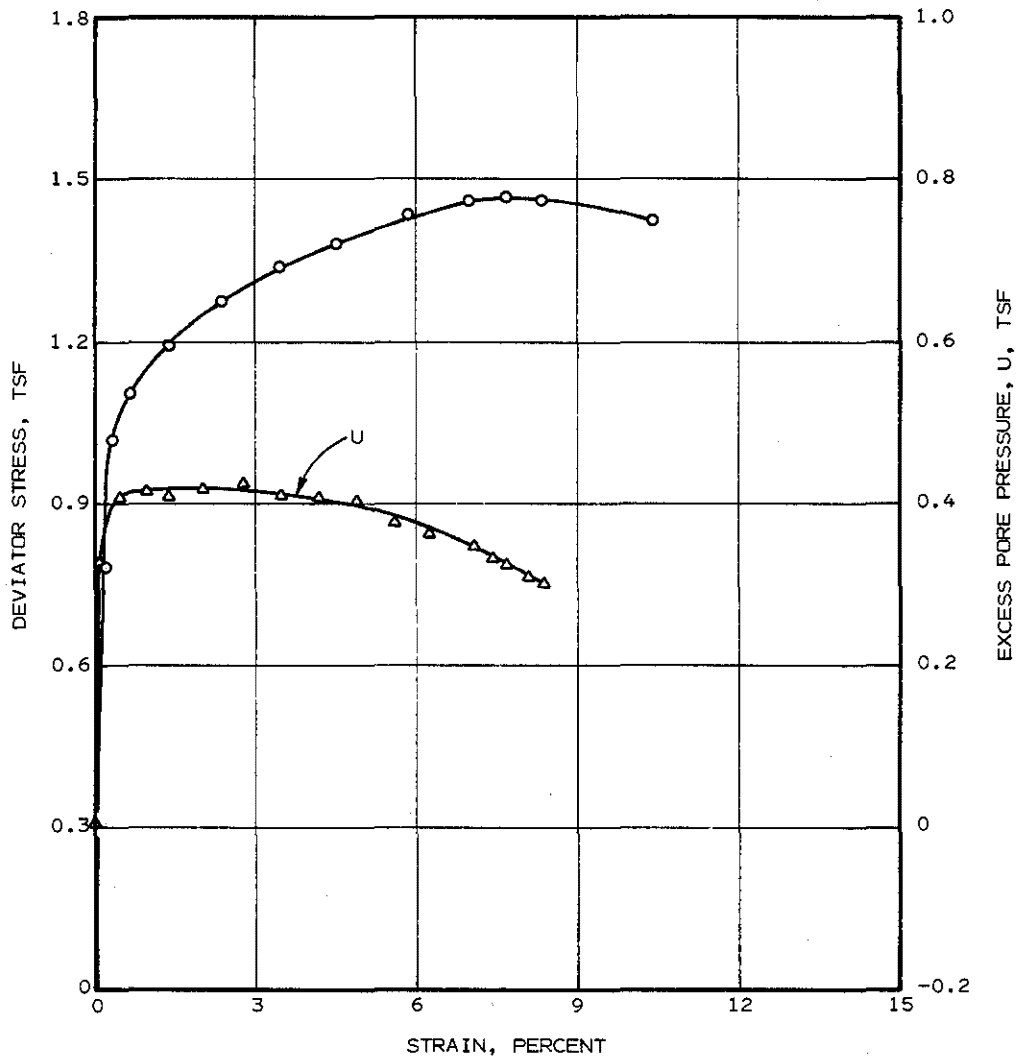
<u>BORING NO.</u>	<u>DEPTH, FT.</u>	<u>CONFINING PRESSURE, TSF.</u>	<u>MATERIAL</u>
CB-1	9	3.02	VERY STIFF BROWN AND LIGHT GRAY CLAY

PORE PRESSURE-STRAIN AND
STRESS-STRAIN CURVES
TRIAxIAL COMPRESSION TEST
CONSOLIDATED UNDRAINED



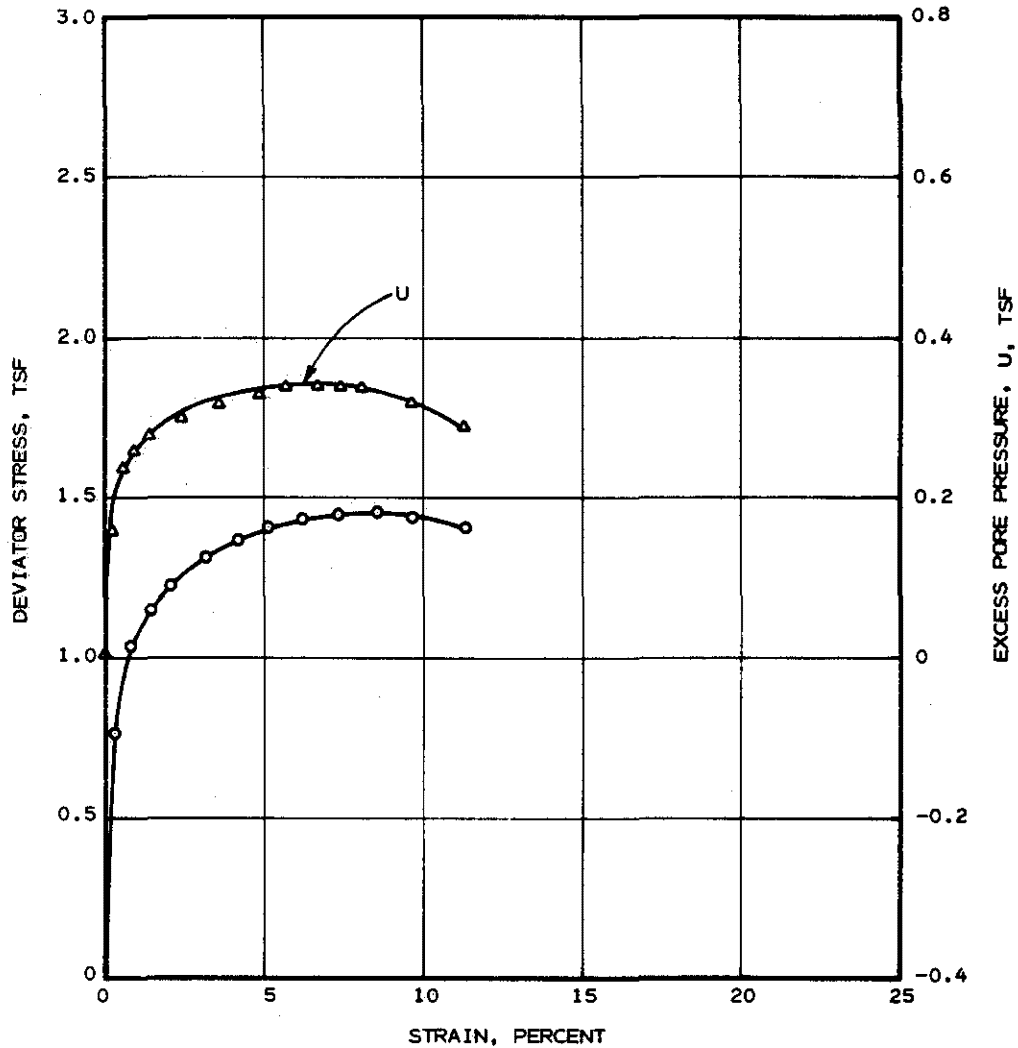
<u>BORING NO.</u>	<u>DEPTH, FT.</u>	<u>CONFINING PRESSURE, TSF</u>	<u>MATERIAL</u>
CB-3	19	1.15	STIFF RED AND LIGHT GRAY CLAY, SLICKENSIDED WITH CALCAREOUS NODULES

PORE PRESSURE-STRAIN AND
STRESS-STRAIN CURVES
TRIAxIAL COMPRESSION TEST
CONSOLIDATED UNDRAINED



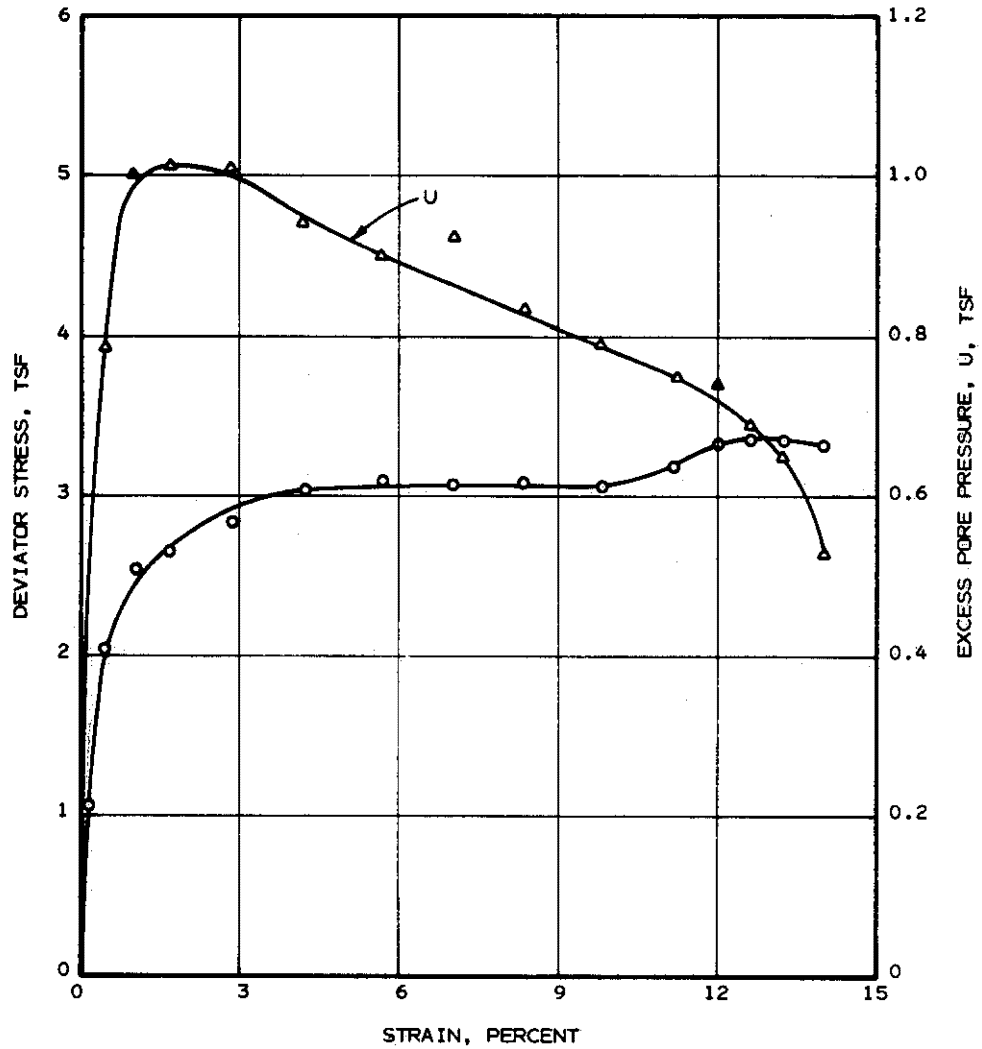
<u>BORING NO.</u>	<u>DEPTH, FT.</u>	<u>CONFINING PRESSURE, TSF</u>	<u>MATERIAL</u>
CB-1	18.5	1.44	STIFF RED AND LIGHT GRAY CLAY, SLICKENSIDED WITH CALCAREOUS NODULES

PORE PRESSURE — STRAIN AND
STRESS-STRAIN CURVES
TRIAXIAL COMPRESSION TEST
CONSOLIDATED UNDRAINED



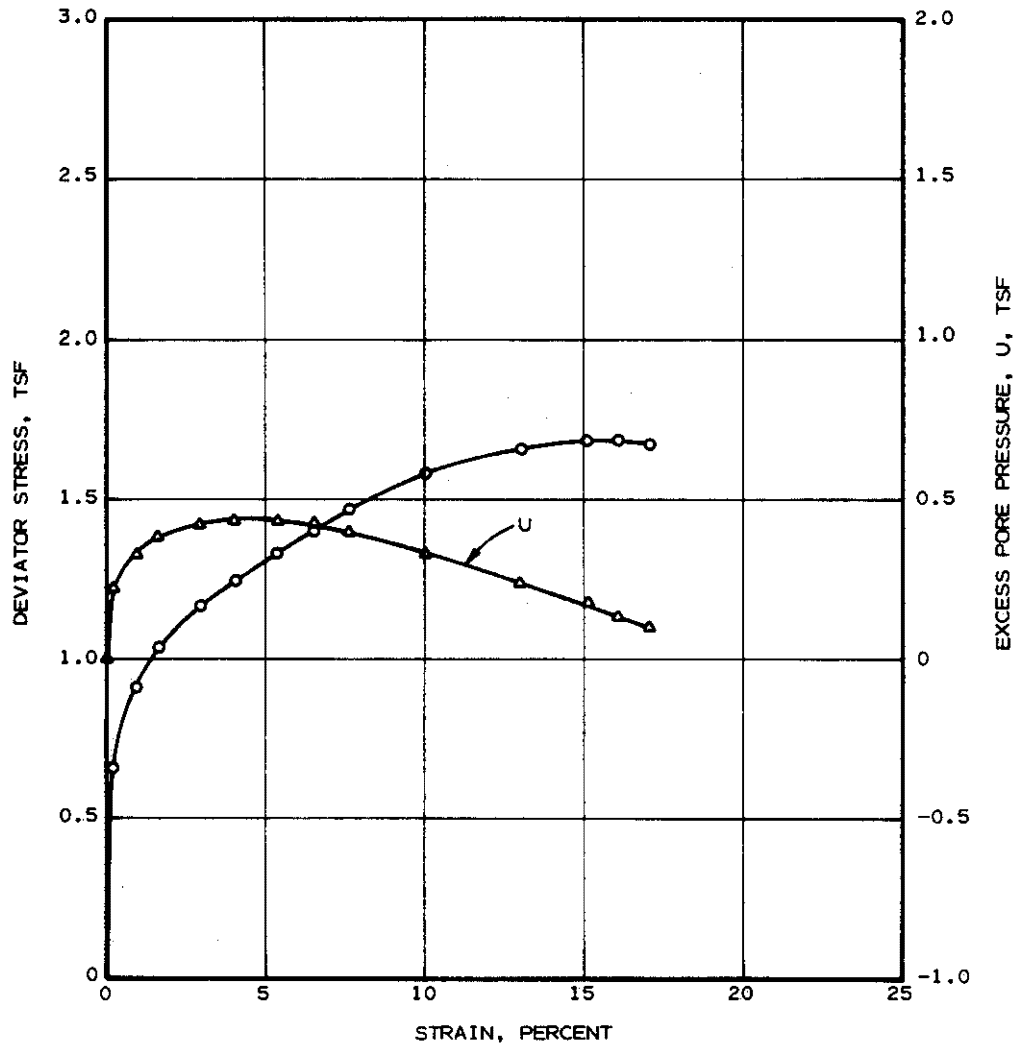
<u>BORING NO.</u>	<u>DEPTH, FT.</u>	<u>CONFINING PRESSURE, TSF</u>	<u>MATERIAL</u>
CB-1	19.5	1.87	STIFF RED AND LIGHT GRAY CLAY, SLICKENSIDED WITH CALCAREOUS NODULES

PORE PRESSURE-STRAIN AND
STRESS-STRAIN CURVES
TRIAxIAL COMPRESSION TEST
CONSOLIDATED UNDRAINED



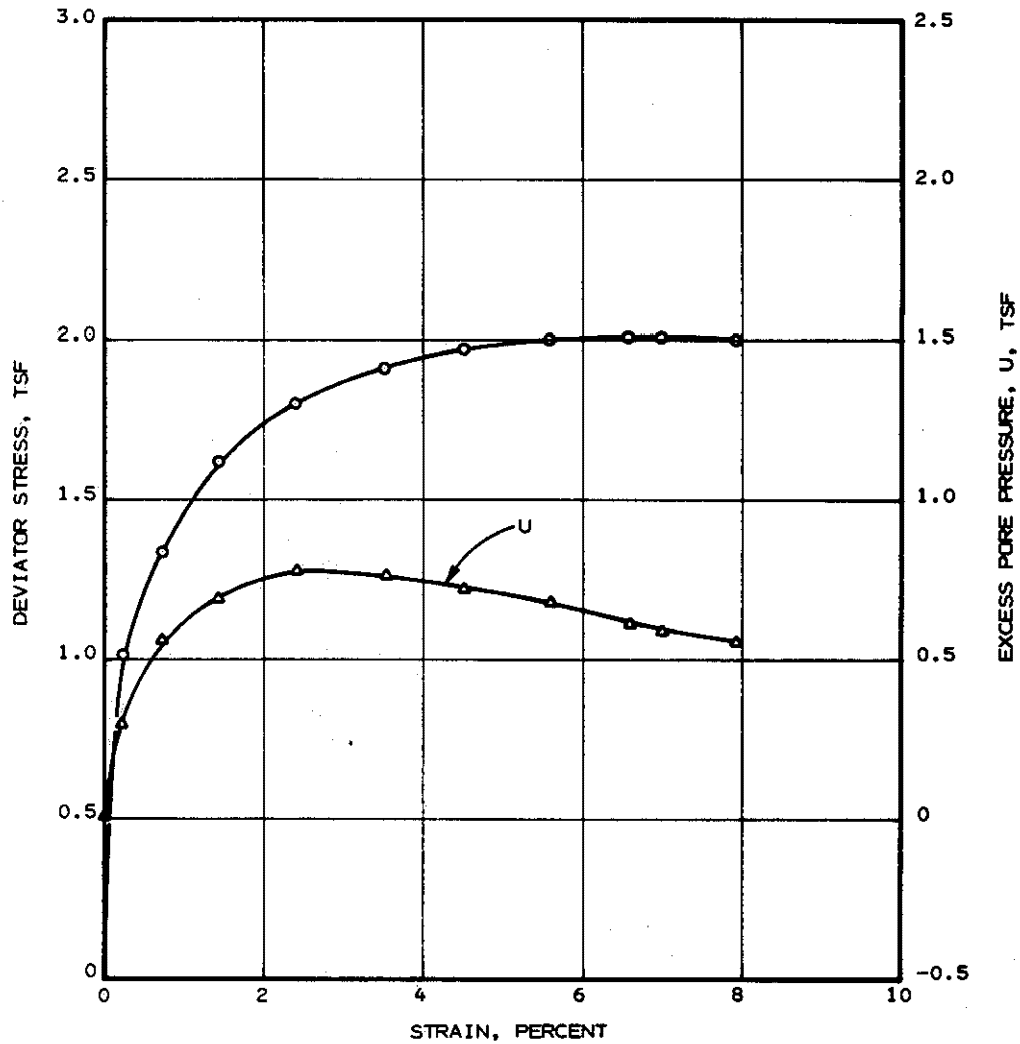
<u>BORING NO.</u>	<u>DEPTH, FT.</u>	<u>CONFINING PRESSURE, TSF</u>	<u>MATERIAL</u>
CB-2	19	2.74	STIFF RED AND LIGHT GRAY CLAY, SLICKENSIDED WITH CALCAREOUS NODULES

PORE PRESSURE-STRAIN AND
STRESS-STRAIN CURVES
TRIAxIAL COMPRESSION TEST
CONSOLIDATED UNDRAINED



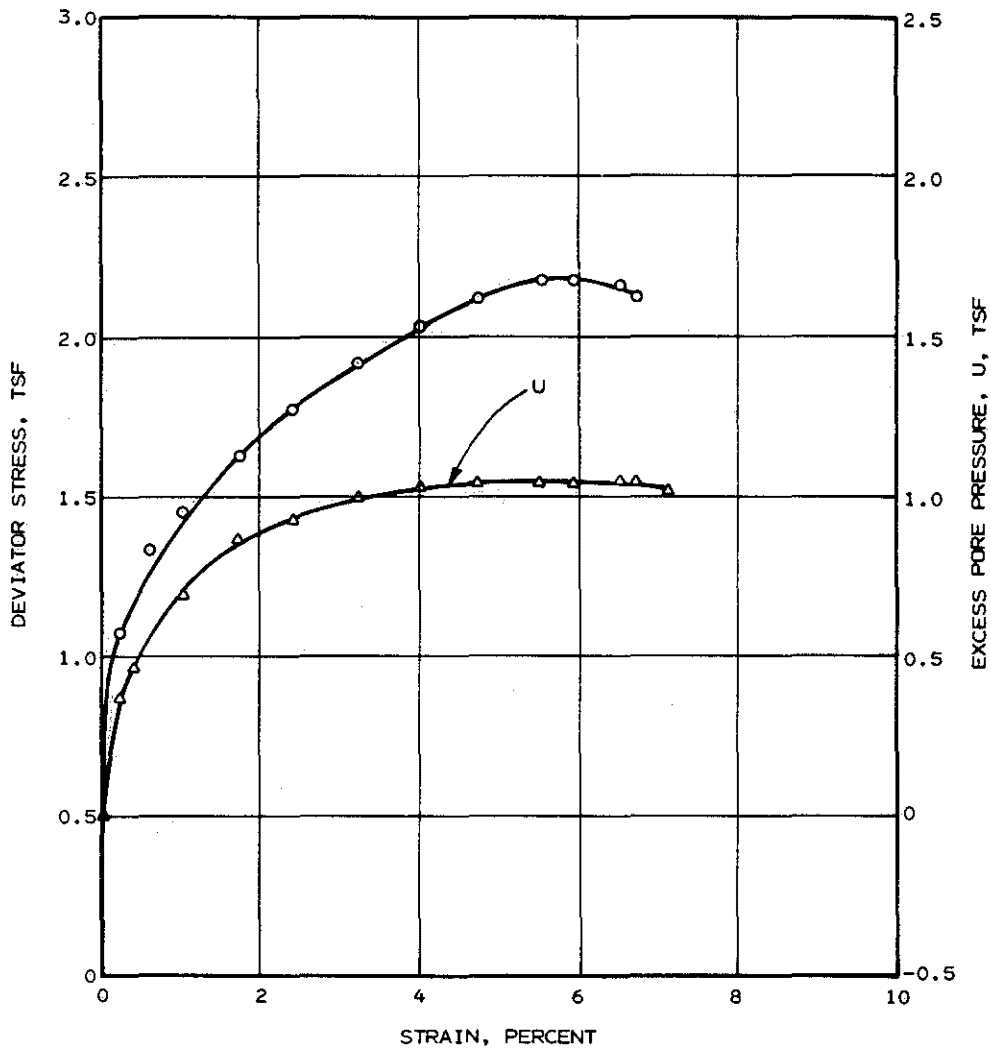
BORING NO.	DEPTH, FT.	CONFINING PRESSURE, TSF	MATERIAL
CB-2	23	1.22	VERY STIFF RED AND LIGHT GRAY CLAY, SLICKENSIDED

PORE PRESSURE-STRAIN AND
STRESS-STRAIN CURVES
TRIAxIAL COMPRESSION TEST
CONSOLIDATED UNDRAINED



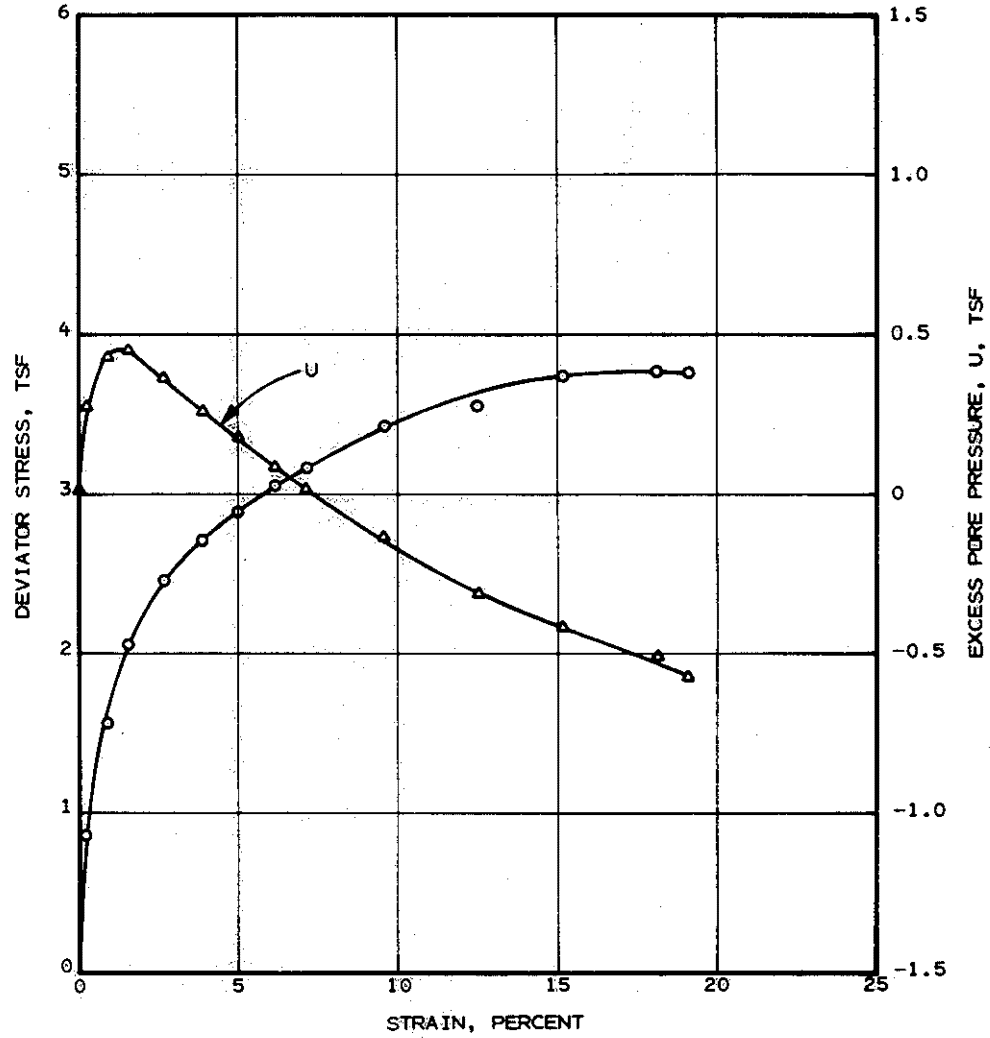
<u>BORING NO.</u>	<u>DEPTH, FT.</u>	<u>CONFINING PRESSURE, TSF</u>	<u>MATERIAL</u>
CB-3	23.5	1.80	STIFF RED AND LIGHT GRAY CLAY, SLICKENSIDED WITH CALCAREOUS NODULES

PORE PRESSURE-STRAIN AND
STRESS-STRAIN CURVES
TRIAXIAL COMPRESSION TEST
CONSOLIDATED UNDRAINED



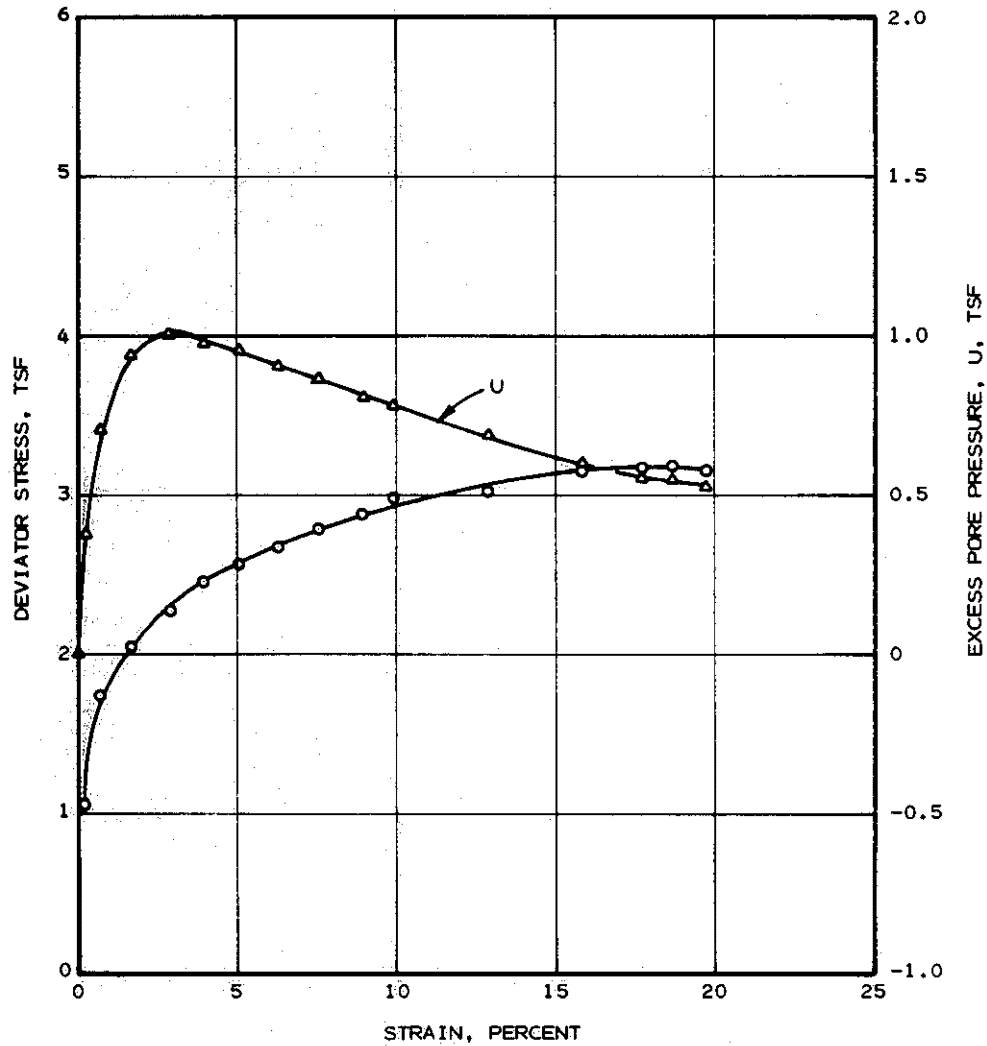
BORING NO.	DEPTH, FT.	CONFINING PRESSURE, TSF	MATERIAL
CB-2	23	2.38	VERY STIFF RED AND LIGHT GRAY CLAY, SLICKENSIDED

PORE PRESSURE-STRAIN AND
STRESS-STRAIN CURVES
TRIAxIAL COMPRESSION TEST
CONSOLIDATED UNDRAINED



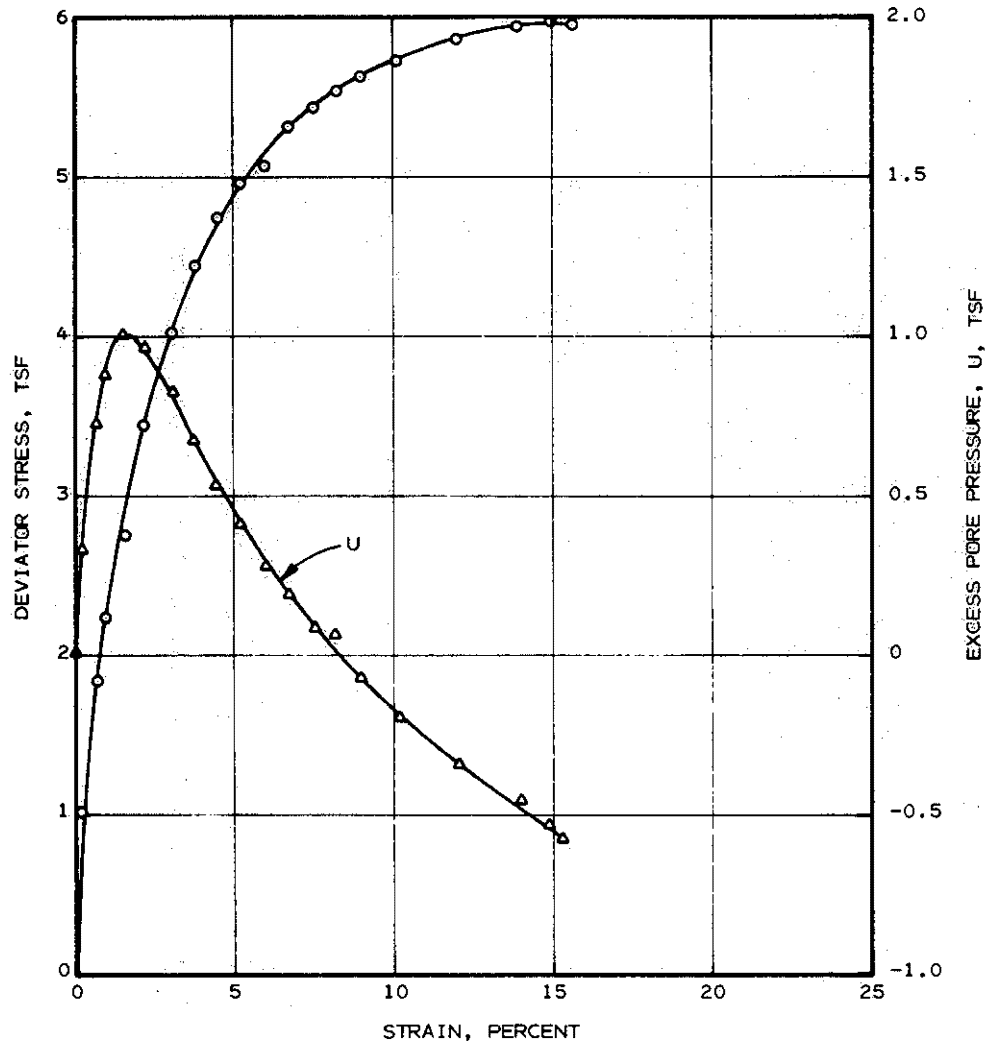
<u>BORING NO.</u>	<u>DEPTH, FT.</u>	<u>CONFINING PRESSURE, TSF</u>	<u>MATERIAL</u>
CB-1	33.5	1.30	VERY STIFF LIGHT GRAY AND TAN SANDY CLAY

PORE PRESSURE-STRAIN AND
STRESS-STRAIN CURVES
TRIAxIAL COMPRESSION TEST
CONSOLIDATED UNDRAINED



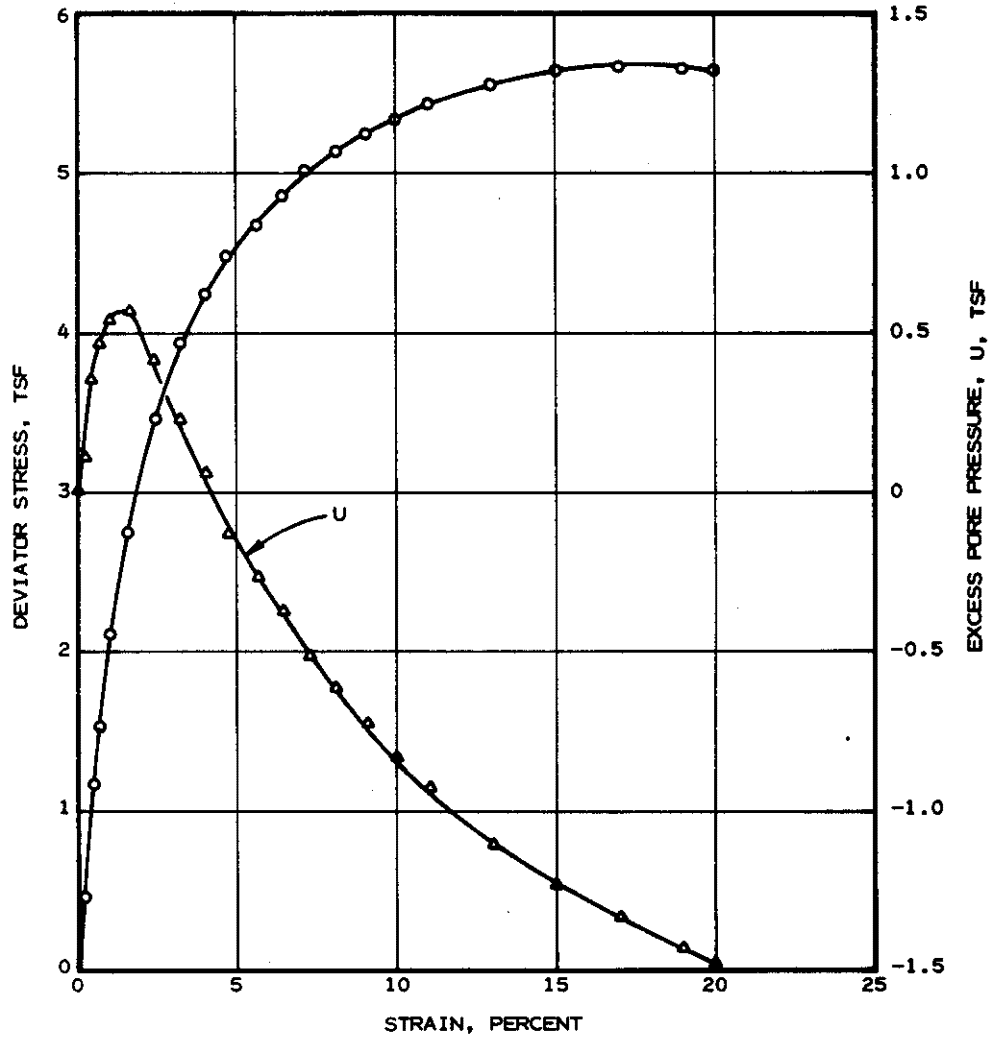
<u>BORING NO.</u>	<u>DEPTH, FT.</u>	<u>CONFINING PRESSURE, TSF</u>	<u>MATERIAL</u>
CB-1	32.5	2.09	VERY STIFF LIGHT GRAY AND TAN SANDY CLAY

PORE PRESSURE-STRAIN AND
STRESS-STRAIN CURVES
TRIAxIAL COMPRESSION TEST
CONSOLIDATED UNDRAINED



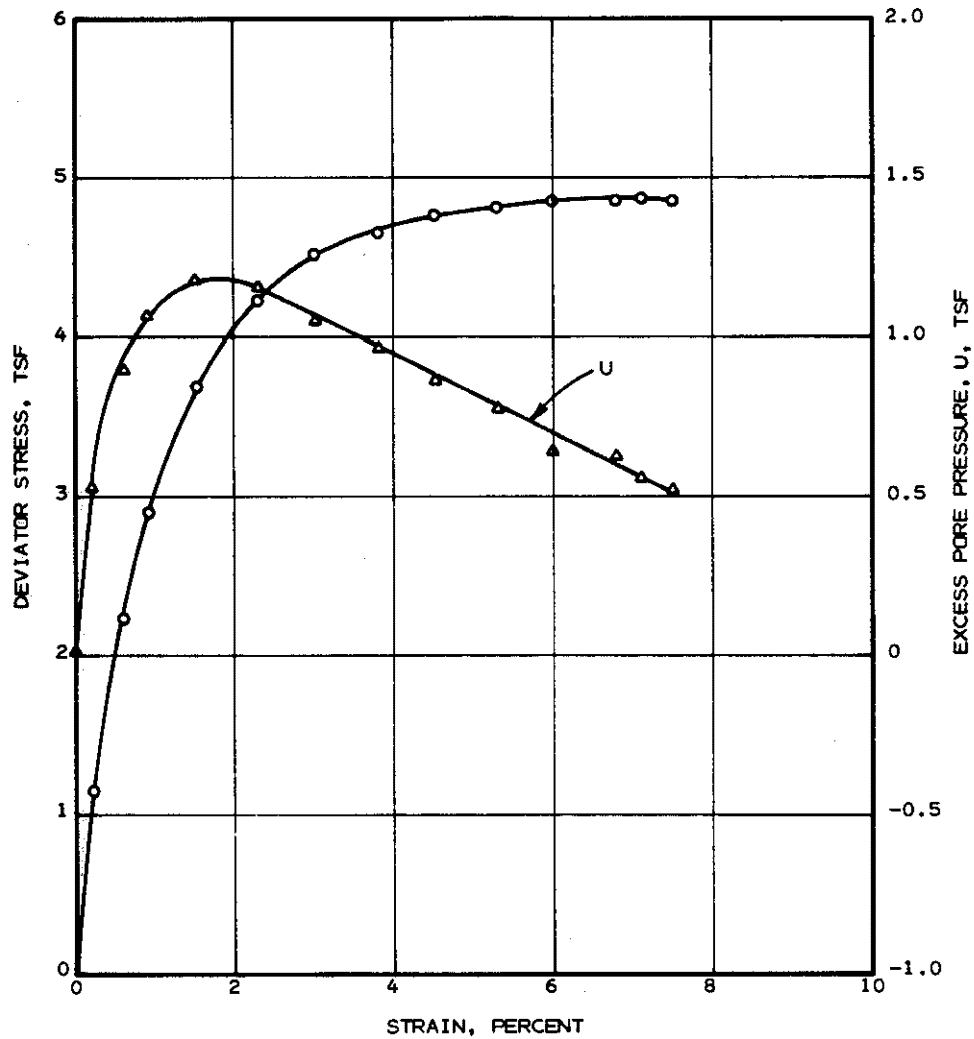
<u>BORING NO.</u>	<u>DEPTH, FT.</u>	<u>CONFINING PRESSURE, TSF</u>	<u>MATERIAL</u>
CB-3A	33.5	2.59	VERY STIFF LIGHT GRAY AND TAN SANDY CLAY

PORE PRESSURE-STRAIN AND
STRESS-STRAIN CURVES
TRIAxIAL COMPRESSION TEST
CONSOLIDATED UNDRAINED



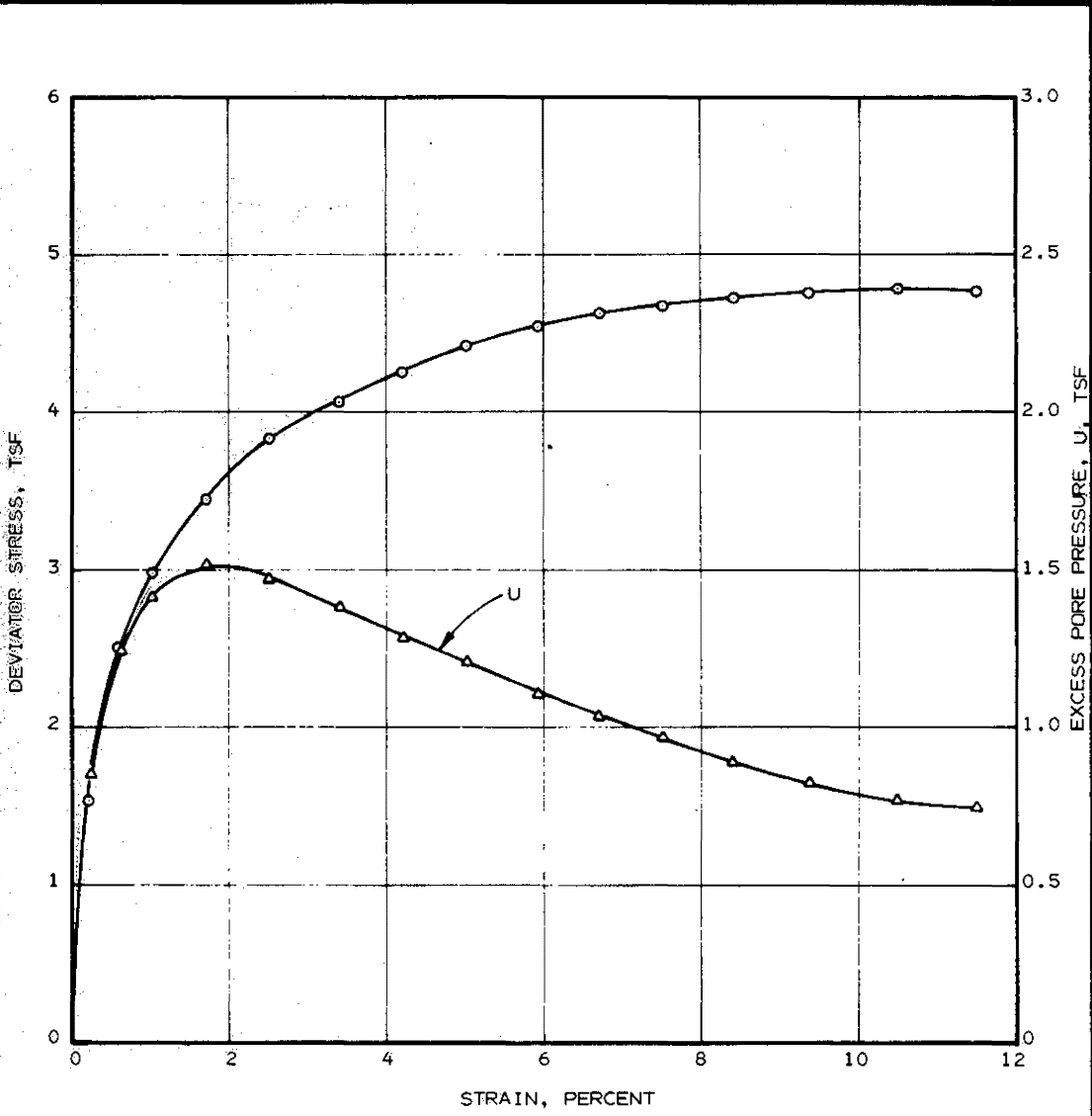
<u>BORING NO.</u>	<u>DEPTH, FT.</u>	<u>CONFINING PRESSURE, TSF</u>	<u>MATERIAL</u>
CB-2	37	1.87	STIFF LIGHT GRAY AND TAN SANDY CLAY

PORE PRESSURE-STRAIN AND
STRESS-STRAIN CURVES
TRIAxIAL COMPRESSION TEST
CONSOLIDATED UNDRAINED



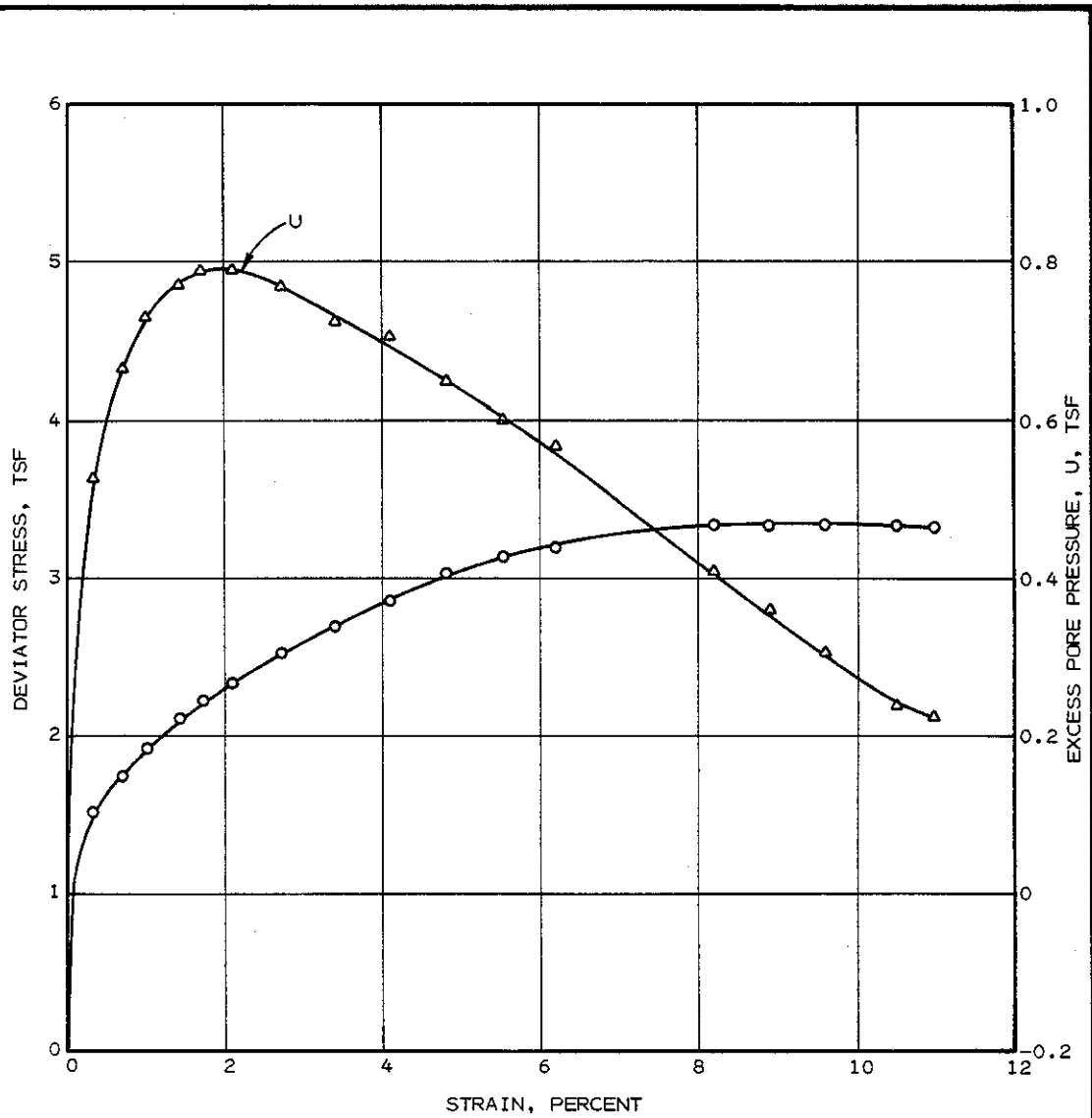
BORING NO.	DEPTH, FT.	CONFINING PRESSURE, TSF	MATERIAL
CB-2	37	2.95	STIFF LIGHT GRAY AND TAN SANDY CLAY

PORE PRESSURE-STRAIN AND
STRESS-STRAIN CURVES
TRIAXIAL COMPRESSION TEST
CONSOLIDATED UNDRAINED



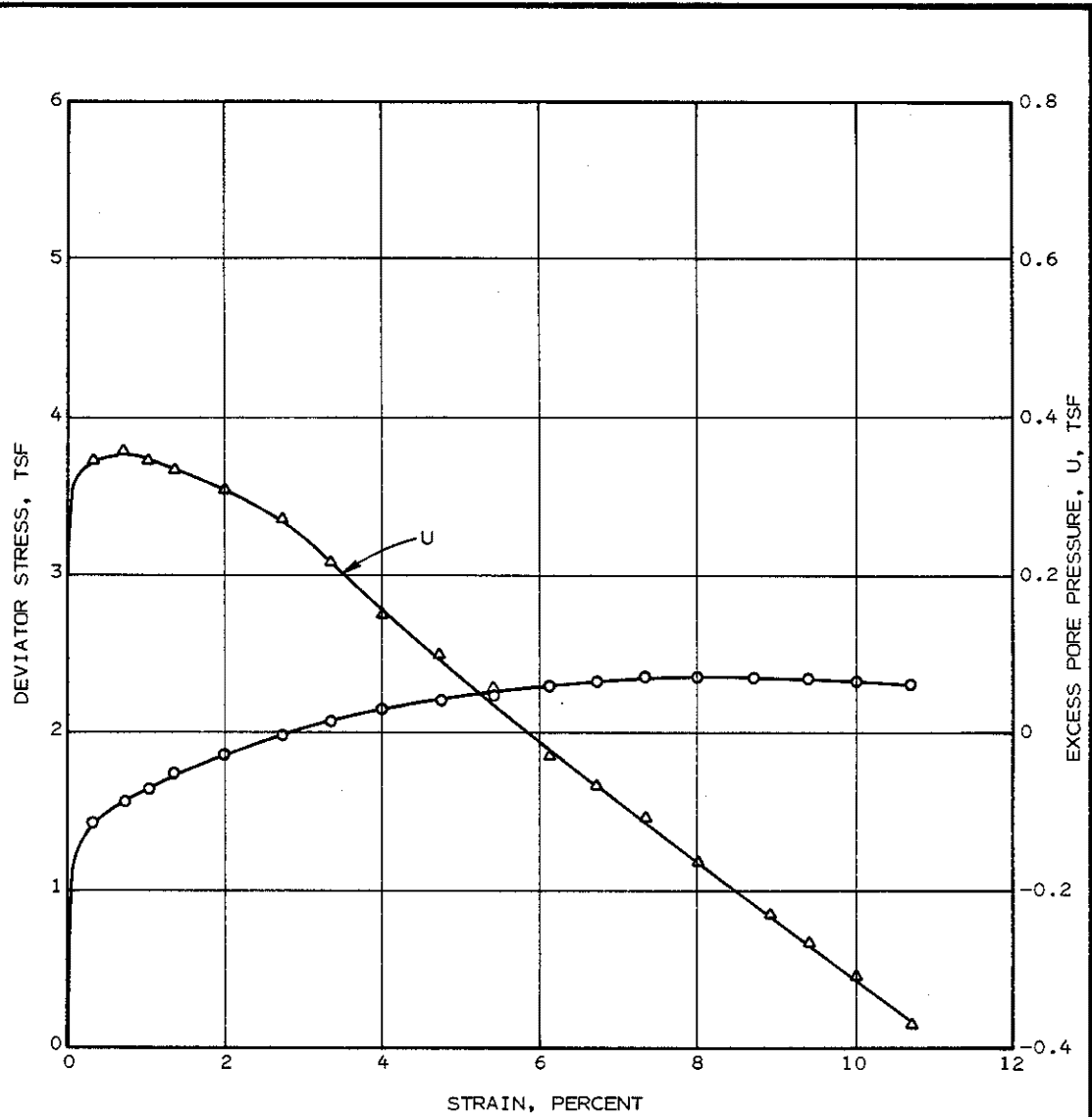
BORING NO.	DEPTH, FT.	CONFINING PRESSURE, TSF	MATERIAL
CB-1	37.5	4.03	STIFF LIGHT GRAY AND TAN SANDY CLAY

PORE PRESSURE-STRAIN AND
STRESS-STRAIN CURVES
TRIAXIAL COMPRESSION TEST
CONSOLIDATED UNDRAINED



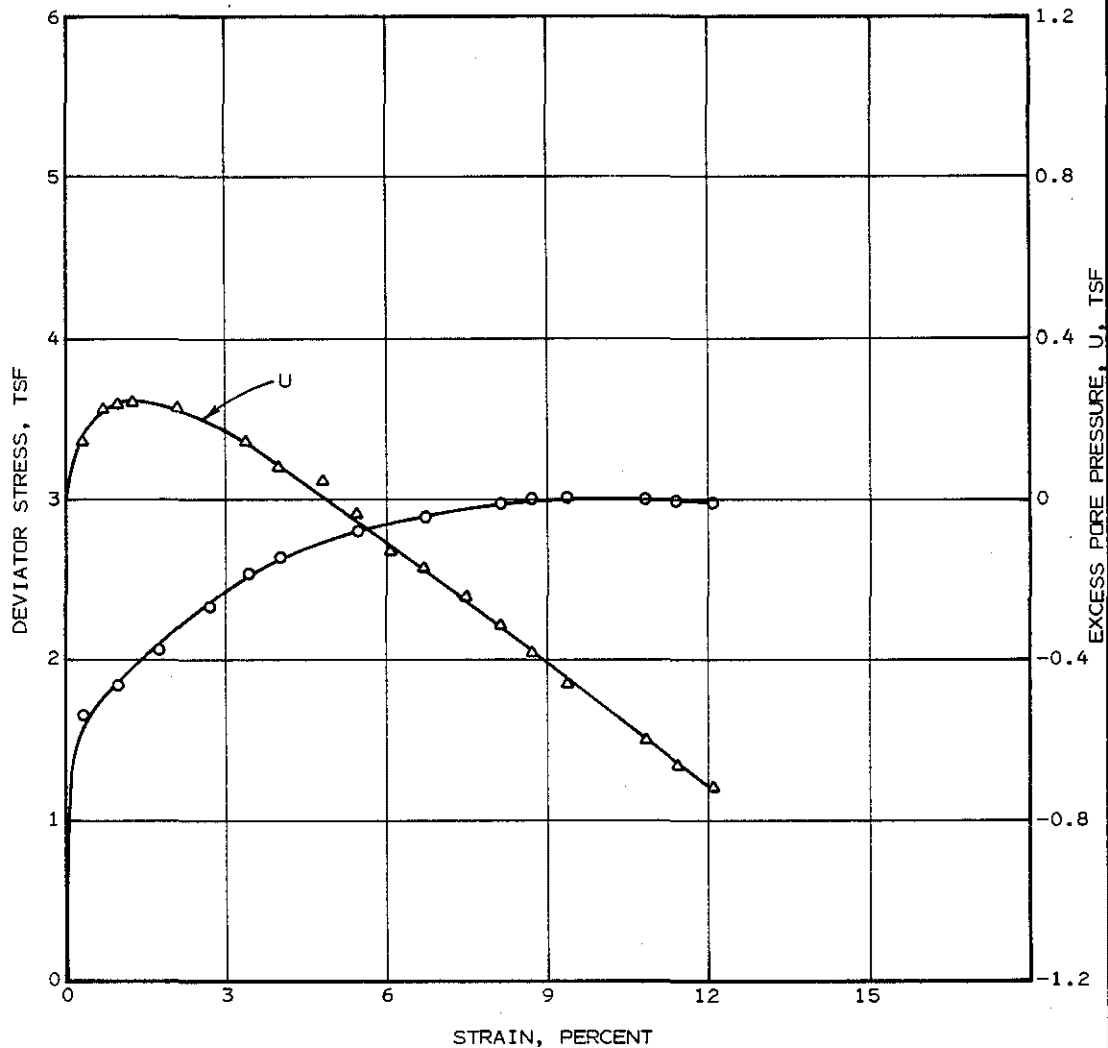
<u>BORING NO.</u>	<u>DEPTH, FT.</u>	<u>CONFINING PRESSURE, TSF</u>	<u>MATERIAL</u>
CB-2	17	2.02	RED AND LIGHT GRAY CLAY, SLICKENSIDED

PORE PRESSURE-STRAIN AND
 STRESS-STRAIN CURVES
 TRIAXIAL COMPRESSION TEST
 REMOLDED ANISOTROPIC CONSOLIDATED UNDRAINED



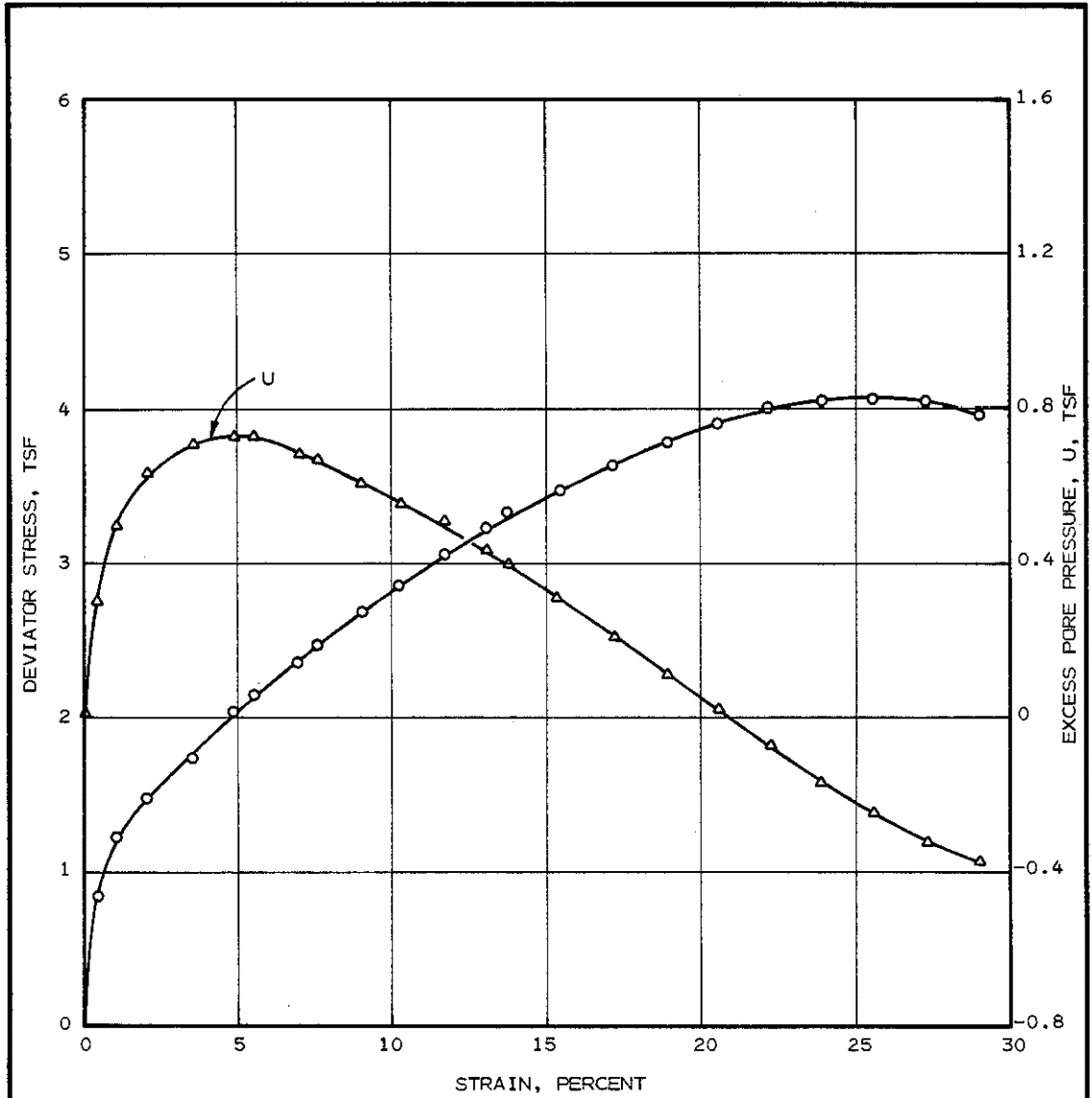
BORING NO.	DEPTH, FT.	CONFINING PRESSURE, TSF	MATERIAL
CB-2	17	1.12	RED AND LIGHT GRAY CLAY

PORE PRESSURE-STRAIN AND
 STRESS-STRAIN CURVES
 TRIAXIAL COMPRESSION TEST
 REMOLDED ANISOTROPIC CONSOLIDATED UNDRAINED



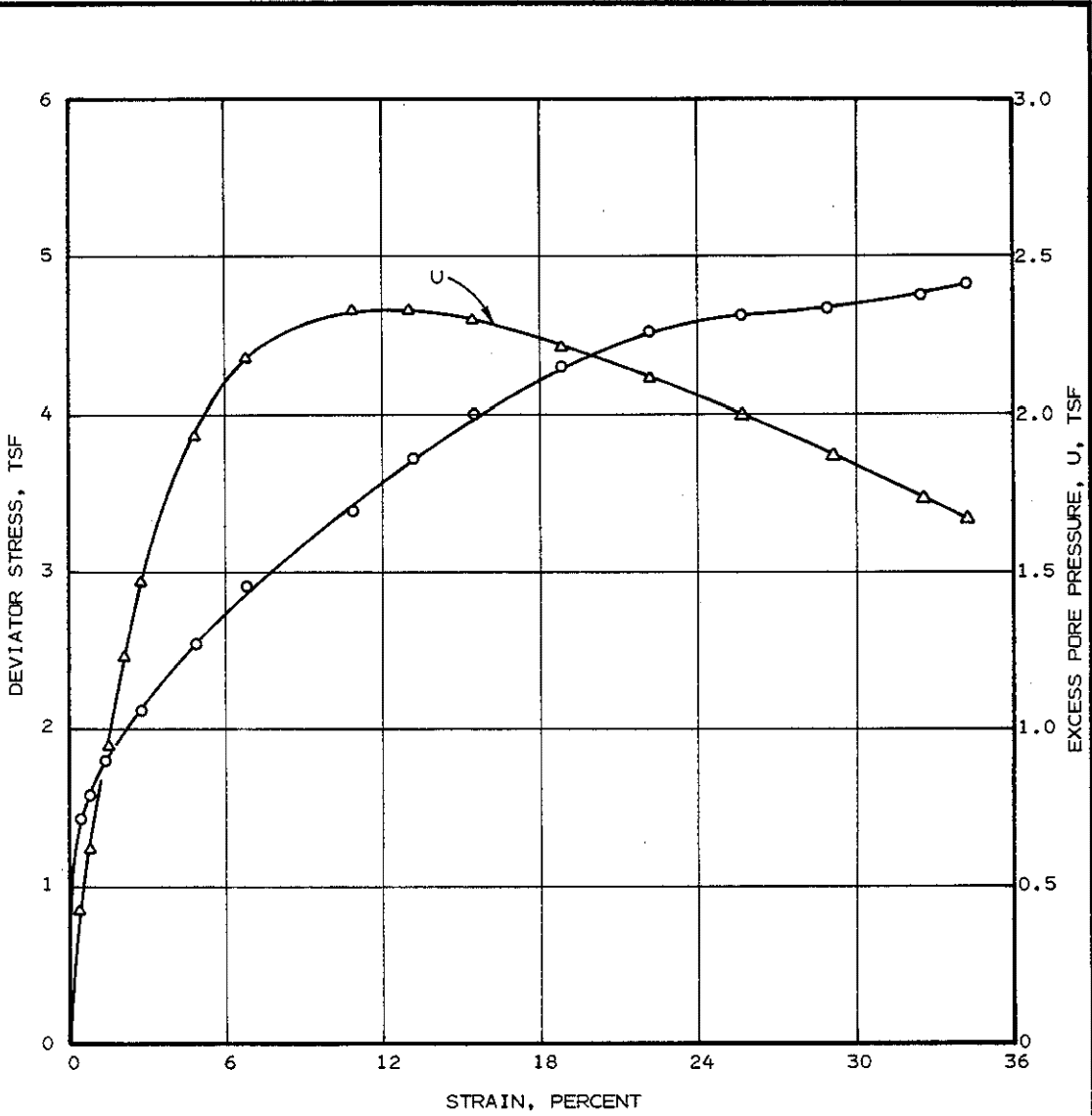
BORING NO.	DEPTH, FT.	CONFINING PRESSURE, TSF	MATERIAL
CB-2	17	1.51	RED AND LIGHT GRAY CLAY, SLICKENSIDED

PORE PRESSURE-STRAIN AND
STRESS-STRAIN CURVES
TRIAXIAL COMPRESSION TEST
REMOLDED ANISOTROPIC CONSOLIDATED UNDRAINED



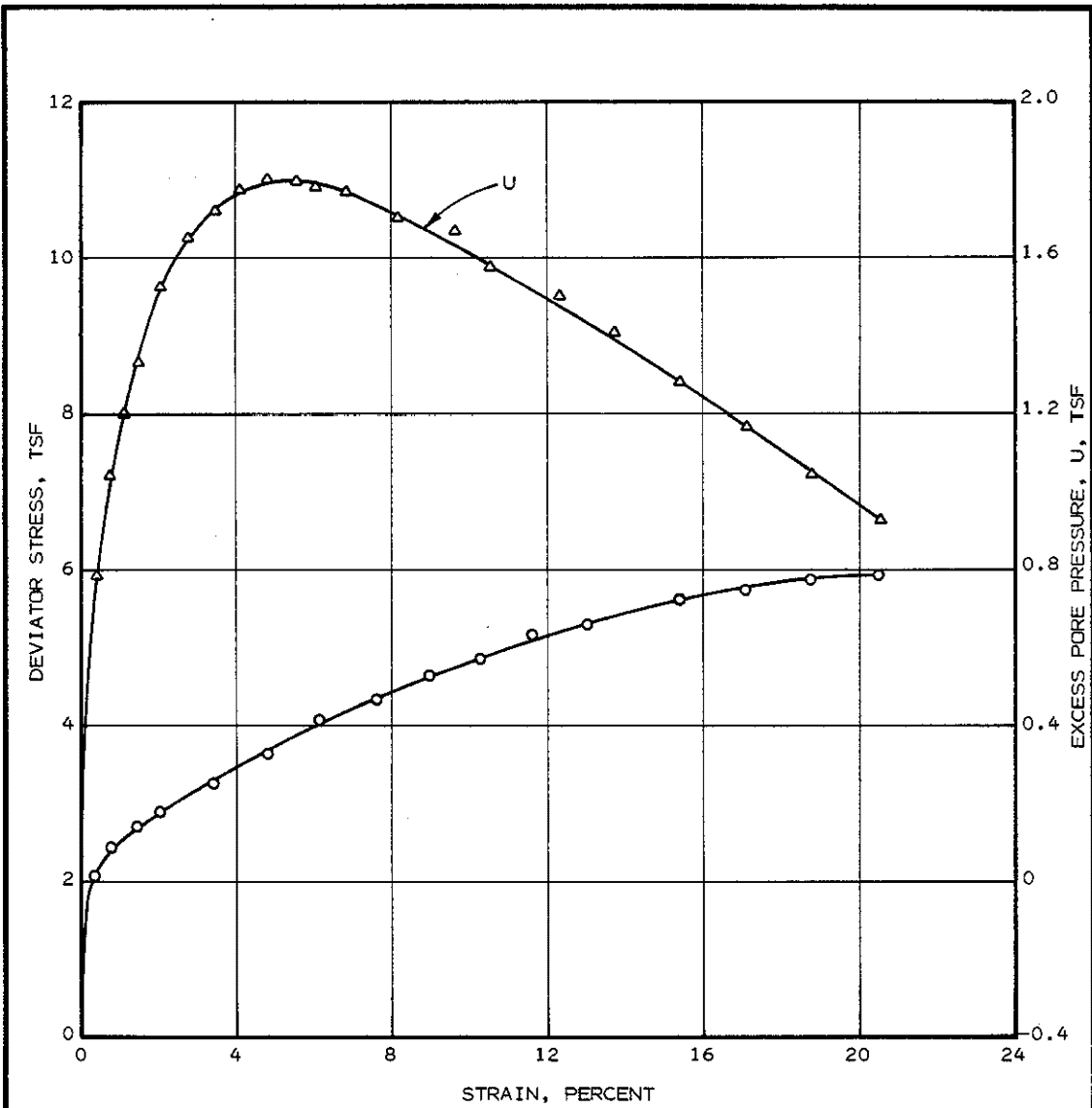
<u>BORING NO.</u>	<u>DEPTH, FT.</u>	<u>CONFINING PRESSURE, TSF</u>	<u>MATERIAL</u>
CB-2	35	1.73	TAN AND LIGHT GRAY SANDY CLAY WITH SAND POCKETS

PORE PRESSURE-STRAIN AND
STRESS-STRAIN CURVES
TRIAXIAL COMPRESSION TEST
REMOLDED ANISOTROPIC CONSOLIDATED UNDRAINED



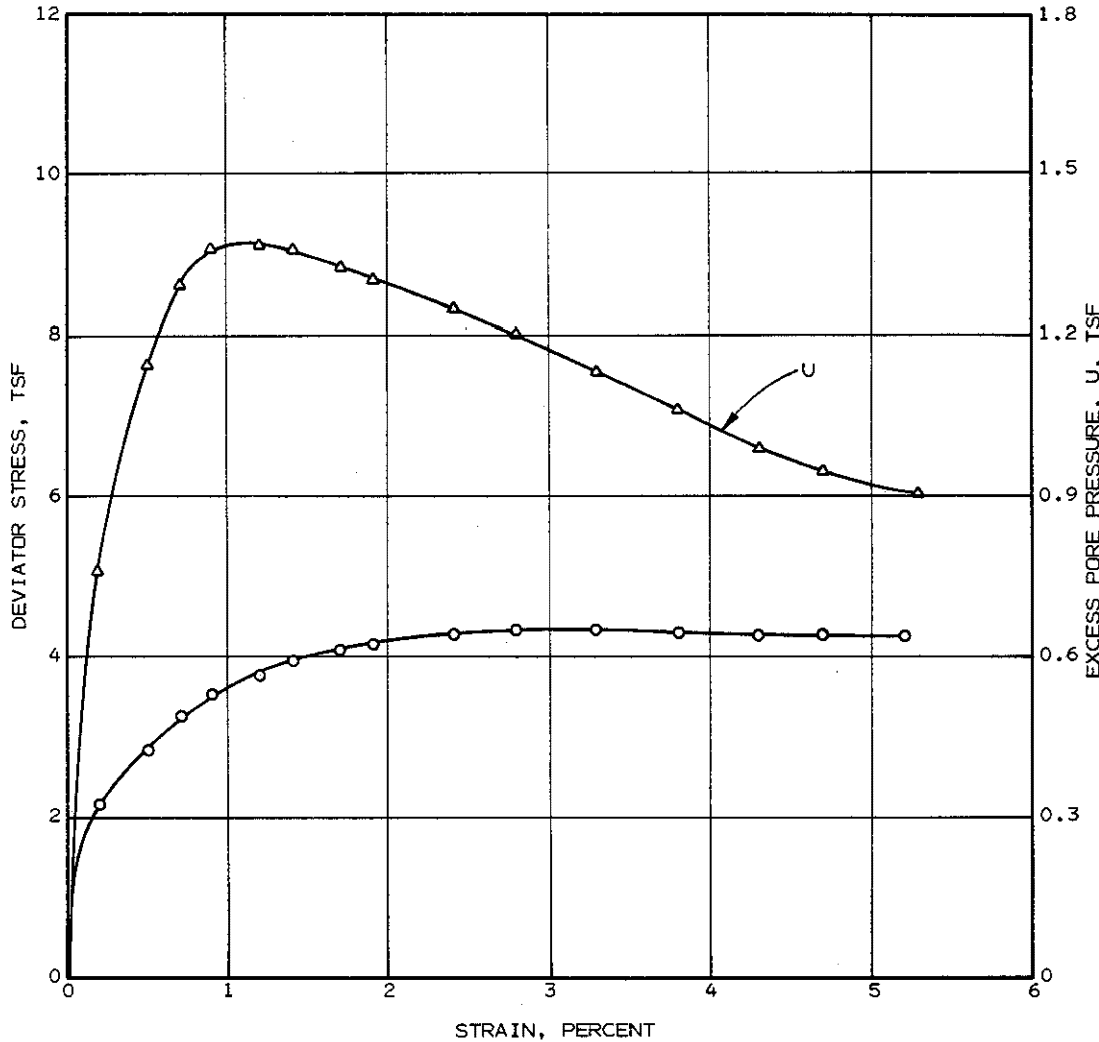
BORING NO.	DEPTH, FT.	CONFINING PRESSURE, TSF	MATERIAL
CB-2	35	2.59	TAN AND LIGHT GRAY SANDY CLAY

PORE PRESSURE-STRAIN AND
STRESS-STRAIN CURVES
TRIAxIAL COMPRESSION TEST
REMOLDED ANISOTROPIC CONSOLIDATED UNDRAINED



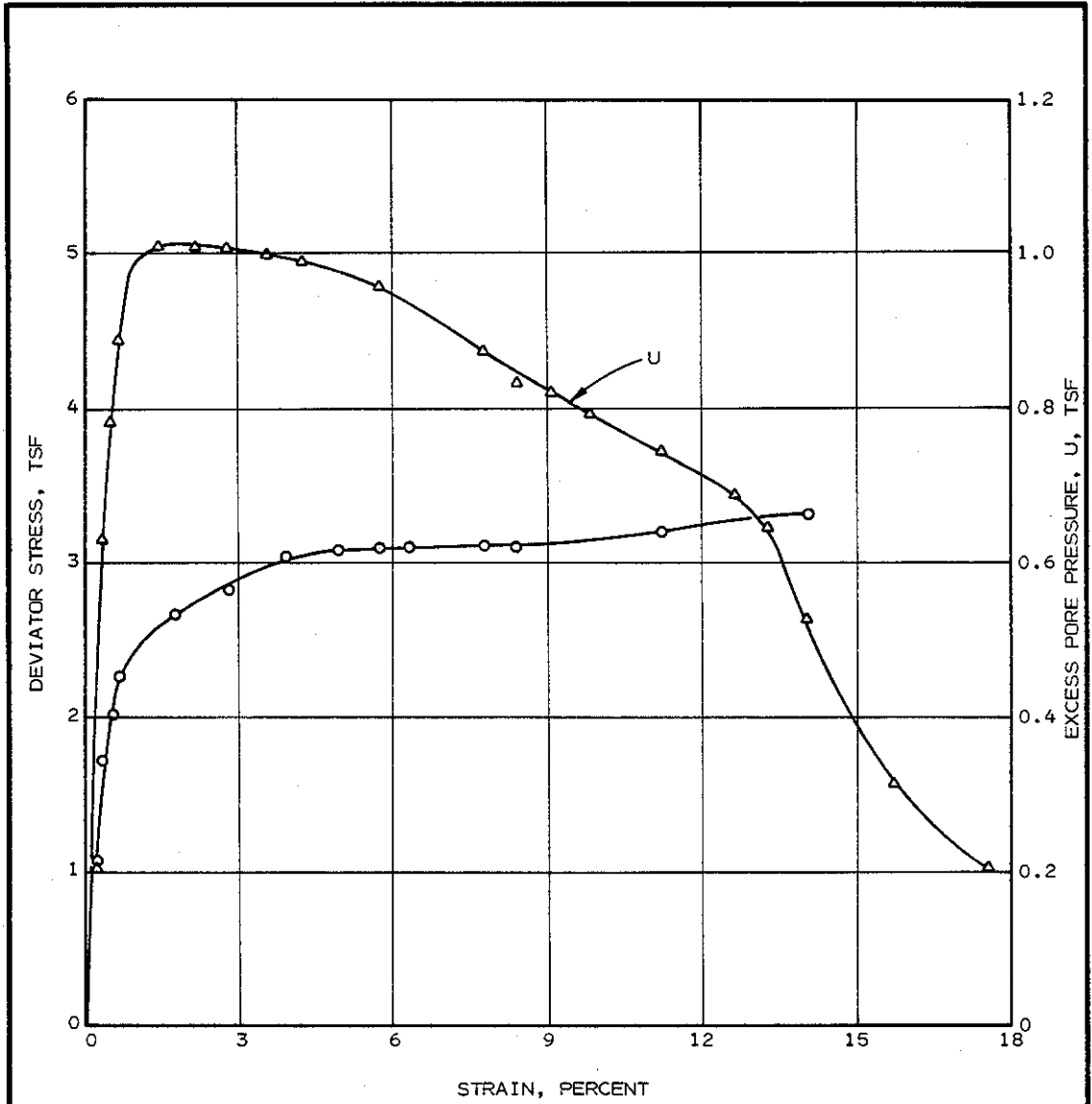
BORING NO.	DEPTH, FT.	CONFINING PRESSURE, TSF	MATERIAL
CB-2	35	3.46	TAN AND LIGHT GRAY SANDY CLAY

PORE PRESSURE-STRAIN AND
STRESS-STRAIN CURVES
TRIAXIAL COMPRESSION TEST
ANISOTROPIC CONSOLIDATED UNDRAINED



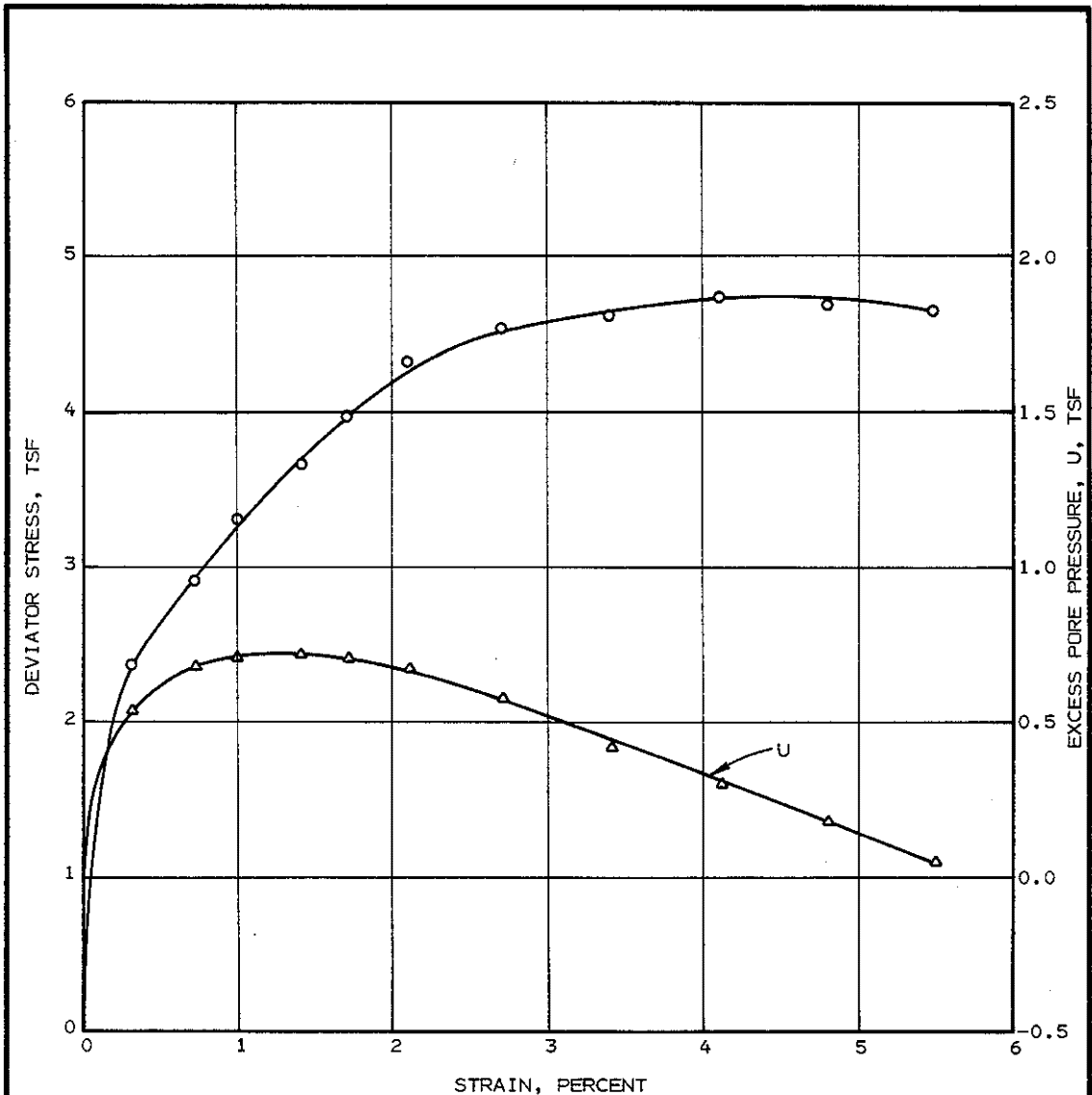
BORING NO.	DEPTH, FT.	MAXIMUM CONSOLIDATION PRESSURE, TSF	FINAL CONFINING PRESSURE, TSF	MATERIAL
CB-2	19	10.8	5.04	VERY STIFF RED AND LIGHT GRAY CLAY, SLICKENSIDED

OCR = 2.1
 PORE PRESSURE-STRAIN AND
 STRESS-STRAIN CURVES
 NSP TRIAXIAL COMPRESSION TEST
 CONSOLIDATED UNDRAINED



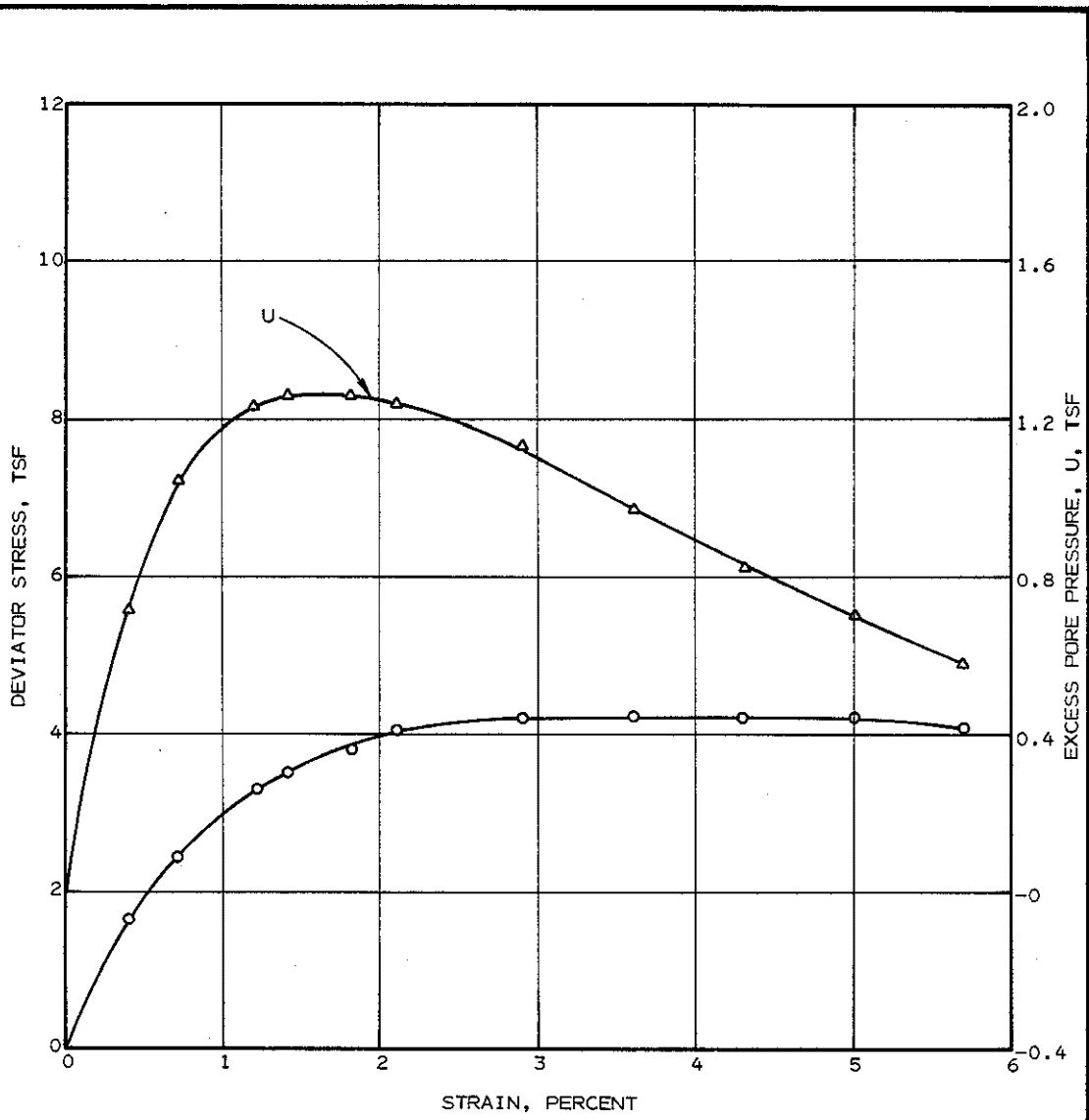
BORING NO.	DEPTH, FT.	MAXIMUM CONSOLIDATION PRESSURE, TSF	FINAL CONFINING PRESSURE, TSF	MATERIAL
CB-2	19	10.8	2.74	VERY STIFF RED AND LIGHT GRAY CLAY WITH CALCAREOUS NODULES, SLICKENSIDED

OCR = 3.95
 PORE PRESSURE-STRAIN AND
 STRESS-STRAIN CURVES
 NSP TRIAXIAL COMPRESSION TEST
 CONSOLIDATED UNDRAINED



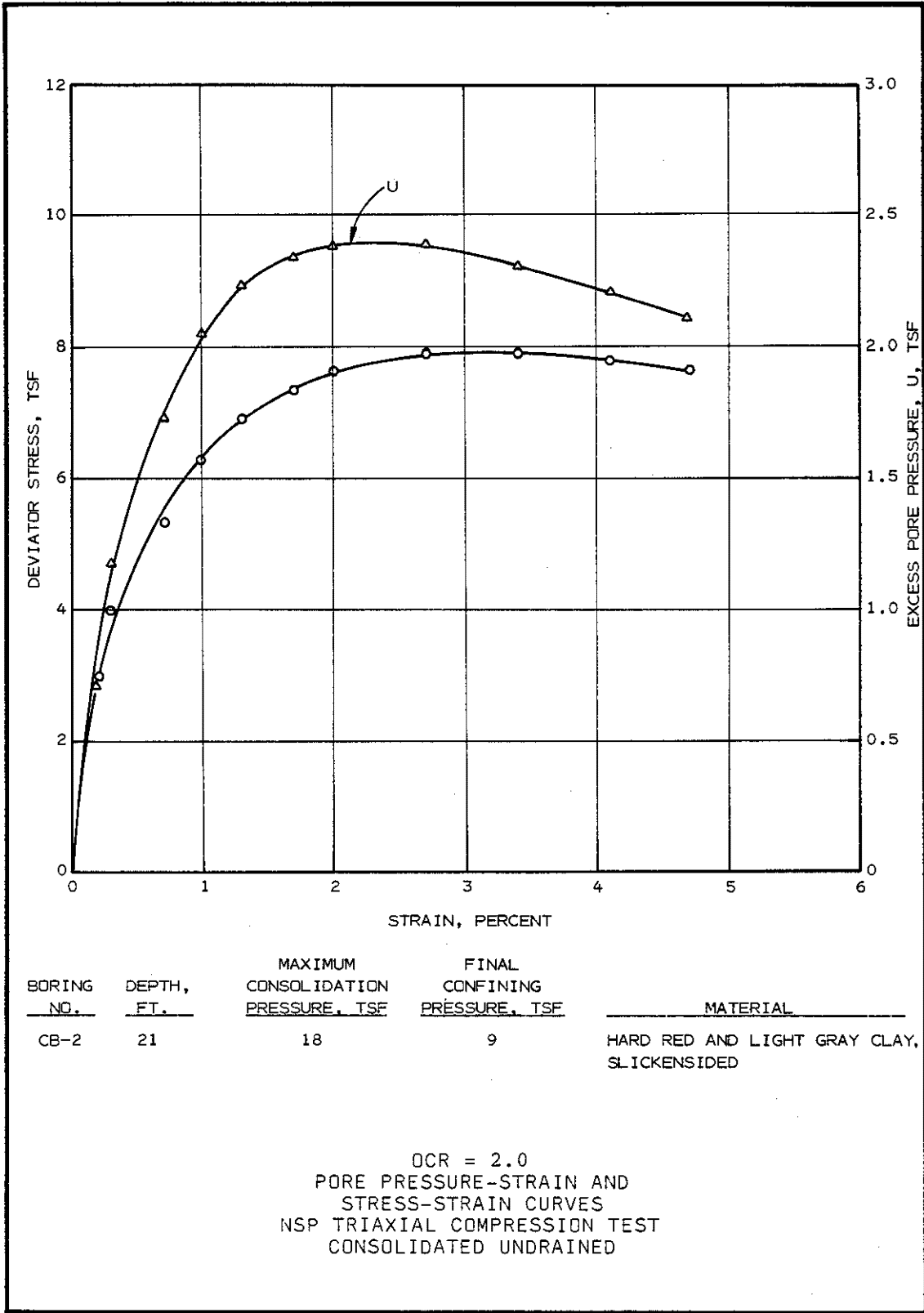
<u>BORING NO.</u>	<u>DEPTH, FT.</u>	<u>MAXIMUM CONSOLIDATION PRESSURE, TSF</u>	<u>FINAL CONFINING PRESSURE, TSF</u>	<u>MATERIAL</u>
CB-2	21	18	1.80	VERY STIFF RED AND LIGHT GRAY CLAY, SLICKENSIDED

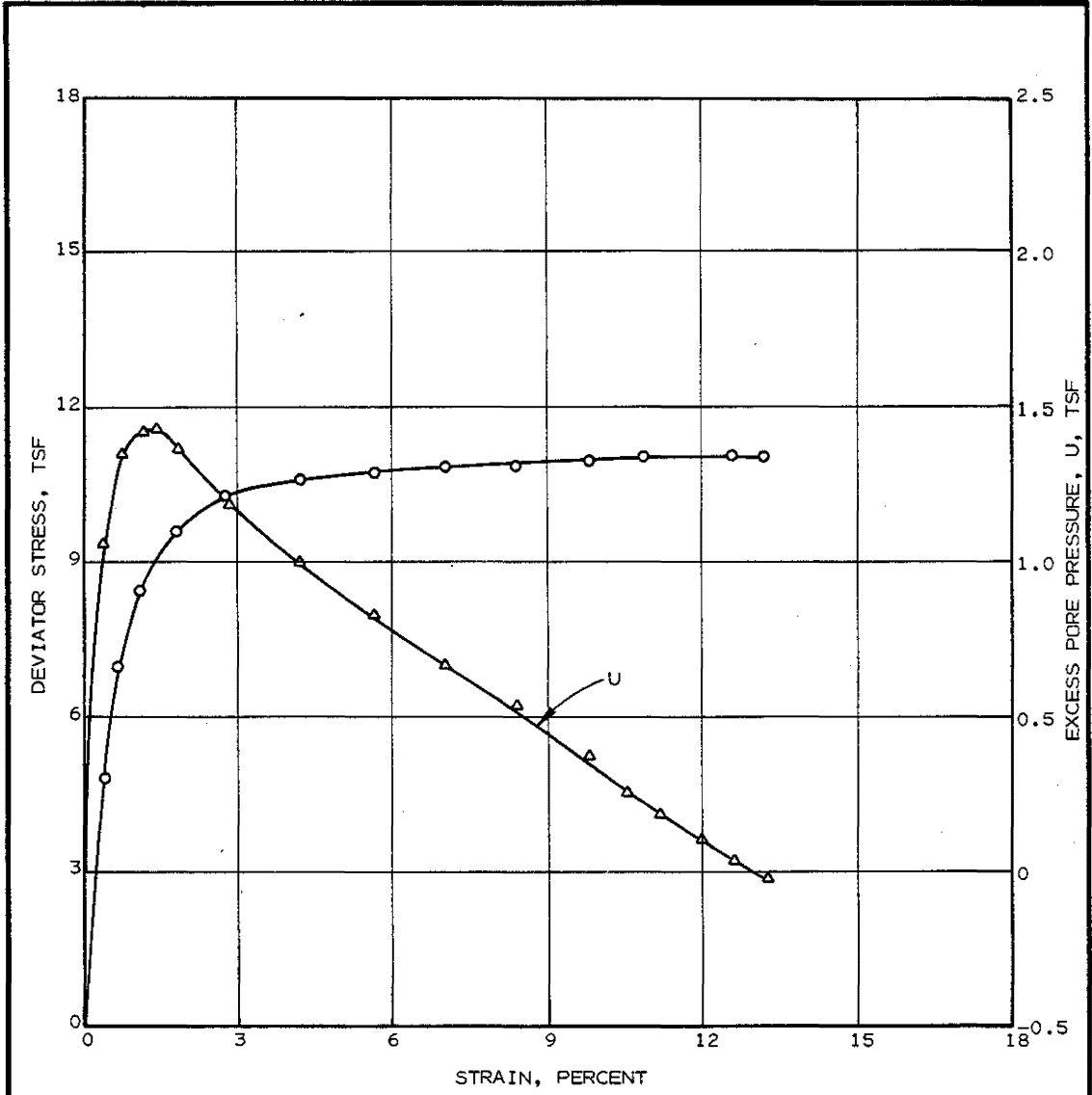
OCR = 10.0
 PORE PRESSURE-STRAIN AND
 STRESS-STRAIN CURVES
 NSP TRIAXIAL COMPRESSION TEST
 CONSOLIDATED UNDRAINED



BORING NO.	DEPTH, FT.	MAXIMUM CONSOLIDATION PRESSURE, TSF	FINAL CONFINING PRESSURE, TSF	MATERIAL
CB-1	21	18	3.60	VERY STIFF RED AND LIGHT GRAY SLICKENSIDED CLAY

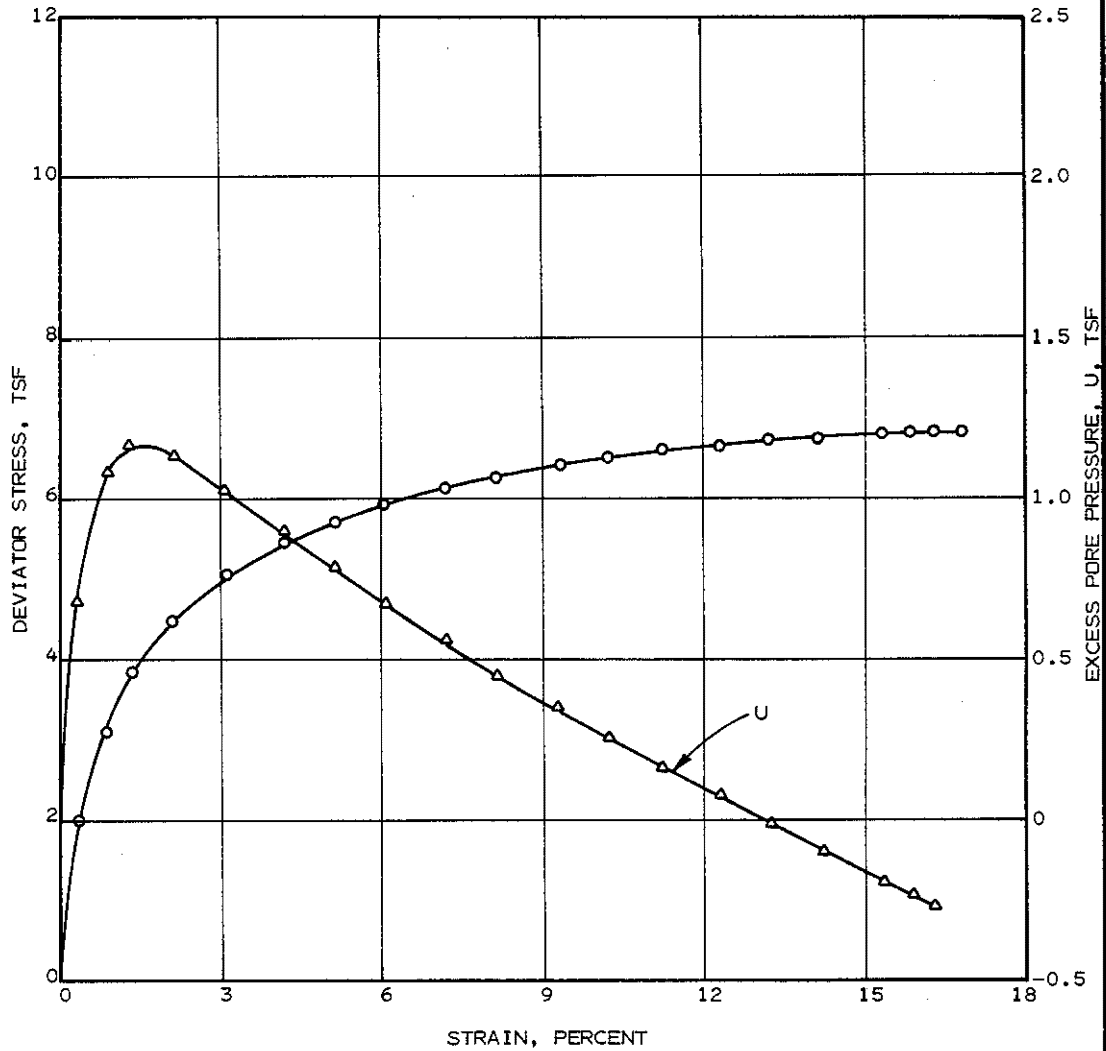
DCR = 5.0
 PORE PRESSURE-STRAIN AND
 STRESS-STRAIN CURVES
 NSP TRIAXIAL COMPRESSION TEST
 CONSOLIDATED UNDRAINED





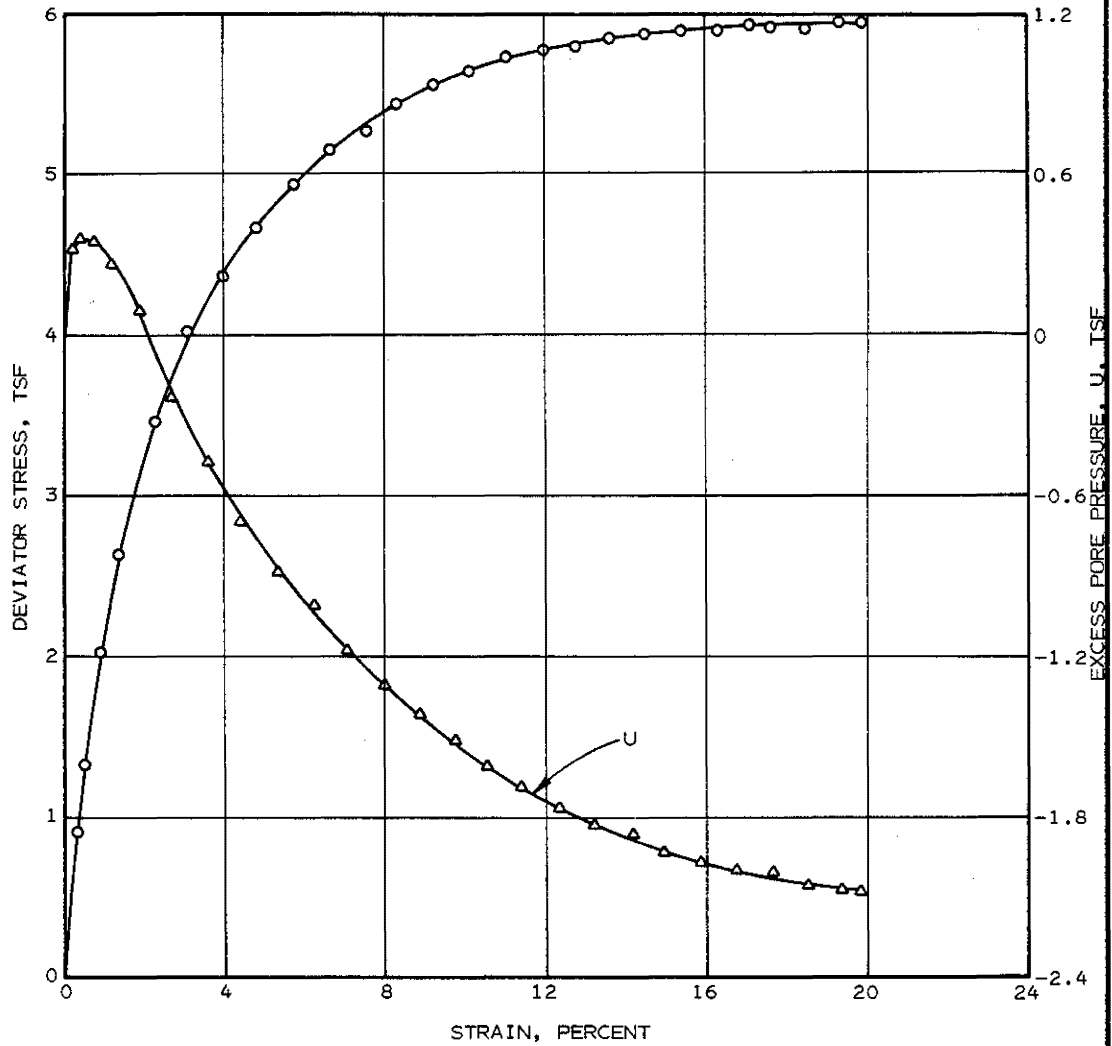
BORING NO.	DEPTH, FT.	MAXIMUM CONSOLIDATION PRESSURE, TSF	FINAL CONFINING PRESSURE, TSF	MATERIAL
CB-1	33	10.8	5.40	HARD YELLOW AND LIGHT GRAY SANDY CLAY

OCR = 2.0
 PORE PRESSURE-STRAIN AND
 STRESS-STRAIN CURVES
 NSP TRIAXIAL COMPRESSION TEST
 CONSOLIDATED UNDRAINED



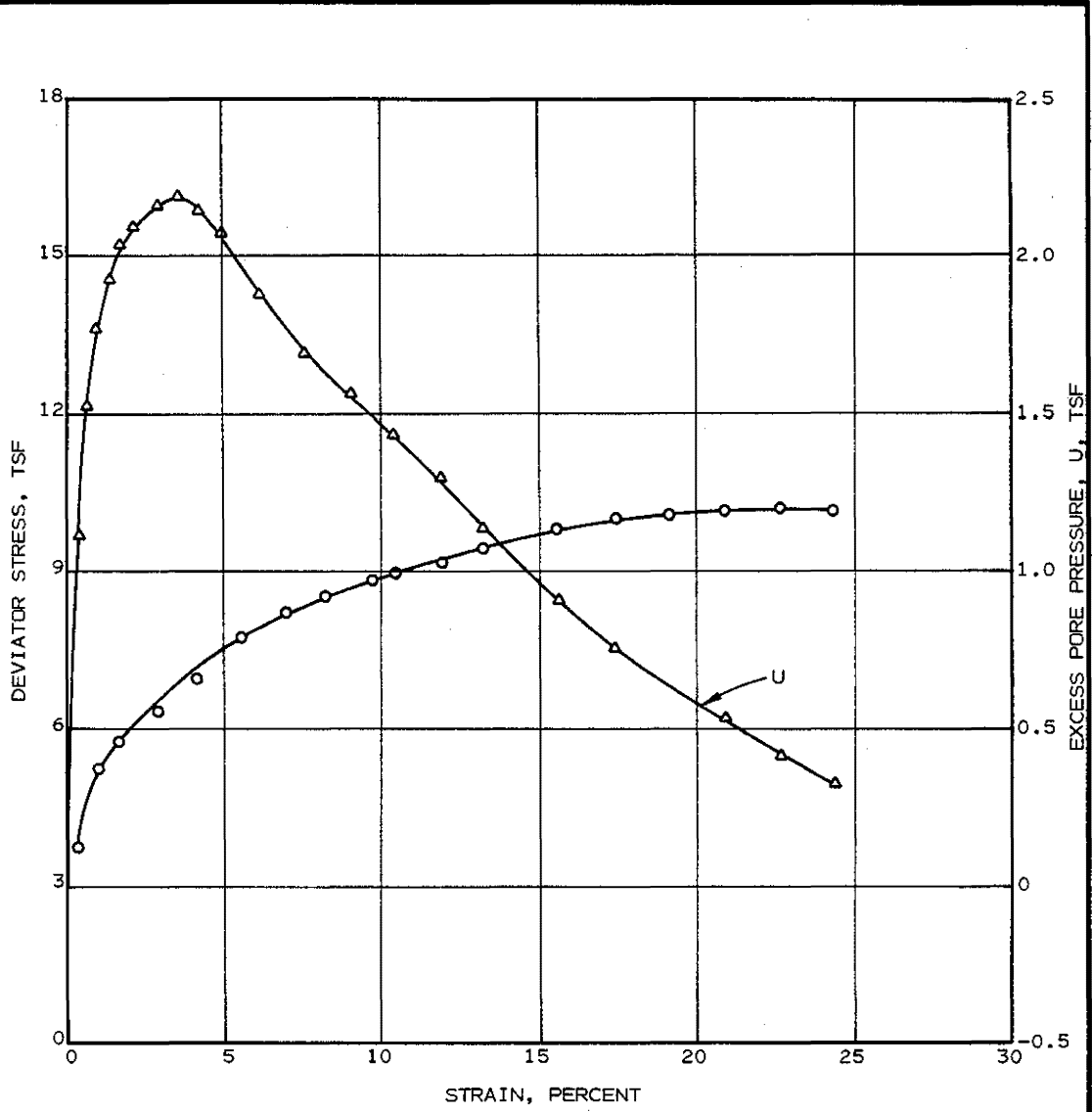
BORING NO.	DEPTH, FT.	MAXIMUM CONSOLIDATION PRESSURE, TSF	FINAL CONFINING PRESSURE, TSF	MATERIAL
CB-1	33	10.8	3.60	HARD TAN AND LIGHT GRAY SANDY CLAY

OCR = 3.0
 PORE PRESSURE-STRAIN AND
 STRESS-STRAIN CURVES
 NSP TRIAXIAL COMPRESSION TEST
 CONSOLIDATED UNDRAINED



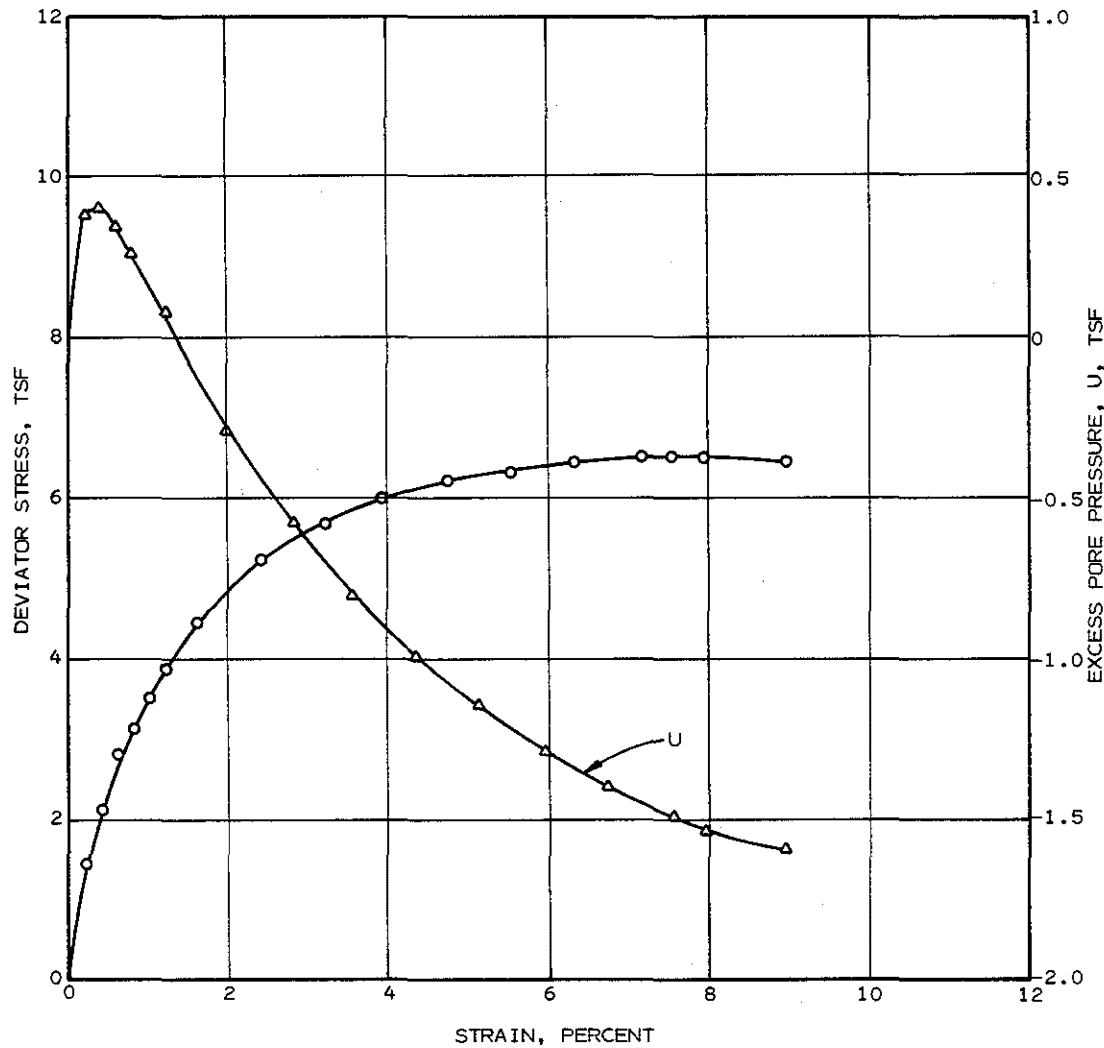
BORING NO.	DEPTH, FT.	MAXIMUM CONSOLIDATION PRESSURE, TSF	FINAL CONFINING PRESSURE, TSF	MATERIAL
CB-1	33	10.8	1.08	VERY STIFF LIGHT GRAY AND TAN SANDY CLAY

OCR = 10.0
 PORE PRESSURE-STRAIN AND
 STRESS-STRAIN CURVES
 NSP TRIAXIAL COMPRESSION TEST
 CONSOLIDATED UNDRAINED



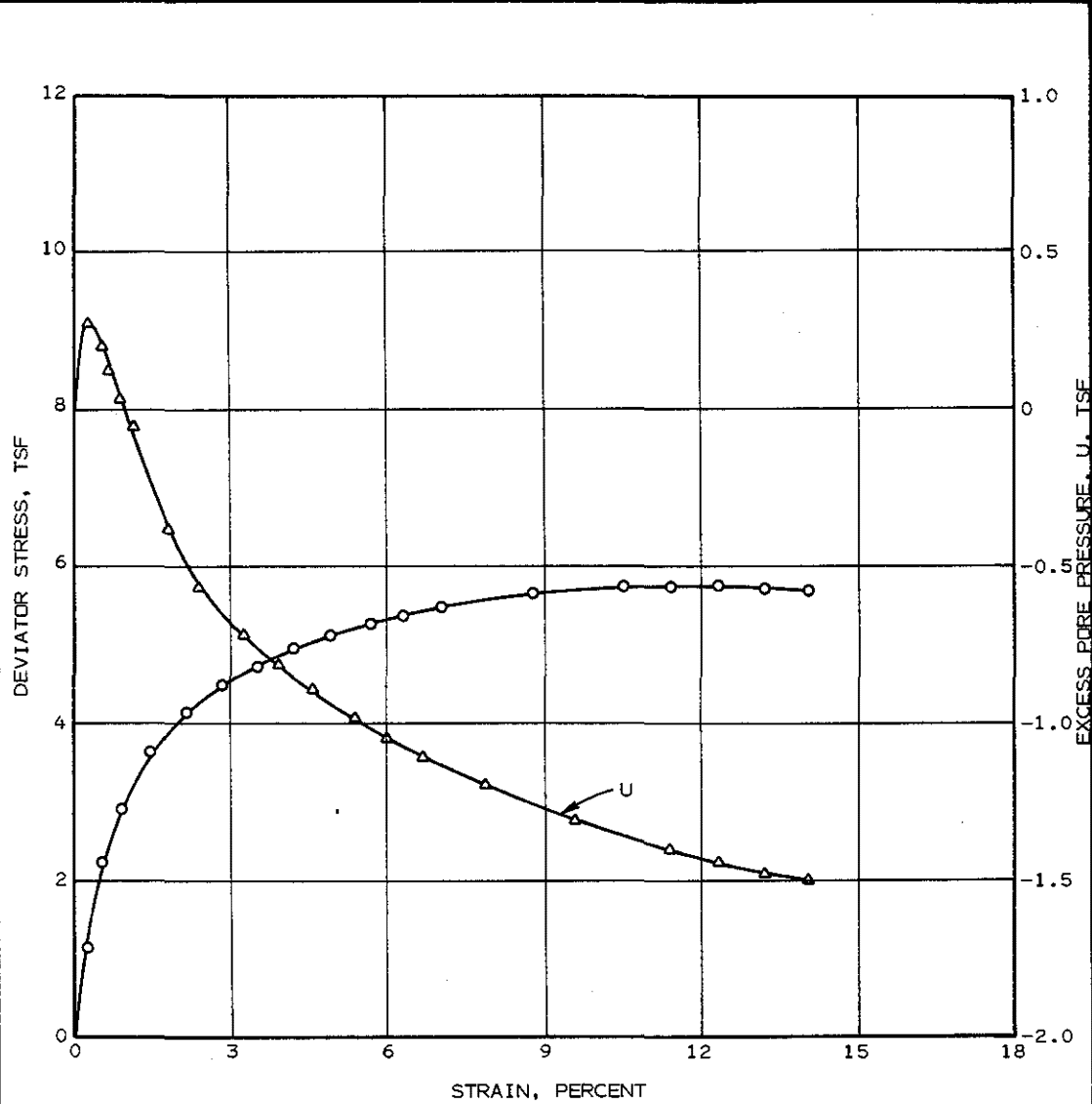
BORING NO.	DEPTH, FT.	MAXIMUM CONSOLIDATION PRESSURE, TSF	FINAL CONFINING PRESSURE, TSF	MATERIAL
CB-1	35	10.8	5.40	HARD YELLOW AND LIGHT GRAY SANDY CLAY

OCR = 2.0
 PORE PRESSURE-STRAIN AND
 STRESS-STRAIN CURVES
 NSP TRIAXIAL COMPRESSION TEST
 CONSOLIDATED UNDRAINED



<u>BORING NO.</u>	<u>DEPTH, FT.</u>	<u>MAXIMUM CONSOLIDATION PRESSURE, TSF</u>	<u>FINAL CONFINING PRESSURE, TSF</u>	<u>MATERIAL</u>
CB-1	35	10.8	2.16	HARD TAN AND LIGHT GRAY SANDY CLAY WITH SAND PARTINGS AND POCKETS

OCR = 5.0
 PORE PRESSURE-STRAIN AND
 STRESS-STRAIN CURVES
 NSP TRIAXIAL COMPRESSION TEST
 CONSOLIDATED UNDRAINED



<u>BORING NO.</u>	<u>DEPTH, FT.</u>	<u>MAXIMUM CONSOLIDATION PRESSURE, TSF</u>	<u>FINAL CONFINING PRESSURE, TSF</u>	<u>MATERIAL</u>
CB-1	35	10.8	1.08	HARD TAN AND LIGHT GRAY SANDY CLAY WITH SAND POCKETS AND SEAMS

OCR = 10.0
 PORE PRESSURE-STRAIN AND
 STRESS-STRAIN CURVES
 NSP TRIAXIAL COMPRESSION TEST
 CONSOLIDATED UNDRAINED

DEPTH, FT: 8'-10'

DESCRIPTION: VERY STIFF BROWN AND LIGHT GRAY CLAY

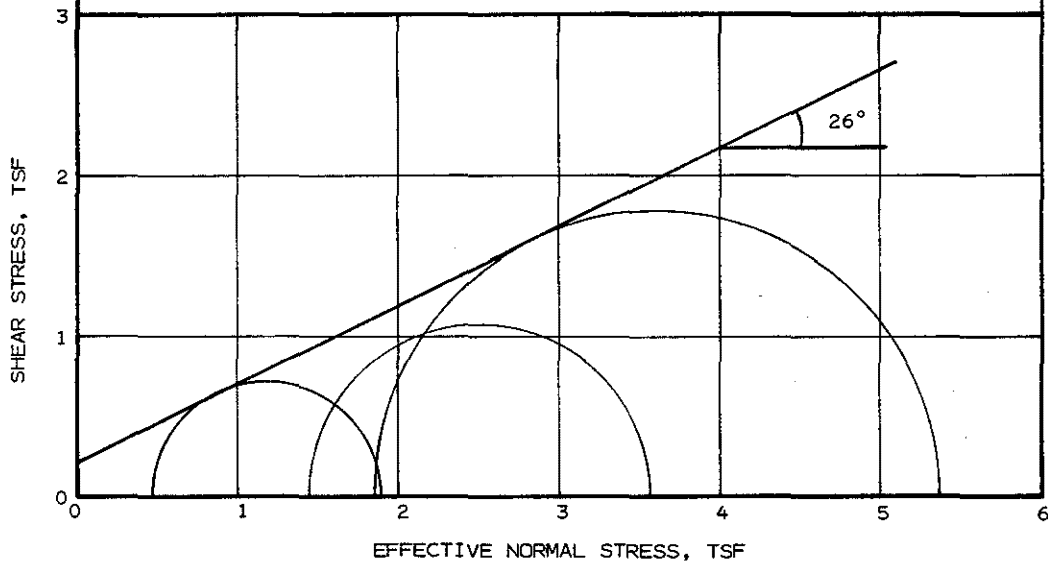
SAMPLE TYPE: UNDISTURBED

UNIT DRY WEIGHT: 105 PCF

WATER CONTENT: INITIAL 20%

ANGLE OF SHEAR, ϕ' : 26°

COHESION, c' : 0.2 TSF



DEPTH, FT: 8'-10'

DESCRIPTION: VERY STIFF BROWN AND LIGHT GRAY CLAY

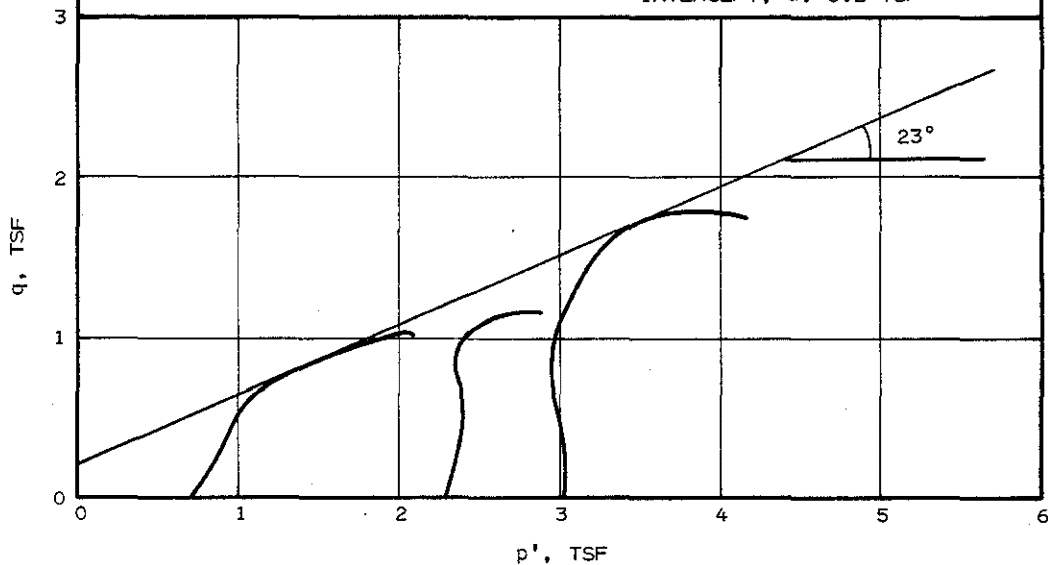
SAMPLE TYPE: UNDISTURBED

UNIT DRY WEIGHT: 105 PCF

WATER CONTENT: INITIAL 20%

ANGLE INCLINATION, α : 23°

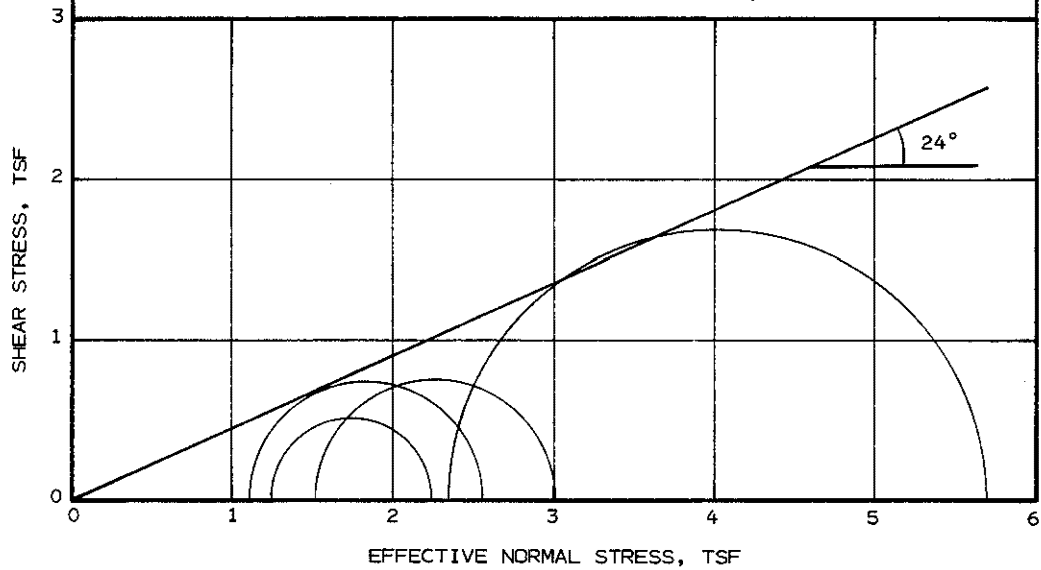
INTERCEPT, a : 0.2 TSF



TRIAxIAL TEST RESULTS
CONSOLIDATED UNDRAINED

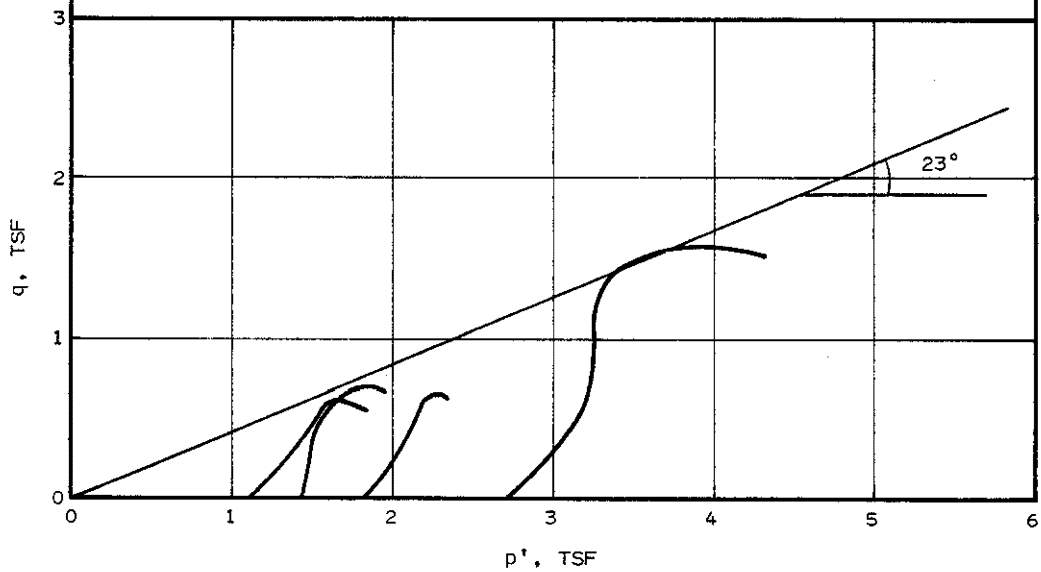
DEPTH, FT: 18'-20'
DESCRIPTION: VERY STIFF RED AND LIGHT
GRAY CLAY
SAMPLE TYPE: UNDISTURBED

UNIT DRY WEIGHT: 108 PCF
WATER CONTENT: INITIAL 25%
ANGLE OF SHEAR, ϕ' : 24°
COHESION, c' : 0.0 TSF



DEPTH, FT: 18'-20'
DESCRIPTION: VERY STIFF RED AND LIGHT
GRAY CLAY
SAMPLE TYPE: UNDISTURBED

UNIT DRY WEIGHT: 108 PCF
WATER CONTENT: INITIAL 25%
ANGLE INCLINATION, α : 23°
INTERCEPT, a : 0.0 TSF



TRIAxIAL TEST RESULTS
CONSOLIDATED UNDRAINED

DEPTH, FT: 22'-24'

DESCRIPTION: VERY STIFF RED AND LIGHT
GRAY CLAY

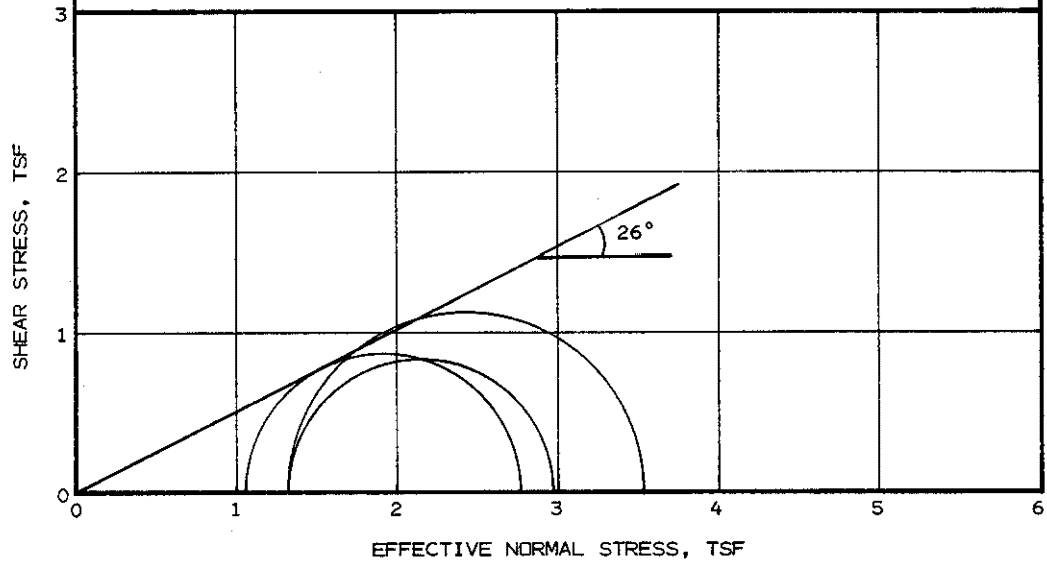
SAMPLE TYPE: UNDISTURBED

UNIT DRY WEIGHT: 97 PCF

WATER CONTENT: INITIAL 26%

ANGLE OF SHEAR, ϕ' : 26°

COHESION, c' : 0.0 TSF



DEPTH, FT: 22'-24'

DESCRIPTION: VERY STIFF RED AND LIGHT
GRAY CLAY

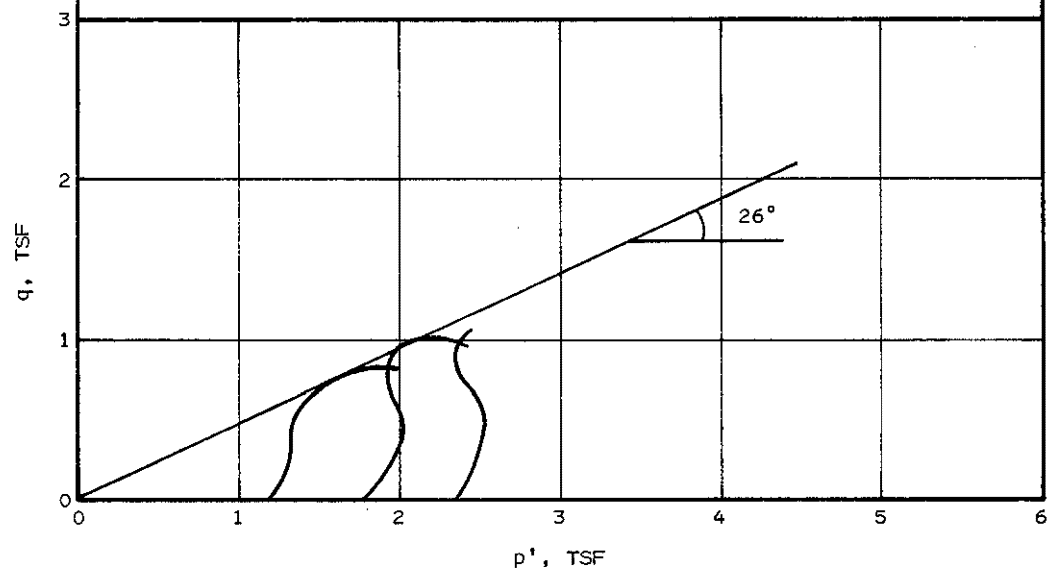
SAMPLE TYPE: UNDISTURBED

UNIT DRY WEIGHT: 97 PCF

WATER CONTENT: INITIAL 26%

ANGLE INCLINATION, α : 26°

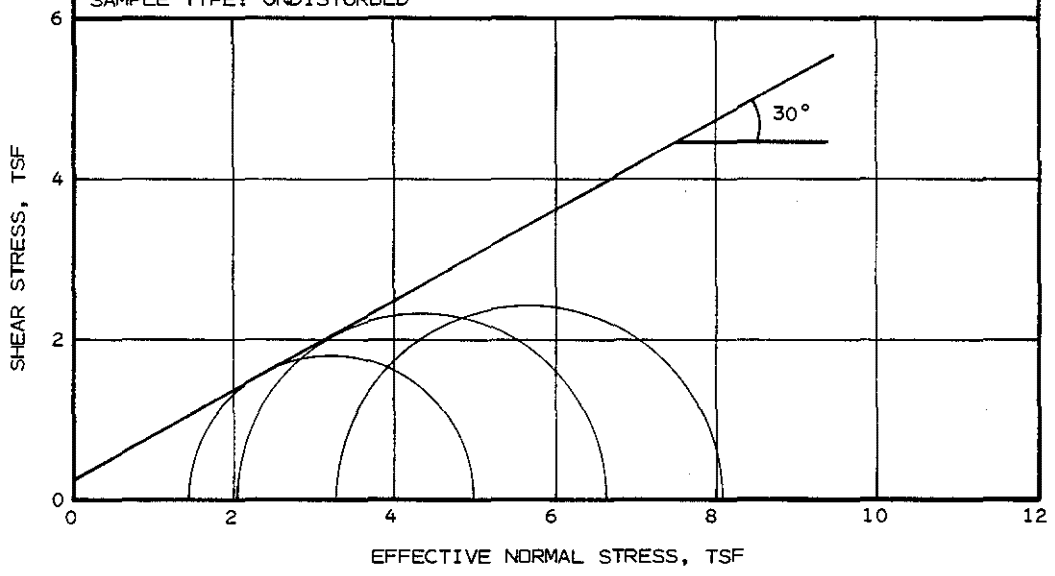
INTERCEPT, a : 0.0 TSF



TRIAXIAL TEST RESULTS
CONSOLIDATED UNDRAINED

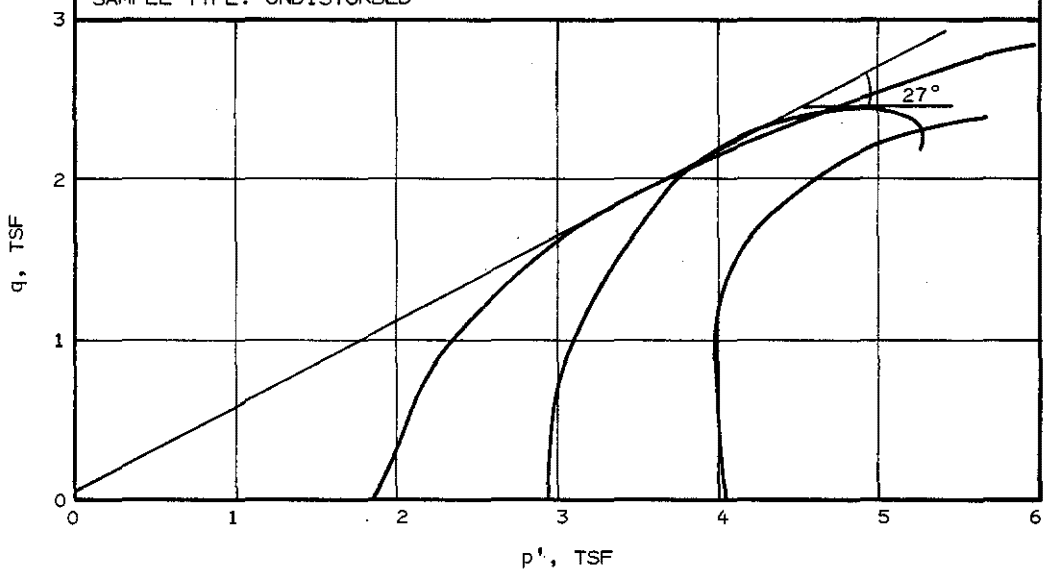
DEPTH, FT: 36'-38'
 DESCRIPTION: VERY STIFF LIGHT GRAY AND TAN SANDY CLAY WITH SAND POCKETS
 SAMPLE TYPE: UNDISTURBED

UNIT DRY WEIGHT: 116 PCF
 WATER CONTENT: INITIAL 15%
 ANGLE OF SHEAR, ϕ' : 30°
 COHESION, c' : 0.27 TSF



DEPTH, FT: 36'-38'
 DESCRIPTION: VERY STIFF LIGHT GRAY AND TAN SANDY CLAY WITH SAND POCKETS
 SAMPLE TYPE: UNDISTURBED

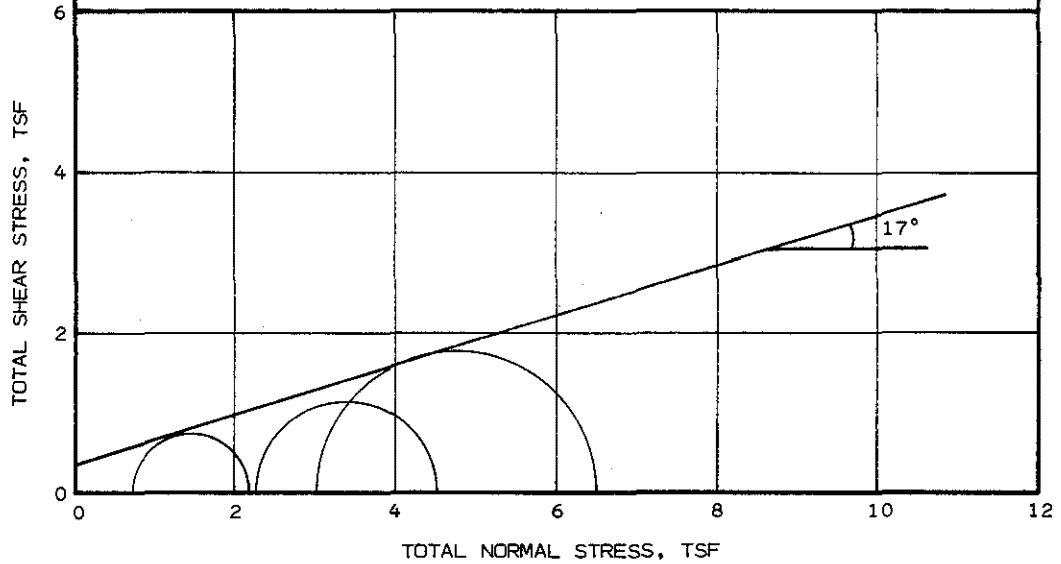
UNIT DRY WEIGHT: 116 PCF
 WATER CONTENT: INITIAL 15%
 ANGLE INCLINATION, α : 27°
 INTERCEPT, a : 0.08 TSF



TRIAXIAL TEST RESULTS
 CONSOLIDATED UNDRAINED

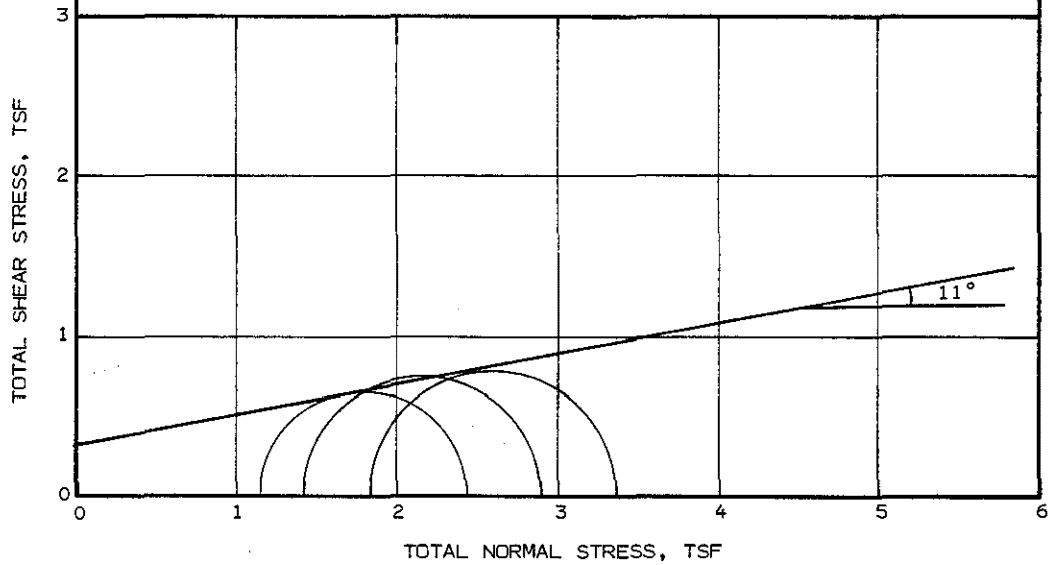
DEPTH, FT: 8'-10'
DESCRIPTION: VERY STIFF BROWN AND LIGHT
GRAY CLAY
SAMPLE TYPE: UNDISTURBED

UNIT DRY WEIGHT: 105 PCF
WATER CONTENT: INITIAL 20%
ANGLE OF SHEAR, ϕ : 17°
COHESION, C: 0.35 TSF



DEPTH, FT: 18'-20'
DESCRIPTION: VERY STIFF RED AND LIGHT
GRAY CLAY
SAMPLE TYPE: UNDISTURBED

UNIT DRY WEIGHT: 108 PCF
WATER CONTENT: INITIAL 25%
ANGLE OF SHEAR, ϕ : 11°
COHESION, C: 0.35 TSF



CIU TRIAXIAL TEST RESULTS

DEPTH, FT: 22'-24'

DESCRIPTION: VERY STIFF RED AND LIGHT GRAY CLAY

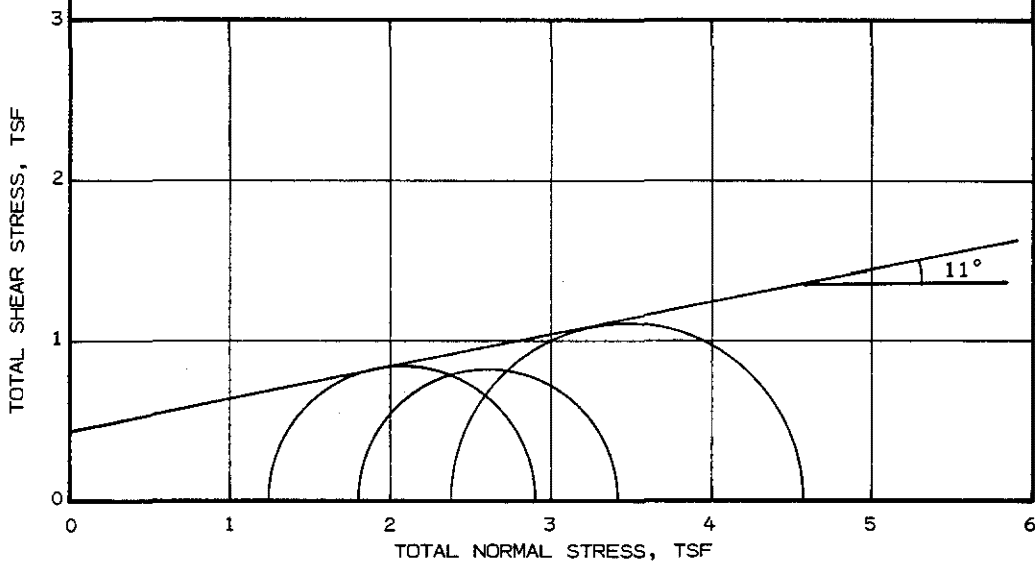
SAMPLE TYPE: UNDISTURBED

UNIT DRY WEIGHT: 97 PCF

WATER CONTENT: INITIAL 26%

ANGLE OF SHEAR, ϕ : 11°

COHESION, C: 0.45 TSF



DEPTH, FT: 32'-34'

DESCRIPTION: VERY STIFF LIGHT GRAY AND BROWN SANDY CLAY

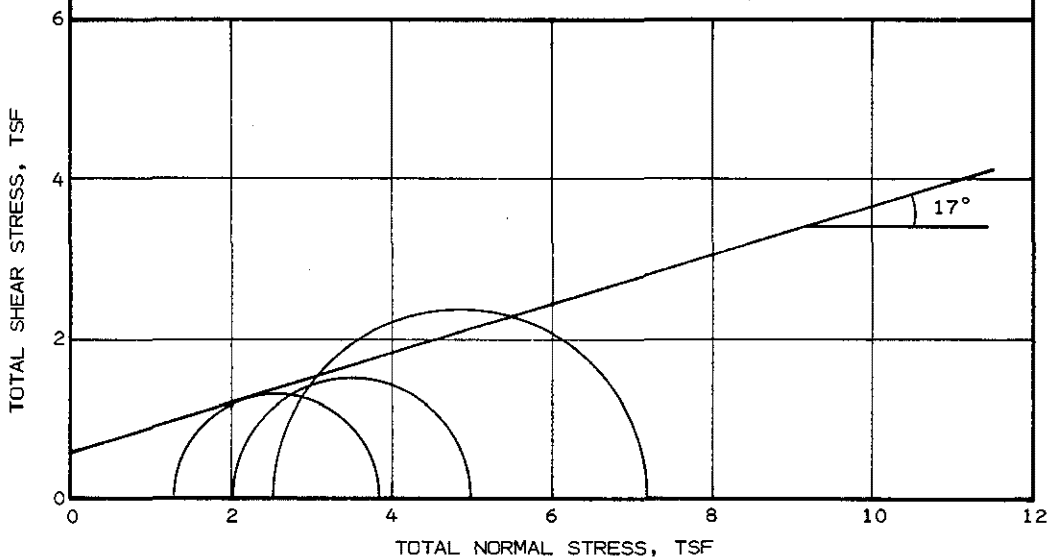
SAMPLE TYPE: UNDISTURBED

UNIT DRY WEIGHT: 116 PCF

WATER CONTENT: INITIAL 15%

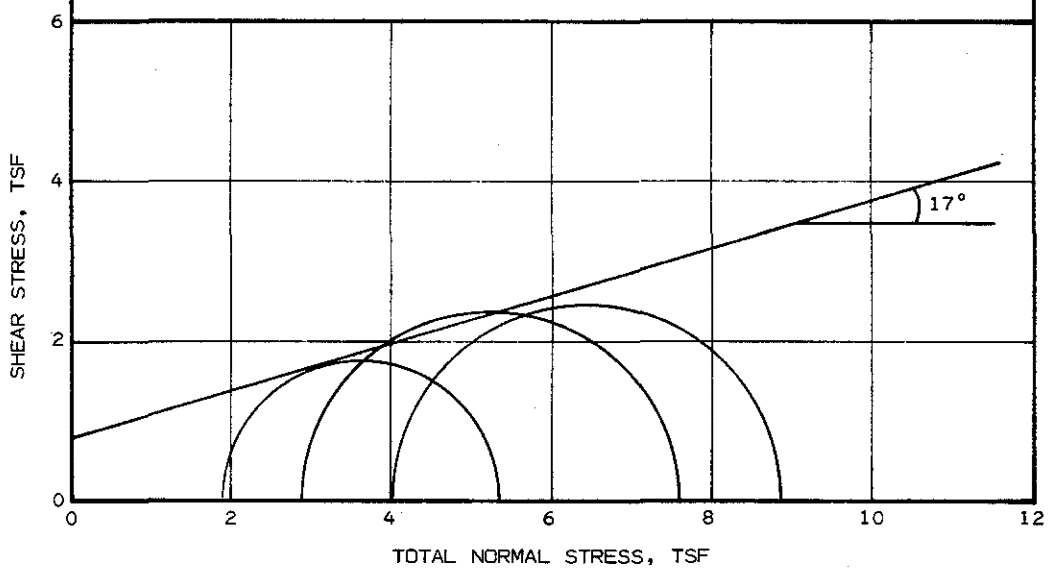
ANGLE OF SHEAR, ϕ : 17°

COHESION, C: 0.60 TSF

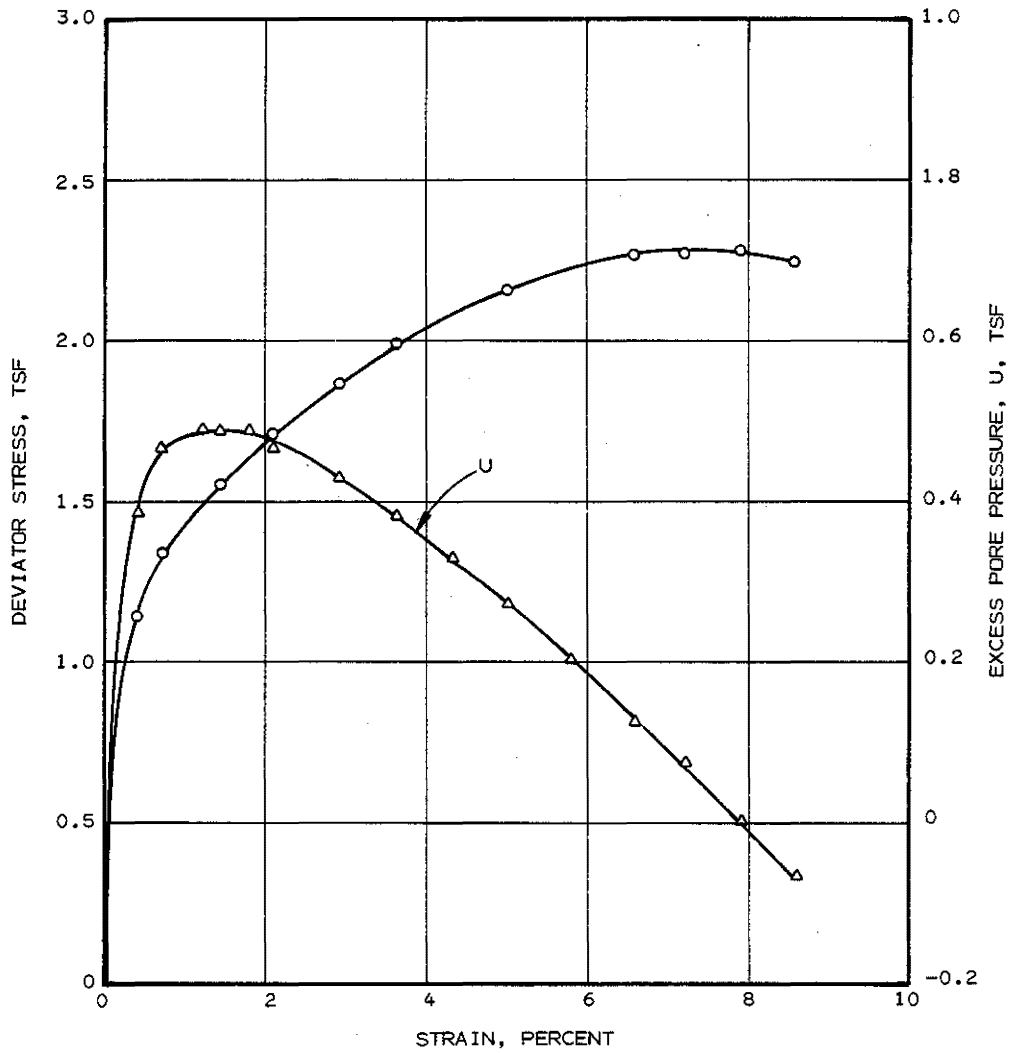


CIU TRIAXIAL TEST RESULTS

DEPTH, FT: 36'-38'	UNIT DRY WEIGHT: 116 PCF
DESCRIPTION: VERY STIFF LIGHT GRAY AND TAN SANDY CLAY	WATER CONTENT: INITIAL 15%
SAMPLE TYPE: UNDISTURBED	ANGLE OF SHEAR, ϕ : 17'
	COHESION, C: 0.80 TSF

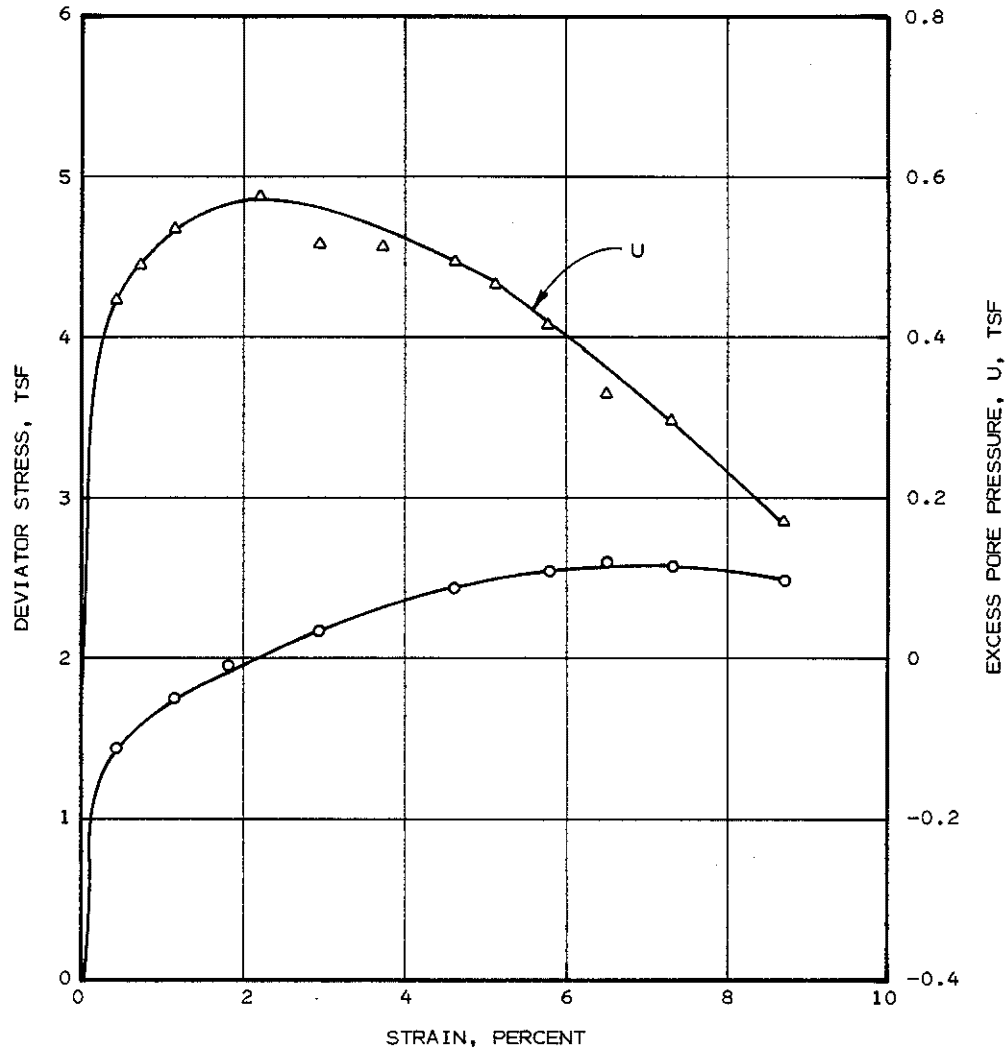


CIU TRIAXIAL TEST RESULTS



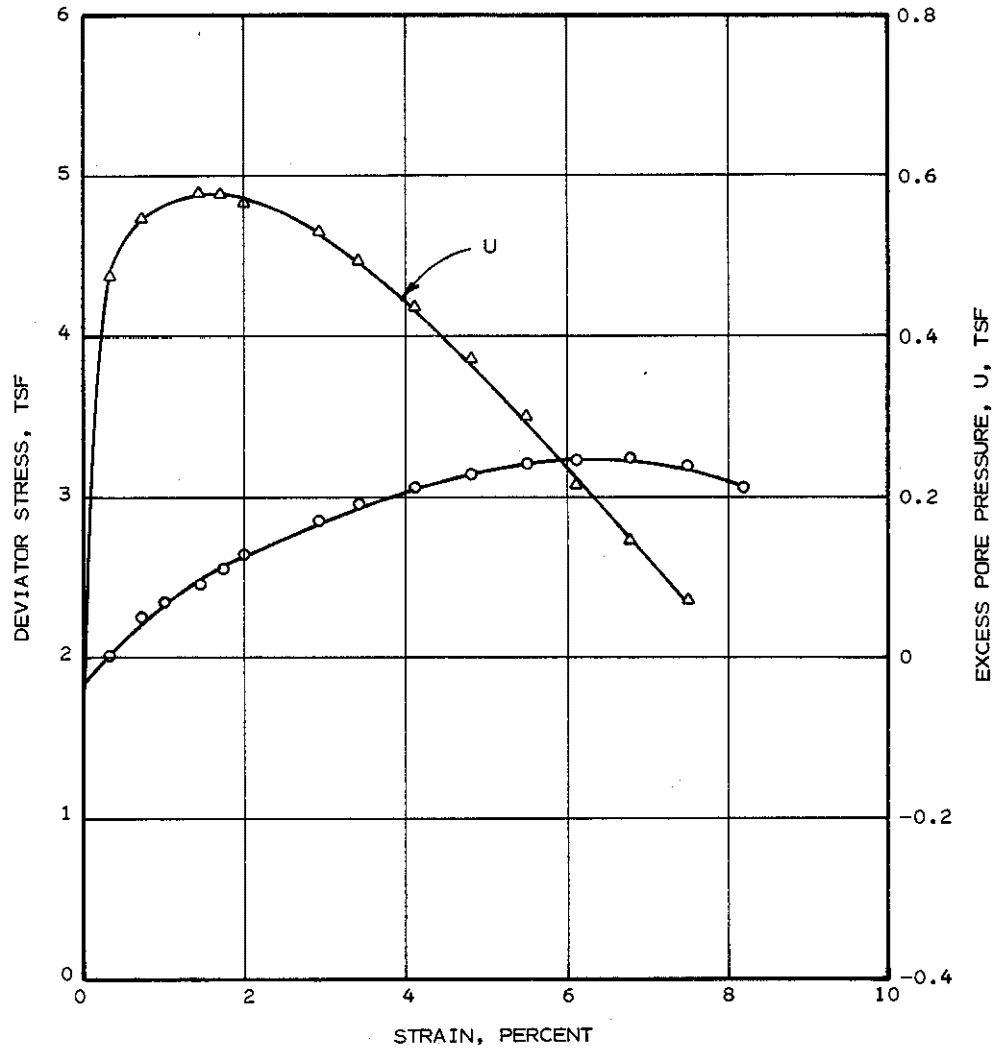
<u>BORING NO.</u>	<u>DEPTH, FT.</u>	<u>CONFINING PRESSURE, TSF</u>	<u>MATERIAL</u>
CB-3	20.5	1.80	RED AND LIGHT GRAY CLAY, SLICKENSIDED

PORE PRESSURE-STRAIN AND
STRESS-STRAIN CURVES
CIU TRIAXIAL COMPRESSION TEST REMOLDED
CONSOLIDATED UNDRAINED



<u>BORING NO.</u>	<u>DEPTH, FT.</u>	<u>CONFINING PRESSURE, TSF</u>	<u>MATERIAL</u>
CB-1	21	2.38	RED AND LIGHT GRAY CLAY, SLICKENSIDED

PORE PRESSURE-STRAIN AND
STRESS-STRAIN CURVES
CIU TRIAXIAL COMPRESSION TEST REMOLDED
CONSOLIDATED UNDRAINED



<u>BORING NO.</u>	<u>DEPTH, FT.</u>	<u>CONFINING PRESSURE, TSF</u>	<u>MATERIAL</u>
CB-3	21	2.95	RED AND LIGHT GRAY CLAY, SLICKENSIDED

PORE PRESSURE-STRAIN AND
STRESS-STRAIN CURVES
CIU TRIAXIAL COMPRESSION TEST REMOLDED
CONSOLIDATED UNDRAINED

DEPTH, FT: 32'-34'

DESCRIPTION: VERY STIFF LIGHT GRAY AND
BROWN SANDY CLAY

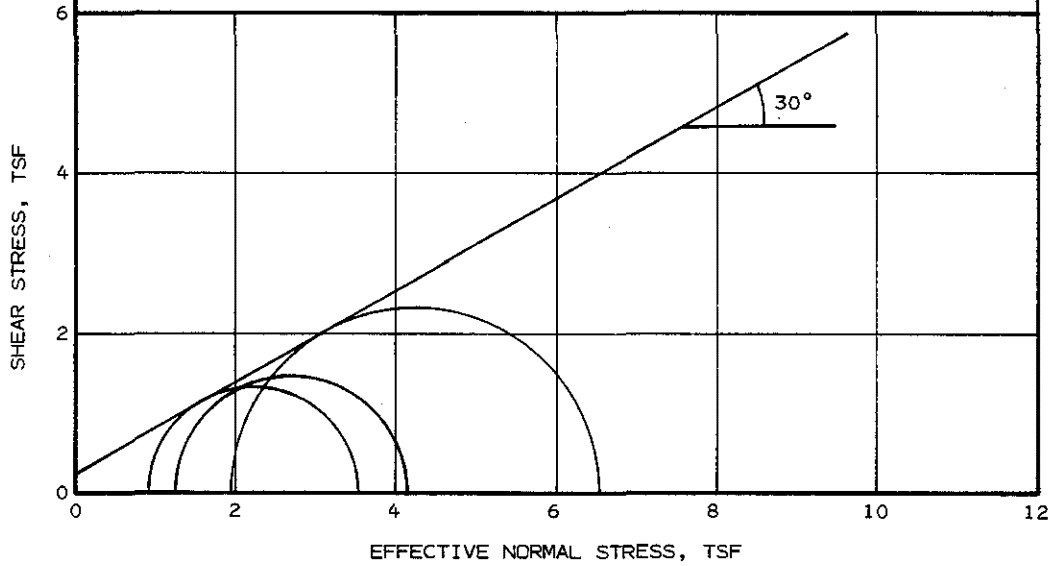
SAMPLE TYPE: UNDISTURBED

UNIT DRY WEIGHT: 116 PCF

WATER CONTENT: INITIAL 15%

ANGLE OF SHEAR, ϕ' : 30°

COHESION, c' : 0.5 TSF



DEPTH, FT: 32'-34'

DESCRIPTION: VERY STIFF LIGHT GRAY AND
BROWN SANDY CLAY

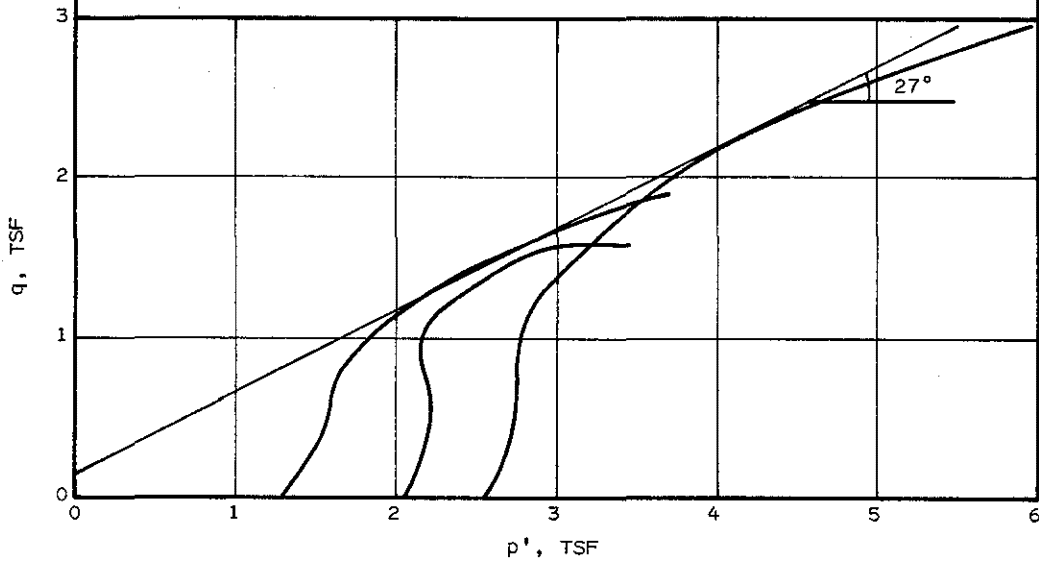
SAMPLE TYPE: UNDISTURBED

UNIT DRY WEIGHT: 116 PCF

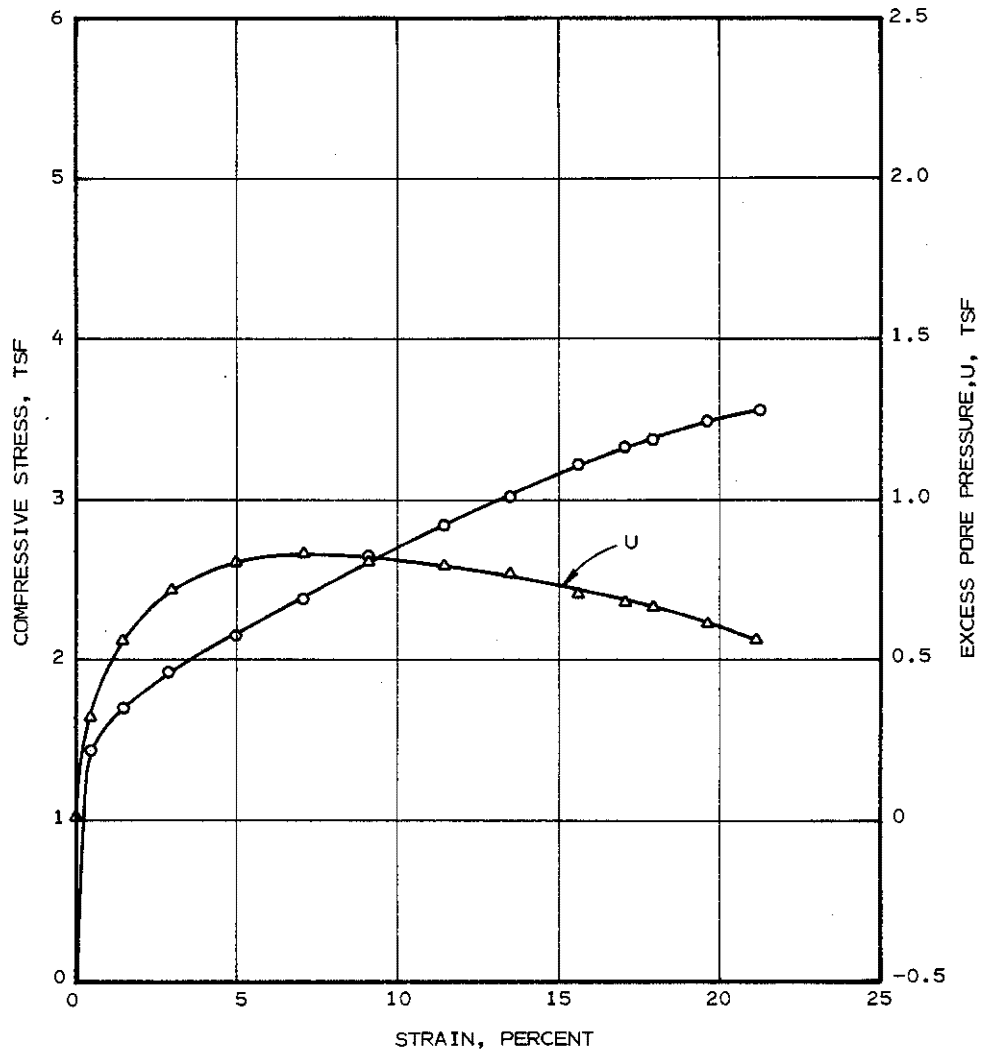
WATER CONTENT: INITIAL 15%

ANGLE INCLINATION, α : 27°

INTERCEPT, a : 0.18 TSF

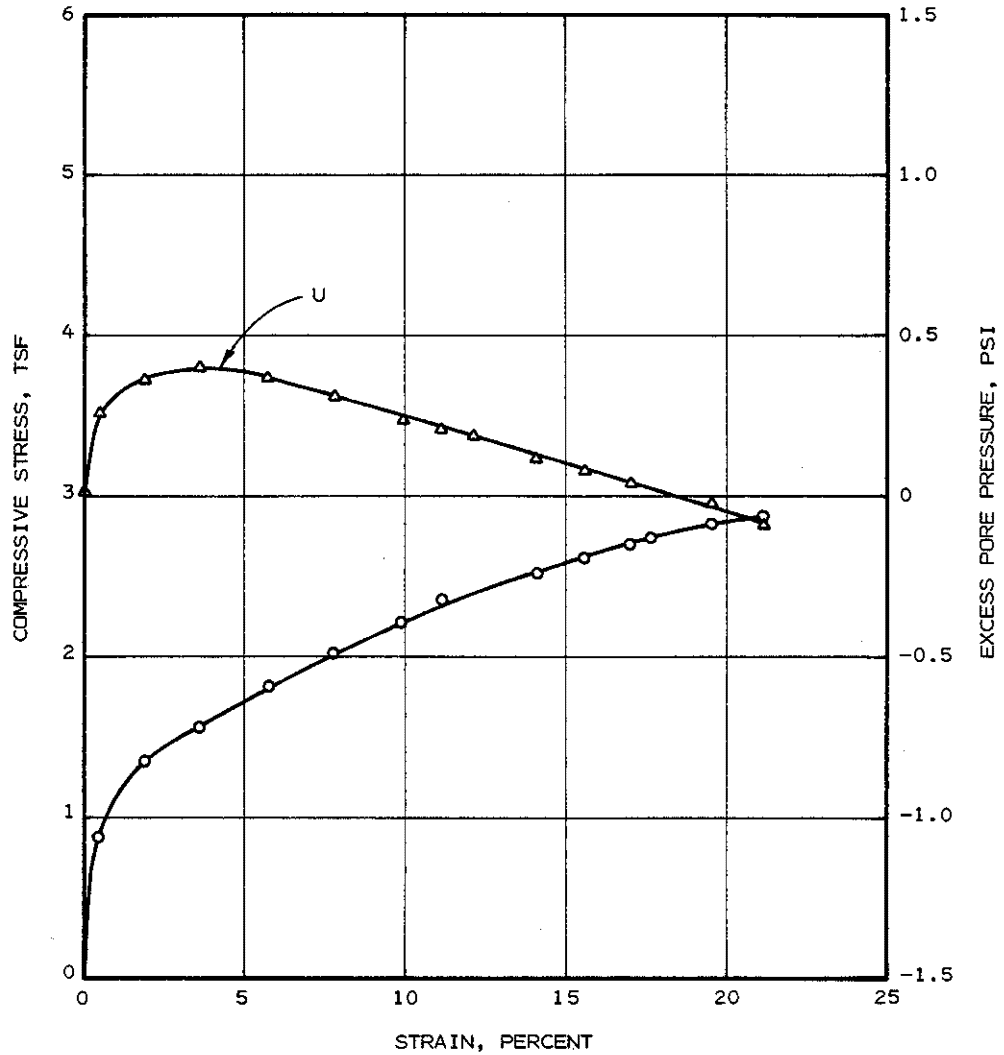


TRIAxIAL TEST RESULTS
CONSOLIDATED UNDRAINED



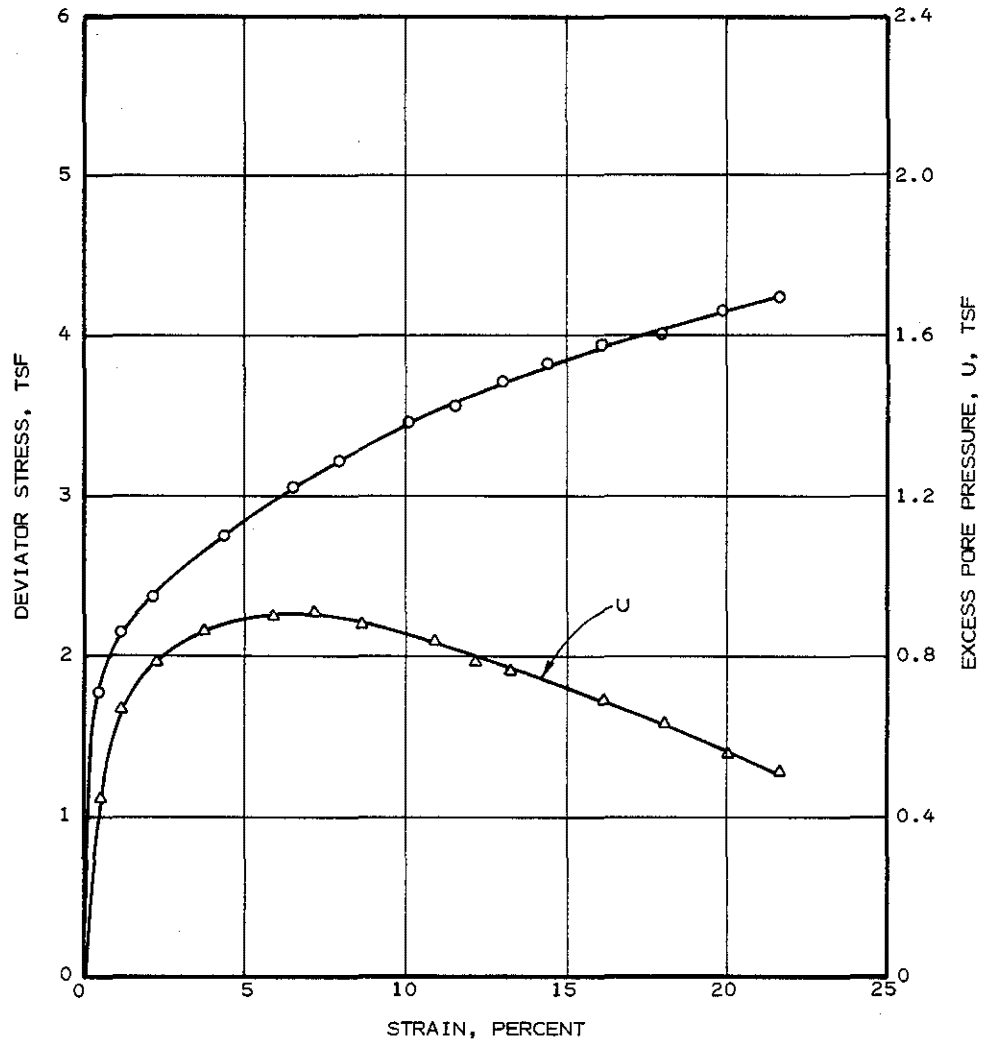
<u>BORING NO.</u>	<u>DEPTH, FT.</u>	<u>CONFINING PRESSURE, TSF</u>	<u>MATERIAL</u>
CB-3	30.5	2.30	TAN AND LIGHT GRAY SANDY CLAY

PORE PRESSURE-STRAIN AND
 STRESS-STRAIN CURVES
 CIU TRIAXIAL COMPRESSION TEST REMOLDED
 CONSOLIDATED UNDRAINED



<u>BORING NO.</u>	<u>DEPTH, FT.</u>	<u>CONFINING PRESSURE, TSF</u>	<u>MATERIAL</u>
CB-3	31	1.51	VERY STIFF TAN AND LIGHT GRAY SANDY CLAY WITH CALCAREOUS DEPOSITS AND NODULES

PORE PRESSURE-STRAIN AND
 STRESS-STRAIN CURVES
 CIU TRIAXIAL COMPRESSION TEST REMOLDED
 CONSOLIDATED UNDRAINED

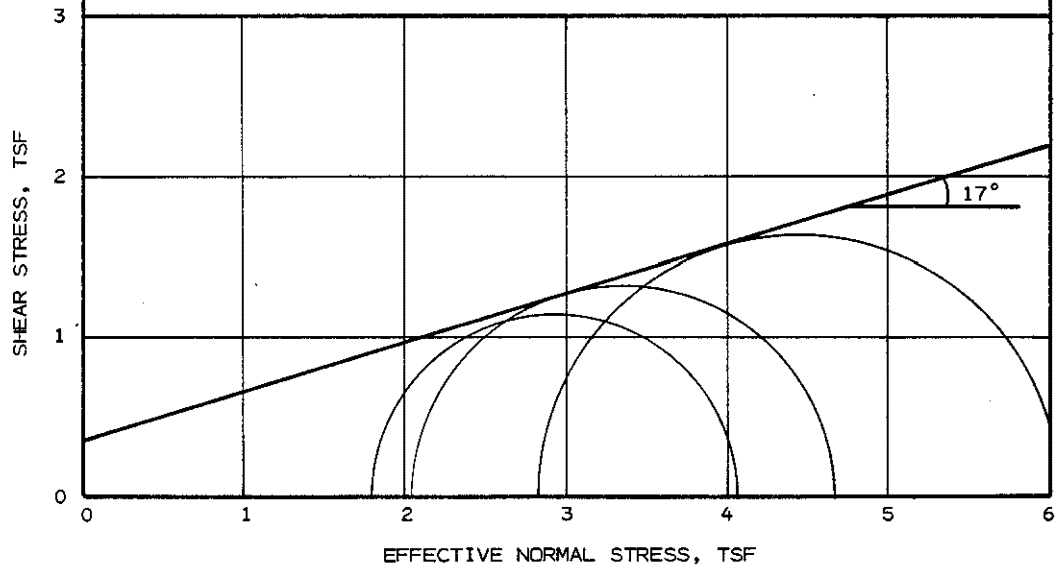


<u>BORING NO.</u>	<u>DEPTH, FT.</u>	<u>CONFINING PRESSURE, TSF</u>	<u>MATERIAL</u>
CB-3	30.5	3.02	TAN AND LIGHT GRAY SANDY CLAY WITH CALCAREOUS DEPOSITS AND NODULES

PORE PRESSURE-STRAIN AND
STRESS-STRAIN CURVES
CIU TRIAXIAL COMPRESSION TEST REMOLDED
CONSOLIDATED UNDRAINED

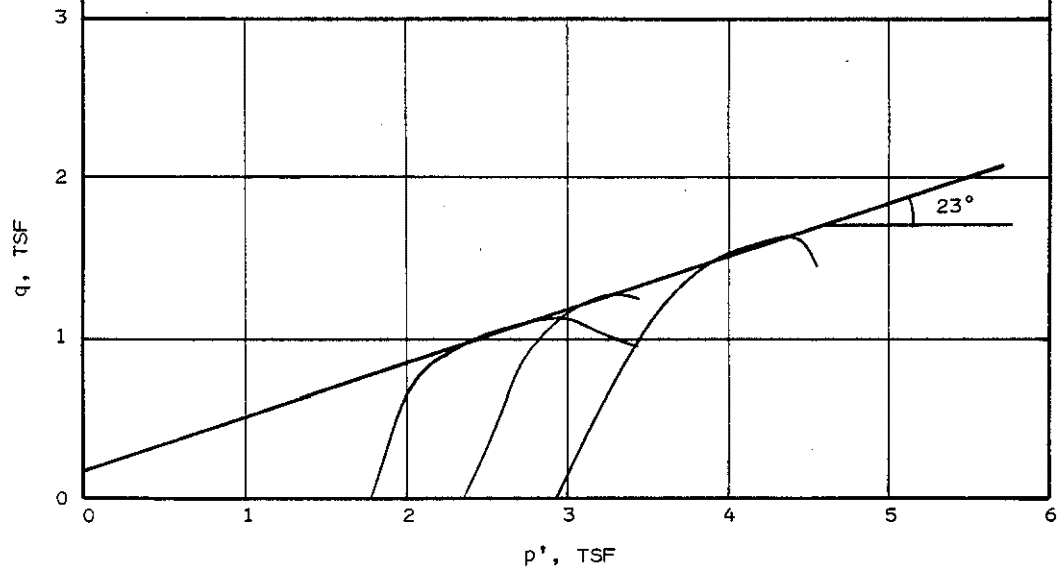
DEPTH, FT: 20'-22'
DESCRIPTION: RED AND LIGHT GRAY CLAY
SAMPLE TYPE: REMOLDED

UNIT DRY WEIGHT: 99 PCF
WATER CONTENT: INITIAL 27%
ANGLE OF SHEAR, ϕ' : 17°
COHESION, c' : 0.36 TSF



DEPTH, FT: 20'-22'
DESCRIPTION: RED AND LIGHT GRAY CLAY
SAMPLE TYPE: REMOLDED

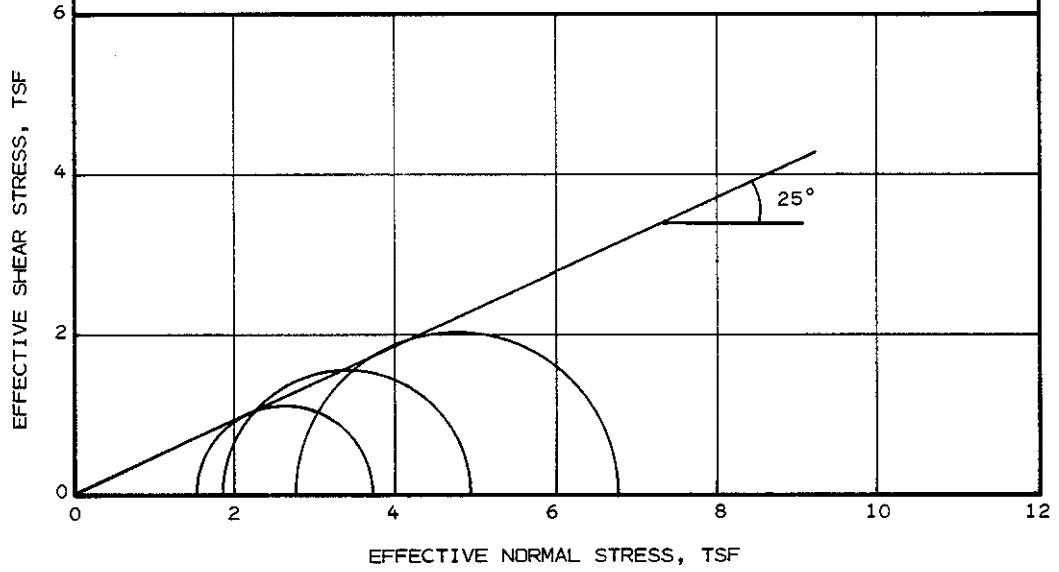
UNIT DRY WEIGHT: 99 PCF
WATER CONTENT: INITIAL 27%
ANGLE INCLINATION, α : 23°
INTERCEPT, a : 0.20 TSF



TRIAXIAL TEST RESULTS REMOLDED
CONSOLIDATED UNDRAINED

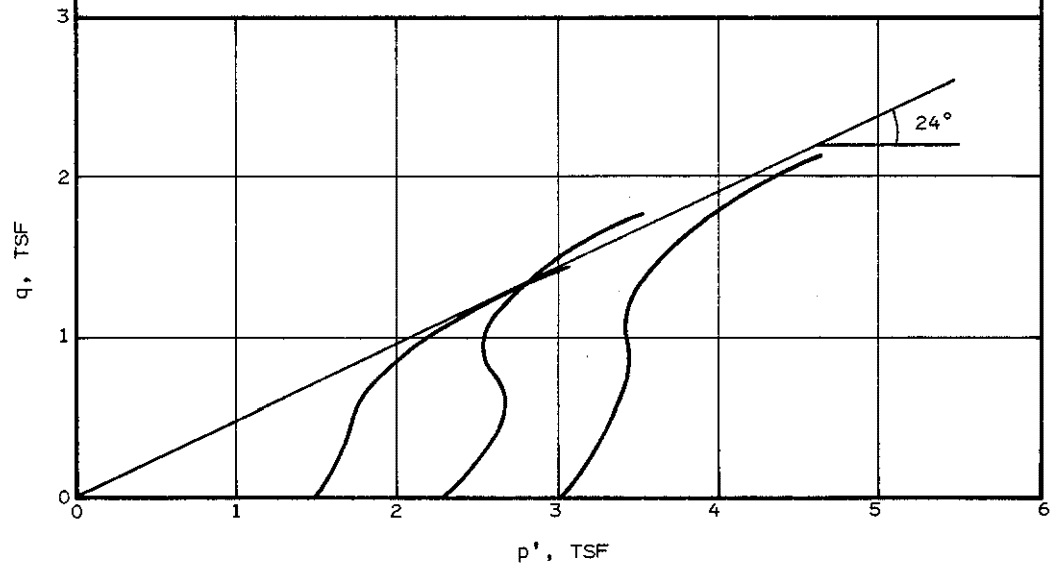
DEPTH, FT: 30'-32'
DESCRIPTION: VERY STIFF TAN AND LIGHT
GRAY SANDY CLAY
SAMPLE TYPE: REMOLDED

UNIT DRY WEIGHT: 119 PCF
WATER CONTENT: INITIAL 14%
ANGLE OF SHEAR, ϕ' : 25°
COHESION, c' : 0.0 TSF



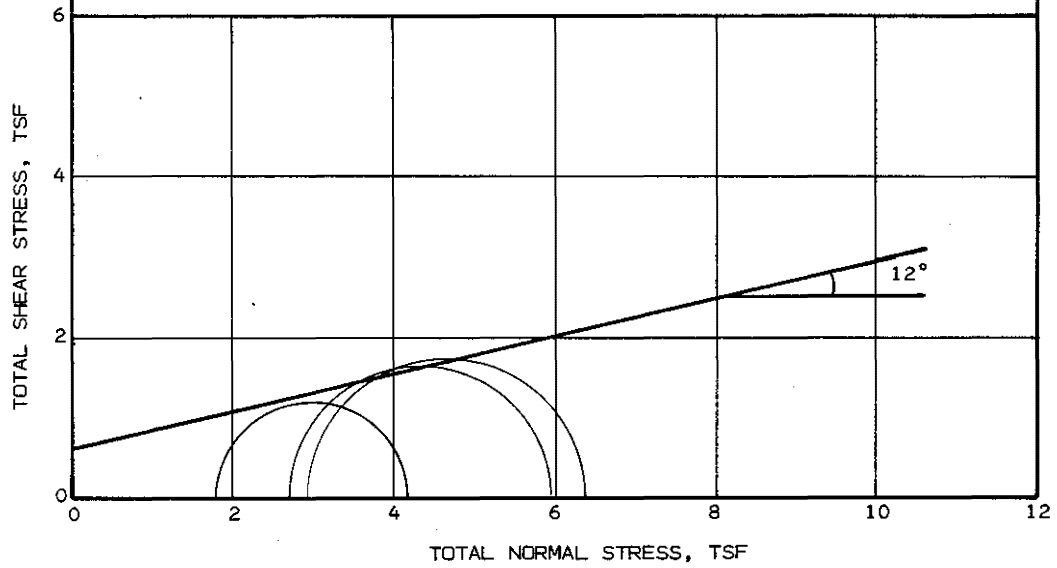
DEPTH, FT: 30'-32'
DESCRIPTION: VERY STIFF TAN AND LIGHT
GRAY SANDY CLAY
SAMPLE TYPE: REMOLDED

UNIT DRY WEIGHT: 119 PCF
WATER CONTENT: INITIAL 14%
ANGLE OF SHEAR, α : 24°
COHESION, a : 0.0 TSF

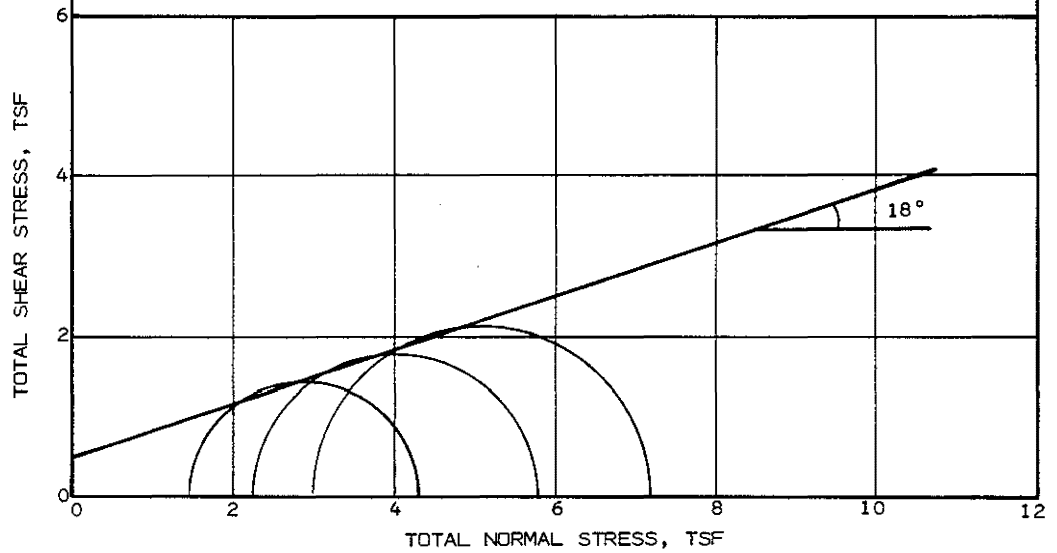


TRIAxIAL TEST RESULTS
CONSOLIDATED UNDRAINED REMOLDED

DEPTH, FT: 20'-22'	UNIT DRY WEIGHT: 99 PCF
DESCRIPTION: RED AND LIGHT GRAY CLAY	WATER CONTENT: INITIAL 27%
SAMPLE TYPE: REMOLDED	ANGLE OF SHEAR, ϕ : 12°
	COHESION, C: 0.60 TSF

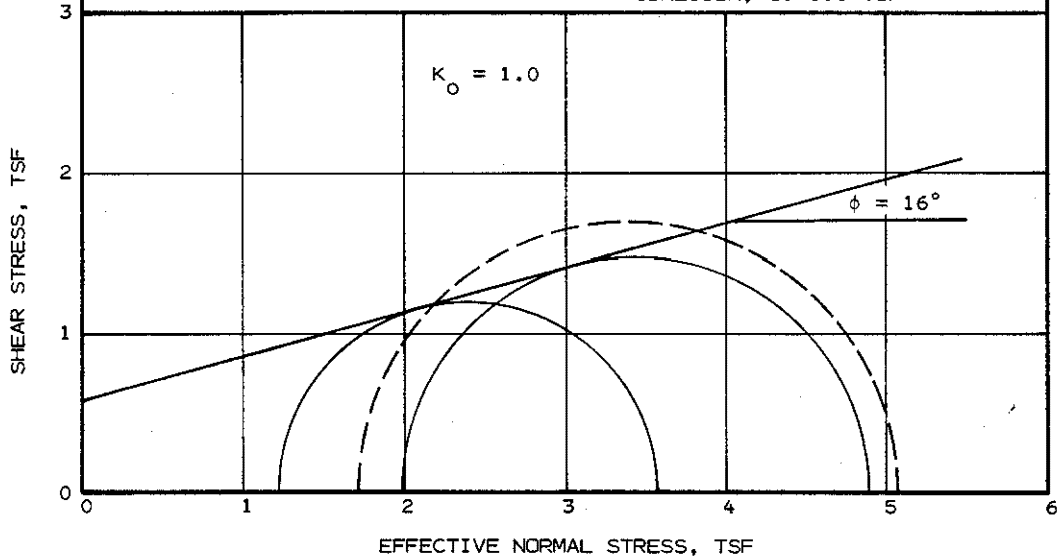


DEPTH, FT: 30'-32'	UNIT DRY WEIGHT: 119 PCF
DESCRIPTION: LIGHT GRAY AND TAN SANDY CLAY	WATER CONTENT: INITIAL 14%
SAMPLE TYPE: REMOLDED	ANGLE OF SHEAR, ϕ : 18°
	COHESION, C: 0.55 TSF

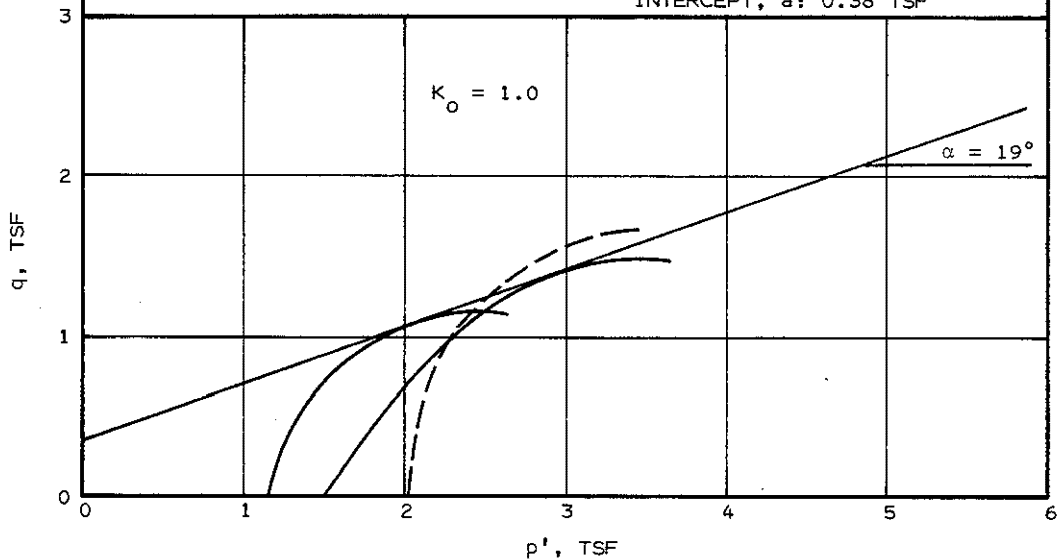


CIU TRIAXIAL TEST RESULTS REMOLDED

DEPTH, FT: 17
 DESCRIPTION: RED AND LIGHT GRAY CLAY
 SAMPLE TYPE: REMOLDED
 UNIT DRY WEIGHT: 101 PCF
 WATER CONTENT: INITIAL 24%
 FINAL 26%
 ANGLE OF SHEAR, ϕ' : 16°
 COHESION, C: 0.6 TSF

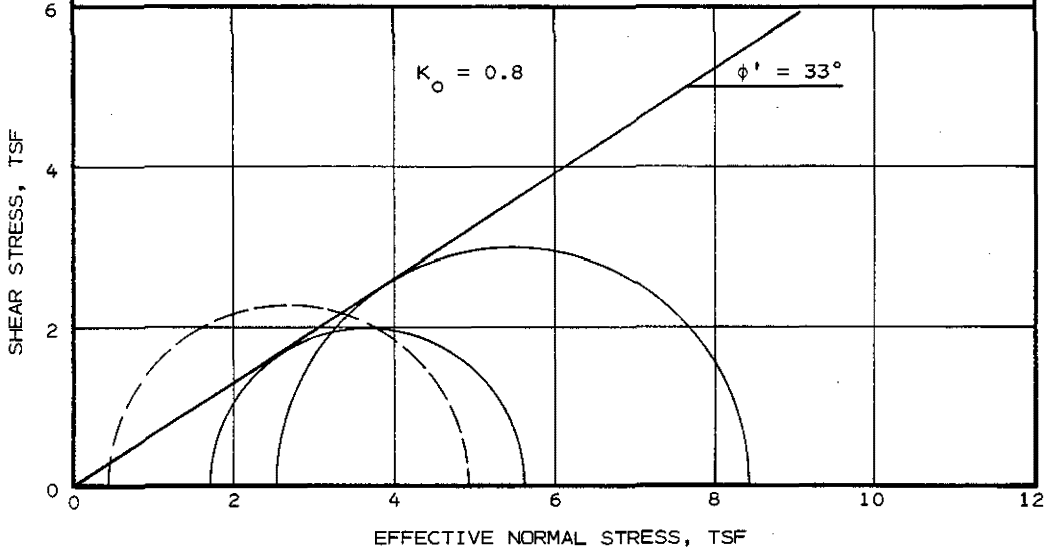


DEPTH, FT: 17
 DESCRIPTION: RED AND LIGHT GRAY CLAY
 SAMPLE TYPE: REMOLDED
 UNIT DRY WEIGHT: 101 PCF
 WATER CONTENT: INITIAL 24%
 FINAL 26%
 ANGLE INCLINATION, α : 19°
 INTERCEPT, a: 0.38 TSF

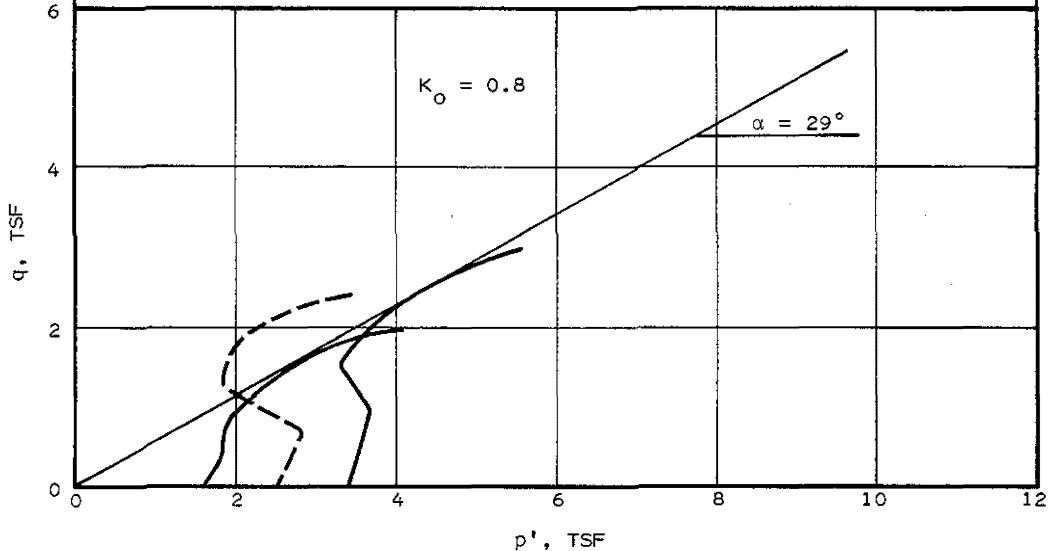


TRIAXIAL TEST RESULTS
 REMOLDED ANISOTROPIC CONSOLIDATED UNDRAINED

DEPTH, FT: 35'	UNIT DRY WEIGHT: 117 PCF
DESCRIPTION: TAN AND LIGHT GRAY SANDY CLAY	WATER CONTENT: INITIAL 16% FINAL 14%
SAMPLE TYPE: REMOLDED	ANGLE OF SHEAR, ϕ' : 33° COHESION, C: 0 TSF



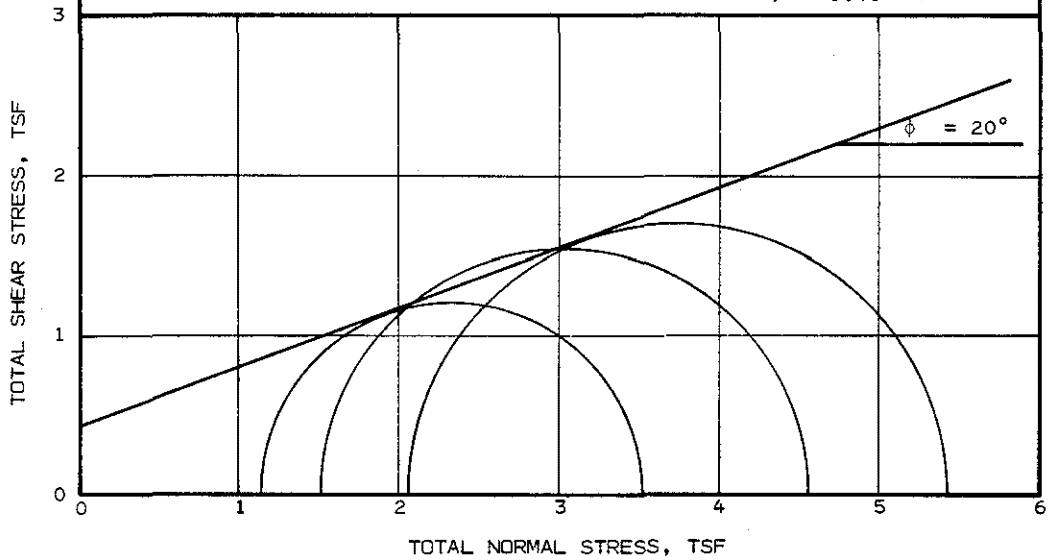
DEPTH, FT: 35'	UNIT DRY WEIGHT: 117 PCF
DESCRIPTION: TAN AND LIGHT GRAY SANDY CLAY	WATER CONTENT: INITIAL 16% FINAL 14%
SAMPLE TYPE: REMOLDED	ANGLE INCLINATION, α : 29° INTERCEPT, a: 0 TSF



TRIAxIAL TEST RESULTS
REMOLDED ANISOTROPIC CONSOLIDATED UNDRAINED

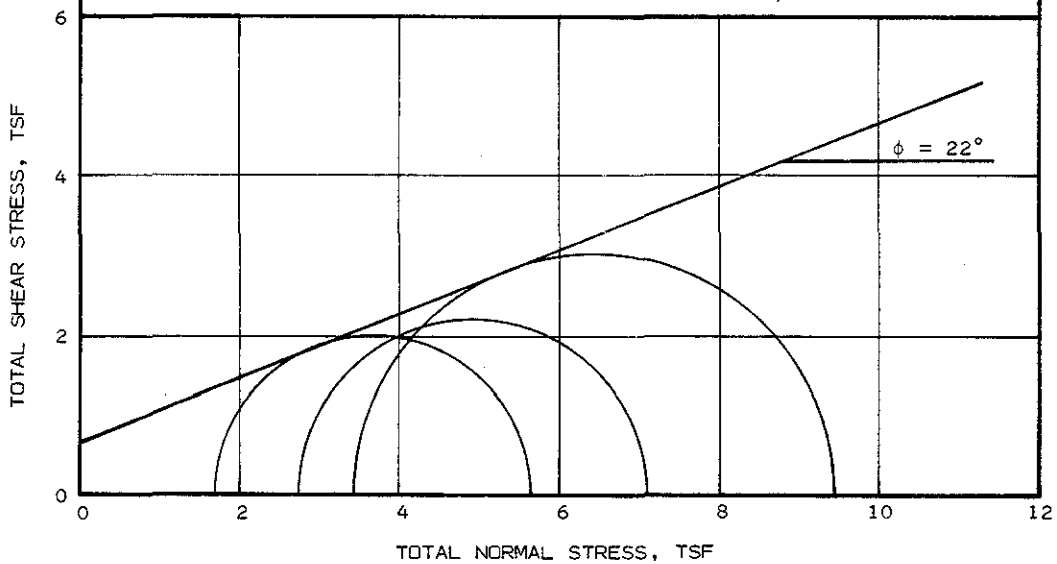
DEPTH, FT: 17'
 DESCRIPTION: RED AND LIGHT GRAY CLAY
 SAMPLE TYPE: REMOLDED

UNIT DRY WEIGHT: 101 PCF
 WATER CONTENT: INITIAL 24%
 FINAL 26%
 ANGLE OF SHEAR, ϕ : 20°
 COHESION, C: 0.40 TSF



DEPTH, FT: 35'
 DESCRIPTION: TAN AND LIGHT GRAY SANDY CLAY
 SAMPLE TYPE: REMOLDED

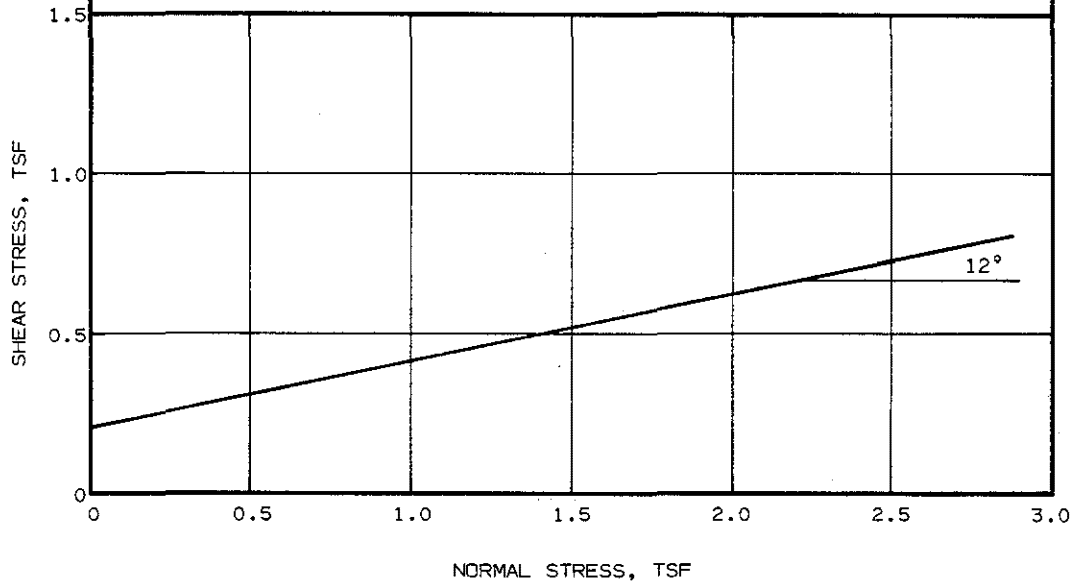
UNIT DRY WEIGHT: 101 PCF
 WATER CONTENT: INITIAL 24%
 FINAL 26%
 ANGLE OF SHEAR, ϕ : 22°
 COHESION, C: 0.70 TSF



CAU TRIAXIAL TEST RESULTS REMOLDED

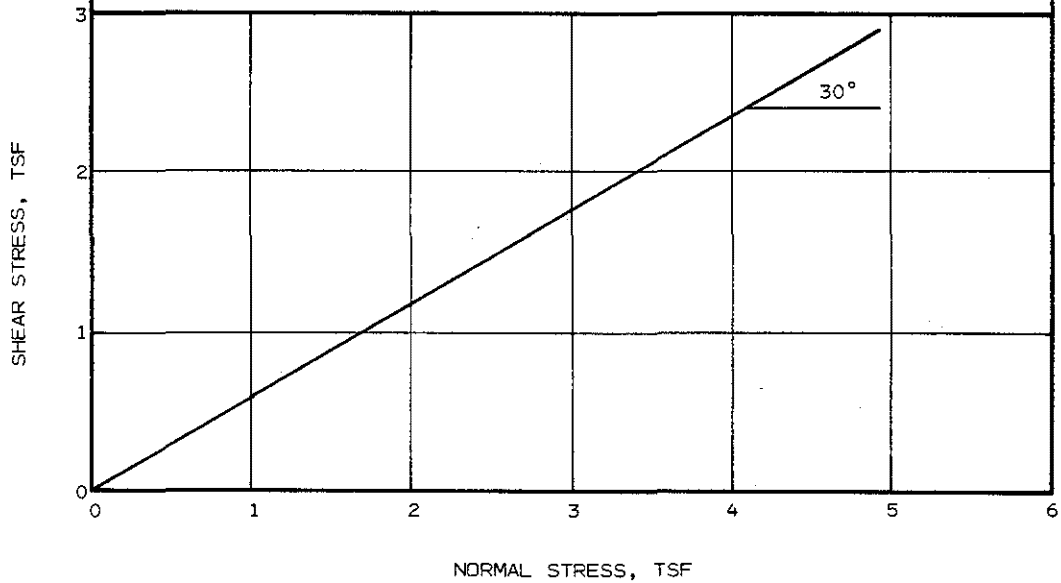
DEPTH, FT: 16'-18'
DESCRIPTION: RED AND LIGHT GRAY CLAY
SAMPLE TYPE: UNDISTURBED

UNIT DRY WEIGHT: 100
WATER CONTENT: INITIAL 24%
ANGLE OF SHEAR, ϕ : 12°
COHESION, C: 0.23 TSF



DEPTH, FT: 30'-32'
DESCRIPTION: LIGHT GRAY AND TAN SANDY CLAY
SAMPLE TYPE: UNDISTURBED

UNIT DRY WEIGHT: 115 PCF
WATER CONTENT: INITIAL 15%
ANGLE OF SHEAR, ϕ : 30°
COHESION, C: 0.0 TSF



RESIDUAL DIRECT SHEAR TEST RESULTS
CONSOLIDATED DRAINED

BORING NO: CB-2 SAMPLE NO:

UNIT DRY WEIGHT: 105 PCF

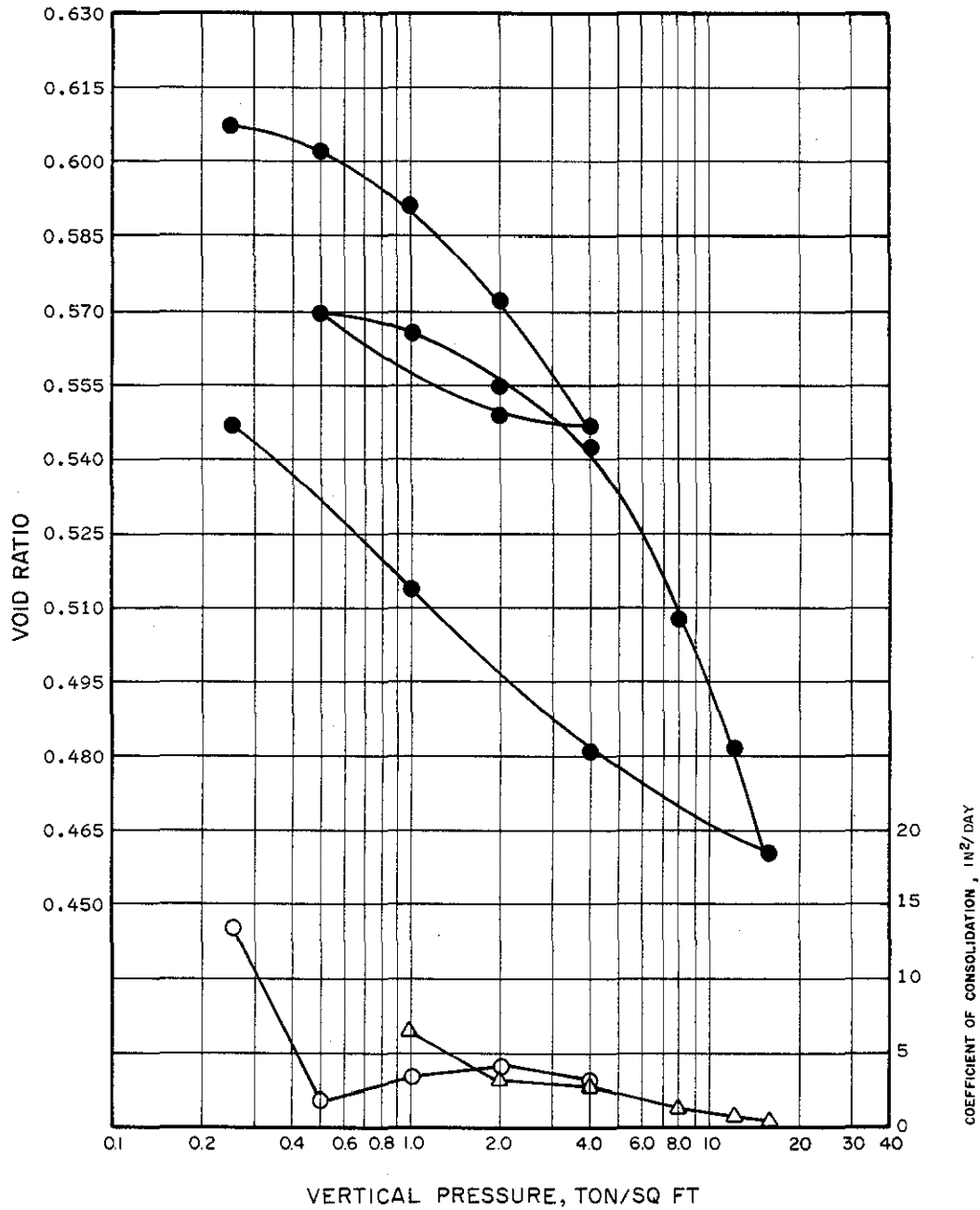
DEPTH, FT: 9.5

WATER CONTENT: 22 %

DESCRIPTION: VERY STIFF GRAY AND TAN
SANDY CLAY WITH SAND POCKETS AND
CALCAREOUS NODULES

LIQUID LIMIT:

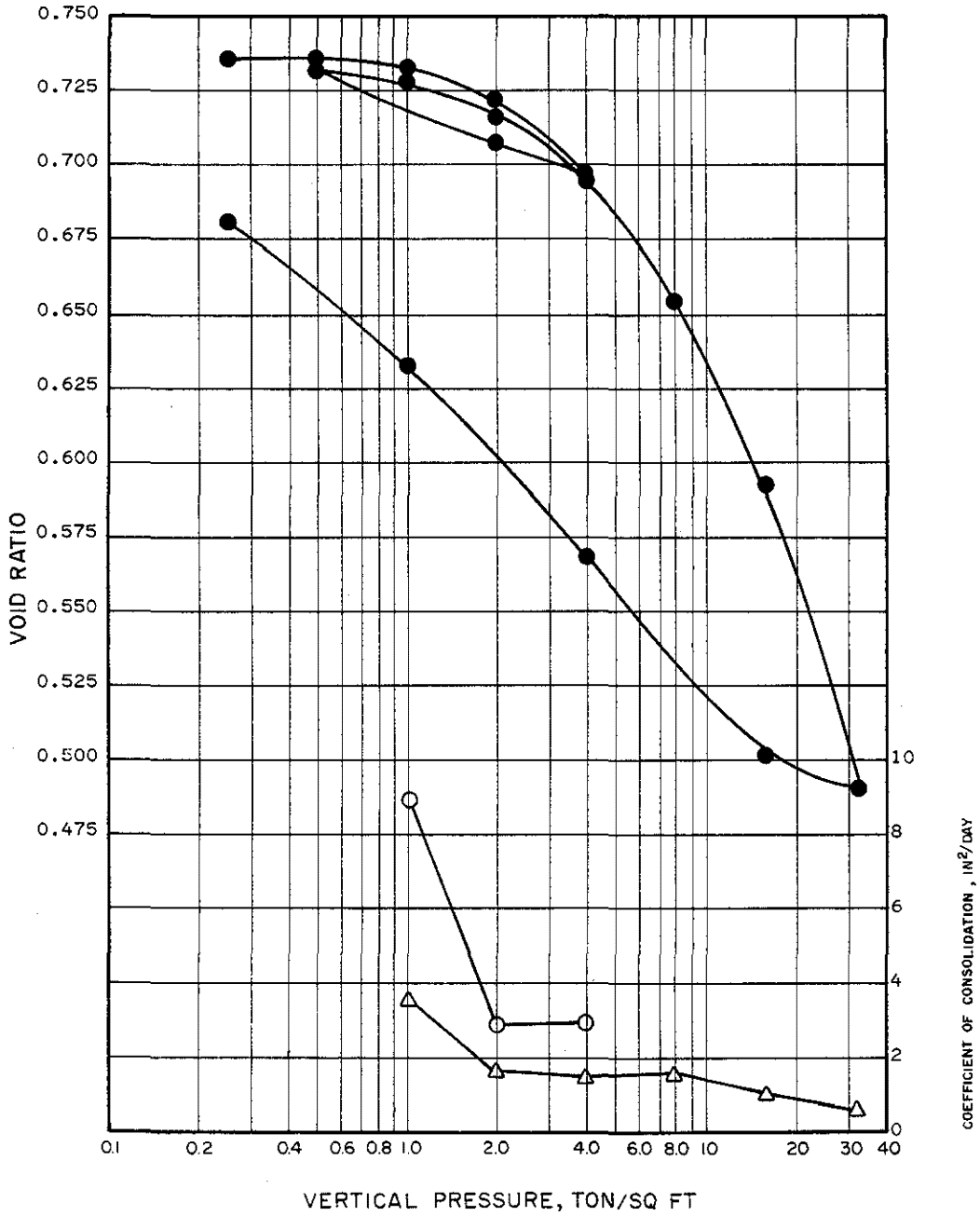
PLASTIC LIMIT:



CONSOLIDATION TEST RESULTS
VERTICAL

BORING NO: CB-2 SAMPLE NO:
 DEPTH, FT: 18-20
 DESCRIPTION: VERY STIFF RED AND LIGHT
 GRAY CLAY, INTENSELY SLICKENSIDED

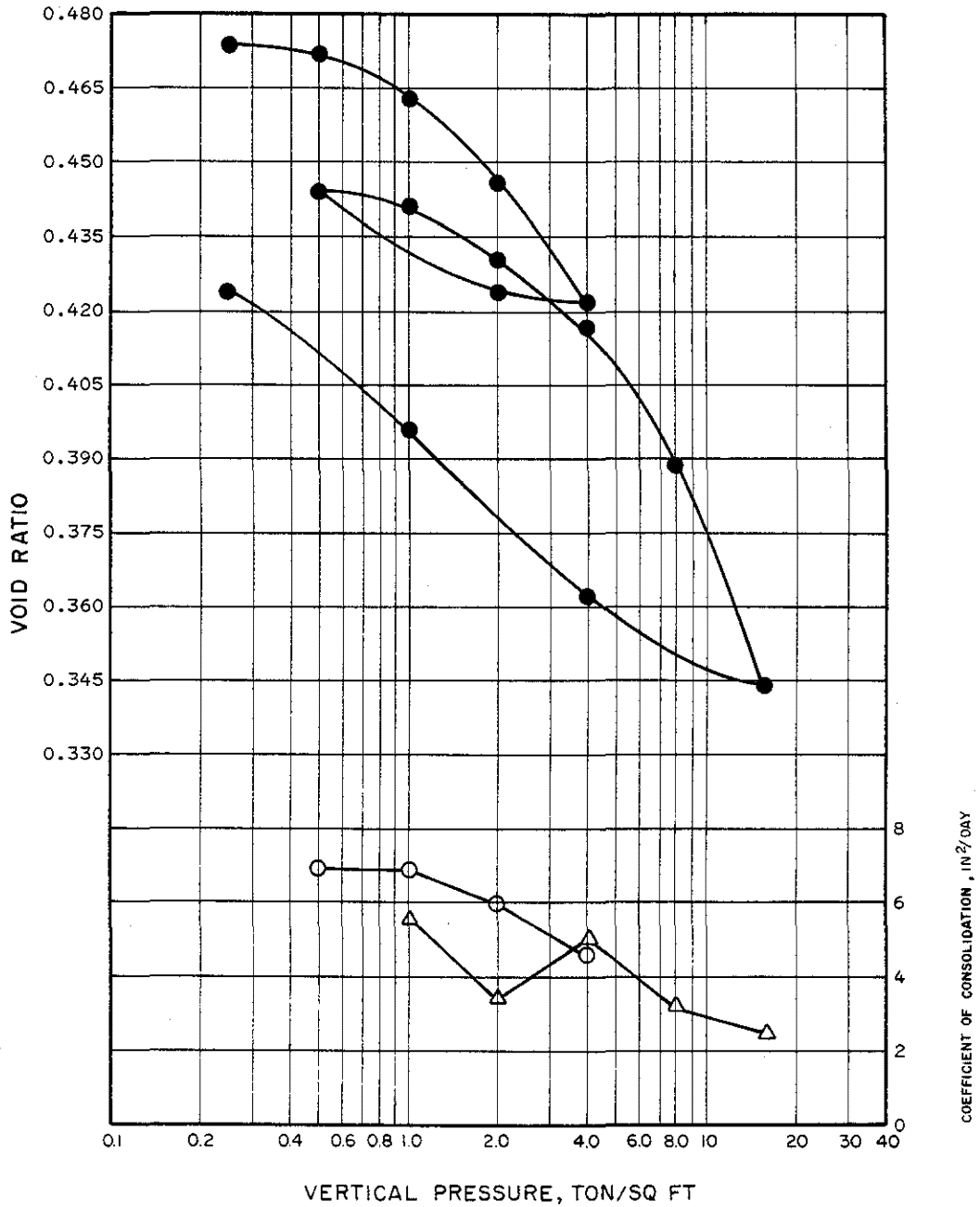
UNIT DRY WEIGHT: 96 PCF
 WATER CONTENT: 30 %
 LIQUID LIMIT:
 PLASTIC LIMIT:



CONSOLIDATION TEST RESULTS
 VERTICAL

BORING NO: CB-2 SAMPLE NO:
 DEPTH, FT: 9
 DESCRIPTION VERY STIFF GRAY AND TAN
 SANDY CLAY WITH SAND POCKETS AND
 CALCAREOUS NODULES

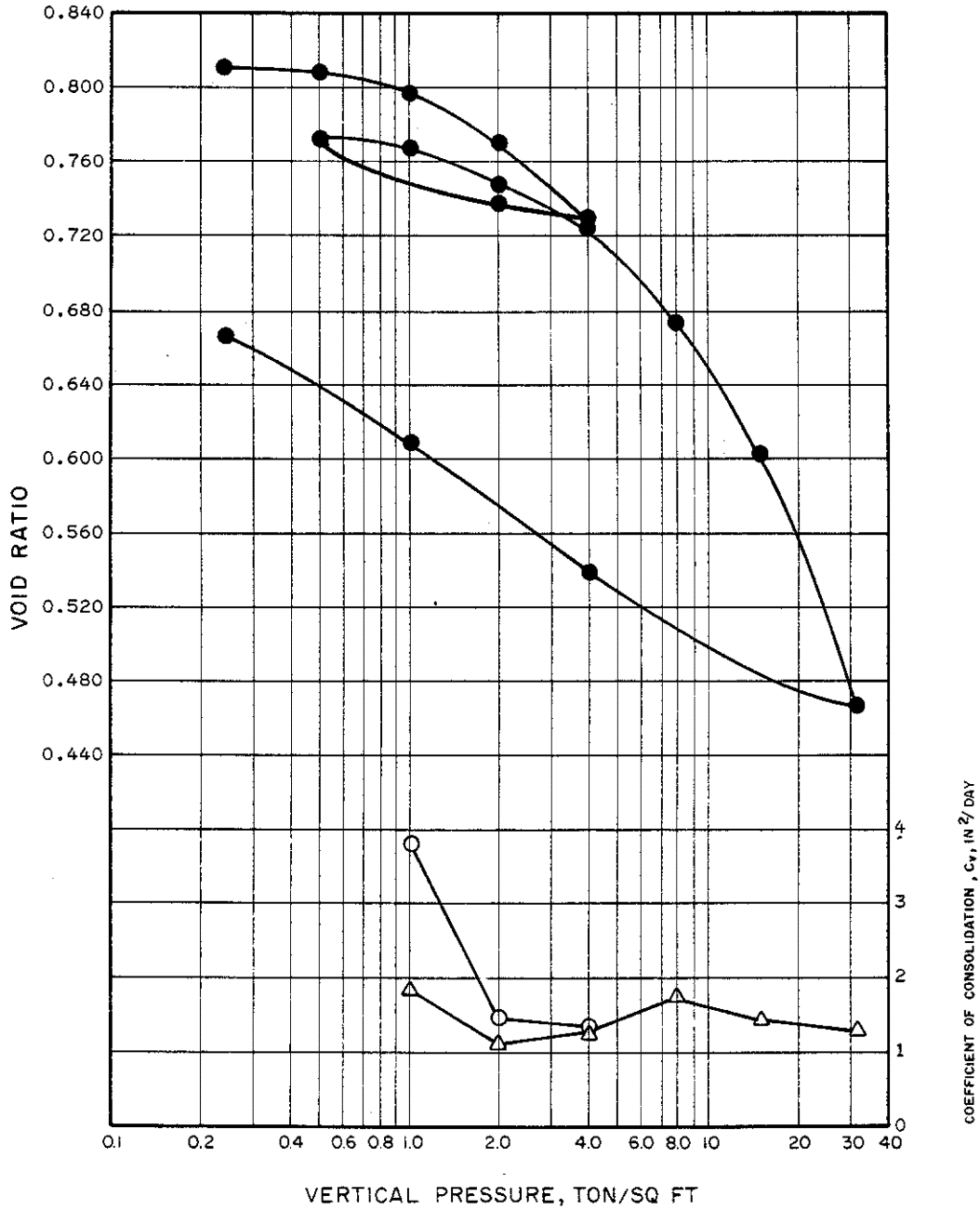
UNIT DRY WEIGHT: 109 PCF
 WATER CONTENT: 20 %
 LIQUID LIMIT:
 PLASTIC LIMIT:



CONSOLIDATION TEST RESULTS
 HORIZONTAL

BORING NO: CB-2 SAMPLE NO:
 DEPTH, FT: 22-24
 DESCRIPTION: VERY STIFF RED AND LIGHT
 GRAY CLAY, SLICKENSIDED

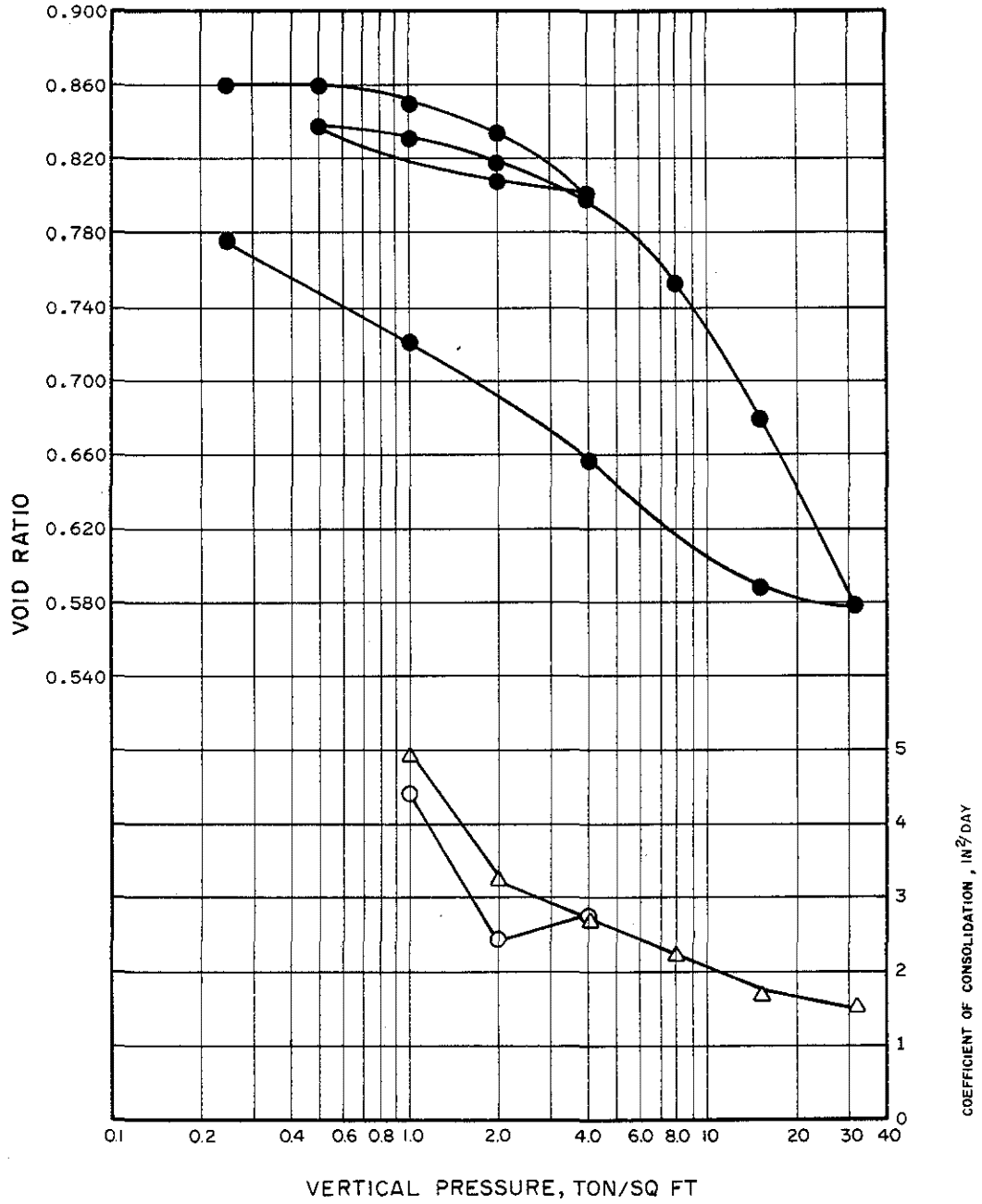
UNIT DRY WEIGHT: 93 PCF
 WATER CONTENT: 34 %
 LIQUID LIMIT:
 PLASTIC LIMIT:



CONSOLIDATION TEST RESULTS
 VERTICAL

BORING NO: CB-2 SAMPLE NO:
 DEPTH, FT: 23.5
 DESCRIPTION: VERY STIFF RED AND LIGHT
 GRAY CLAY, SLICKENSIDED

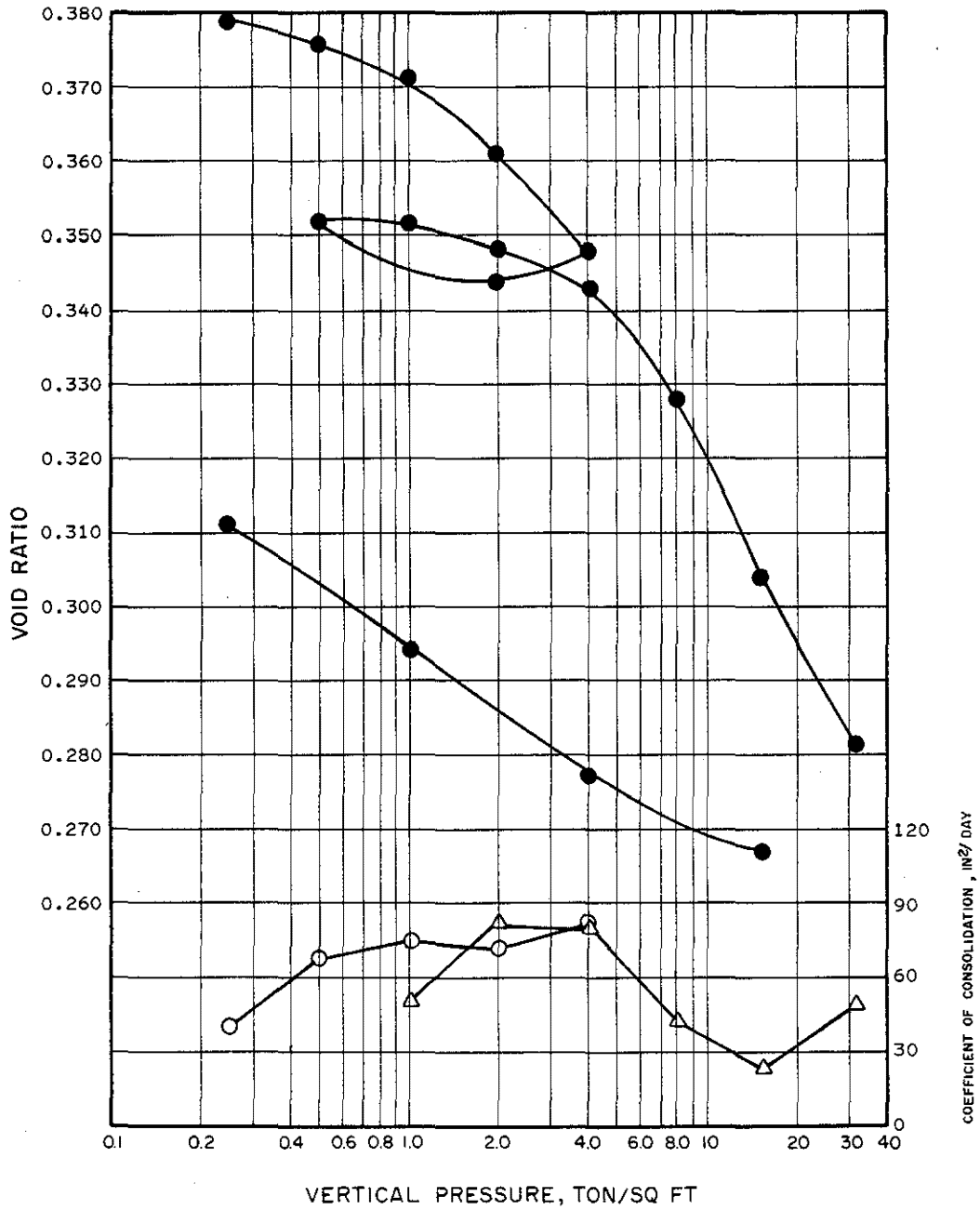
UNIT DRY WEIGHT: 91 PCF
 WATER CONTENT: 32 %
 LIQUID LIMIT:
 PLASTIC LIMIT:



CONSOLIDATION TEST RESULTS
 HORIZONTAL

BORING NO: CB-3 SAMPLE NO:
 DEPTH, FT: 32-34
 DESCRIPTION: STIFF TAN SANDY CLAY

UNIT DRY WEIGHT: 118 PCF
 WATER CONTENT: 15 %
 LIQUID LIMIT:
 PLASTIC LIMIT:



CONSOLIDATION TEST RESULTS
 VERTICAL

BORING NO: CB-2SAMPLE NO:

DEPTH, FT: 32-34

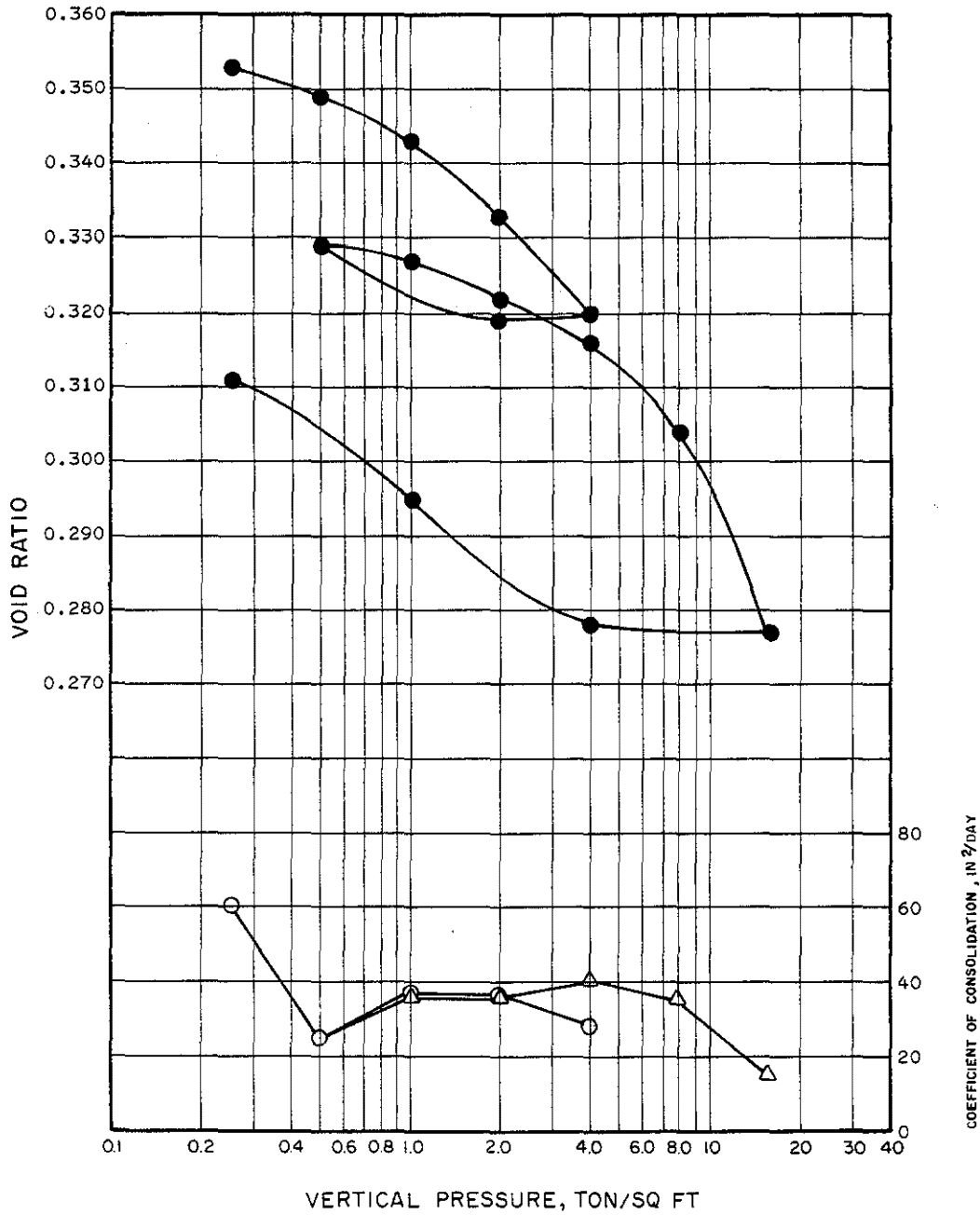
DESCRIPTION: VERY STIFF LIGHT GRAY AND
TAN SANDY CLAY

UNIT DRY WEIGHT: 121 PCF

WATER CONTENT: 15 %

LIQUID LIMIT:

PLASTIC LIMIT:



CONSOLIDATION TEST RESULTS
HORIZONTAL

BORING NO: CB-2 SAMPLE NO:

DEPTH, FT: 36-38

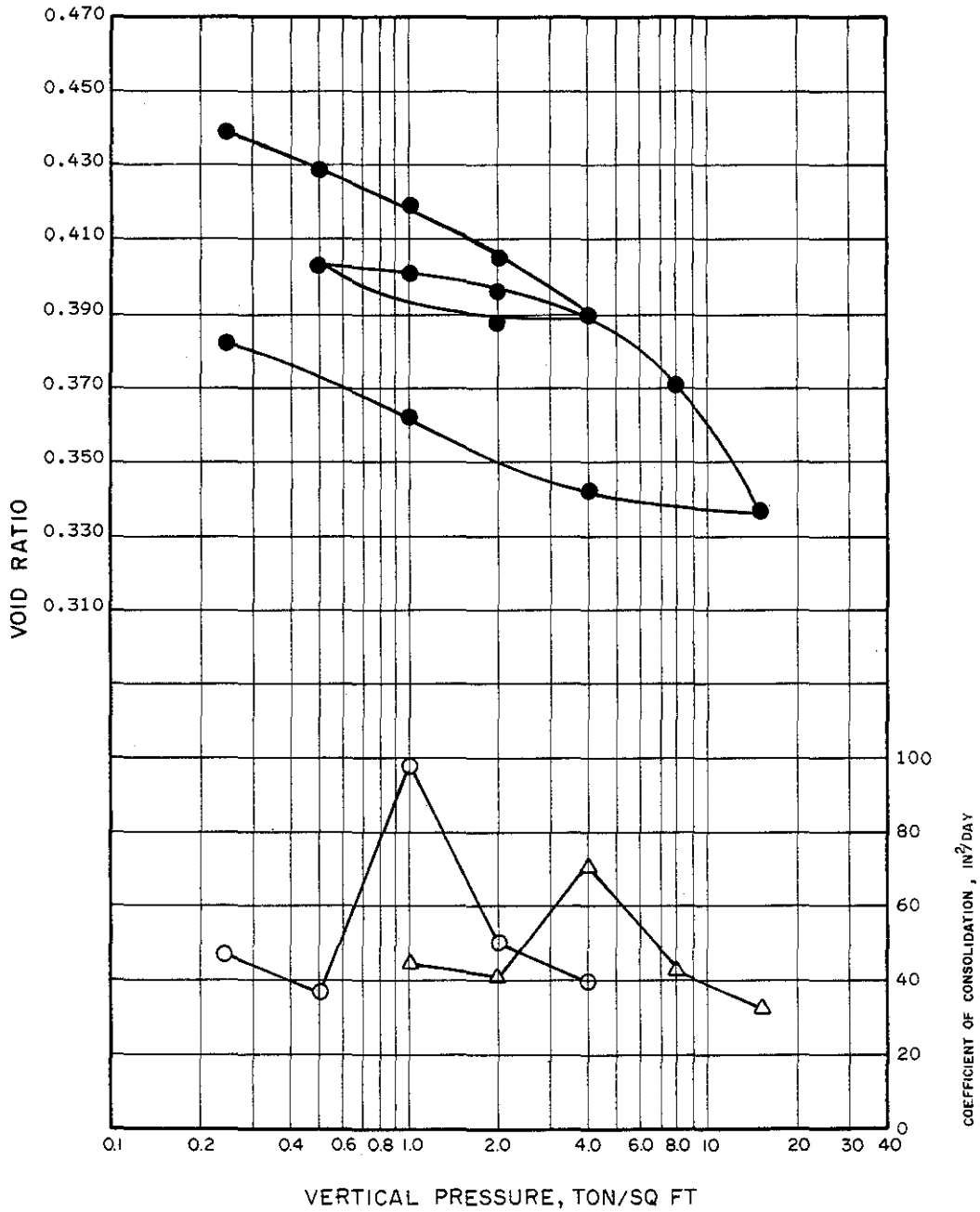
DESCRIPTION: VERY STIFF TAN AND LIGHT
GRAY SANDY CLAY

UNIT DRY WEIGHT: 112 PCF

WATER CONTENT: 16 %

LIQUID LIMIT:

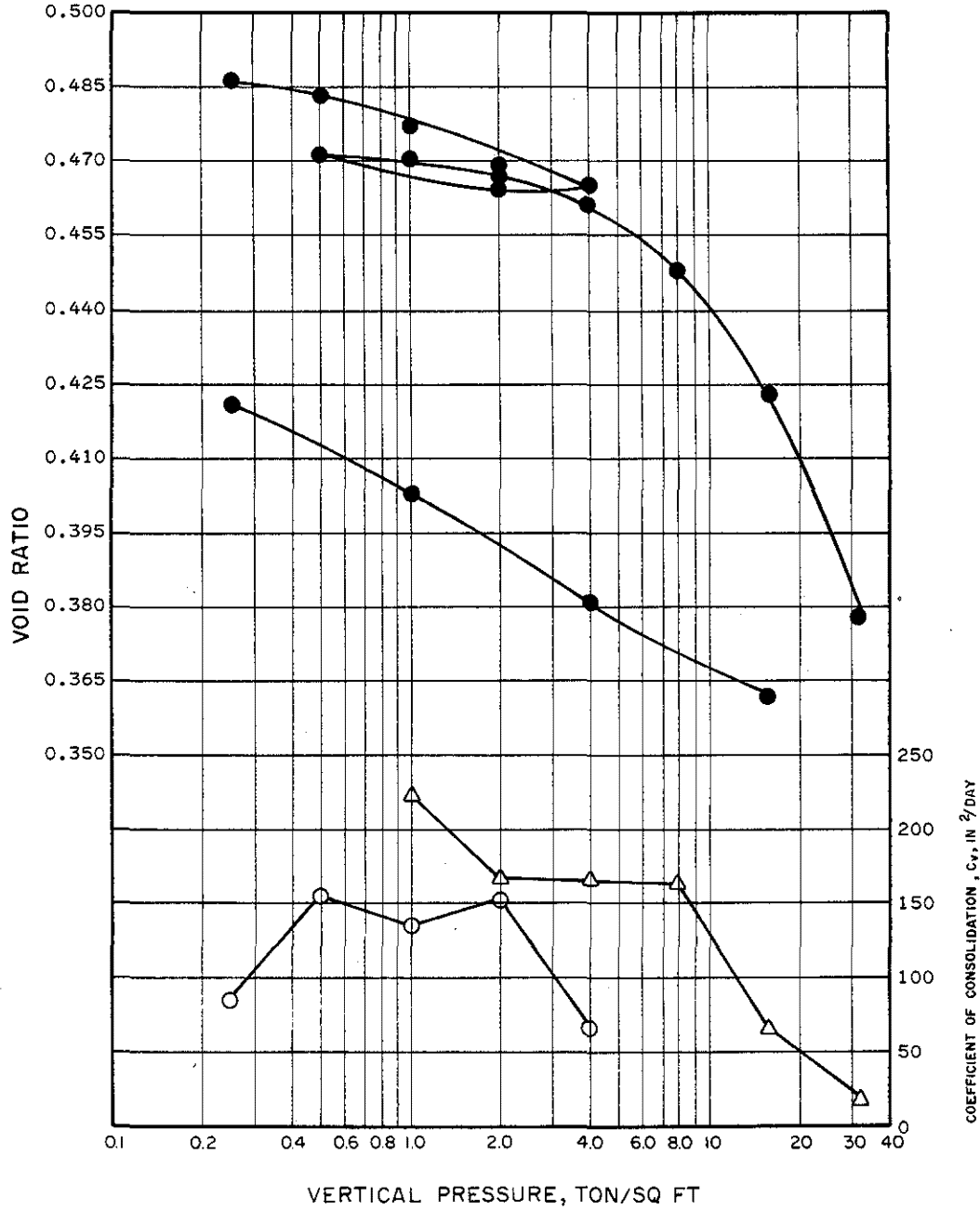
PLASTIC LIMIT:



CONSOLIDATION TEST RESULTS
VERTICAL

BORING NO: CB-2 SAMPLE NO:
 DEPTH, FT: 46-48
 DESCRIPTION: VERY STIFF RED AND TAN
 SILTY CLAY

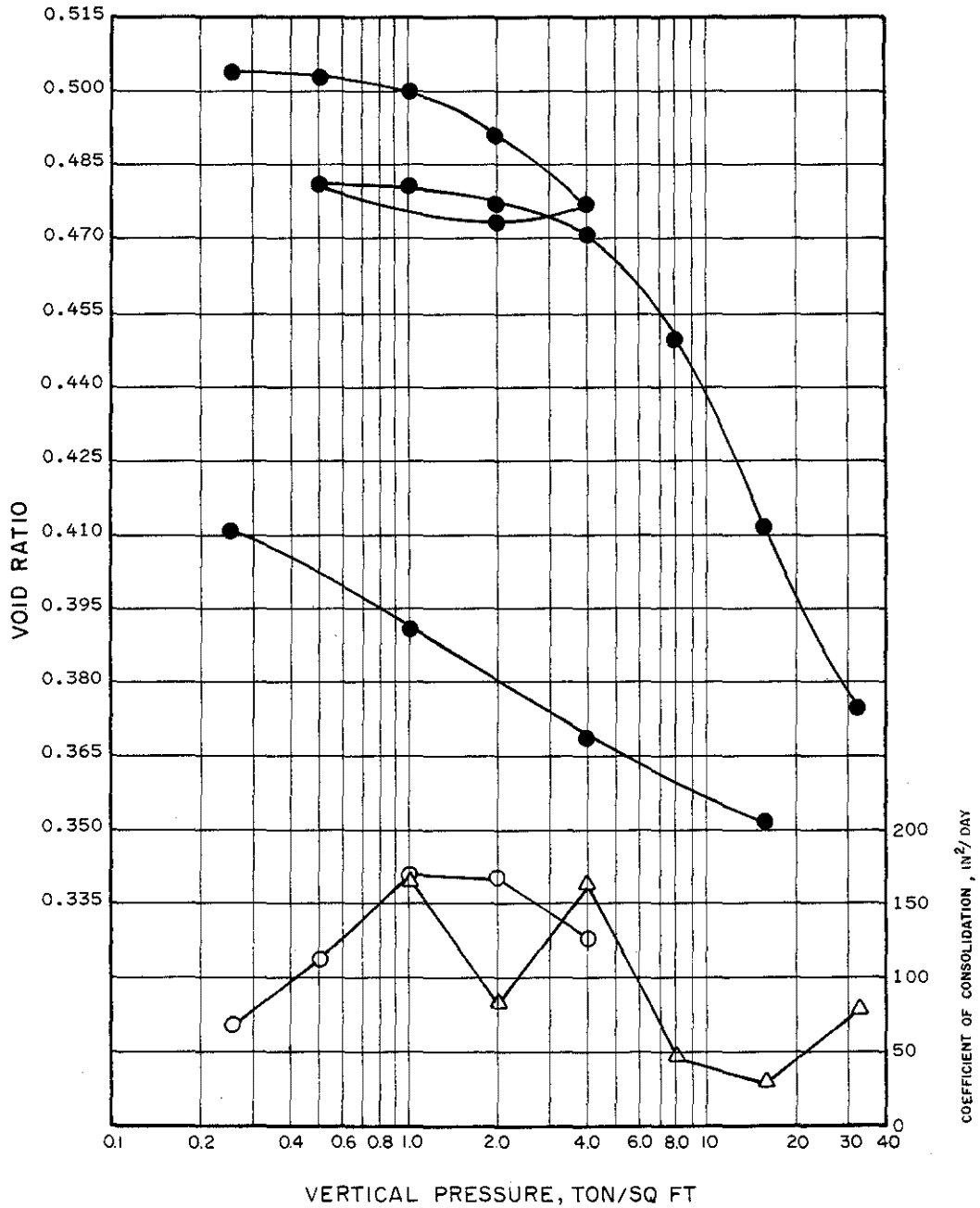
UNIT DRY WEIGHT: 108 PCF
 WATER CONTENT: 18 %
 LIQUID LIMIT:
 PLASTIC LIMIT:



CONSOLIDATION TEST RESULTS
 VERTICAL

BORING NO: CB-3 SAMPLE NO:
 DEPTH, FT: 47
 DESCRIPTION: VERY STIFF RED AND TAN
 VERY SILTY CLAY

UNIT DRY WEIGHT: 107 PCF
 WATER CONTENT: 19 %
 LIQUID LIMIT:
 PLASTIC LIMIT:



CONSOLIDATION TEST RESULTS
 HORIZONTAL

FEDERALLY COORDINATED PROGRAM (FCP) OF HIGHWAY RESEARCH AND DEVELOPMENT

The Offices of Research and Development (R&D) of the Federal Highway Administration (FHWA) are responsible for a broad program of staff and contract research and development and a Federal-aid program, conducted by or through the State highway transportation agencies, that includes the Highway Planning and Research (HP&R) program and the National Cooperative Highway Research Program (NCHRP) managed by the Transportation Research Board. The FCP is a carefully selected group of projects that uses research and development resources to obtain timely solutions to urgent national highway engineering problems.*

The diagonal double stripe on the cover of this report represents a highway and is color-coded to identify the FCP category that the report falls under. A red stripe is used for category 1, dark blue for category 2, light blue for category 3, brown for category 4, gray for category 5, green for categories 6 and 7, and an orange stripe identifies category 0.

FCP Category Descriptions

1. Improved Highway Design and Operation for Safety

Safety R&D addresses problems associated with the responsibilities of the FHWA under the Highway Safety Act and includes investigation of appropriate design standards, roadside hardware, signing, and physical and scientific data for the formulation of improved safety regulations.

2. Reduction of Traffic Congestion, and Improved Operational Efficiency

Traffic R&D is concerned with increasing the operational efficiency of existing highways by advancing technology, by improving designs for existing as well as new facilities, and by balancing the demand-capacity relationship through traffic management techniques such as bus and carpool preferential treatment, motorist information, and rerouting of traffic.

3. Environmental Considerations in Highway Design, Location, Construction, and Operation

Environmental R&D is directed toward identifying and evaluating highway elements that affect

the quality of the human environment. The goals are reduction of adverse highway and traffic impacts, and protection and enhancement of the environment.

4. Improved Materials Utilization and Durability

Materials R&D is concerned with expanding the knowledge and technology of materials properties, using available natural materials, improving structural foundation materials, recycling highway materials, converting industrial wastes into useful highway products, developing extender or substitute materials for those in short supply, and developing more rapid and reliable testing procedures. The goals are lower highway construction costs and extended maintenance-free operation.

5. Improved Design to Reduce Costs, Extend Life Expectancy, and Insure Structural Safety

Structural R&D is concerned with furthering the latest technological advances in structural and hydraulic designs, fabrication processes, and construction techniques to provide safe, efficient highways at reasonable costs.

6. Improved Technology for Highway Construction

This category is concerned with the research, development, and implementation of highway construction technology to increase productivity, reduce energy consumption, conserve dwindling resources, and reduce costs while improving the quality and methods of construction.

7. Improved Technology for Highway Maintenance

This category addresses problems in preserving the Nation's highways and includes activities in physical maintenance, traffic services, management, and equipment. The goal is to maximize operational efficiency and safety to the traveling public while conserving resources.

0. Other New Studies

This category, not included in the seven-volume official statement of the FCP, is concerned with HP&R and NCHRP studies not specifically related to FCP projects. These studies involve R&D support of other FHWA program office research.

* The complete seven-volume official statement of the FCP is available from the National Technical Information Service, Springfield, Va. 22161. Single copies of the introductory volume are available without charge from Program Analysis (HRD-3), Offices of Research and Development, Federal Highway Administration, Washington, D.C. 20590.